**MSC-E Data Report 3/2019**

**July 2019**

# Assessment of transboundary pollution by toxic substances: Heavy metals and POPs

## SUPPLEMENTARY MATERIALS FOR HEAVY METALS

I. Ilyin, A. Gusev, O. Rozovskaya, V. Shatalov, O.Travnikov, I.Strijkina

**MCS-E**

Meteorological Synthesizing
Centre - East

2nd Roshchinsky proezd, 8/5
115419 Moscow
Russia
Phone.: +7 926 906 91 78
Fax: +7 495 956 19 44
E-mail: msce@msceast.org
www.msceast.org

# Contents


Introduction 5

1. Pollution of the EMEP domain in 2017 7

1.1. Lead 7

1.2. Cadmium 8

1.4. Mercury 9

2.TRANSBOUNDARY POLLUTION OF THE EMEP COUNTRIES 10

2.1. Lead 10

2.2. Cadmium 11

2.3. Mercury 13

3. SOURCE-RECEPTOR TABLES 15

Lead 16

Cadmium 20

Mercury 24

4. EVALUATION OF MODELLING RESULTS VS. OBSERVATIONS 28

4.1. Lead 28

*4.1.1. Air concentrations* *28*

*4.1.2. Wet deposition* *34*

4.2. Cadmium 41

*4.2.1. Air concentrations* *41*

*4.2.2. Wet deposition* *47*

4.3. Mercury 54

*4.3.1. Air concentrations* *54*

*4.3.2. Wet deposition* *56*

4.4. Discussion 59

5. POLLUTION OF MARGINAL SEAS 66

5.1. Lead 66

5.2. Cadmium 67

5.3. Mercury 68

6. ECOSYSTEM-SPECIFIC DEPOSITION 69

6.1. Lead 70

6.2. Cadmium 72

6.3. Mercury 74

REFERENCES 76

## Introduction

This report is a supplement to the EMEP Status Report 2/2019 and summarizes the main output modeling results for 2017 on lead (Pb), cadmium (Cd) and mercury (Hg), presented in a form of maps, graphs and tables. Besides, the report contains evaluation of the calculated concentrations and deposition against measurements. The modelling results are based on meteorological data related to 2017, and emission data related to 2016 (the numerical data are available in the internet: http://en.msceast.org/index.php/pollution-assessment/emep-domain-menu/data-hm-pop-menu). The updated Information based on emissions for 2017 will be available on the internet (www.msceast.org).

In *Chapter 1* maps of annual mean air concentrations, total and wet deposition of Pb, Cd and Hg are presented. Spatial resolution of the maps is 0.1°x0.1°.

*Chapter 2* is focused on transboundary aspects of atmospheric pollution in the EMEP region. It presents country-averaged deposition fluxes split in three components: contribution of EMEP anthropogenic emissions, secondary sources (wind re-suspension and natural emission) within the EMEP region and sources outside the EMEP countries (non-EMEP sources). Furthermore, for each EMEP country fraction of anthropogenic deposition caused by national and foreign sources is presented. Finally, export of emitted lead, cadmium and mercury to other countries is characterized. Deposition to the EMEP region caused by sources of each EMEP country is presented as a sum of two parts. First part is a mass deposited within national's territory. The second part means mass of a pollutant emitted by a country and deposited to other EMEP countries.

Source-receptor tables are presented in *Chapter 3*. The tables give information about contribution of emission sources of each EMEP country to deposition in other EMEP counties. The columns of the table reveal deposition from a country to other countries. The rows contain deposition to a country from countries-contributors.

*Chapter 4* is focused on the evaluation of modelling results against concentrations and wet deposition observed at the EMEP monitoring stations. The chapter contains tables with statistical indicators for each station, diagrams showing comparison of modelled and observed annual mean air concentrations or annual sums of wet deposition, and time series of modelled and measured monthly mean pollution levels. The possible reasons of the discrepancies between calculated and observed levels are discussed.

Statistical indicators used in the chapter for evaluation of the agreement between modelled (*M*) and observed (*O*) parameters include Mean Relative Bais (MRB), Pearson's correlation coefficient (Rc) and Normalized root mean square error (NRMSE), calculated by formulae (1), (2) and (3), respectively:

$$MNB = \frac{\left(\overline{M} - \overline{O}\right)}{\overline{O}} \cdot 100\% \qquad (1)$$

$$Rc = \frac{\sum_{1}^{N}\left(M - \overline{M}\right)\cdot\left(O - \overline{O}\right)}{\sqrt{\sum_{1}^{N}\left(M - \overline{M}\right)^{2} \cdot \sum_{1}^{N}\left(O - \overline{O}\right)^{2}}} \qquad (2)$$

$$NRMSE = \frac{1}{\overline{O}} \cdot \sqrt{\frac{\sum_{i}^{N} (M_i - O_i)^2}{N}} \qquad (3)$$

Besides, fraction of fitting modelled and observed values within two-fold or three-fold difference (F2, F3) was calculated.

Maps of deposition of Pb, Cd and Hg to marginal seas (the Baltic, Black, Caspian, North and Mediterranean) of the EMEP region and maps of ecosystem-dependent deposition are presented in *Chapters 5* and *6*, respectively.

# 1. Pollution of the EMEP domain in 2017

## 1.1. Lead

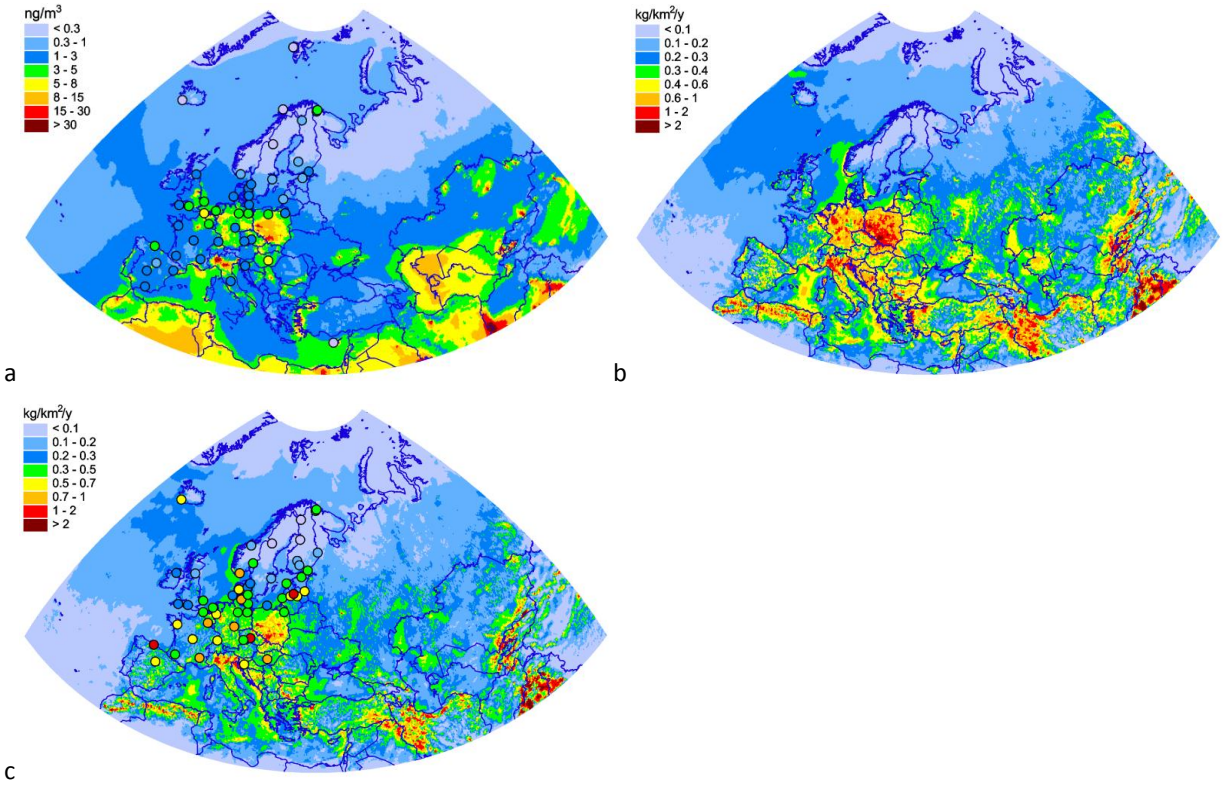


***Fig. 1.1***. *Concentrations in air (a), total (b) and wet (c) deposition flux of Pb in 2017*

## 1.2. Cadmium

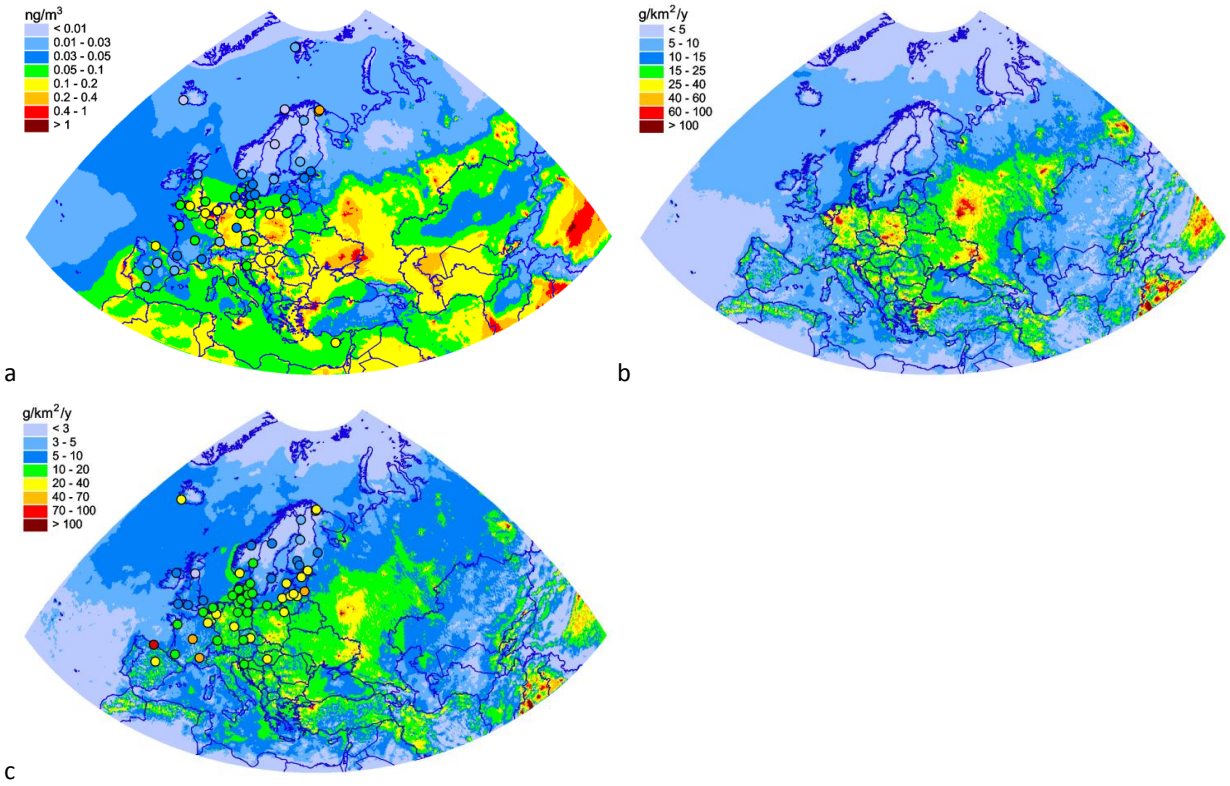


***Fig. 1.2****.Concentrations in air (a), total (b) and wet (c) deposition flux of Cd in 2017*

## 1.4. Mercury

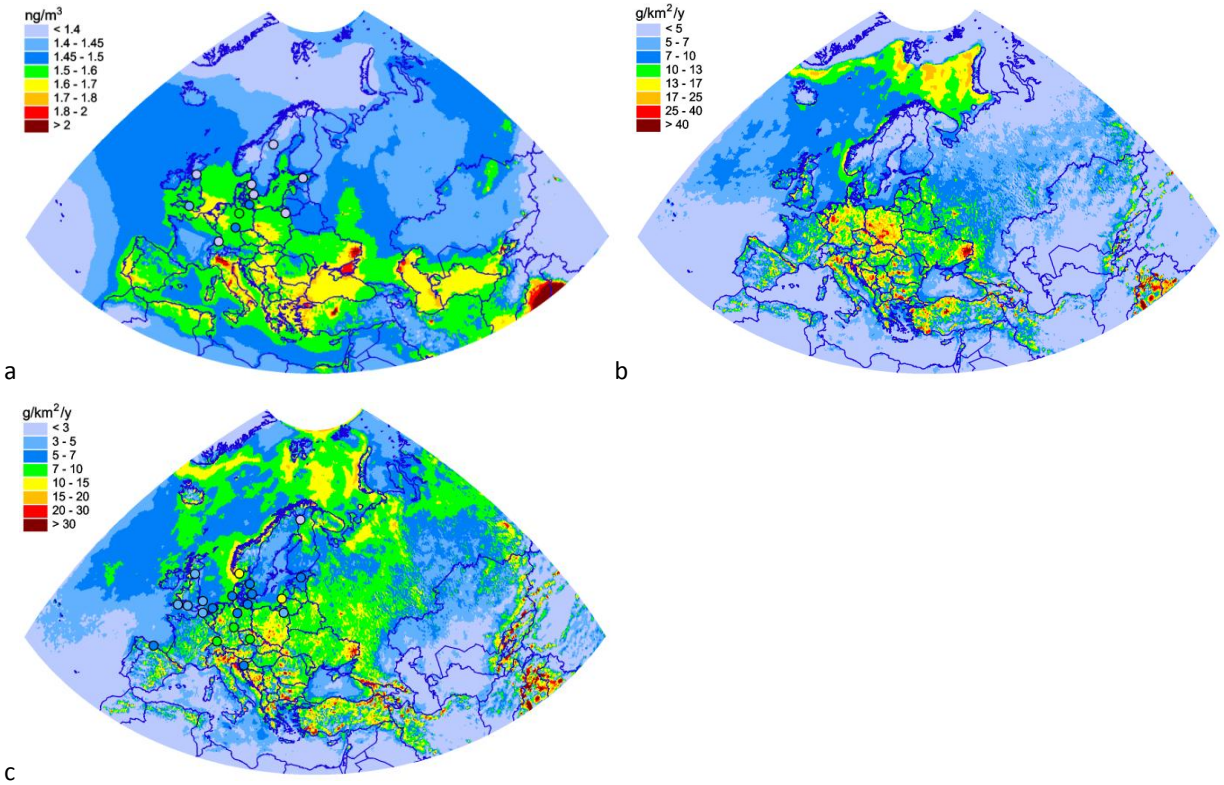


***Fig. 1.3****.Concentrations in air (a), net deposition flux (b) and wet deposition flux (c) deposition flux of Hg in 2017*

# 2.TRANSBOUNDARY POLLUTION OF THE EMEP COUNTRIES

## 2.1. Lead

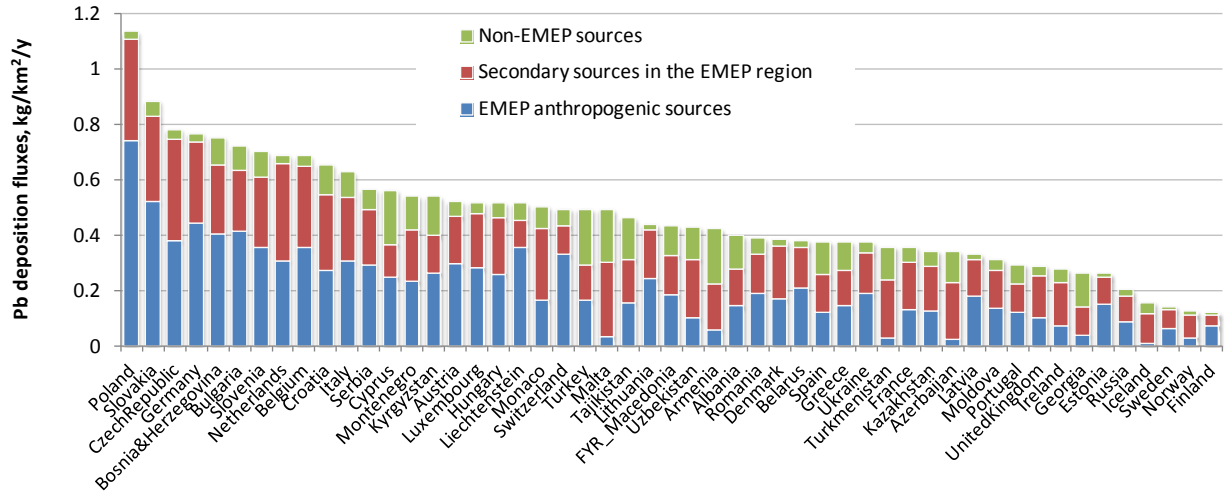


***Fig. 2.1.*** *Country-average deposition fluxes of Pb to EMEP countries*

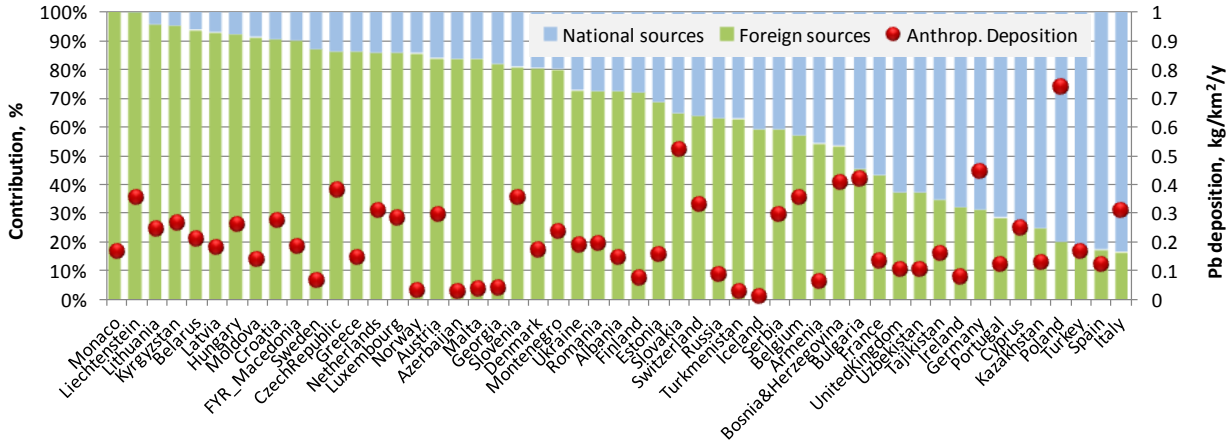


***Fig. 2.2.*** *Relative contribution of national sources and transboundary transport to Pb deposition in the EMEP countries*

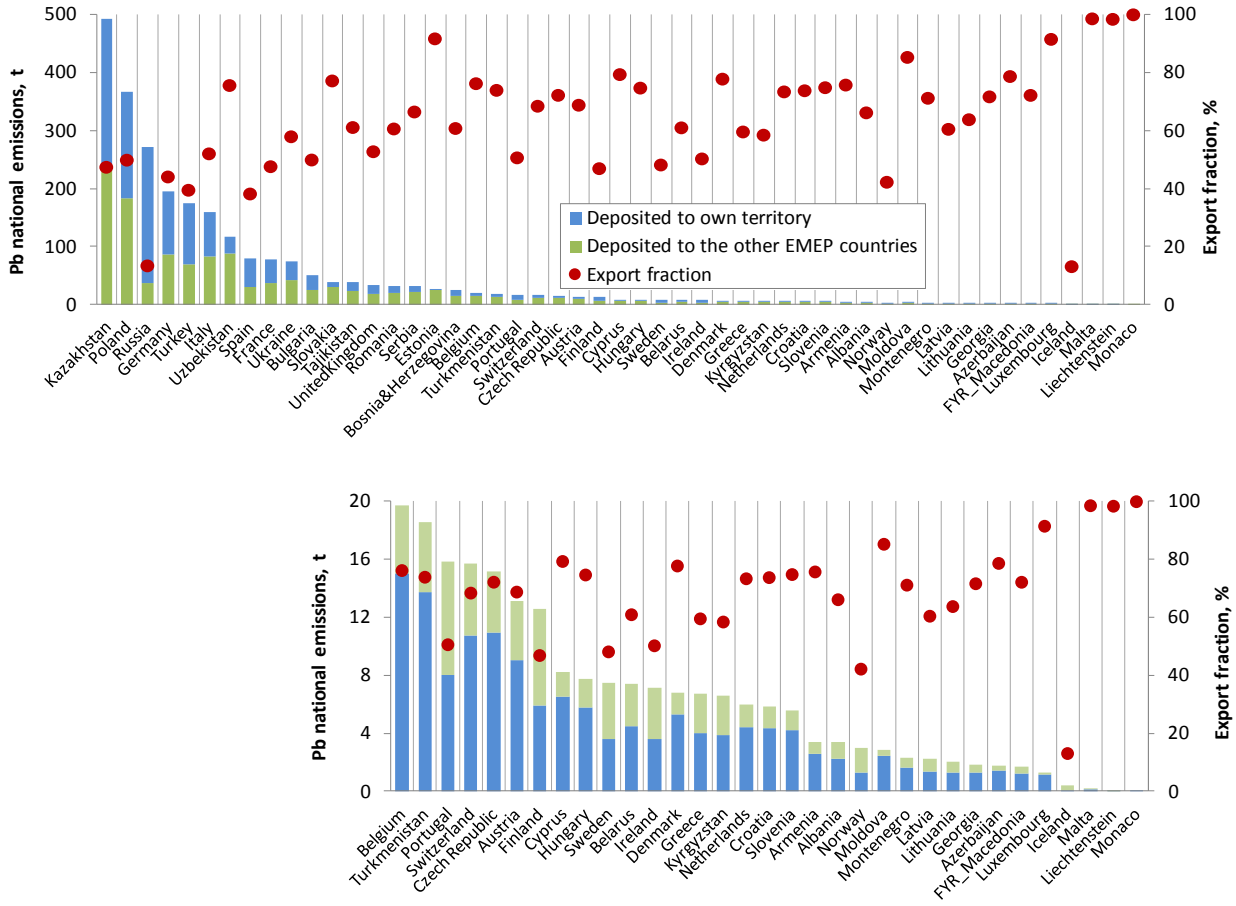


***Fig. 2.3.*** *Contribution of EMEP countries to transboundary transport of Pb. Red circle - fraction of total anthropogenic deposition to the EMEP countries exported outside the country.*

## 2.2. Cadmium

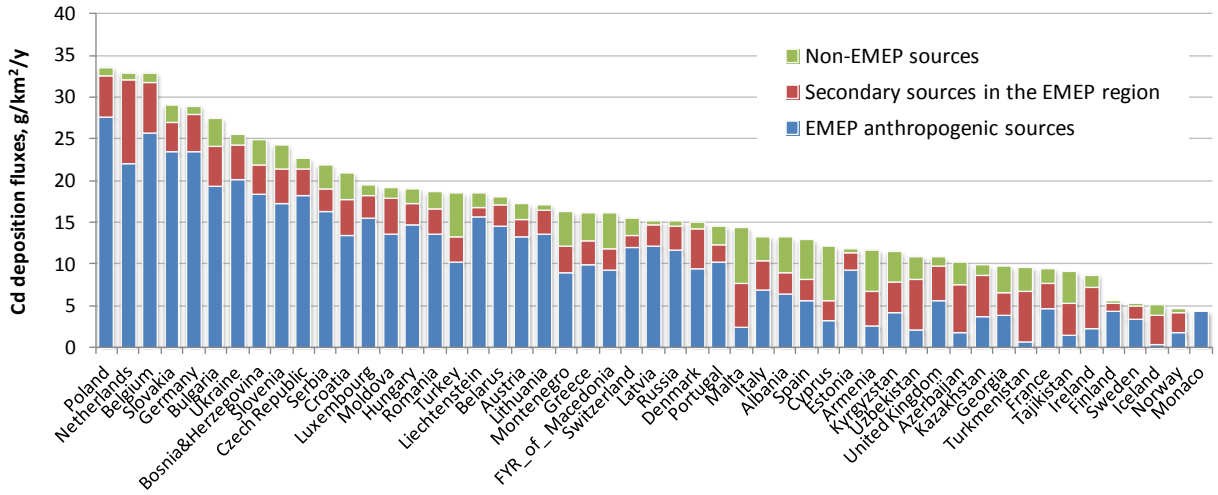


***Fig. 2.4.*** *Country-average deposition fluxes of Cd to EMEP countries*

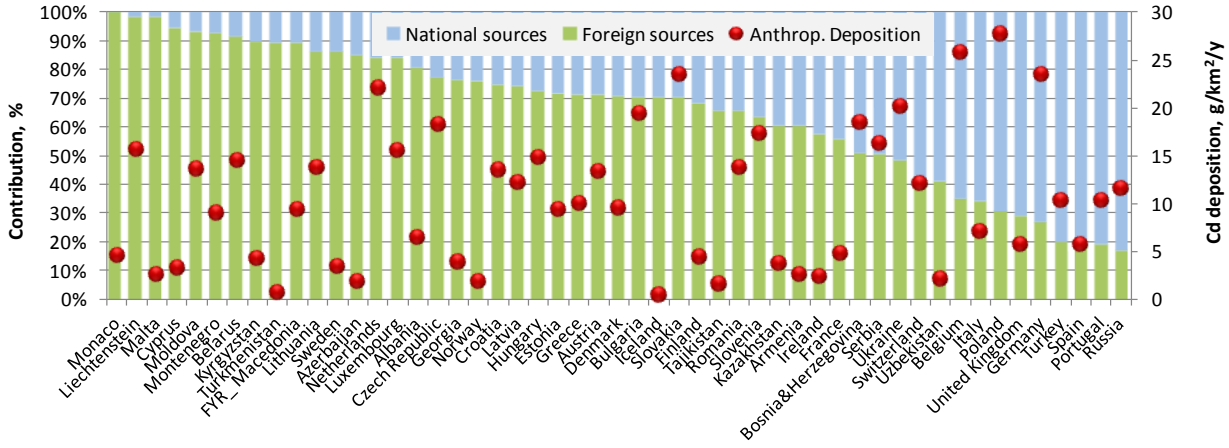


***Fig. 2.5.*** *Relative contribution of national sources and transboundary transport to Cd deposition in the EMEP countries*

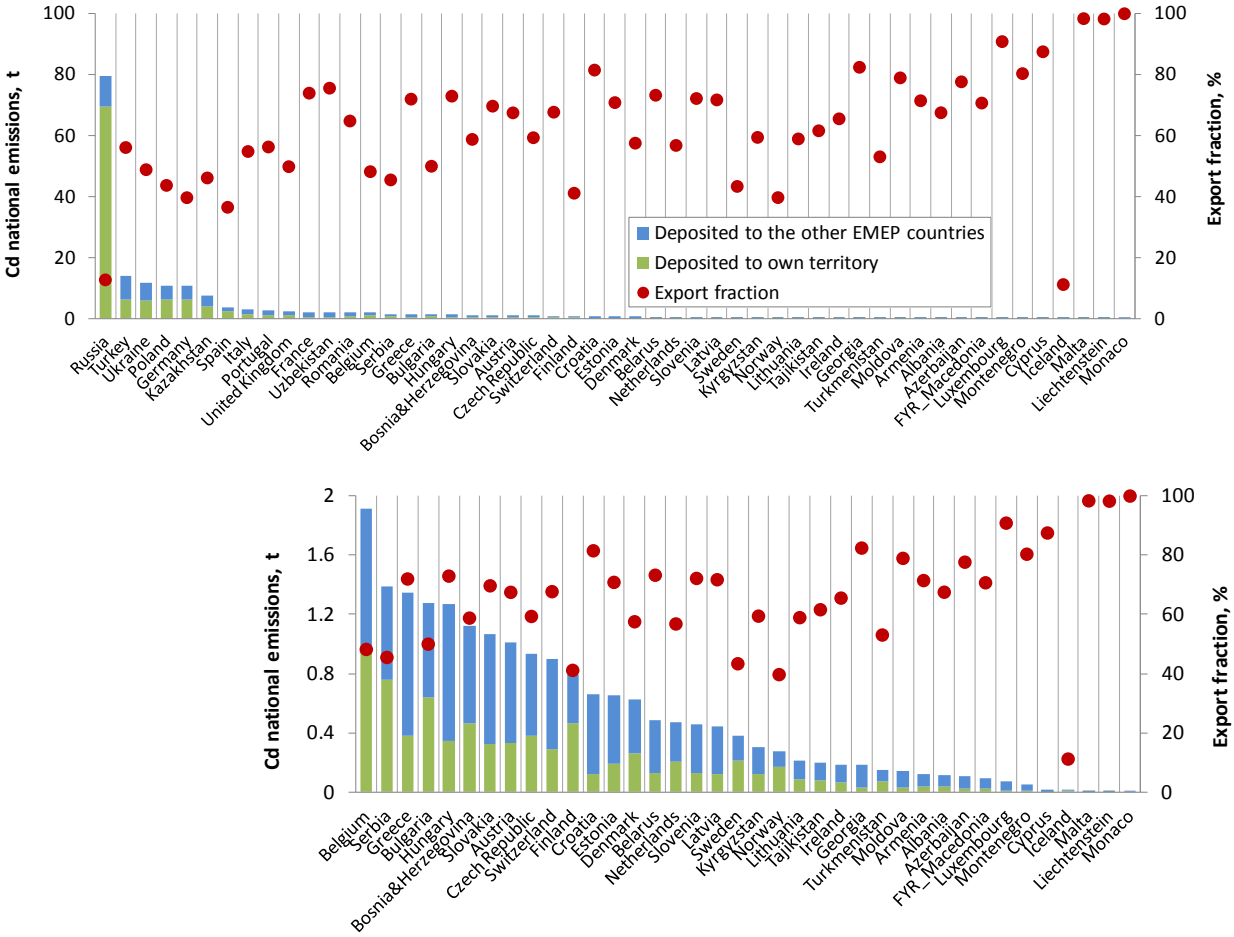


***Fig. 2.6****. Contribution of EMEP countries to transboundary transport of Cd. Red circle - fraction of total anthropogenic deposition to the EMEP countries exported outside the country.*

## 2.3. Mercury

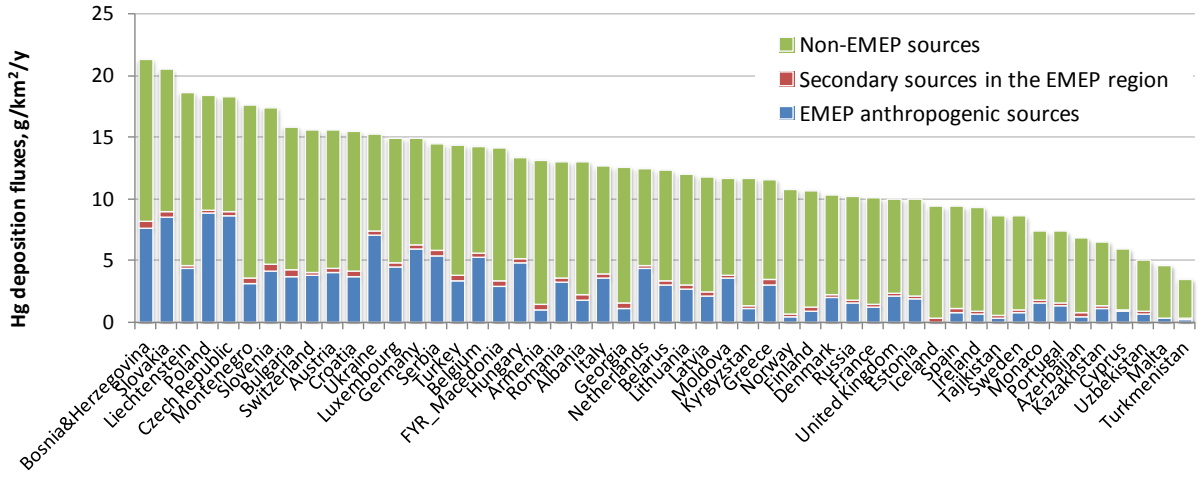


***Fig. 2.7.*** *Country-average deposition fluxes of Hg to EMEP countries*

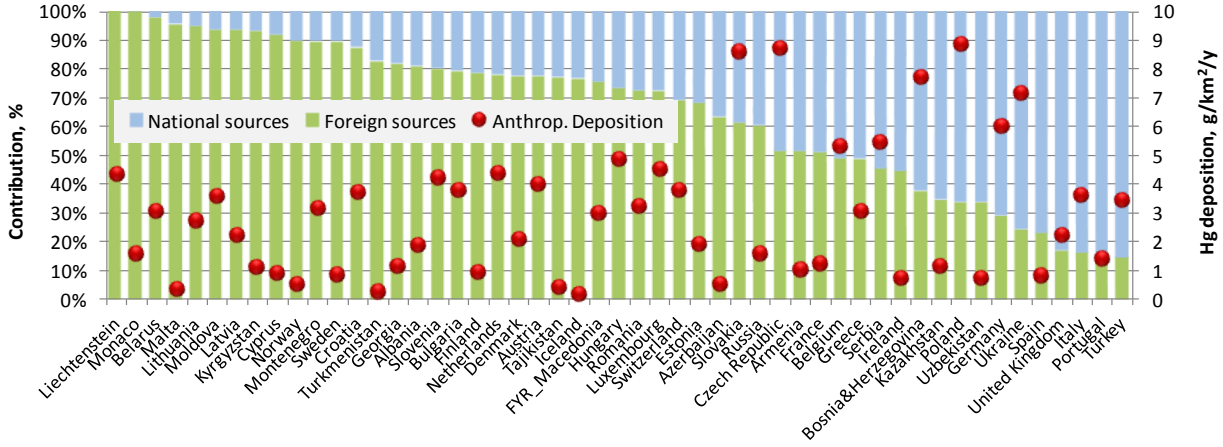


***Fig. 2.8.*** *Relative contribution of national sources and transboundary transport to Hg deposition in the EMEP countries*

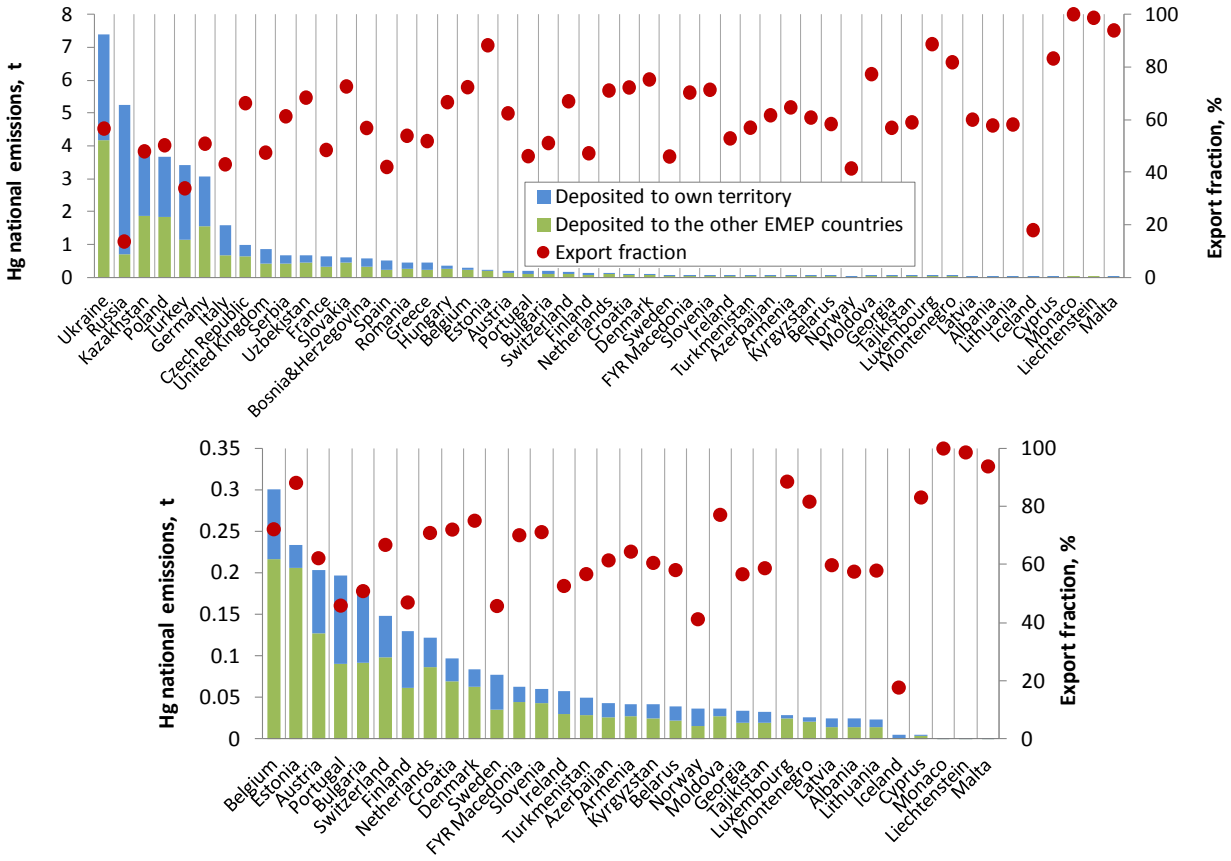


***Fig. 2.9.*** *Contribution of EMEP countries to transboundary transport of Hg. Red circle - fraction of total anthropogenic deposition to the EMEP countries exported outside the country.*

# 3. SOURCE-RECEPTOR TABLES

***Table 3.1.*** *Codes of countries, regions and seas*

| Country/Region/Sea | Code | Country/Region/Sea | Code |
|---|---|---|---|
| Albania | AL | Monaco | MC |
| Armenia | AM | Montenegro | ME |
| Austria | AT | Netherlands | NL |
| Azerbaijan | AZ | Norway | NO |
| Belarus | BY | Poland | PL |
| Belgium | BE | Portugal | PT |
| Bosnia and Herzegovina | BA | Republic of Moldova | MD |
| Bulgaria | BG | Romania | RO |
| Croatia | HR | Russian Federation | RU |
| Cyprus | CY | Serbia | RS |
| Czech Republic | CZ | Slovakia | SK |
| Denmark | DK | Slovenia | SI |
| Estonia | EE | Spain | ES |
| Finland | FI | Sweden | SE |
| France | FR | Switzerland | CH |
| Georgia | GE | The Former Yugoslav Republic of Macedonia | MK |
| Germany | DE | Tajikistan | TJ |
| Greece | GR | Turkey | TR |
| Hungary | HU | Turkmenistan | TM |
| Iceland | IS | Ukraine | UA |
| Ireland | IE | United Kingdom | GB |
| Italy | IT | Uzbekistan | UZ |
| Kazakhstan | KZ | | |
| Kyrgyzstan | KY | | |
| Latvia | LV | | |
| Lithuania | LT | | |
| Luxembourg | LU | | |
| Malta | MT | | |

***Table 3.2**. Matrix of Pb country-to-country deposition from anthropogenic sources in 2017, kg*

Receptors ↓ Emitters →

| code | AL | AM | AT | AZ | BA | BE | BG | BY | CH | CY | CZ | DE | DK |
|---|---|---|---|---|---|---|---|---|---|---|---|---|---|
| **AL** | **1154.9** | 0.1 | 14.0 | 0.1 | 154.6 | 2.3 | 248.6 | 0.8 | 12.7 | 1.3 | 9.6 | 46.8 | 0.7 |
| **AM** | 0.8 | **825.3** | 0.9 | 92.3 | 2.8 | 0.3 | 9.6 | 0.3 | 1.1 | 68.6 | 0.7 | 5.0 | 0.1 |
| **AT** | 7.5 | 0.0 | **4091.6** | 0.0 | 182.2 | 85.9 | 60.1 | 4.3 | 1065.3 | 0.3 | 421.3 | 6351.9 | 10.3 |
| **AZ** | 1.2 | 223.2 | 1.6 | **377.7** | 4.6 | 0.6 | 16.7 | 0.9 | 2.0 | 69.6 | 1.9 | 11.9 | 0.4 |
| **BA** | 68.3 | 0.1 | 204.1 | 0.1 | **9781.0** | 20.0 | 311.9 | 4.3 | 73.4 | 1.4 | 152.7 | 532.3 | 6.6 |
| **BE** | 0.2 | 0.0 | 13.1 | 0.0 | 1.9 | **4687.1** | 2.1 | 0.9 | 54.2 | 0.0 | 12.1 | 1411.6 | 5.5 |
| **BG** | 121.0 | 8.0 | 111.4 | 4.8 | 493.7 | 17.3 | **25247.2** | 19.9 | 56.8 | 70.0 | 82.7 | 402.1 | 5.4 |
| **BY** | 39.5 | 5.1 | 214.0 | 4.6 | 352.3 | 149.1 | 789.1 | **2877.9** | 115.3 | 7.8 | 438.6 | 2592.1 | 168.5 |
| **CH** | 0.8 | 0.0 | 58.1 | 0.0 | 11.7 | 38.3 | 2.9 | 0.2 | **4969.0** | 0.0 | 9.9 | 1215.0 | 1.4 |
| **CY** | 1.0 | 0.1 | 0.5 | 0.0 | 2.4 | 0.1 | 10.5 | 0.2 | 0.5 | **1697.4** | 0.4 | 2.2 | 0.0 |
| **CZ** | 4.7 | 0.1 | 874.7 | 0.1 | 244.6 | 223.9 | 60.0 | 7.8 | 359.7 | 0.3 | **4222.5** | 8868.5 | 33.5 |
| **DE** | 3.8 | 0.3 | 911.3 | 0.3 | 85.0 | 5611.1 | 60.2 | 33.0 | 3489.2 | 0.7 | 998.8 | **108976.0** | 362.6 |
| **DK** | 0.3 | 0.0 | 25.7 | 0.0 | 11.6 | 284.3 | 5.5 | 8.4 | 34.6 | 0.0 | 40.0 | 2325.9 | **1514.6** |
| **EE** | 1.8 | 0.2 | 24.1 | 0.3 | 28.0 | 42.4 | 33.9 | 61.4 | 22.4 | 0.3 | 40.8 | 546.0 | 81.3 |
| **ES** | 4.3 | 0.0 | 23.8 | 0.0 | 47.5 | 56.1 | 11.1 | 0.2 | 72.0 | 0.2 | 12.1 | 240.6 | 2.0 |
| **FI** | 5.4 | 0.6 | 78.7 | 0.7 | 76.9 | 122.2 | 90.0 | 117.6 | 79.8 | 1.1 | 129.3 | 1283.3 | 190.0 |
| **FR** | 16.7 | 0.0 | 132.6 | 0.0 | 165.5 | 1925.1 | 79.5 | 3.2 | 1512.4 | 0.7 | 76.3 | 5001.6 | 26.0 |
| **GB** | 0.5 | 0.0 | 26.0 | 0.0 | 3.7 | 734.5 | 12.4 | 5.7 | 54.6 | 0.2 | 26.1 | 1638.6 | 60.3 |
| **GE** | 3.6 | 204.3 | 4.5 | 55.3 | 16.1 | 1.2 | 82.0 | 2.2 | 3.4 | 89.1 | 3.8 | 21.4 | 0.8 |
| **GR** | 312.3 | 2.1 | 44.8 | 1.3 | 295.4 | 7.4 | 2506.1 | 7.1 | 37.5 | 98.9 | 32.6 | 166.0 | 2.4 |
| **HR** | 47.2 | 0.1 | 380.3 | 0.0 | 1762.9 | 21.4 | 232.6 | 3.8 | 91.1 | 1.0 | 166.0 | 628.9 | 5.6 |
| **HU** | 57.0 | 0.5 | 796.7 | 0.3 | 1328.4 | 43.1 | 514.2 | 16.0 | 142.2 | 1.7 | 472.3 | 1419.4 | 14.0 |
| **IE** | 0.1 | 0.0 | 8.2 | 0.0 | 1.0 | 80.6 | 2.4 | 0.5 | 14.4 | 0.0 | 4.3 | 233.2 | 4.8 |
| **IS** | 0.1 | 0.0 | 1.6 | 0.0 | 0.5 | 17.5 | 1.1 | 0.6 | 4.2 | 0.0 | 2.4 | 101.1 | 8.2 |
| **IT** | 141.2 | 0.1 | 423.7 | 0.1 | 1099.9 | 49.8 | 331.9 | 2.3 | 1067.9 | 2.8 | 116.5 | 1363.2 | 6.6 |
| **KY** | 1.7 | 23.7 | 2.5 | 15.4 | 8.3 | 0.9 | 21.8 | 0.8 | 4.1 | 42.5 | 1.6 | 14.3 | 0.3 |
| **KZ** | 39.8 | 473.5 | 95.8 | 341.5 | 233.9 | 35.5 | 783.6 | 80.6 | 89.6 | 366.7 | 96.8 | 605.5 | 26.0 |
| **LI** | 0.0 | 0.0 | 0.9 | 0.0 | 0.0 | 0.2 | 0.0 | 0.0 | 27.5 | 0.0 | 0.1 | 9.0 | 0.0 |
| **LT** | 5.1 | 0.3 | 78.3 | 0.3 | 89.5 | 96.6 | 91.6 | 337.7 | 45.0 | 0.4 | 154.9 | 1449.4 | 199.0 |
| **LU** | 0.0 | 0.0 | 1.8 | 0.0 | 0.3 | 70.6 | 0.3 | 0.1 | 11.9 | 0.0 | 1.7 | 202.1 | 0.3 |
| **LV** | 4.1 | 0.3 | 54.2 | 0.4 | 68.3 | 77.0 | 83.5 | 178.7 | 36.2 | 0.5 | 103.8 | 1117.6 | 177.1 |
| **MC** | 0.0 | 0.0 | 0.0 | 0.0 | 0.0 | 0.0 | 0.0 | 0.0 | 0.0 | 0.0 | 0.0 | 0.0 | 0.0 |
| **MD** | 7.7 | 3.2 | 19.5 | 1.9 | 38.5 | 4.5 | 184.6 | 20.0 | 10.3 | 7.1 | 17.1 | 102.3 | 4.6 |
| **ME** | 110.1 | 0.0 | 16.3 | 0.0 | 436.8 | 2.0 | 112.1 | 0.4 | 10.3 | 0.5 | 12.3 | 49.6 | 0.7 |
| **MK** | 318.5 | 0.5 | 18.2 | 0.3 | 130.8 | 2.5 | 975.8 | 1.2 | 12.3 | 3.5 | 12.9 | 59.2 | 0.8 |
| **MT** | 0.1 | 0.0 | 0.1 | 0.0 | 0.3 | 0.0 | 0.2 | 0.0 | 0.1 | 0.0 | 0.0 | 0.1 | 0.0 |
| **NL** | 0.3 | 0.0 | 16.2 | 0.0 | 2.2 | 2598.1 | 3.7 | 2.8 | 44.4 | 0.0 | 19.3 | 2552.3 | 15.7 |
| **NO** | 1.2 | 0.6 | 41.6 | 0.6 | 25.1 | 325.6 | 27.9 | 21.8 | 59.0 | 0.7 | 78.5 | 2166.4 | 400.1 |
| **PL** | 30.6 | 2.0 | 954.8 | 2.2 | 747.5 | 894.0 | 338.8 | 353.5 | 469.9 | 1.8 | 3696.3 | 19732.7 | 644.3 |
| **PT** | 0.1 | 0.0 | 1.5 | 0.0 | 1.1 | 6.6 | 0.3 | 0.0 | 4.2 | 0.0 | 0.8 | 25.7 | 0.4 |
| **RO** | 167.9 | 10.7 | 417.2 | 6.3 | 1212.0 | 47.1 | 4011.2 | 54.5 | 177.4 | 38.3 | 233.2 | 1327.5 | 23.9 |
| **RS** | 208.7 | 1.3 | 215.8 | 0.6 | 1821.9 | 21.9 | 2041.4 | 12.4 | 70.4 | 4.3 | 173.8 | 620.4 | 9.2 |
| **RU** | 256.6 | 752.2 | 808.8 | 601.9 | 1818.1 | 543.9 | 5568.5 | 2344.0 | 646.0 | 747.4 | 1056.7 | 7827.8 | 689.2 |
| **SE** | 3.6 | 0.4 | 125.3 | 0.6 | 85.6 | 489.4 | 51.9 | 90.3 | 155.2 | 0.6 | 246.9 | 5207.6 | 1914.9 |
| **SI** | 8.7 | 0.0 | 429.3 | 0.0 | 155.3 | 10.9 | 61.5 | 0.5 | 56.9 | 0.2 | 49.7 | 377.8 | 1.6 |
| **SK** | 18.6 | 0.2 | 607.3 | 0.1 | 560.7 | 45.6 | 193.6 | 10.6 | 126.9 | 0.7 | 852.2 | 1491.1 | 16.1 |
| **TJ** | 0.8 | 12.5 | 1.0 | 8.1 | 3.2 | 0.4 | 8.9 | 0.4 | 1.7 | 21.9 | 0.8 | 6.3 | 0.2 |
| **TM** | 1.9 | 82.5 | 3.1 | 73.9 | 7.5 | 1.1 | 27.6 | 2.0 | 3.9 | 67.2 | 2.9 | 21.4 | 1.0 |
| **TR** | 103.5 | 636.4 | 91.2 | 83.6 | 313.1 | 21.7 | 2123.1 | 40.9 | 73.3 | 4582.5 | 73.2 | 437.7 | 10.9 |
| **UA** | 109.9 | 38.1 | 626.2 | 30.9 | 986.2 | 191.6 | 2791.3 | 643.2 | 261.2 | 145.9 | 807.6 | 3911.3 | 145.1 |
| **UZ** | 2.8 | 89.7 | 4.3 | 65.3 | 13.3 | 1.6 | 45.3 | 3.0 | 5.4 | 80.9 | 3.7 | 26.1 | 1.3 |
| **SUM,t** | 3.4 | 3.4 | 13.1 | 1.8 | 24.9 | 19.7 | 50.3 | 7.4 | 15.7 | 8.2 | 15.2 | 194.7 | 6.8 |
| **Emiss 2016, t** | 5.8 | 5.0 | 15.6 | 2.9 | 33.9 | 26.9 | 66.7 | 8.0 | 19.2 | 26.8 | 17.2 | 233.5 | 11.0 |
| **code** | **AL** | **AM** | **AT** | **AZ** | **BA** | **BE** | **BG** | **BY** | **CH** | **CY** | **CZ** | **DE** | **DK** |

***Table 3.2**. Matrix of Pb country-to-country deposition from anthropogenic sources in 2017, kg (continued)*

Receptors ↓ Emitters →

| code | EE | ES | FI | FR | GB | GE | GR | HR | HU | IE | IS | IT | KY | KZ |
|---|---|---|---|---|---|---|---|---|---|---|---|---|---|---|
| **AL** | 0.5 | 93.5 | 0.2 | 71.7 | 2.8 | 0.1 | 125.7 | 23.0 | 14.1 | 0.5 | 0.0 | 1196.2 | 0.0 | 2.5 |
| **AM** | 0.3 | 10.2 | 0.1 | 4.3 | 0.4 | 144.5 | 4.2 | 0.6 | 0.5 | 0.1 | 0.0 | 30.9 | 0.2 | 81.3 |
| **AT** | 16.5 | 493.3 | 5.9 | 884.0 | 90.6 | 0.0 | 4.7 | 214.9 | 119.5 | 9.7 | 0.1 | 7124.1 | 0.0 | 1.6 |
| **AZ** | 1.2 | 16.6 | 0.3 | 6.6 | 1.0 | 125.8 | 5.4 | 1.0 | 1.1 | 0.1 | 0.0 | 48.9 | 1.1 | 461.8 |
| **BA** | 4.8 | 282.5 | 2.1 | 240.5 | 21.5 | 0.1 | 29.6 | 522.1 | 240.5 | 2.1 | 0.1 | 3968.6 | 0.0 | 4.3 |
| **BE** | 3.4 | 239.0 | 1.3 | 3020.2 | 696.6 | 0.0 | 0.2 | 1.3 | 1.9 | 49.3 | 0.4 | 91.8 | 0.0 | 0.1 |
| **BG** | 9.5 | 222.7 | 2.5 | 151.1 | 17.3 | 6.4 | 555.4 | 73.9 | 156.7 | 2.0 | 0.1 | 1504.7 | 0.5 | 181.3 |
| **BY** | 404.7 | 287.3 | 80.1 | 390.7 | 293.0 | 5.6 | 91.5 | 76.8 | 184.1 | 26.9 | 0.6 | 1555.8 | 0.6 | 244.0 |
| **CH** | 0.5 | 422.7 | 0.5 | 1304.8 | 44.2 | 0.0 | 0.6 | 14.6 | 2.6 | 5.6 | 0.1 | 5430.2 | 0.0 | 0.2 |
| **CY** | 0.1 | 4.7 | 0.0 | 2.4 | 0.2 | 0.1 | 9.2 | 0.5 | 0.3 | 0.0 | 0.0 | 30.1 | 0.0 | 0.7 |
| **CZ** | 17.2 | 284.6 | 6.8 | 811.3 | 220.4 | 0.1 | 2.8 | 130.9 | 208.5 | 18.8 | 0.3 | 1521.3 | 0.0 | 2.7 |
| **DE** | 84.6 | 1724.6 | 40.5 | 10868.2 | 3887.3 | 0.3 | 4.9 | 60.1 | 82.8 | 321.4 | 3.1 | 4034.6 | 0.0 | 16.1 |
| **DK** | 21.8 | 138.2 | 7.9 | 444.8 | 718.4 | 0.0 | 0.2 | 4.5 | 8.4 | 60.6 | 1.1 | 125.1 | 0.0 | 3.0 |
| **EE** | **2201.9** | 73.7 | 308.9 | 91.5 | 102.2 | 0.3 | 4.6 | 7.6 | 16.2 | 9.0 | 0.2 | 158.9 | 0.0 | 10.6 |
| **ES** | 0.4 | **49293.8** | 0.4 | 1935.1 | 135.0 | 0.0 | 4.1 | 20.6 | 6.5 | 45.2 | 0.9 | 2271.1 | 0.0 | 0.4 |
| **FI** | 3813.6 | 212.2 | **6684.4** | 278.8 | 407.6 | 0.6 | 11.1 | 20.6 | 49.0 | 33.7 | 1.4 | 483.4 | 0.2 | 49.0 |
| **FR** | 9.4 | 10338.2 | 4.2 | **41071.0** | 2460.7 | 0.0 | 14.3 | 70.7 | 22.3 | 317.0 | 2.9 | 6667.9 | 0.0 | 1.1 |
| **GB** | 9.7 | 1062.2 | 4.2 | 2209.1 | **15784.9** | 0.0 | 0.7 | 2.0 | 7.1 | 1965.3 | 9.0 | 135.9 | 0.0 | 3.6 |
| **GE** | 1.9 | 27.3 | 0.4 | 11.3 | 2.3 | **521.0** | 14.0 | 2.8 | 3.5 | 0.3 | 0.0 | 93.3 | 0.4 | 118.1 |
| **GR** | 3.6 | 234.9 | 1.0 | 158.0 | 8.3 | 2.0 | **2714.7** | 47.8 | 46.8 | 1.2 | 0.0 | 2203.9 | 0.2 | 56.7 |
| **HR** | 5.3 | 470.0 | 1.9 | 350.5 | 22.6 | 0.1 | 23.5 | **1543.1** | 274.4 | 2.4 | 0.1 | 5397.9 | 0.0 | 2.2 |
| **HU** | 10.4 | 370.0 | 3.8 | 361.6 | 46.3 | 0.4 | 35.8 | 424.1 | **1955.9** | 4.7 | 0.1 | 3338.5 | 0.0 | 6.2 |
| **IE** | 1.8 | 277.2 | 0.9 | 265.6 | 535.8 | 0.0 | 0.2 | 0.7 | 1.6 | **3550.5** | 3.8 | 35.6 | 0.0 | 0.3 |
| **IS** | 1.3 | 23.6 | 1.4 | 43.5 | 129.2 | 0.0 | 0.1 | 0.2 | 0.4 | 29.1 | **337.2** | 11.9 | 0.0 | 3.8 |
| **IT** | 4.3 | 2973.5 | 2.4 | 3259.3 | 61.5 | 0.1 | 87.2 | 475.5 | 102.2 | 9.0 | 0.2 | **76845.0** | 0.0 | 5.2 |
| **KY** | 1.3 | 34.5 | 0.3 | 12.8 | 1.7 | 8.9 | 4.9 | 1.5 | 1.2 | 0.2 | 0.0 | 78.7 | **2742.3** | 14933.2 |
| **KZ** | 222.8 | 561.9 | 48.2 | 257.8 | 64.5 | 210.8 | 97.2 | 43.3 | 62.4 | 7.4 | 0.6 | 1566.8 | 2719.6 | **258669.0** |
| **LI** | 0.0 | 1.7 | 0.0 | 4.0 | 0.2 | 0.0 | 0.0 | 0.1 | 0.0 | 0.0 | 0.0 | 17.3 | 0.0 | 0.0 |
| **LT** | 131.9 | 105.8 | 48.6 | 175.9 | 247.1 | 0.3 | 9.7 | 26.0 | 53.5 | 23.2 | 0.3 | 426.2 | 0.0 | 14.1 |
| **LU** | 0.1 | 23.9 | 0.1 | 238.2 | 21.1 | 0.0 | 0.0 | 0.2 | 0.2 | 1.8 | 0.0 | 15.5 | 0.0 | 0.0 |
| **LV** | 498.2 | 96.1 | 122.2 | 148.4 | 199.8 | 0.4 | 9.6 | 18.0 | 38.2 | 19.0 | 0.3 | 326.7 | 0.0 | 21.4 |
| **MC** | 0.0 | 0.2 | 0.0 | 0.7 | 0.0 | 0.0 | 0.0 | 0.0 | 0.0 | 0.0 | 0.0 | 1.1 | 0.0 | 0.0 |
| **MD** | 4.3 | 27.9 | 1.3 | 23.8 | 6.6 | 2.7 | 31.5 | 8.8 | 19.7 | 0.6 | 0.0 | 175.3 | 0.3 | 97.1 |
| **ME** | 0.4 | 60.0 | 0.2 | 44.6 | 2.5 | 0.0 | 18.0 | 30.0 | 20.2 | 0.3 | 0.0 | 994.4 | 0.0 | 1.1 |
| **MK** | 0.7 | 67.9 | 0.3 | 48.0 | 2.7 | 0.4 | 252.4 | 17.9 | 24.1 | 0.4 | 0.0 | 594.8 | 0.0 | 9.7 |
| **MT** | 0.0 | 1.4 | 0.0 | 0.7 | 0.0 | 0.0 | 0.1 | 0.1 | 0.0 | 0.0 | 0.0 | 6.0 | 0.0 | 0.0 |
| **NL** | 4.9 | 185.3 | 2.3 | 1837.1 | 1299.9 | 0.0 | 0.3 | 1.3 | 4.1 | 89.3 | 0.6 | 71.0 | 0.0 | 0.3 |
| **NO** | 150.1 | 389.6 | 119.8 | 630.9 | 1350.7 | 0.5 | 2.1 | 7.8 | 20.8 | 120.1 | 9.9 | 206.8 | 0.2 | 56.5 |
| **PL** | 205.7 | 766.3 | 78.7 | 1788.2 | 1299.5 | 1.8 | 27.8 | 255.9 | 586.0 | 111.6 | 1.9 | 3201.4 | 0.2 | 75.6 |
| **PT** | 0.0 | 2873.4 | 0.0 | 80.2 | 15.2 | 0.0 | 0.1 | 0.6 | 0.2 | 3.1 | 0.1 | 69.1 | 0.0 | 0.1 |
| **RO** | 26.6 | 364.8 | 7.6 | 354.0 | 54.5 | 8.8 | 327.3 | 227.8 | 730.2 | 5.6 | 0.2 | 3496.1 | 0.6 | 223.9 |
| **RS** | 8.1 | 234.0 | 2.9 | 202.1 | 25.4 | 1.3 | 139.3 | 211.9 | 479.6 | 2.4 | 0.1 | 2474.9 | 0.1 | 23.0 |
| **RU** | 17221.8 | 2127.4 | 3883.9 | 1936.0 | 1280.2 | 540.2 | 794.2 | 361.1 | 617.1 | 120.0 | 6.8 | 9936.9 | 778.5 | 203358.0 |
| **SE** | 1042.1 | 514.5 | 1032.5 | 963.9 | 1495.5 | 0.4 | 3.1 | 27.5 | 59.6 | 129.8 | 4.3 | 578.8 | 0.2 | 35.7 |
| **SI** | 1.2 | 186.3 | 0.5 | 176.3 | 11.7 | 0.0 | 5.5 | 411.4 | 63.2 | 1.3 | 0.0 | 3055.6 | 0.0 | 0.7 |
| **SK** | 9.2 | 210.0 | 3.1 | 256.7 | 50.3 | 0.2 | 16.5 | 174.3 | 623.7 | 4.8 | 0.1 | 1582.2 | 0.0 | 4.2 |
| **TJ** | 0.6 | 14.6 | 0.1 | 5.1 | 0.8 | 5.1 | 2.2 | 0.6 | 0.6 | 0.1 | 0.0 | 33.5 | 88.4 | 1263.4 |
| **TM** | 4.2 | 29.1 | 0.8 | 10.6 | 2.1 | 34.7 | 7.2 | 1.6 | 1.9 | 0.3 | 0.0 | 76.7 | 19.7 | 2476.5 |
| **TR** | 33.6 | 599.3 | 7.5 | 275.5 | 31.1 | 135.0 | 845.8 | 61.1 | 78.3 | 3.8 | 0.1 | 2696.0 | 1.7 | 501.1 |
| **UA** | 208.7 | 615.7 | 53.3 | 661.9 | 266.4 | 43.6 | 349.4 | 239.1 | 745.6 | 25.1 | 0.7 | 3894.7 | 4.1 | 1419.4 |
| **UZ** | 8.1 | 37.6 | 1.5 | 15.9 | 3.6 | 35.6 | 9.4 | 2.5 | 2.7 | 0.5 | 0.0 | 118.7 | 234.7 | 7619.2 |
| **SUM,t** | 26.4 | 79.7 | 12.6 | 78.4 | 33.4 | 1.8 | 6.7 | 5.9 | 7.7 | 7.1 | 0.4 | 160.0 | 6.6 | 492.1 |
| **Emiss 2016, t** | 32.5 | 153.0 | 15.9 | 110.8 | 64.4 | 2.5 | 14.7 | 8.0 | 8.9 | 13.4 | 1.7 | 272.1 | 12.2 | 695.9 |
| **code** | **EE** | **ES** | **FI** | **FR** | **GB** | **GE** | **GR** | **HR** | **HU** | **IE** | **IS** | **IT** | **KY** | **KZ** |

***Table 3.2**. Matrix of Pb country-to-country deposition from anthropogenic sources in 2017, kg (continued)*

Receptors ↓ Emitters →

| code | LI | LT | LU | LV | MC | MD | ME | MK | MT | NL | NO | PL | PT |
|---|---|---|---|---|---|---|---|---|---|---|---|---|---|
| **AL** | 0.0 | 0.1 | 0.2 | 0.1 | 0.0 | 1.6 | 126.9 | 78.1 | 4.8 | 0.6 | 0.1 | 112.2 | 8.9 |
| **AM** | 0.0 | 0.0 | 0.0 | 0.0 | 0.0 | 0.6 | 0.4 | 0.4 | 0.2 | 0.1 | 0.0 | 17.1 | 1.3 |
| **AT** | 2.9 | 1.9 | 14.3 | 2.1 | 0.2 | 1.2 | 9.1 | 3.3 | 1.5 | 22.1 | 1.2 | 1491.3 | 50.1 |
| **AZ** | 0.0 | 0.1 | 0.1 | 0.1 | 0.0 | 1.4 | 0.6 | 0.6 | 0.2 | 0.2 | 0.1 | 51.6 | 2.0 |
| **BA** | 0.1 | 0.8 | 2.3 | 0.6 | 0.1 | 4.6 | 204.4 | 14.3 | 4.7 | 5.9 | 0.8 | 1339.3 | 26.4 |
| **BE** | 0.0 | 0.4 | 74.2 | 0.4 | 0.0 | 0.0 | 0.2 | 0.1 | 0.0 | 222.8 | 1.8 | 177.0 | 27.4 |
| **BG** | 0.1 | 2.5 | 1.7 | 1.7 | 0.1 | 104.9 | 55.8 | 106.3 | 5.9 | 5.3 | 0.9 | 1215.1 | 29.6 |
| **BY** | 0.2 | 238.6 | 9.0 | 109.7 | 0.1 | 147.3 | 28.7 | 26.1 | 2.1 | 62.7 | 22.6 | 21995.2 | 33.7 |
| **CH** | 6.0 | 0.1 | 5.7 | 0.1 | 0.3 | 0.1 | 0.7 | 0.3 | 0.4 | 9.1 | 0.4 | 69.3 | 33.9 |
| **CY** | 0.0 | 0.0 | 0.0 | 0.0 | 0.0 | 0.4 | 0.4 | 0.4 | 0.3 | 0.0 | 0.0 | 7.0 | 0.4 |
| **CZ** | 0.6 | 2.3 | 31.1 | 2.2 | 0.1 | 1.9 | 8.0 | 2.7 | 0.8 | 62.2 | 3.1 | 8967.6 | 28.9 |
| **DE** | 4.8 | 12.7 | 598.7 | 14.1 | 0.3 | 2.3 | 4.1 | 2.5 | 0.7 | 2019.5 | 26.7 | 12389.8 | 192.6 |
| **DK** | 0.0 | 5.8 | 8.3 | 4.6 | 0.0 | 0.7 | 0.5 | 0.3 | 0.1 | 157.2 | 19.1 | 1393.2 | 25.4 |
| **EE** | 0.0 | 59.0 | 1.7 | 185.2 | 0.0 | 3.9 | 1.7 | 1.3 | 0.1 | 20.6 | 14.7 | 2074.6 | 9.3 |
| **ES** | 0.1 | 0.1 | 3.6 | 0.1 | 0.2 | 0.4 | 3.6 | 1.2 | 2.8 | 7.5 | 0.7 | 120.8 | 5124.7 |
| **FI** | 0.1 | 66.0 | 3.8 | 128.7 | 0.0 | 8.5 | 4.8 | 3.8 | 0.4 | 60.4 | 112.9 | 5147.4 | 26.1 |
| **FR** | 0.5 | 1.7 | 186.2 | 1.6 | 1.4 | 0.7 | 12.0 | 6.3 | 4.9 | 217.2 | 8.5 | 838.9 | 784.6 |
| **GB** | 0.1 | 3.0 | 15.9 | 2.2 | 0.0 | 0.4 | 0.3 | 0.3 | 0.1 | 243.0 | 15.8 | 685.8 | 236.3 |
| **GE** | 0.0 | 0.3 | 0.1 | 0.2 | 0.0 | 5.0 | 1.7 | 2.0 | 0.4 | 0.4 | 0.2 | 103.2 | 3.7 |
| **GR** | 0.0 | 0.9 | 0.7 | 0.6 | 0.1 | 23.2 | 61.0 | 166.3 | 12.9 | 2.2 | 0.4 | 485.7 | 22.4 |
| **HR** | 0.1 | 0.8 | 2.6 | 0.7 | 0.2 | 3.1 | 62.8 | 12.9 | 4.8 | 5.7 | 0.7 | 1336.4 | 41.4 |
| **HU** | 0.2 | 2.1 | 6.0 | 1.5 | 0.1 | 8.1 | 74.4 | 32.9 | 3.2 | 11.8 | 1.3 | 4548.4 | 37.6 |
| **IE** | 0.0 | 0.3 | 3.2 | 0.3 | 0.0 | 0.1 | 0.1 | 0.1 | 0.0 | 21.8 | 1.9 | 65.0 | 89.0 |
| **IS** | 0.0 | 0.2 | 0.8 | 0.2 | 0.0 | 0.0 | 0.0 | 0.0 | 0.0 | 7.3 | 7.5 | 60.9 | 3.5 |
| **IT** | 1.4 | 0.7 | 6.0 | 0.6 | 2.3 | 4.7 | 96.2 | 31.5 | 25.0 | 11.5 | 1.2 | 1058.7 | 244.2 |
| **KY** | 0.0 | 0.1 | 0.1 | 0.1 | 0.0 | 0.9 | 1.0 | 1.1 | 0.2 | 0.2 | 0.2 | 32.6 | 4.5 |
| **KZ** | 0.1 | 10.3 | 2.3 | 11.8 | 0.1 | 77.3 | 21.3 | 27.1 | 2.8 | 11.7 | 12.4 | 2717.3 | 89.7 |
| **LI** | **0.3** | 0.0 | 0.0 | 0.0 | 0.0 | 0.0 | 0.0 | 0.0 | 0.0 | 0.0 | 0.0 | 0.3 | 0.2 |
| **LT** | 0.1 | **736.5** | 3.6 | 105.5 | 0.0 | 11.3 | 5.3 | 3.4 | 0.4 | 46.6 | 15.2 | 9681.8 | 12.6 |
| **LU** | 0.0 | 0.0 | **107.2** | 0.0 | 0.0 | 0.0 | 0.0 | 0.0 | 0.0 | 7.5 | 0.1 | 16.0 | 2.8 |
| **LV** | 0.0 | 273.1 | 2.9 | **878.3** | 0.0 | 10.9 | 4.3 | 3.0 | 0.3 | 39.3 | 20.0 | 5624.0 | 11.9 |
| **MC** | 0.0 | 0.0 | 0.0 | 0.0 | **0.0** | 0.0 | 0.0 | 0.0 | 0.0 | 0.0 | 0.0 | 0.0 | 0.0 |
| **MD** | 0.0 | 2.3 | 0.4 | 1.3 | 0.0 | **420.1** | 3.8 | 4.6 | 0.6 | 1.6 | 0.6 | 657.3 | 3.4 |
| **ME** | 0.0 | 0.1 | 0.2 | 0.1 | 0.0 | 1.0 | **661.3** | 8.7 | 2.6 | 0.6 | 0.1 | 127.5 | 5.1 |
| **MK** | 0.0 | 0.2 | 0.3 | 0.1 | 0.0 | 4.7 | 36.4 | **478.4** | 2.2 | 0.7 | 0.1 | 154.8 | 8.6 |
| **MT** | 0.0 | 0.0 | 0.0 | 0.0 | 0.0 | 0.0 | 0.0 | 0.0 | **2.1** | 0.0 | 0.0 | 0.2 | 0.1 |
| **NL** | 0.0 | 0.9 | 20.7 | 1.0 | 0.0 | 0.1 | 0.2 | 0.1 | 0.0 | **1602.9** | 3.1 | 474.1 | 20.2 |
| **NO** | 0.1 | 11.4 | 12.6 | 15.9 | 0.0 | 2.6 | 1.2 | 1.1 | 0.1 | 151.3 | **1730.8** | 2412.7 | 72.3 |
| **PL** | 0.7 | 79.0 | 53.1 | 40.6 | 0.2 | 30.2 | 38.3 | 18.0 | 2.4 | 362.4 | 44.3 | **184284.0** | 96.0 |
| **PT** | 0.0 | 0.0 | 0.4 | 0.0 | 0.0 | 0.0 | 0.1 | 0.0 | 0.1 | 1.2 | 0.2 | 11.6 | **7834.8** |
| **RO** | 0.2 | 7.5 | 5.5 | 4.4 | 0.1 | 259.4 | 108.1 | 111.6 | 7.6 | 14.1 | 3.2 | 4431.8 | 46.6 |
| **RS** | 0.1 | 1.9 | 2.4 | 1.3 | 0.1 | 16.0 | 336.7 | 239.1 | 4.2 | 7.4 | 1.1 | 2116.7 | 27.6 |
| **RU** | 0.8 | 379.1 | 27.5 | 577.9 | 0.5 | 634.0 | 154.8 | 177.0 | 16.8 | 234.7 | 287.3 | 39260.8 | 258.5 |
| **SE** | 0.2 | 58.9 | 17.8 | 80.0 | 0.0 | 4.5 | 4.4 | 2.2 | 0.2 | 259.7 | 606.2 | 8328.7 | 79.0 |
| **SI** | 0.1 | 0.1 | 1.5 | 0.1 | 0.1 | 0.7 | 9.0 | 3.5 | 1.2 | 2.7 | 0.2 | 319.5 | 16.5 |
| **SK** | 0.2 | 1.7 | 5.9 | 1.3 | 0.1 | 5.2 | 27.6 | 10.9 | 1.6 | 12.9 | 1.4 | 8136.0 | 23.0 |
| **TJ** | 0.0 | 0.0 | 0.0 | 0.0 | 0.0 | 0.4 | 0.4 | 0.5 | 0.1 | 0.1 | 0.1 | 16.0 | 1.9 |
| **TM** | 0.0 | 0.3 | 0.1 | 0.3 | 0.0 | 2.7 | 0.8 | 1.2 | 0.3 | 0.4 | 0.3 | 100.9 | 3.6 |
| **TR** | 0.1 | 4.5 | 1.9 | 3.7 | 0.1 | 113.7 | 42.5 | 53.1 | 18.3 | 7.1 | 2.2 | 1581.5 | 69.8 |
| **UA** | 0.4 | 63.4 | 14.8 | 38.3 | 0.2 | 926.8 | 75.2 | 76.6 | 8.8 | 66.0 | 20.6 | 30301.5 | 77.4 |
| **UZ** | 0.0 | 0.4 | 0.1 | 0.5 | 0.0 | 3.4 | 1.4 | 1.9 | 0.3 | 0.5 | 0.5 | 111.5 | 4.8 |
| **SUM,t** | 0.0 | 2.0 | 1.3 | 2.2 | 0.0 | 2.9 | 2.3 | 1.7 | 0.1 | 6.0 | 3.0 | 366.7 | 15.9 |
| **Emiss 2016, t** | 0.0 | 2.3 | 1.5 | 2.7 | 0.0 | 3.5 | 3.6 | 2.5 | 0.8 | 8.9 | 5.0 | 418.3 | 40.0 |
| **code** | **LI** | **LT** | **LU** | **LV** | **MC** | **MD** | **ME** | **MK** | **MT** | **NL** | **NO** | **PL** | **PT** |

***Table 3.2**. Matrix of Pb country-to-country deposition from anthropogenic sources in 2017, kg (continued)*

Receptors ↓ Emitters →

| code | RO | RS | RU | SE | SI | SK | TJ | TM | TR | UA | UZ | SUM, t |
|---|---|---|---|---|---|---|---|---|---|---|---|---|
| **AL** | 44.8 | 340.7 | 10.8 | 0.2 | 8.4 | 50.0 | 0.0 | 0.2 | 146.3 | 21.0 | 0.2 | 4.13 |
| **AM** | 5.9 | 3.2 | 24.8 | 0.1 | 0.5 | 2.7 | 0.3 | 52.0 | 365.4 | 17.6 | 18.2 | 1.80 |
| **AT** | 60.3 | 160.3 | 14.6 | 2.7 | 740.0 | 897.5 | 0.0 | 0.1 | 16.8 | 15.6 | 0.1 | 24.75 |
| **AZ** | 13.4 | 5.5 | 115.6 | 0.2 | 0.9 | 6.0 | 6.0 | 207.3 | 323.4 | 46.9 | 100.8 | 2.27 |
| **BA** | 250.5 | 1386.5 | 27.1 | 1.9 | 101.4 | 824.8 | 0.1 | 0.3 | 127.2 | 49.4 | 0.4 | 20.85 |
| **BE** | 1.5 | 2.7 | 3.2 | 2.3 | 2.4 | 14.7 | 0.0 | 0.0 | 1.2 | 0.8 | 0.0 | 10.83 |
| **BG** | 3083.2 | 2291.4 | 572.4 | 2.1 | 48.0 | 515.7 | 2.2 | 31.2 | 7421.7 | 1119.0 | 25.7 | 46.17 |
| **BY** | 850.8 | 550.0 | 2382.5 | 70.6 | 71.4 | 1113.5 | 2.5 | 27.5 | 1905.6 | 2041.0 | 23.2 | 43.11 |
| **CH** | 1.6 | 5.1 | 1.0 | 0.6 | 17.9 | 15.2 | 0.0 | 0.0 | 2.3 | 0.9 | 0.0 | 13.70 |
| **CY** | 4.6 | 2.7 | 4.0 | 0.0 | 0.3 | 1.4 | 0.0 | 0.1 | 514.6 | 6.2 | 0.1 | 2.31 |
| **CZ** | 78.8 | 293.6 | 27.2 | 6.8 | 160.0 | 2106.5 | 0.0 | 0.3 | 18.9 | 28.1 | 0.2 | 29.96 |
| **DE** | 58.1 | 106.4 | 132.1 | 51.6 | 103.1 | 624.7 | 0.1 | 1.6 | 32.3 | 54.9 | 1.2 | 158.10 |
| **DK** | 7.5 | 14.8 | 36.1 | 41.6 | 5.6 | 57.5 | 0.0 | 0.2 | 2.3 | 11.1 | 0.3 | 7.58 |
| **EE** | 32.9 | 39.8 | 288.8 | 73.9 | 7.8 | 92.8 | 0.1 | 2.0 | 101.0 | 56.6 | 1.1 | 6.94 |
| **ES** | 7.8 | 18.1 | 3.3 | 0.9 | 22.1 | 33.9 | 0.0 | 0.1 | 16.6 | 3.4 | 0.1 | 59.56 |
| **FI** | 81.6 | 100.9 | 1726.8 | 1333.8 | 23.7 | 304.6 | 0.8 | 5.4 | 208.6 | 129.7 | 5.4 | 23.71 |
| **FR** | 25.3 | 101.5 | 23.1 | 10.2 | 76.4 | 113.8 | 0.0 | 0.2 | 70.8 | 11.0 | 0.2 | 72.42 |
| **GB** | 9.0 | 9.3 | 41.6 | 14.7 | 3.2 | 48.0 | 0.1 | 0.3 | 8.2 | 9.8 | 0.5 | 25.10 |
| **GE** | 58.8 | 24.4 | 163.6 | 0.4 | 2.4 | 16.1 | 1.0 | 59.8 | 918.0 | 155.7 | 26.5 | 2.83 |
| **GR** | 339.5 | 652.0 | 197.3 | 0.9 | 24.3 | 167.2 | 0.8 | 6.8 | 7511.4 | 336.2 | 6.4 | 19.01 |
| **HR** | 192.4 | 824.1 | 23.0 | 1.9 | 474.3 | 791.8 | 0.0 | 0.2 | 83.6 | 36.4 | 0.2 | 15.34 |
| **HU** | 519.2 | 1984.5 | 100.4 | 3.6 | 310.3 | 4868.0 | 0.0 | 1.2 | 192.8 | 108.6 | 0.7 | 24.18 |
| **IE** | 1.8 | 3.2 | 4.5 | 2.1 | 1.2 | 7.9 | 0.0 | 0.0 | 1.4 | 1.1 | 0.0 | 5.23 |
| **IS** | 0.7 | 0.9 | 11.1 | 3.8 | 0.3 | 3.1 | 0.0 | 0.1 | 1.3 | 1.3 | 0.2 | 0.82 |
| **IT** | 155.8 | 442.5 | 34.2 | 2.3 | 511.3 | 424.2 | 0.1 | 0.6 | 285.1 | 59.9 | 0.6 | 91.83 |
| **KY** | 9.8 | 9.0 | 81.6 | 0.3 | 1.4 | 5.9 | 6773.0 | 461.8 | 170.9 | 27.5 | 26870.1 | 52.41 |
| **KZ** | 661.8 | 291.8 | 14525.9 | 30.2 | 44.0 | 324.3 | 7382.5 | 5362.4 | 3222.4 | 3135.7 | 37822.5 | 343.59 |
| **LI** | 0.0 | 0.0 | 0.0 | 0.0 | 0.1 | 0.1 | 0.0 | 0.0 | 0.0 | 0.0 | 0.0 | 0.06 |
| **LT** | 107.9 | 132.2 | 449.3 | 62.5 | 27.7 | 334.5 | 0.1 | 1.9 | 118.0 | 136.2 | 1.2 | 15.80 |
| **LU** | 0.2 | 0.3 | 0.2 | 0.1 | 0.3 | 1.6 | 0.0 | 0.0 | 0.1 | 0.1 | 0.0 | 0.73 |
| **LV** | 89.3 | 106.3 | 455.1 | 88.9 | 18.1 | 227.9 | 0.2 | 2.5 | 195.5 | 130.5 | 1.6 | 11.58 |
| **MC** | 0.0 | 0.0 | 0.0 | 0.0 | 0.0 | 0.0 | 0.0 | 0.0 | 0.0 | 0.0 | 0.0 | 0.00 |
| **MD** | 416.4 | 65.9 | 327.5 | 1.9 | 8.1 | 83.5 | 0.8 | 10.7 | 966.3 | 747.4 | 9.5 | 4.56 |
| **ME** | 34.3 | 326.0 | 5.4 | 0.2 | 9.0 | 69.9 | 0.0 | 0.1 | 53.8 | 11.1 | 0.1 | 3.24 |
| **MK** | 113.8 | 589.3 | 24.3 | 0.3 | 9.4 | 79.0 | 0.1 | 1.2 | 591.9 | 50.9 | 0.9 | 4.70 |
| **MT** | 0.0 | 0.1 | 0.1 | 0.0 | 0.0 | 0.1 | 0.0 | 0.0 | 0.6 | 0.1 | 0.0 | 0.01 |
| **NL** | 3.3 | 4.0 | 20.2 | 4.6 | 2.4 | 27.8 | 0.0 | 0.0 | 2.6 | 3.0 | 0.0 | 10.94 |
| **NO** | 26.5 | 41.8 | 367.7 | 400.9 | 9.3 | 132.0 | 1.2 | 4.0 | 45.9 | 58.4 | 6.1 | 11.72 |
| **PL** | 463.5 | 1074.4 | 850.4 | 132.1 | 268.1 | 5195.4 | 0.5 | 13.0 | 156.3 | 568.5 | 9.4 | 230.05 |
| **PT** | 0.2 | 0.4 | 0.2 | 0.2 | 0.9 | 1.1 | 0.0 | 0.0 | 1.1 | 0.1 | 0.0 | 10.94 |
| **RO** | **12528.5** | 3040.4 | 966.3 | 8.3 | 178.1 | 1927.2 | 1.8 | 40.2 | 5843.7 | 1995.5 | 31.0 | 45.12 |
| **RS** | 998.0 | **10622.4** | 106.0 | 2.6 | 80.3 | 1282.7 | 0.2 | 2.9 | 818.0 | 175.2 | 2.3 | 25.85 |
| **RU** | 4581.1 | 2531.7 | **235303.0** | 1161.6 | 347.4 | 3127.3 | 2894.8 | 4639.3 | 24000.9 | 28501.3 | 13328.7 | 629.05 |
| **SE** | 58.6 | 111.7 | 801.4 | **3865.5** | 31.2 | 375.4 | 0.6 | 4.5 | 67.8 | 88.2 | 4.3 | 29.11 |
| **SI** | 52.4 | 126.4 | 4.4 | 0.5 | **1413.5** | 176.2 | 0.0 | 0.0 | 15.1 | 8.6 | 0.0 | 7.22 |
| **SK** | 219.2 | 747.2 | 82.5 | 3.8 | 156.9 | **8975.6** | 0.0 | 0.7 | 68.7 | 80.5 | 0.4 | 25.42 |
| **TJ** | 4.2 | 3.5 | 30.4 | 0.1 | 0.6 | 3.0 | **14739.1** | 427.4 | 85.7 | 12.1 | 5664.1 | 22.47 |
| **TM** | 27.2 | 9.5 | 270.5 | 0.7 | 1.7 | 9.1 | 741.4 | **4845.8** | 325.5 | 95.7 | 3564.2 | 12.96 |
| **TR** | 1263.8 | 632.6 | 1751.4 | 5.9 | 45.5 | 314.1 | 5.0 | 154.0 | **106050.0** | 2232.2 | 95.1 | 128.31 |
| **UA** | 4127.7 | 1734.7 | 8425.4 | 61.8 | 226.2 | 3510.0 | 21.8 | 211.3 | 11557.0 | **30862.7** | 210.1 | 111.83 |
| **UZ** | 36.4 | 15.6 | 394.4 | 1.1 | 2.6 | 13.0 | 5193.7 | 2002.2 | 393.0 | 129.9 | **28418.3** | 45.16 |
| **SUM,t** | 31.7 | 31.6 | 271.2 | 7.5 | 5.6 | 39.3 | 37.8 | 18.6 | 175.0 | 73.4 | 116.3 | |
| **Emiss 2016, t** | 39.0 | 38.6 | 328.3 | 10.9 | 7.0 | 44.6 | 63.7 | 39.0 | 343.0 | 85.5 | 184.8 | |
| **code** | **RO** | **RS** | **RU** | **SE** | **SI** | **SK** | **TJ** | **TM** | **TR** | **UA** | **UZ** | |

***Table 3.3**. Matrix of Cd country-to-country deposition from anthropogenic sources in 2017, kg*

Receptors ↓ Emitters →

| code | AL | AM | AT | AZ | BA | BE | BG | BY | CH | CY | CZ | DE | DK |
|---|---|---|---|---|---|---|---|---|---|---|---|---|---|
| **AL** | **36.2** | 0.0 | 1.1 | 0.0 | 6.2 | 0.2 | 5.6 | 0.1 | 0.7 | 0.0 | 0.6 | 2.5 | 0.0 |
| **AM** | 0.0 | **30.0** | 0.1 | 5.0 | 0.1 | 0.0 | 0.2 | 0.0 | 0.1 | 0.1 | 0.0 | 0.2 | 0.0 |
| **AT** | 0.3 | 0.0 | **324.0** | 0.0 | 7.8 | 7.9 | 1.6 | 0.3 | 61.6 | 0.0 | 35.3 | 360.0 | 0.6 |
| **AZ** | 0.0 | 9.2 | 0.1 | **23.5** | 0.2 | 0.1 | 0.4 | 0.1 | 0.1 | 0.1 | 0.1 | 0.6 | 0.0 |
| **BA** | 3.1 | 0.0 | 18.4 | 0.0 | **464.0** | 1.8 | 7.1 | 0.3 | 3.9 | 0.0 | 9.7 | 29.0 | 0.3 |
| **BE** | 0.0 | 0.0 | 0.9 | 0.0 | 0.1 | **512.0** | 0.1 | 0.1 | 3.1 | 0.0 | 0.9 | 85.2 | 0.4 |
| **BG** | 3.4 | 0.3 | 8.5 | 0.3 | 21.2 | 1.6 | **640.0** | 1.5 | 3.1 | 0.1 | 4.9 | 20.8 | 0.3 |
| **BY** | 1.2 | 0.2 | 16.0 | 0.3 | 15.0 | 13.6 | 20.0 | **265.0** | 6.5 | 0.0 | 25.4 | 136.0 | 9.1 |
| **CH** | 0.0 | 0.0 | 4.6 | 0.0 | 0.4 | 3.5 | 0.1 | 0.0 | **291.0** | 0.0 | 0.7 | 74.3 | 0.1 |
| **CY** | 0.0 | 0.0 | 0.0 | 0.0 | 0.1 | 0.0 | 0.3 | 0.0 | 0.0 | **1.8** | 0.0 | 0.1 | 0.0 |
| **CZ** | 0.2 | 0.0 | 78.6 | 0.0 | 10.6 | 21.3 | 1.5 | 0.6 | 20.9 | 0.0 | **330.0** | 521.0 | 1.8 |
| **DE** | 0.1 | 0.0 | 71.9 | 0.0 | 3.4 | 612.0 | 1.5 | 2.4 | 206.0 | 0.0 | 73.3 | **6100.0** | 23.5 |
| **DK** | 0.0 | 0.0 | 1.9 | 0.0 | 0.5 | 28.5 | 0.1 | 0.6 | 1.9 | 0.0 | 2.4 | 127.0 | **125.0** |
| **EE** | 0.1 | 0.0 | 1.8 | 0.0 | 1.2 | 3.9 | 0.8 | 4.8 | 1.2 | 0.0 | 2.4 | 28.6 | 4.5 |
| **ES** | 0.1 | 0.0 | 1.6 | 0.0 | 1.8 | 5.0 | 0.3 | 0.0 | 3.8 | 0.0 | 0.7 | 13.2 | 0.1 |
| **FI** | 0.2 | 0.0 | 5.8 | 0.0 | 3.3 | 11.0 | 2.2 | 8.4 | 4.4 | 0.0 | 7.4 | 67.7 | 10.7 |
| **FR** | 0.6 | 0.0 | 9.4 | 0.0 | 7.0 | 186.0 | 1.7 | 0.2 | 82.4 | 0.0 | 5.6 | 301.0 | 1.4 |
| **GB** | 0.0 | 0.0 | 1.9 | 0.0 | 0.2 | 68.0 | 0.4 | 0.4 | 3.2 | 0.0 | 1.9 | 93.6 | 3.7 |
| **GE** | 0.1 | 15.0 | 0.3 | 3.9 | 0.7 | 0.1 | 2.1 | 0.2 | 0.2 | 0.2 | 0.2 | 1.1 | 0.0 |
| **GR** | 8.4 | 0.1 | 3.4 | 0.1 | 12.1 | 0.7 | 66.7 | 0.5 | 2.0 | 0.2 | 1.9 | 8.7 | 0.1 |
| **HR** | 2.0 | 0.0 | 34.0 | 0.0 | 78.4 | 2.0 | 5.7 | 0.3 | 5.1 | 0.0 | 11.4 | 35.0 | 0.3 |
| **HU** | 2.5 | 0.0 | 78.6 | 0.0 | 59.2 | 3.9 | 11.7 | 1.1 | 8.1 | 0.0 | 29.3 | 77.1 | 0.6 |
| **IE** | 0.0 | 0.0 | 0.6 | 0.0 | 0.0 | 7.8 | 0.1 | 0.0 | 0.9 | 0.0 | 0.3 | 13.5 | 0.3 |
| **IS** | 0.0 | 0.0 | 0.1 | 0.0 | 0.0 | 1.7 | 0.0 | 0.0 | 0.2 | 0.0 | 0.1 | 5.5 | 0.4 |
| **IT** | 5.7 | 0.0 | 33.4 | 0.0 | 46.2 | 4.2 | 7.9 | 0.2 | 55.4 | 0.0 | 7.6 | 73.3 | 0.4 |
| **KY** | 0.0 | 0.9 | 0.1 | 0.8 | 0.3 | 0.1 | 0.4 | 0.0 | 0.2 | 0.1 | 0.1 | 0.7 | 0.0 |
| **KZ** | 1.1 | 19.5 | 6.4 | 19.5 | 9.2 | 3.0 | 18.3 | 5.7 | 4.9 | 0.7 | 5.2 | 31.3 | 1.4 |
| **LI** | 0.0 | 0.0 | 0.1 | 0.0 | 0.0 | 0.0 | 0.0 | 0.0 | 1.6 | 0.0 | 0.0 | 0.5 | 0.0 |
| **LT** | 0.2 | 0.0 | 5.9 | 0.0 | 3.7 | 8.9 | 2.2 | 28.9 | 2.5 | 0.0 | 9.0 | 74.7 | 10.7 |
| **LU** | 0.0 | 0.0 | 0.1 | 0.0 | 0.0 | 8.9 | 0.0 | 0.0 | 0.7 | 0.0 | 0.1 | 12.0 | 0.0 |
| **LV** | 0.2 | 0.0 | 4.1 | 0.0 | 2.9 | 7.0 | 2.0 | 14.6 | 2.0 | 0.0 | 6.0 | 57.5 | 9.6 |
| **MC** | 0.0 | 0.0 | 0.0 | 0.0 | 0.0 | 0.0 | 0.0 | 0.0 | 0.0 | 0.0 | 0.0 | 0.0 | 0.0 |
| **MD** | 0.2 | 0.1 | 1.5 | 0.1 | 1.6 | 0.4 | 5.4 | 1.6 | 0.6 | 0.0 | 0.9 | 5.4 | 0.2 |
| **ME** | 6.1 | 0.0 | 1.3 | 0.0 | 20.3 | 0.2 | 2.6 | 0.0 | 0.5 | 0.0 | 0.8 | 2.6 | 0.0 |
| **MK** | 7.6 | 0.0 | 1.4 | 0.0 | 5.4 | 0.2 | 20.9 | 0.1 | 0.7 | 0.0 | 0.7 | 3.1 | 0.0 |
| **MT** | 0.0 | 0.0 | 0.0 | 0.0 | 0.0 | 0.0 | 0.0 | 0.0 | 0.0 | 0.0 | 0.0 | 0.0 | 0.0 |
| **NL** | 0.0 | 0.0 | 1.2 | 0.0 | 0.1 | 326.0 | 0.1 | 0.2 | 2.6 | 0.0 | 1.4 | 154.0 | 1.1 |
| **NO** | 0.0 | 0.0 | 3.2 | 0.0 | 1.1 | 30.7 | 0.6 | 1.6 | 3.2 | 0.0 | 4.4 | 114.0 | 24.1 |
| **PL** | 1.1 | 0.1 | 75.9 | 0.1 | 32.1 | 83.5 | 7.5 | 28.6 | 25.8 | 0.0 | 223.0 | 1070.0 | 35.9 |
| **PT** | 0.0 | 0.0 | 0.1 | 0.0 | 0.0 | 0.6 | 0.0 | 0.0 | 0.3 | 0.0 | 0.1 | 1.5 | 0.0 |
| **RO** | 5.5 | 0.5 | 34.5 | 0.4 | 55.8 | 4.4 | 112.0 | 4.2 | 10.2 | 0.1 | 15.3 | 73.1 | 1.2 |
| **RS** | 8.3 | 0.1 | 18.7 | 0.0 | 81.7 | 2.0 | 42.3 | 0.9 | 4.0 | 0.0 | 10.9 | 33.7 | 0.4 |
| **RU** | 8.3 | 33.7 | 59.0 | 36.3 | 76.6 | 49.7 | 139.0 | 186.0 | 36.7 | 1.6 | 60.7 | 416.0 | 37.9 |
| **SE** | 0.2 | 0.0 | 9.2 | 0.0 | 3.8 | 46.6 | 1.2 | 6.7 | 8.7 | 0.0 | 15.3 | 278.0 | 125.0 |
| **SI** | 0.3 | 0.0 | 33.8 | 0.0 | 6.7 | 1.0 | 1.6 | 0.0 | 3.2 | 0.0 | 3.5 | 20.7 | 0.1 |
| **SK** | 0.8 | 0.0 | 58.1 | 0.0 | 25.3 | 4.2 | 4.7 | 0.8 | 7.4 | 0.0 | 53.1 | 81.2 | 0.8 |
| **TJ** | 0.0 | 0.5 | 0.1 | 0.4 | 0.1 | 0.0 | 0.2 | 0.0 | 0.1 | 0.0 | 0.0 | 0.3 | 0.0 |
| **TM** | 0.0 | 3.8 | 0.2 | 4.3 | 0.3 | 0.1 | 0.7 | 0.1 | 0.2 | 0.1 | 0.2 | 1.1 | 0.0 |
| **TR** | 2.9 | 22.4 | 6.6 | 4.2 | 12.9 | 1.9 | 61.6 | 3.0 | 4.0 | 8.4 | 4.2 | 22.5 | 0.6 |
| **UA** | 3.7 | 1.9 | 49.3 | 1.9 | 44.0 | 17.4 | 76.0 | 52.4 | 15.0 | 0.3 | 45.6 | 208.0 | 7.9 |
| **UZ** | 0.1 | 3.8 | 0.3 | 3.7 | 0.5 | 0.1 | 1.1 | 0.2 | 0.3 | 0.2 | 0.2 | 1.3 | 0.1 |
| **SUM** | 111.3 | 142.2 | 1068.0 | 105.0 | 1124.1 | 2093.7 | 1278.1 | 622.6 | 900.9 | 14.0 | 1012.8 | 10838.2 | 440.8 |
| **Emiss 2016** | 194.0 | 208.5 | 1241.1 | 170.0 | 1485.4 | 2767.5 | 1686.7 | 667.0 | 1092.4 | 52.7 | 1132.6 | 12921.0 | 723.6 |
| **code** | **AL** | **AM** | **AT** | **AZ** | **BA** | **BE** | **BG** | **BY** | **CH** | **CY** | **CZ** | **DE** | **DK** |

***Table 3.3**. Matrix of Cd country-to-country deposition from anthropogenic sources in 2017, kg (continued)*

Receptors ↓ Emitters →

| code | EE | ES | FI | FR | GB | GE | GR | HR | HU | IE | IS | IT | KY | KZ |
|---|---|---|---|---|---|---|---|---|---|---|---|---|---|---|
| **AL** | 0.0 | 4.0 | 0.0 | 2.7 | 0.1 | 0.0 | 19.7 | 1.6 | 2.2 | 0.0 | 0.0 | 45.0 | 0.0 | 0.0 |
| **AM** | 0.0 | 0.4 | 0.0 | 0.1 | 0.0 | 6.8 | 0.5 | 0.0 | 0.1 | 0.0 | 0.0 | 1.0 | 0.0 | 1.2 |
| **AT** | 0.4 | 19.5 | 0.3 | 25.6 | 4.5 | 0.0 | 0.6 | 20.4 | 22.3 | 0.2 | 0.0 | 73.2 | 0.0 | 0.0 |
| **AZ** | 0.0 | 0.7 | 0.0 | 0.2 | 0.0 | 9.5 | 0.7 | 0.1 | 0.2 | 0.0 | 0.0 | 1.4 | 0.0 | 7.2 |
| **BA** | 0.1 | 11.3 | 0.1 | 8.3 | 1.0 | 0.0 | 4.1 | 56.5 | 40.0 | 0.0 | 0.0 | 81.2 | 0.0 | 0.1 |
| **BE** | 0.1 | 9.4 | 0.1 | 97.5 | 42.7 | 0.0 | 0.0 | 0.1 | 0.3 | 1.1 | 0.0 | 1.4 | 0.0 | 0.0 |
| **BG** | 0.2 | 9.7 | 0.1 | 4.9 | 0.8 | 0.7 | 74.4 | 7.3 | 24.1 | 0.0 | 0.0 | 45.6 | 0.0 | 2.4 |
| **BY** | 9.2 | 11.8 | 4.0 | 11.7 | 13.2 | 0.5 | 12.5 | 8.3 | 28.6 | 0.6 | 0.0 | 31.7 | 0.0 | 3.6 |
| **CH** | 0.0 | 15.8 | 0.0 | 32.1 | 2.3 | 0.0 | 0.1 | 1.0 | 0.3 | 0.1 | 0.0 | 63.6 | 0.0 | 0.0 |
| **CY** | 0.0 | 0.2 | 0.0 | 0.1 | 0.0 | 0.0 | 1.5 | 0.0 | 0.0 | 0.0 | 0.0 | 1.4 | 0.0 | 0.0 |
| **CZ** | 0.4 | 11.7 | 0.3 | 23.4 | 10.8 | 0.0 | 0.4 | 14.2 | 34.4 | 0.4 | 0.0 | 23.6 | 0.0 | 0.0 |
| **DE** | 2.0 | 69.9 | 1.9 | 330.0 | 210.0 | 0.0 | 0.7 | 5.5 | 12.1 | 7.1 | 0.1 | 56.9 | 0.0 | 0.2 |
| **DK** | 0.5 | 5.6 | 0.4 | 13.0 | 35.3 | 0.0 | 0.0 | 0.5 | 1.2 | 1.3 | 0.0 | 1.9 | 0.0 | 0.0 |
| **EE** | **123.0** | 2.9 | 16.0 | 2.5 | 4.7 | 0.0 | 0.6 | 0.9 | 2.5 | 0.2 | 0.0 | 2.9 | 0.0 | 0.2 |
| **ES** | 0.0 | **2250.0** | 0.0 | 52.5 | 7.6 | 0.0 | 0.5 | 1.7 | 0.9 | 1.1 | 0.0 | 30.9 | 0.0 | 0.0 |
| **FI** | 101.0 | 8.3 | **467.0** | 7.9 | 18.6 | 0.1 | 1.4 | 2.5 | 7.5 | 0.7 | 0.0 | 8.7 | 0.0 | 0.7 |
| **FR** | 0.2 | 425.0 | 0.2 | **1150.0** | 145.0 | 0.0 | 2.0 | 7.1 | 3.4 | 7.1 | 0.1 | 128.0 | 0.0 | 0.0 |
| **GB** | 0.2 | 46.3 | 0.2 | 62.3 | **990.0** | 0.0 | 0.1 | 0.2 | 1.2 | 43.2 | 0.2 | 2.2 | 0.0 | 0.0 |
| **GE** | 0.0 | 1.2 | 0.0 | 0.4 | 0.1 | **64.8** | 1.9 | 0.3 | 0.5 | 0.0 | 0.0 | 2.6 | 0.0 | 1.8 |
| **GR** | 0.1 | 9.8 | 0.1 | 5.6 | 0.4 | 0.2 | **379.0** | 3.8 | 7.3 | 0.0 | 0.0 | 92.5 | 0.0 | 0.8 |
| **HR** | 0.1 | 18.8 | 0.1 | 13.4 | 1.1 | 0.0 | 3.0 | **192.0** | 51.6 | 0.0 | 0.0 | 108.0 | 0.0 | 0.0 |
| **HU** | 0.2 | 14.8 | 0.2 | 11.2 | 2.2 | 0.0 | 4.7 | 57.2 | **379.0** | 0.1 | 0.0 | 63.4 | 0.0 | 0.1 |
| **IE** | 0.0 | 12.7 | 0.1 | 6.8 | 35.9 | 0.0 | 0.0 | 0.1 | 0.3 | **69.5** | 0.1 | 0.7 | 0.0 | 0.0 |
| **IS** | 0.0 | 0.9 | 0.1 | 1.3 | 5.9 | 0.0 | 0.0 | 0.0 | 0.1 | 0.6 | **10.0** | 0.3 | 0.0 | 0.1 |
| **IT** | 0.1 | 116.0 | 0.1 | 120.0 | 2.9 | 0.0 | 12.1 | 41.4 | 16.1 | 0.2 | 0.0 | **1380.0** | 0.0 | 0.1 |
| **KY** | 0.0 | 1.4 | 0.0 | 0.4 | 0.1 | 0.7 | 0.6 | 0.1 | 0.1 | 0.0 | 0.0 | 1.7 | **88.6** | 230.0 |
| **KZ** | 3.9 | 23.4 | 2.2 | 7.7 | 2.9 | 19.0 | 12.2 | 3.8 | 8.8 | 0.2 | 0.0 | 31.9 | 82.3 | **4040.0** |
| **LI** | 0.0 | 0.1 | 0.0 | 0.1 | 0.0 | 0.0 | 0.0 | 0.0 | 0.0 | 0.0 | 0.0 | 0.2 | 0.0 | 0.0 |
| **LT** | 3.6 | 4.4 | 2.4 | 5.2 | 11.1 | 0.0 | 1.3 | 2.8 | 8.2 | 0.5 | 0.0 | 7.6 | 0.0 | 0.2 |
| **LU** | 0.0 | 1.0 | 0.0 | 7.5 | 1.3 | 0.0 | 0.0 | 0.0 | 0.0 | 0.0 | 0.0 | 0.2 | 0.0 | 0.0 |
| **LV** | 16.9 | 3.9 | 6.0 | 4.3 | 9.0 | 0.0 | 1.3 | 2.0 | 6.0 | 0.4 | 0.0 | 6.0 | 0.0 | 0.3 |
| **MC** | 0.0 | 0.0 | 0.0 | 0.0 | 0.0 | 0.0 | 0.0 | 0.0 | 0.0 | 0.0 | 0.0 | 0.0 | 0.0 | 0.0 |
| **MD** | 0.1 | 1.2 | 0.1 | 0.7 | 0.3 | 0.3 | 4.3 | 0.9 | 3.0 | 0.0 | 0.0 | 4.7 | 0.0 | 1.4 |
| **ME** | 0.0 | 2.5 | 0.0 | 1.6 | 0.1 | 0.0 | 2.5 | 2.2 | 3.2 | 0.0 | 0.0 | 31.4 | 0.0 | 0.0 |
| **MK** | 0.0 | 2.9 | 0.0 | 1.7 | 0.1 | 0.0 | 38.3 | 1.5 | 3.7 | 0.0 | 0.0 | 18.8 | 0.0 | 0.1 |
| **MT** | 0.0 | 0.1 | 0.0 | 0.0 | 0.0 | 0.0 | 0.0 | 0.0 | 0.0 | 0.0 | 0.0 | 0.7 | 0.0 | 0.0 |
| **NL** | 0.1 | 7.6 | 0.1 | 62.0 | 75.8 | 0.0 | 0.0 | 0.2 | 0.6 | 2.0 | 0.0 | 1.2 | 0.0 | 0.0 |
| **NO** | 3.7 | 16.4 | 6.6 | 17.4 | 62.5 | 0.1 | 0.3 | 0.9 | 3.1 | 2.6 | 0.3 | 3.5 | 0.0 | 0.8 |
| **PL** | 4.7 | 31.8 | 3.7 | 50.7 | 62.1 | 0.2 | 3.8 | 28.0 | 93.6 | 2.4 | 0.0 | 57.0 | 0.0 | 1.1 |
| **PT** | 0.0 | 171.0 | 0.0 | 2.2 | 0.8 | 0.0 | 0.0 | 0.1 | 0.0 | 0.1 | 0.0 | 1.2 | 0.0 | 0.0 |
| **RO** | 0.6 | 15.9 | 0.4 | 11.3 | 2.6 | 0.9 | 44.8 | 26.6 | 131.0 | 0.1 | 0.0 | 85.7 | 0.0 | 3.2 |
| **RS** | 0.2 | 9.9 | 0.1 | 7.0 | 1.2 | 0.1 | 19.9 | 25.8 | 80.9 | 0.0 | 0.0 | 56.3 | 0.0 | 0.3 |
| **RU** | 361.0 | 88.4 | 217.0 | 58.9 | 58.0 | 60.7 | 105.0 | 38.5 | 95.2 | 2.5 | 0.2 | 205.0 | 27.4 | 2980.0 |
| **SE** | 24.5 | 21.0 | 59.8 | 26.9 | 70.7 | 0.0 | 0.5 | 3.5 | 9.3 | 2.8 | 0.1 | 9.8 | 0.0 | 0.5 |
| **SI** | 0.0 | 7.5 | 0.0 | 6.5 | 0.5 | 0.0 | 0.7 | 44.5 | 11.1 | 0.0 | 0.0 | 49.0 | 0.0 | 0.0 |
| **SK** | 0.2 | 8.6 | 0.1 | 7.8 | 2.4 | 0.0 | 2.2 | 20.3 | 115.0 | 0.1 | 0.0 | 31.0 | 0.0 | 0.1 |
| **TJ** | 0.0 | 0.6 | 0.0 | 0.2 | 0.0 | 0.5 | 0.3 | 0.0 | 0.1 | 0.0 | 0.0 | 0.7 | 4.0 | 19.5 |
| **TM** | 0.1 | 1.3 | 0.0 | 0.3 | 0.1 | 3.2 | 1.0 | 0.1 | 0.3 | 0.0 | 0.0 | 2.1 | 0.8 | 40.3 |
| **TR** | 0.7 | 25.2 | 0.4 | 9.3 | 1.4 | 10.1 | 124.0 | 5.4 | 11.8 | 0.1 | 0.0 | 102.0 | 0.0 | 6.9 |
| **UA** | 4.6 | 25.9 | 2.7 | 19.8 | 12.4 | 5.9 | 47.2 | 27.0 | 129.0 | 0.5 | 0.0 | 88.8 | 0.2 | 21.3 |
| **UZ** | 0.1 | 1.6 | 0.1 | 0.5 | 0.2 | 3.2 | 1.2 | 0.2 | 0.4 | 0.0 | 0.0 | 2.9 | 12.2 | 130.0 |
| **SUM** | 663.0 | 3549.9 | 792.9 | 2293.3 | 1910.7 | 187.8 | 931.9 | 657.1 | 1350.4 | 147.9 | 11.3 | 3047.6 | 215.7 | 7494.6 |
| **Emiss 2016** | 809.4 | 7037.9 | 976.2 | 3345.8 | 3493.1 | 255.0 | 2000.3 | 845.7 | 1517.6 | 284.3 | 44.6 | 6792.2 | 448.0 | 10453.2 |
| **code** | **EE** | **ES** | **FI** | **FR** | **GB** | **GE** | **GR** | **HR** | **HU** | **IE** | **IS** | **IT** | **KY** | **KZ** |

***Table 3.3**. Matrix of Cd country-to-country deposition from anthropogenic sources in 2017, kg (continued)*

Receptors ↓ Emitters →

| code | LI | LT | LU | LV | MC | MD | ME | MK | MT | NL | NO | PL | PT |
|---|---|---|---|---|---|---|---|---|---|---|---|---|---|
| **AL** | 0.0 | 0.0 | 0.0 | 0.0 | 0.0 | 0.1 | 1.3 | 4.5 | 0.0 | 0.0 | 0.0 | 3.1 | 0.8 |
| **AM** | 0.0 | 0.0 | 0.0 | 0.0 | 0.0 | 0.0 | 0.0 | 0.0 | 0.0 | 0.0 | 0.0 | 0.5 | 0.1 |
| **AT** | 0.5 | 0.2 | 0.7 | 0.3 | 0.0 | 0.1 | 0.2 | 0.2 | 0.0 | 1.6 | 0.1 | 32.2 | 3.6 |
| **AZ** | 0.0 | 0.0 | 0.0 | 0.0 | 0.0 | 0.1 | 0.0 | 0.0 | 0.0 | 0.0 | 0.0 | 1.5 | 0.2 |
| **BA** | 0.0 | 0.1 | 0.1 | 0.1 | 0.0 | 0.3 | 5.2 | 0.7 | 0.0 | 0.4 | 0.1 | 35.0 | 2.0 |
| **BE** | 0.0 | 0.0 | 4.7 | 0.1 | 0.0 | 0.0 | 0.0 | 0.0 | 0.0 | 19.8 | 0.2 | 4.2 | 2.0 |
| **BG** | 0.0 | 0.3 | 0.1 | 0.3 | 0.0 | 6.4 | 1.4 | 5.7 | 0.0 | 0.4 | 0.1 | 36.4 | 2.4 |
| **BY** | 0.0 | 35.7 | 0.5 | 23.9 | 0.0 | 9.2 | 0.8 | 1.3 | 0.0 | 4.0 | 2.1 | 819.0 | 2.6 |
| **CH** | 1.1 | 0.0 | 0.3 | 0.0 | 0.0 | 0.0 | 0.0 | 0.0 | 0.0 | 0.7 | 0.0 | 1.5 | 2.3 |
| **CY** | 0.0 | 0.0 | 0.0 | 0.0 | 0.0 | 0.0 | 0.0 | 0.0 | 0.0 | 0.0 | 0.0 | 0.2 | 0.0 |
| **CZ** | 0.1 | 0.3 | 1.7 | 0.4 | 0.0 | 0.1 | 0.3 | 0.1 | 0.0 | 4.4 | 0.3 | 198.0 | 2.1 |
| **DE** | 0.9 | 1.5 | 34.7 | 2.4 | 0.0 | 0.1 | 0.1 | 0.1 | 0.0 | 168.0 | 2.6 | 259.0 | 13.9 |
| **DK** | 0.0 | 0.7 | 0.5 | 0.8 | 0.0 | 0.0 | 0.0 | 0.0 | 0.0 | 10.5 | 1.9 | 41.2 | 1.8 |
| **EE** | 0.0 | 8.8 | 0.1 | 41.2 | 0.0 | 0.3 | 0.1 | 0.1 | 0.0 | 1.3 | 1.4 | 66.0 | 0.7 |
| **ES** | 0.0 | 0.0 | 0.2 | 0.0 | 0.0 | 0.0 | 0.1 | 0.1 | 0.0 | 0.6 | 0.1 | 2.5 | 412.0 |
| **FI** | 0.0 | 8.8 | 0.2 | 23.0 | 0.0 | 0.5 | 0.2 | 0.2 | 0.0 | 3.7 | 9.7 | 163.0 | 1.9 |
| **FR** | 0.1 | 0.2 | 9.8 | 0.3 | 0.1 | 0.0 | 0.3 | 0.3 | 0.0 | 17.1 | 0.7 | 19.5 | 58.0 |
| **GB** | 0.0 | 0.4 | 0.9 | 0.4 | 0.0 | 0.0 | 0.0 | 0.0 | 0.0 | 16.2 | 1.4 | 20.4 | 18.2 |
| **GE** | 0.0 | 0.0 | 0.0 | 0.0 | 0.0 | 0.3 | 0.0 | 0.1 | 0.0 | 0.0 | 0.0 | 2.9 | 0.3 |
| **GR** | 0.0 | 0.1 | 0.0 | 0.1 | 0.0 | 1.3 | 1.0 | 9.8 | 0.1 | 0.2 | 0.0 | 14.6 | 1.8 |
| **HR** | 0.0 | 0.1 | 0.1 | 0.1 | 0.0 | 0.2 | 1.1 | 0.6 | 0.0 | 0.4 | 0.1 | 35.9 | 3.2 |
| **HU** | 0.0 | 0.2 | 0.3 | 0.3 | 0.0 | 0.5 | 2.1 | 1.6 | 0.0 | 0.8 | 0.1 | 133.0 | 2.9 |
| **IE** | 0.0 | 0.0 | 0.2 | 0.1 | 0.0 | 0.0 | 0.0 | 0.0 | 0.0 | 1.5 | 0.2 | 1.6 | 7.3 |
| **IS** | 0.0 | 0.0 | 0.0 | 0.0 | 0.0 | 0.0 | 0.0 | 0.0 | 0.0 | 0.5 | 0.6 | 1.6 | 0.3 |
| **IT** | 0.2 | 0.1 | 0.3 | 0.1 | 0.2 | 0.3 | 1.9 | 1.7 | 0.2 | 0.8 | 0.1 | 25.4 | 18.8 |
| **KY** | 0.0 | 0.0 | 0.0 | 0.0 | 0.0 | 0.0 | 0.0 | 0.0 | 0.0 | 0.0 | 0.0 | 0.8 | 0.3 |
| **KZ** | 0.0 | 1.2 | 0.1 | 1.9 | 0.0 | 4.3 | 0.5 | 1.4 | 0.0 | 0.8 | 1.0 | 77.0 | 7.1 |
| **LI** | **0.1** | 0.0 | 0.0 | 0.0 | 0.0 | 0.0 | 0.0 | 0.0 | 0.0 | 0.0 | 0.0 | 0.0 | 0.0 |
| **LT** | 0.0 | **124.0** | 0.2 | 23.5 | 0.0 | 0.8 | 0.2 | 0.2 | 0.0 | 3.0 | 1.4 | 333.0 | 0.9 |
| **LU** | 0.0 | 0.0 | **6.5** | 0.0 | 0.0 | 0.0 | 0.0 | 0.0 | 0.0 | 0.7 | 0.0 | 0.3 | 0.2 |
| **LV** | 0.0 | 42.4 | 0.1 | **204.0** | 0.0 | 0.7 | 0.1 | 0.1 | 0.0 | 2.5 | 1.9 | 182.0 | 0.9 |
| **MC** | 0.0 | 0.0 | 0.0 | 0.0 | **0.0** | 0.0 | 0.0 | 0.0 | 0.0 | 0.0 | 0.0 | 0.0 | 0.0 |
| **MD** | 0.0 | 0.3 | 0.0 | 0.2 | 0.0 | **32.7** | 0.1 | 0.3 | 0.0 | 0.1 | 0.1 | 22.4 | 0.3 |
| **ME** | 0.0 | 0.0 | 0.0 | 0.0 | 0.0 | 0.1 | **9.7** | 0.5 | 0.0 | 0.0 | 0.0 | 3.7 | 0.4 |
| **MK** | 0.0 | 0.0 | 0.0 | 0.0 | 0.0 | 0.2 | 0.6 | **26.8** | 0.0 | 0.0 | 0.0 | 4.8 | 0.7 |
| **MT** | 0.0 | 0.0 | 0.0 | 0.0 | 0.0 | 0.0 | 0.0 | 0.0 | **0.0** | 0.0 | 0.0 | 0.0 | 0.0 |
| **NL** | 0.0 | 0.1 | 1.3 | 0.2 | 0.0 | 0.0 | 0.0 | 0.0 | 0.0 | **128.0** | 0.3 | 11.0 | 1.4 |
| **NO** | 0.0 | 1.4 | 0.6 | 2.6 | 0.0 | 0.1 | 0.0 | 0.0 | 0.0 | 9.7 | **168.0** | 67.8 | 5.4 |
| **PL** | 0.1 | 9.7 | 2.7 | 7.2 | 0.0 | 1.9 | 1.2 | 0.9 | 0.0 | 24.5 | 4.0 | **5950.0** | 7.1 |
| **PT** | 0.0 | 0.0 | 0.0 | 0.0 | 0.0 | 0.0 | 0.0 | 0.0 | 0.0 | 0.1 | 0.0 | 0.3 | **758.0** |
| **RO** | 0.0 | 0.9 | 0.3 | 0.8 | 0.0 | 19.6 | 3.1 | 6.0 | 0.1 | 1.0 | 0.3 | 146.0 | 3.8 |
| **RS** | 0.0 | 0.2 | 0.1 | 0.2 | 0.0 | 0.9 | 9.6 | 10.8 | 0.0 | 0.5 | 0.1 | 66.2 | 2.2 |
| **RU** | 0.1 | 50.1 | 1.4 | 116.0 | 0.0 | 37.3 | 4.2 | 9.2 | 0.1 | 15.0 | 24.1 | 1230.0 | 20.4 |
| **SE** | 0.0 | 8.0 | 0.9 | 14.4 | 0.0 | 0.3 | 0.1 | 0.1 | 0.0 | 16.5 | 53.5 | 242.0 | 5.8 |
| **SI** | 0.0 | 0.0 | 0.1 | 0.0 | 0.0 | 0.0 | 0.2 | 0.2 | 0.0 | 0.2 | 0.0 | 8.7 | 1.2 |
| **SK** | 0.0 | 0.2 | 0.3 | 0.2 | 0.0 | 0.3 | 0.8 | 0.5 | 0.0 | 0.9 | 0.1 | 248.0 | 1.7 |
| **TJ** | 0.0 | 0.0 | 0.0 | 0.0 | 0.0 | 0.0 | 0.0 | 0.0 | 0.0 | 0.0 | 0.0 | 0.4 | 0.1 |
| **TM** | 0.0 | 0.0 | 0.0 | 0.0 | 0.0 | 0.2 | 0.0 | 0.1 | 0.0 | 0.0 | 0.0 | 2.8 | 0.3 |
| **TR** | 0.0 | 0.5 | 0.1 | 0.6 | 0.0 | 6.4 | 0.8 | 3.0 | 0.1 | 0.5 | 0.2 | 46.8 | 5.7 |
| **UA** | 0.1 | 8.0 | 0.7 | 6.8 | 0.0 | 59.7 | 2.2 | 4.1 | 0.1 | 4.4 | 1.9 | 1060.0 | 6.0 |
| **UZ** | 0.0 | 0.0 | 0.0 | 0.1 | 0.0 | 0.2 | 0.0 | 0.1 | 0.0 | 0.0 | 0.0 | 3.1 | 0.4 |
| **SUM** | 3.6 | 304.7 | 71.0 | 472.6 | 0.6 | 185.5 | 49.4 | 91.5 | 1.2 | 461.0 | 278.6 | 11625.1 | 1389.4 |
| **Emiss 2016** | 4.2 | 345.3 | 83.5 | 556.2 | 1.0 | 222.6 | 71.5 | 130.9 | 6.0 | 653.2 | 447.7 | 13109.4 | 3583.4 |
| **code** | **LI** | **LT** | **LU** | **LV** | **MC** | **MD** | **ME** | **MK** | **MT** | **NL** | **NO** | **PL** | **PT** |

***Table 3.3**. Matrix of Cd country-to-country deposition from anthropogenic sources in 2017, kg (continued)*

Receptors ↓ Emitters →

| code | RO | RS | RU | SE | SI | SK | TJ | TM | TR | UA | UZ | SUM |
|---|---|---|---|---|---|---|---|---|---|---|---|---|
| **AL** | 2.7 | 22.7 | 2.9 | 0.0 | 0.6 | 1.4 | 0.0 | 0.0 | 10.4 | 3.9 | 0.0 | 182.9 |
| **AM** | 0.3 | 0.2 | 10.1 | 0.0 | 0.0 | 0.1 | 0.0 | 0.3 | 14.5 | 2.9 | 0.3 | 75.2 |
| **AT** | 5.2 | 10.2 | 3.6 | 0.2 | 63.3 | 24.9 | 0.0 | 0.0 | 1.3 | 2.5 | 0.0 | 1117.3 |
| **AZ** | 0.8 | 0.3 | 69.4 | 0.0 | 0.1 | 0.2 | 0.0 | 1.4 | 14.2 | 8.5 | 1.8 | 153 |
| **BA** | 17.9 | 89.5 | 6.6 | 0.1 | 7.8 | 22.7 | 0.0 | 0.0 | 7.7 | 8.1 | 0.0 | 944.7 |
| **BE** | 0.1 | 0.2 | 0.6 | 0.2 | 0.2 | 0.4 | 0.0 | 0.0 | 0.1 | 0.1 | 0.0 | 788.4 |
| **BG** | 171.0 | 137.0 | 158.0 | 0.1 | 3.7 | 14.3 | 0.0 | 0.2 | 508.0 | 215.0 | 0.5 | 2137.5 |
| **BY** | 71.1 | 33.4 | 639.0 | 4.8 | 6.0 | 32.8 | 0.0 | 0.2 | 122.0 | 552.0 | 0.5 | 3004.9 |
| **CH** | 0.1 | 0.3 | 0.2 | 0.0 | 1.2 | 0.3 | 0.0 | 0.0 | 0.1 | 0.1 | 0.0 | 498.2 |
| **CY** | 0.3 | 0.2 | 1.1 | 0.0 | 0.0 | 0.0 | 0.0 | 0.0 | 21.4 | 1.2 | 0.0 | 29.9 |
| **CZ** | 7.5 | 17.7 | 6.6 | 0.5 | 13.7 | 61.9 | 0.0 | 0.0 | 1.5 | 4.5 | 0.0 | 1427.8 |
| **DE** | 5.4 | 6.1 | 30.1 | 3.6 | 7.9 | 15.9 | 0.0 | 0.0 | 2.4 | 9.0 | 0.0 | 8354.2 |
| **DK** | 0.7 | 0.9 | 8.7 | 3.2 | 0.5 | 1.5 | 0.0 | 0.0 | 0.1 | 2.0 | 0.0 | 422.6 |
| **EE** | 3.6 | 2.4 | 72.1 | 5.1 | 0.7 | 2.7 | 0.0 | 0.0 | 6.0 | 10.5 | 0.0 | 428.8 |
| **ES** | 0.8 | 1.0 | 0.7 | 0.1 | 1.6 | 0.8 | 0.0 | 0.0 | 0.8 | 0.6 | 0.0 | 2793.8 |
| **FI** | 8.6 | 6.1 | 395.0 | 42.6 | 2.1 | 8.7 | 0.0 | 0.0 | 10.9 | 24.0 | 0.1 | 1454.8 |
| **FR** | 2.2 | 6.0 | 4.7 | 0.7 | 6.5 | 2.9 | 0.0 | 0.0 | 3.2 | 1.8 | 0.0 | 2597.8 |
| **GB** | 1.1 | 0.7 | 9.1 | 1.0 | 0.3 | 1.5 | 0.0 | 0.0 | 0.5 | 2.0 | 0.0 | 1393.5 |
| **GE** | 3.4 | 1.5 | 87.9 | 0.0 | 0.2 | 0.4 | 0.0 | 0.3 | 51.2 | 26.3 | 0.4 | 272.9 |
| **GR** | 22.7 | 39.7 | 56.0 | 0.1 | 1.8 | 4.7 | 0.0 | 0.0 | 482.0 | 69.3 | 0.1 | 1309.9 |
| **HR** | 15.4 | 52.4 | 5.3 | 0.1 | 42.9 | 22.4 | 0.0 | 0.0 | 5.3 | 5.7 | 0.0 | 753.6 |
| **HU** | 63.1 | 125.0 | 23.9 | 0.2 | 30.0 | 149.0 | 0.0 | 0.0 | 14.3 | 16.8 | 0.0 | 1369.3 |
| **IE** | 0.2 | 0.2 | 1.0 | 0.1 | 0.1 | 0.2 | 0.0 | 0.0 | 0.1 | 0.2 | 0.0 | 162.7 |
| **IS** | 0.1 | 0.1 | 2.3 | 0.2 | 0.0 | 0.1 | 0.0 | 0.0 | 0.1 | 0.2 | 0.0 | 33.4 |
| **IT** | 11.6 | 27.1 | 8.3 | 0.2 | 40.2 | 11.1 | 0.0 | 0.0 | 16.7 | 9.9 | 0.0 | 2098.5 |
| **KY** | 0.5 | 0.4 | 23.5 | 0.0 | 0.1 | 0.1 | 27.4 | 2.6 | 6.7 | 4.0 | 451.0 | 844.8 |
| **KZ** | 42.3 | 16.7 | 4210.0 | 1.4 | 3.1 | 8.8 | 40.6 | 32.8 | 164.0 | 541.0 | 680.0 | 10200.5 |
| **LI** | 0.0 | 0.0 | 0.0 | 0.0 | 0.0 | 0.0 | 0.0 | 0.0 | 0.0 | 0.0 | 0.0 | 2.7 |
| **LT** | 10.8 | 7.8 | 130.0 | 4.7 | 2.3 | 9.8 | 0.0 | 0.0 | 7.9 | 29.8 | 0.0 | 884.3 |
| **LU** | 0.0 | 0.0 | 0.0 | 0.0 | 0.0 | 0.0 | 0.0 | 0.0 | 0.0 | 0.0 | 0.0 | 39.5 |
| **LV** | 9.1 | 6.5 | 120.0 | 7.0 | 1.6 | 6.7 | 0.0 | 0.0 | 12.4 | 27.8 | 0.0 | 787.8 |
| **MC** | 0.0 | 0.0 | 0.0 | 0.0 | 0.0 | 0.0 | 0.0 | 0.0 | 0.0 | 0.0 | 0.0 | 0 |
| **MD** | 40.0 | 4.0 | 85.1 | 0.1 | 0.6 | 2.4 | 0.0 | 0.1 | 60.4 | 172.0 | 0.2 | 456.4 |
| **ME** | 2.0 | 21.0 | 1.4 | 0.0 | 0.7 | 2.0 | 0.0 | 0.0 | 2.9 | 2.0 | 0.0 | 124.3 |
| **MK** | 5.9 | 38.2 | 6.6 | 0.0 | 0.7 | 2.2 | 0.0 | 0.0 | 34.3 | 9.1 | 0.0 | 237.3 |
| **MT** | 0.0 | 0.0 | 0.0 | 0.0 | 0.0 | 0.0 | 0.0 | 0.0 | 0.0 | 0.0 | 0.0 | 0.8 |
| **NL** | 0.3 | 0.3 | 3.8 | 0.3 | 0.2 | 0.7 | 0.0 | 0.0 | 0.2 | 0.5 | 0.0 | 784.9 |
| **NO** | 2.6 | 2.5 | 85.0 | 23.5 | 0.8 | 3.6 | 0.0 | 0.0 | 2.6 | 11.5 | 0.1 | 688.9 |
| **PL** | 52.2 | 64.5 | 215.0 | 9.6 | 22.9 | 185.0 | 0.0 | 0.1 | 11.0 | 103.0 | 0.2 | 8595.5 |
| **PT** | 0.0 | 0.0 | 0.0 | 0.0 | 0.1 | 0.0 | 0.0 | 0.0 | 0.0 | 0.0 | 0.0 | 936.5 |
| **RO** | **1120.0** | 198.0 | 257.0 | 0.5 | 15.6 | 58.5 | 0.0 | 0.2 | 373.0 | 384.0 | 0.6 | 3229.6 |
| **RS** | 72.0 | **711.0** | 27.6 | 0.2 | 6.7 | 37.2 | 0.0 | 0.0 | 47.6 | 31.4 | 0.0 | 1429.2 |
| **RU** | 326.0 | 156.0 | **69400.0** | 48.7 | 28.5 | 91.5 | 17.4 | 29.4 | 1420.0 | 5110.0 | 241.0 | 83815.7 |
| **SE** | 6.1 | 6.9 | 181.0 | **215.0** | 3.0 | 10.8 | 0.0 | 0.0 | 4.4 | 17.7 | 0.1 | 1510.7 |
| **SI** | 4.1 | 8.2 | 1.1 | 0.0 | **130.0** | 5.0 | 0.0 | 0.0 | 0.9 | 1.4 | 0.0 | 352 |
| **SK** | 26.5 | 47.8 | 19.7 | 0.3 | 13.9 | **343.0** | 0.0 | 0.0 | 5.1 | 11.7 | 0.0 | 1145.2 |
| **TJ** | 0.2 | 0.2 | 9.3 | 0.0 | 0.0 | 0.1 | **76.3** | 2.6 | 3.3 | 1.8 | 99.2 | 221.1 |
| **TM** | 1.7 | 0.6 | 95.5 | 0.0 | 0.1 | 0.3 | 5.4 | **34.2** | 13.9 | 16.9 | 71.9 | 304.6 |
| **TR** | 79.8 | 38.5 | 535.0 | 0.3 | 3.4 | 8.6 | 0.0 | 0.8 | **6410.0** | 416.0 | 1.6 | 8011.2 |
| **UA** | 351.0 | 108.0 | 2410.0 | 4.0 | 19.3 | 111.0 | 0.1 | 1.4 | 732.0 | **6180.0** | 4.2 | 11983.7 |
| **UZ** | 2.3 | 0.9 | 126.0 | 0.1 | 0.2 | 0.3 | 31.2 | 13.1 | 16.3 | 22.4 | **548.0** | 929.2 |
| **SUM** | 2571.4 | 2018.6 | 79545.8 | 378.7 | 485.1 | 1268.7 | 198.6 | 119.8 | 10623.6 | 14071.2 | 2102.1 | |
| **Emiss 2016** | 3048.8 | 2426.6 | 93439.4 | 540.0 | 600.2 | 1411.1 | 320.2 | 227.9 | 18680.3 | 16339.9 | 3277.1 | |
| **code** | **RO** | **RS** | **RU** | **SE** | **SI** | **SK** | **TJ** | **TM** | **TR** | **UA** | **UZ** | |

***Table 3.4**. Matrix of Hg country-to-country deposition from anthropogenic sources in 2017, kg*

Receptors ↓ Emitters →

| code | AL | AM | AT | AZ | BA | BE | BG | BY | CH | CY | CZ | DE | DK |
|---|---|---|---|---|---|---|---|---|---|---|---|---|---|
| **AL** | **10.3** | 0.0 | 0.2 | 0.0 | 2.8 | 0.1 | 0.9 | 0.0 | 0.1 | 0.0 | 0.6 | 1.1 | 0.0 |
| **AM** | 0.0 | **14.9** | 0.0 | 1.7 | 0.1 | 0.0 | 0.1 | 0.0 | 0.0 | 0.0 | 0.1 | 0.2 | 0.0 |
| **AT** | 0.1 | 0.0 | **77.0** | 0.0 | 3.6 | 1.4 | 0.2 | 0.0 | 10.5 | 0.0 | 28.0 | 87.8 | 0.2 |
| **AZ** | 0.0 | 2.7 | 0.0 | **16.3** | 0.1 | 0.0 | 0.1 | 0.0 | 0.0 | 0.0 | 0.2 | 0.5 | 0.0 |
| **BA** | 0.6 | 0.0 | 2.9 | 0.0 | **247.3** | 0.4 | 0.8 | 0.0 | 0.7 | 0.0 | 8.4 | 9.9 | 0.1 |
| **BE** | 0.0 | 0.0 | 0.1 | 0.0 | 0.1 | **83.4** | 0.0 | 0.0 | 0.4 | 0.0 | 0.8 | 25.1 | 0.1 |
| **BG** | 0.6 | 0.1 | 1.5 | 0.1 | 10.9 | 0.4 | **88.7** | 0.1 | 0.6 | 0.0 | 4.2 | 7.4 | 0.1 |
| **BY** | 0.2 | 0.1 | 2.2 | 0.1 | 6.9 | 2.3 | 2.4 | **16.1** | 1.0 | 0.0 | 19.7 | 46.3 | 1.8 |
| **CH** | 0.0 | 0.0 | 1.0 | 0.0 | 0.3 | 0.6 | 0.0 | 0.0 | **49.0** | 0.0 | 0.7 | 17.4 | 0.0 |
| **CY** | 0.0 | 0.0 | 0.0 | 0.0 | 0.1 | 0.0 | 0.0 | 0.0 | 0.0 | **0.7** | 0.0 | 0.1 | 0.0 |
| **CZ** | 0.0 | 0.0 | 12.3 | 0.0 | 3.9 | 3.0 | 0.2 | 0.0 | 2.9 | 0.0 | **332.4** | 135.5 | 0.5 |
| **DE** | 0.0 | 0.0 | 13.1 | 0.0 | 1.7 | 79.2 | 0.2 | 0.1 | 29.2 | 0.0 | 87.0 | **1517.4** | 4.5 |
| **DK** | 0.0 | 0.0 | 0.2 | 0.0 | 0.2 | 3.0 | 0.0 | 0.0 | 0.3 | 0.0 | 2.0 | 30.9 | **20.9** |
| **EE** | 0.0 | 0.0 | 0.3 | 0.0 | 0.5 | 0.6 | 0.1 | 0.2 | 0.2 | 0.0 | 2.3 | 10.2 | 0.9 |
| **ES** | 0.0 | 0.0 | 0.4 | 0.0 | 1.0 | 0.7 | 0.1 | 0.0 | 0.6 | 0.0 | 0.8 | 4.4 | 0.0 |
| **FI** | 0.1 | 0.0 | 1.2 | 0.0 | 2.1 | 2.5 | 0.4 | 0.5 | 0.8 | 0.0 | 8.5 | 33.4 | 3.0 |
| **FR** | 0.1 | 0.0 | 1.6 | 0.0 | 2.7 | 24.9 | 0.2 | 0.0 | 14.0 | 0.0 | 5.1 | 85.0 | 0.4 |
| **GB** | 0.0 | 0.0 | 0.3 | 0.0 | 0.1 | 7.0 | 0.1 | 0.0 | 0.4 | 0.0 | 1.9 | 24.2 | 0.7 |
| **GE** | 0.0 | 2.7 | 0.1 | 2.5 | 0.6 | 0.1 | 0.4 | 0.0 | 0.1 | 0.1 | 0.4 | 1.0 | 0.0 |
| **GR** | 1.4 | 0.0 | 0.7 | 0.0 | 5.9 | 0.2 | 9.8 | 0.0 | 0.4 | 0.0 | 1.8 | 3.7 | 0.1 |
| **HR** | 0.3 | 0.0 | 5.7 | 0.0 | 36.5 | 0.4 | 0.5 | 0.0 | 0.7 | 0.0 | 9.4 | 10.1 | 0.1 |
| **HU** | 0.4 | 0.0 | 11.9 | 0.0 | 26.5 | 0.7 | 1.4 | 0.1 | 1.0 | 0.0 | 25.5 | 21.9 | 0.2 |
| **IE** | 0.0 | 0.0 | 0.1 | 0.0 | 0.0 | 0.7 | 0.0 | 0.0 | 0.1 | 0.0 | 0.2 | 2.8 | 0.1 |
| **IS** | 0.0 | 0.0 | 0.1 | 0.0 | 0.0 | 0.3 | 0.0 | 0.0 | 0.1 | 0.0 | 0.3 | 2.6 | 0.1 |
| **IT** | 1.1 | 0.0 | 6.6 | 0.0 | 20.3 | 0.9 | 1.1 | 0.0 | 9.6 | 0.0 | 7.3 | 21.5 | 0.1 |
| **KY** | 0.0 | 0.3 | 0.1 | 0.3 | 0.2 | 0.1 | 0.1 | 0.0 | 0.1 | 0.0 | 0.2 | 0.7 | 0.0 |
| **KZ** | 0.3 | 4.0 | 2.0 | 5.2 | 5.3 | 1.6 | 2.7 | 0.6 | 1.3 | 0.2 | 7.8 | 20.8 | 0.6 |
| **LI** | 0.0 | 0.0 | 0.0 | 0.0 | 0.0 | 0.0 | 0.0 | 0.0 | 0.4 | 0.0 | 0.0 | 0.1 | 0.0 |
| **LT** | 0.0 | 0.0 | 0.9 | 0.0 | 1.6 | 1.3 | 0.4 | 1.6 | 0.4 | 0.0 | 7.6 | 25.2 | 1.9 |
| **LU** | 0.0 | 0.0 | 0.0 | 0.0 | 0.0 | 1.2 | 0.0 | 0.0 | 0.1 | 0.0 | 0.1 | 3.4 | 0.0 |
| **LV** | 0.0 | 0.0 | 0.7 | 0.0 | 1.4 | 1.0 | 0.3 | 0.7 | 0.3 | 0.0 | 5.5 | 20.0 | 1.7 |
| **MC** | 0.0 | 0.0 | 0.0 | 0.0 | 0.0 | 0.0 | 0.0 | 0.0 | 0.0 | 0.0 | 0.0 | 0.0 | 0.0 |
| **MD** | 0.0 | 0.0 | 0.2 | 0.0 | 0.8 | 0.1 | 0.8 | 0.1 | 0.1 | 0.0 | 1.0 | 2.2 | 0.1 |
| **ME** | 1.3 | 0.0 | 0.2 | 0.0 | 12.1 | 0.1 | 0.3 | 0.0 | 0.1 | 0.0 | 0.8 | 1.1 | 0.0 |
| **MK** | 1.6 | 0.0 | 0.3 | 0.0 | 2.5 | 0.1 | 3.5 | 0.0 | 0.1 | 0.0 | 0.7 | 1.2 | 0.0 |
| **MT** | 0.0 | 0.0 | 0.0 | 0.0 | 0.0 | 0.0 | 0.0 | 0.0 | 0.0 | 0.0 | 0.0 | 0.0 | 0.0 |
| **NL** | 0.0 | 0.0 | 0.2 | 0.0 | 0.0 | 37.7 | 0.0 | 0.0 | 0.3 | 0.0 | 1.2 | 38.8 | 0.2 |
| **NO** | 0.0 | 0.0 | 0.7 | 0.0 | 0.6 | 4.8 | 0.1 | 0.1 | 0.7 | 0.0 | 6.2 | 44.9 | 5.1 |
| **PL** | 0.2 | 0.0 | 10.1 | 0.0 | 13.0 | 10.8 | 1.2 | 1.6 | 3.6 | 0.0 | 201.5 | 369.9 | 6.9 |
| **PT** | 0.0 | 0.0 | 0.0 | 0.0 | 0.0 | 0.1 | 0.0 | 0.0 | 0.1 | 0.0 | 0.1 | 0.8 | 0.0 |
| **RO** | 0.9 | 0.1 | 5.2 | 0.1 | 27.7 | 1.1 | 14.7 | 0.3 | 1.6 | 0.0 | 13.2 | 23.3 | 0.4 |
| **RS** | 1.4 | 0.0 | 2.7 | 0.0 | 42.3 | 0.5 | 6.1 | 0.1 | 0.6 | 0.0 | 9.1 | 10.8 | 0.1 |
| **RU** | 1.8 | 8.3 | 14.6 | 12.2 | 43.2 | 14.9 | 21.8 | 12.2 | 8.7 | 0.6 | 71.3 | 207.8 | 10.7 |
| **SE** | 0.0 | 0.0 | 1.6 | 0.0 | 1.5 | 6.3 | 0.2 | 0.4 | 1.2 | 0.0 | 15.0 | 89.0 | 20.0 |
| **SI** | 0.1 | 0.0 | 7.3 | 0.0 | 3.1 | 0.2 | 0.2 | 0.0 | 0.5 | 0.0 | 2.8 | 5.1 | 0.0 |
| **SK** | 0.1 | 0.0 | 7.8 | 0.0 | 10.7 | 0.8 | 0.6 | 0.0 | 1.0 | 0.0 | 44.0 | 24.0 | 0.2 |
| **TJ** | 0.0 | 0.1 | 0.0 | 0.1 | 0.1 | 0.0 | 0.0 | 0.0 | 0.0 | 0.0 | 0.1 | 0.3 | 0.0 |
| **TM** | 0.0 | 0.7 | 0.1 | 1.3 | 0.3 | 0.1 | 0.1 | 0.0 | 0.1 | 0.0 | 0.3 | 0.9 | 0.0 |
| **TR** | 0.7 | 6.9 | 1.8 | 1.1 | 8.4 | 0.9 | 10.0 | 0.3 | 1.2 | 2.1 | 5.3 | 12.4 | 0.3 |
| **UA** | 0.6 | 0.3 | 7.3 | 0.4 | 21.1 | 3.3 | 9.3 | 3.0 | 2.5 | 0.1 | 38.0 | 70.9 | 1.7 |
| **UZ** | 0.0 | 0.6 | 0.1 | 0.8 | 0.3 | 0.1 | 0.2 | 0.0 | 0.1 | 0.0 | 0.4 | 1.0 | 0.0 |
| **SUM** | 24.7 | 42.1 | 203.8 | 42.4 | 570.2 | 299.9 | 180.6 | 38.5 | 147.6 | 4.1 | 979.7 | 3074.7 | 84.1 |
| **Emiss 2016** | 0.19 | 0.34 | 0.95 | 0.26 | 1.74 | 1.37 | 0.81 | 0.20 | 0.69 | 0.09 | 2.65 | 9.78 | 0.32 |
| **code** | **AL** | **AM** | **AT** | **AZ** | **BA** | **BE** | **BG** | **BY** | **CH** | **CY** | **CZ** | **DE** | **DK** |

***Table 3.4**. Matrix of Hg country-to-country deposition from anthropogenic sources in 2017, kg (continued)*

Receptors ↓ Emitters →

| code | EE | ES | FI | FR | GB | GE | GR | HR | HU | IE | IS | IT | KY | KZ |
|---|---|---|---|---|---|---|---|---|---|---|---|---|---|---|
| **AL** | 0.0 | 0.7 | 0.0 | 0.6 | 0.2 | 0.0 | 9.6 | 0.4 | 0.6 | 0.0 | 0.0 | 8.8 | 0.0 | 0.0 |
| **AM** | 0.0 | 0.1 | 0.0 | 0.1 | 0.0 | 2.3 | 0.2 | 0.0 | 0.0 | 0.0 | 0.0 | 0.4 | 0.0 | 0.3 |
| **AT** | 0.1 | 3.3 | 0.0 | 7.0 | 2.5 | 0.0 | 0.3 | 3.2 | 4.3 | 0.1 | 0.0 | 55.8 | 0.0 | 0.0 |
| **AZ** | 0.0 | 0.1 | 0.0 | 0.1 | 0.1 | 2.7 | 0.3 | 0.0 | 0.1 | 0.0 | 0.0 | 0.5 | 0.0 | 2.7 |
| **BA** | 0.1 | 2.0 | 0.0 | 1.9 | 0.8 | 0.0 | 1.9 | 6.8 | 9.4 | 0.0 | 0.0 | 28.8 | 0.0 | 0.0 |
| **BE** | 0.0 | 1.6 | 0.0 | 26.4 | 13.9 | 0.0 | 0.0 | 0.0 | 0.1 | 0.3 | 0.0 | 0.7 | 0.0 | 0.0 |
| **BG** | 0.1 | 1.7 | 0.1 | 1.6 | 0.8 | 0.1 | 26.4 | 1.1 | 5.6 | 0.0 | 0.0 | 12.0 | 0.0 | 0.7 |
| **BY** | 3.3 | 2.4 | 0.6 | 3.5 | 7.5 | 0.1 | 4.4 | 1.0 | 6.4 | 0.4 | 0.0 | 11.4 | 0.0 | 1.6 |
| **CH** | 0.0 | 2.8 | 0.0 | 9.1 | 1.1 | 0.0 | 0.1 | 0.3 | 0.1 | 0.1 | 0.0 | 71.7 | 0.0 | 0.0 |
| **CY** | 0.0 | 0.0 | 0.0 | 0.0 | 0.0 | 0.0 | 0.4 | 0.0 | 0.0 | 0.0 | 0.0 | 0.2 | 0.0 | 0.0 |
| **CZ** | 0.1 | 2.0 | 0.1 | 6.4 | 4.8 | 0.0 | 0.2 | 1.3 | 7.2 | 0.2 | 0.0 | 11.6 | 0.0 | 0.0 |
| **DE** | 0.6 | 12.0 | 0.3 | 86.4 | 71.0 | 0.0 | 0.4 | 0.9 | 2.5 | 2.3 | 0.0 | 33.4 | 0.0 | 0.1 |
| **DK** | 0.1 | 1.2 | 0.1 | 2.9 | 12.1 | 0.0 | 0.0 | 0.0 | 0.2 | 0.4 | 0.0 | 0.9 | 0.0 | 0.0 |
| **EE** | **27.7** | 0.6 | 2.0 | 0.8 | 2.4 | 0.0 | 0.3 | 0.1 | 0.5 | 0.1 | 0.0 | 1.2 | 0.0 | 0.1 |
| **ES** | 0.0 | **303.2** | 0.0 | 11.8 | 3.5 | 0.0 | 0.3 | 0.4 | 0.3 | 0.4 | 0.0 | 13.2 | 0.0 | 0.0 |
| **FI** | 32.9 | 2.4 | **68.6** | 3.6 | 12.8 | 0.0 | 0.8 | 0.4 | 1.9 | 0.6 | 0.0 | 4.9 | 0.0 | 1.2 |
| **FR** | 0.1 | 65.5 | 0.1 | **324.8** | 52.5 | 0.0 | 1.1 | 1.3 | 0.7 | 2.4 | 0.0 | 43.5 | 0.0 | 0.1 |
| **GB** | 0.1 | 8.6 | 0.1 | 14.2 | **446.7** | 0.0 | 0.1 | 0.0 | 0.2 | 13.7 | 0.1 | 1.1 | 0.0 | 0.1 |
| **GE** | 0.0 | 0.3 | 0.0 | 0.2 | 0.2 | **14.9** | 1.1 | 0.1 | 0.3 | 0.0 | 0.0 | 1.3 | 0.0 | 0.6 |
| **GR** | 0.1 | 1.7 | 0.0 | 1.4 | 0.5 | 0.0 | **207.1** | 0.8 | 1.8 | 0.0 | 0.0 | 15.7 | 0.0 | 0.3 |
| **HR** | 0.0 | 3.0 | 0.0 | 2.4 | 0.7 | 0.0 | 1.3 | **27.0** | 11.0 | 0.0 | 0.0 | 39.3 | 0.0 | 0.0 |
| **HU** | 0.1 | 2.4 | 0.0 | 2.4 | 1.3 | 0.0 | 2.1 | 5.2 | **121.2** | 0.1 | 0.0 | 20.8 | 0.0 | 0.0 |
| **IE** | 0.0 | 2.1 | 0.0 | 1.4 | 11.4 | 0.0 | 0.0 | 0.0 | 0.0 | **27.1** | 0.0 | 0.3 | 0.0 | 0.0 |
| **IS** | 0.0 | 0.3 | 0.0 | 0.5 | 3.6 | 0.0 | 0.0 | 0.0 | 0.0 | 0.3 | **3.8** | 0.3 | 0.0 | 0.2 |
| **IT** | 0.1 | 16.3 | 0.0 | 19.1 | 2.0 | 0.0 | 6.1 | 12.3 | 3.7 | 0.1 | 0.0 | **908.7** | 0.0 | 0.1 |
| **KY** | 0.0 | 0.4 | 0.0 | 0.2 | 0.2 | 0.1 | 0.3 | 0.1 | 0.1 | 0.0 | 0.0 | 1.1 | **16.4** | 59.7 |
| **KZ** | 2.3 | 5.1 | 1.0 | 4.0 | 4.2 | 2.5 | 5.6 | 1.0 | 3.7 | 0.3 | 0.0 | 14.9 | 17.3 | **2056.3** |
| **LI** | 0.0 | 0.0 | 0.0 | 0.0 | 0.0 | 0.0 | 0.0 | 0.0 | 0.0 | 0.0 | 0.0 | 0.2 | 0.0 | 0.0 |
| **LT** | 1.2 | 1.0 | 0.3 | 1.5 | 4.8 | 0.0 | 0.6 | 0.3 | 1.7 | 0.2 | 0.0 | 3.1 | 0.0 | 0.2 |
| **LU** | 0.0 | 0.2 | 0.0 | 2.2 | 0.5 | 0.0 | 0.0 | 0.0 | 0.0 | 0.0 | 0.0 | 0.1 | 0.0 | 0.0 |
| **LV** | 5.9 | 0.9 | 0.8 | 1.3 | 4.2 | 0.0 | 0.6 | 0.3 | 1.3 | 0.2 | 0.0 | 2.7 | 0.0 | 0.3 |
| **MC** | 0.0 | 0.0 | 0.0 | 0.0 | 0.0 | 0.0 | 0.0 | 0.0 | 0.0 | 0.0 | 0.0 | 0.0 | 0.0 | 0.0 |
| **MD** | 0.0 | 0.3 | 0.0 | 0.3 | 0.2 | 0.0 | 1.7 | 0.1 | 0.9 | 0.0 | 0.0 | 1.4 | 0.0 | 0.3 |
| **ME** | 0.0 | 0.5 | 0.0 | 0.4 | 0.1 | 0.0 | 1.2 | 0.4 | 0.9 | 0.0 | 0.0 | 7.3 | 0.0 | 0.0 |
| **MK** | 0.0 | 0.5 | 0.0 | 0.4 | 0.1 | 0.0 | 16.9 | 0.3 | 0.9 | 0.0 | 0.0 | 4.0 | 0.0 | 0.0 |
| **MT** | 0.0 | 0.0 | 0.0 | 0.0 | 0.0 | 0.0 | 0.0 | 0.0 | 0.0 | 0.0 | 0.0 | 0.1 | 0.0 | 0.0 |
| **NL** | 0.0 | 1.2 | 0.0 | 12.2 | 23.0 | 0.0 | 0.0 | 0.0 | 0.1 | 0.5 | 0.0 | 0.5 | 0.0 | 0.0 |
| **NO** | 1.5 | 3.7 | 1.9 | 6.1 | 30.6 | 0.0 | 0.2 | 0.1 | 0.9 | 1.3 | 0.1 | 2.4 | 0.0 | 0.9 |
| **PL** | 1.5 | 6.1 | 0.5 | 13.9 | 25.7 | 0.0 | 2.0 | 2.7 | 21.6 | 1.1 | 0.0 | 22.8 | 0.0 | 0.5 |
| **PT** | 0.0 | 15.9 | 0.0 | 0.5 | 0.4 | 0.0 | 0.0 | 0.0 | 0.0 | 0.0 | 0.0 | 0.5 | 0.0 | 0.0 |
| **RO** | 0.3 | 3.2 | 0.1 | 3.5 | 2.2 | 0.1 | 17.6 | 3.4 | 29.8 | 0.1 | 0.0 | 27.0 | 0.0 | 1.1 |
| **RS** | 0.1 | 1.5 | 0.0 | 1.6 | 0.9 | 0.0 | 8.2 | 2.8 | 19.8 | 0.0 | 0.0 | 15.6 | 0.0 | 0.1 |
| **RU** | 143.6 | 25.1 | 37.0 | 28.5 | 53.0 | 8.2 | 49.0 | 7.6 | 29.7 | 2.8 | 0.2 | 99.8 | 5.5 | 1719.3 |
| **SE** | 8.4 | 4.6 | 14.5 | 7.9 | 31.2 | 0.0 | 0.3 | 0.4 | 1.9 | 1.2 | 0.1 | 4.7 | 0.0 | 0.9 |
| **SI** | 0.0 | 1.3 | 0.0 | 1.2 | 0.3 | 0.0 | 0.3 | 7.7 | 2.1 | 0.0 | 0.0 | 25.1 | 0.0 | 0.0 |
| **SK** | 0.1 | 1.4 | 0.0 | 2.1 | 1.5 | 0.0 | 1.0 | 1.9 | 32.7 | 0.1 | 0.0 | 11.2 | 0.0 | 0.0 |
| **TJ** | 0.0 | 0.2 | 0.0 | 0.1 | 0.1 | 0.1 | 0.2 | 0.0 | 0.0 | 0.0 | 0.0 | 0.5 | 0.4 | 5.2 |
| **TM** | 0.1 | 0.3 | 0.0 | 0.2 | 0.2 | 0.4 | 0.4 | 0.1 | 0.2 | 0.0 | 0.0 | 1.0 | 0.2 | 19.5 |
| **TR** | 0.4 | 5.1 | 0.2 | 3.6 | 2.0 | 1.7 | 40.6 | 1.4 | 4.0 | 0.1 | 0.0 | 24.1 | 0.0 | 3.2 |
| **UA** | 1.7 | 5.8 | 0.6 | 7.0 | 8.4 | 0.5 | 16.5 | 3.3 | 30.5 | 0.4 | 0.0 | 30.7 | 0.0 | 6.6 |
| **UZ** | 0.1 | 0.3 | 0.0 | 0.3 | 0.2 | 0.4 | 0.5 | 0.1 | 0.2 | 0.0 | 0.0 | 1.1 | 1.7 | 51.9 |
| **SUM** | 233.0 | 520.8 | 129.4 | 627.7 | 846.7 | 34.3 | 428.2 | 96.8 | 361.3 | 57.3 | 4.6 | 1588.4 | 41.6 | 3934.4 |
| **Emiss 2016** | 0.62 | 3.86 | 0.59 | 3.23 | 3.96 | 0.22 | 2.15 | 0.50 | 1.17 | 0.33 | 0.06 | 8.91 | 0.80 | 18.67 |
| **code** | **EE** | **ES** | **FI** | **FR** | **GB** | **GE** | **GR** | **HR** | **HU** | **IE** | **IS** | **IT** | **KY** | **KZ** |

***Table 3.4**. Matrix of Hg country-to-country deposition from anthropogenic sources in 2017, kg (continued)*

Receptors ↓ Emitters →

| code | LI | LT | LU | LV | MC | MD | ME | MK | MT | NL | NO | PL | PT |
|---|---|---|---|---|---|---|---|---|---|---|---|---|---|
| **AL** | 0.0 | 0.0 | 0.0 | 0.0 | 0.0 | 0.0 | 0.4 | 3.1 | 0.0 | 0.0 | 0.0 | 1.4 | 0.1 |
| **AM** | 0.0 | 0.0 | 0.0 | 0.0 | 0.0 | 0.0 | 0.0 | 0.0 | 0.0 | 0.0 | 0.0 | 0.3 | 0.0 |
| **AT** | 0.0 | 0.0 | 0.3 | 0.0 | 0.0 | 0.0 | 0.1 | 0.1 | 0.0 | 0.6 | 0.0 | 19.7 | 0.7 |
| **AZ** | 0.0 | 0.0 | 0.0 | 0.0 | 0.0 | 0.0 | 0.0 | 0.0 | 0.0 | 0.0 | 0.0 | 0.8 | 0.0 |
| **BA** | 0.0 | 0.0 | 0.1 | 0.0 | 0.0 | 0.0 | 3.0 | 0.4 | 0.0 | 0.2 | 0.0 | 15.8 | 0.4 |
| **BE** | 0.0 | 0.0 | 1.9 | 0.0 | 0.0 | 0.0 | 0.0 | 0.0 | 0.0 | 5.3 | 0.0 | 1.6 | 0.3 |
| **BG** | 0.0 | 0.0 | 0.1 | 0.0 | 0.0 | 1.0 | 0.7 | 3.9 | 0.0 | 0.2 | 0.0 | 12.3 | 0.4 |
| **BY** | 0.0 | 2.0 | 0.2 | 1.2 | 0.0 | 1.2 | 0.4 | 0.8 | 0.0 | 1.3 | 0.2 | 190.1 | 0.6 |
| **CH** | 0.0 | 0.0 | 0.1 | 0.0 | 0.0 | 0.0 | 0.0 | 0.0 | 0.0 | 0.2 | 0.0 | 0.9 | 0.4 |
| **CY** | 0.0 | 0.0 | 0.0 | 0.0 | 0.0 | 0.0 | 0.0 | 0.0 | 0.0 | 0.0 | 0.0 | 0.1 | 0.0 |
| **CZ** | 0.0 | 0.0 | 0.6 | 0.0 | 0.0 | 0.0 | 0.1 | 0.1 | 0.0 | 1.3 | 0.1 | 113.4 | 0.4 |
| **DE** | 0.0 | 0.1 | 12.7 | 0.1 | 0.0 | 0.0 | 0.1 | 0.1 | 0.0 | 34.4 | 0.3 | 123.4 | 2.5 |
| **DK** | 0.0 | 0.0 | 0.1 | 0.0 | 0.0 | 0.0 | 0.0 | 0.0 | 0.0 | 2.3 | 0.3 | 9.7 | 0.4 |
| **EE** | 0.0 | 0.6 | 0.0 | 1.7 | 0.0 | 0.0 | 0.0 | 0.0 | 0.0 | 0.4 | 0.1 | 17.6 | 0.1 |
| **ES** | 0.0 | 0.0 | 0.1 | 0.0 | 0.0 | 0.0 | 0.0 | 0.0 | 0.0 | 0.2 | 0.0 | 1.9 | 47.7 |
| **FI** | 0.0 | 0.7 | 0.2 | 1.3 | 0.0 | 0.1 | 0.1 | 0.1 | 0.0 | 1.8 | 1.4 | 54.5 | 0.7 |
| **FR** | 0.0 | 0.0 | 3.7 | 0.0 | 0.0 | 0.0 | 0.1 | 0.2 | 0.0 | 4.5 | 0.2 | 9.1 | 8.7 |
| **GB** | 0.0 | 0.0 | 0.3 | 0.0 | 0.0 | 0.0 | 0.0 | 0.0 | 0.0 | 3.8 | 0.2 | 7.2 | 2.7 |
| **GE** | 0.0 | 0.0 | 0.0 | 0.0 | 0.0 | 0.1 | 0.0 | 0.1 | 0.0 | 0.0 | 0.0 | 2.0 | 0.1 |
| **GR** | 0.0 | 0.0 | 0.0 | 0.0 | 0.0 | 0.2 | 0.4 | 7.2 | 0.0 | 0.1 | 0.0 | 5.8 | 0.4 |
| **HR** | 0.0 | 0.0 | 0.1 | 0.0 | 0.0 | 0.0 | 0.5 | 0.3 | 0.0 | 0.1 | 0.0 | 14.7 | 0.6 |
| **HU** | 0.0 | 0.0 | 0.1 | 0.0 | 0.0 | 0.1 | 1.0 | 0.9 | 0.0 | 0.3 | 0.0 | 48.0 | 0.5 |
| **IE** | 0.0 | 0.0 | 0.0 | 0.0 | 0.0 | 0.0 | 0.0 | 0.0 | 0.0 | 0.3 | 0.0 | 0.5 | 0.9 |
| **IS** | 0.0 | 0.0 | 0.0 | 0.0 | 0.0 | 0.0 | 0.0 | 0.0 | 0.0 | 0.2 | 0.1 | 1.2 | 0.1 |
| **IT** | 0.0 | 0.0 | 0.1 | 0.0 | 0.0 | 0.0 | 0.9 | 1.0 | 0.0 | 0.3 | 0.0 | 12.6 | 3.1 |
| **KY** | 0.0 | 0.0 | 0.0 | 0.0 | 0.0 | 0.0 | 0.0 | 0.0 | 0.0 | 0.0 | 0.0 | 0.8 | 0.1 |
| **KZ** | 0.0 | 0.2 | 0.1 | 0.2 | 0.0 | 0.9 | 0.3 | 0.9 | 0.0 | 0.7 | 0.4 | 37.5 | 1.6 |
| **LI** | **0.0** | 0.0 | 0.0 | 0.0 | 0.0 | 0.0 | 0.0 | 0.0 | 0.0 | 0.0 | 0.0 | 0.0 | 0.0 |
| **LT** | 0.0 | **10.0** | 0.1 | 1.3 | 0.0 | 0.1 | 0.1 | 0.1 | 0.0 | 0.9 | 0.2 | 73.5 | 0.2 |
| **LU** | 0.0 | 0.0 | **3.3** | 0.0 | 0.0 | 0.0 | 0.0 | 0.0 | 0.0 | 0.2 | 0.0 | 0.2 | 0.0 |
| **LV** | 0.0 | 3.4 | 0.1 | **9.9** | 0.0 | 0.1 | 0.1 | 0.1 | 0.0 | 0.7 | 0.2 | 44.8 | 0.2 |
| **MC** | 0.0 | 0.0 | 0.0 | 0.0 | **0.0** | 0.0 | 0.0 | 0.0 | 0.0 | 0.0 | 0.0 | 0.0 | 0.0 |
| **MD** | 0.0 | 0.0 | 0.0 | 0.0 | 0.0 | **8.2** | 0.0 | 0.2 | 0.0 | 0.1 | 0.0 | 8.2 | 0.1 |
| **ME** | 0.0 | 0.0 | 0.0 | 0.0 | 0.0 | 0.0 | **4.7** | 0.3 | 0.0 | 0.0 | 0.0 | 1.7 | 0.1 |
| **MK** | 0.0 | 0.0 | 0.0 | 0.0 | 0.0 | 0.0 | 0.2 | **18.7** | 0.0 | 0.0 | 0.0 | 1.8 | 0.1 |
| **MT** | 0.0 | 0.0 | 0.0 | 0.0 | 0.0 | 0.0 | 0.0 | 0.0 | **0.0** | 0.0 | 0.0 | 0.0 | 0.0 |
| **NL** | 0.0 | 0.0 | 0.4 | 0.0 | 0.0 | 0.0 | 0.0 | 0.0 | 0.0 | **35.4** | 0.0 | 3.6 | 0.2 |
| **NO** | 0.0 | 0.1 | 0.3 | 0.2 | 0.0 | 0.0 | 0.0 | 0.0 | 0.0 | 3.1 | **21.3** | 27.3 | 1.3 |
| **PL** | 0.0 | 0.6 | 1.0 | 0.4 | 0.0 | 0.3 | 0.5 | 0.5 | 0.0 | 6.3 | 0.4 | **1825.3** | 1.6 |
| **PT** | 0.0 | 0.0 | 0.0 | 0.0 | 0.0 | 0.0 | 0.0 | 0.0 | 0.0 | 0.0 | 0.0 | 0.3 | **106.6** |
| **RO** | 0.0 | 0.1 | 0.2 | 0.1 | 0.0 | 3.3 | 1.5 | 3.6 | 0.0 | 0.4 | 0.1 | 50.5 | 0.8 |
| **RS** | 0.0 | 0.0 | 0.1 | 0.0 | 0.0 | 0.1 | 5.5 | 8.0 | 0.0 | 0.2 | 0.0 | 21.3 | 0.3 |
| **RU** | 0.0 | 4.2 | 1.2 | 6.6 | 0.0 | 6.7 | 2.5 | 6.4 | 0.0 | 8.4 | 4.5 | 419.1 | 6.8 |
| **SE** | 0.0 | 0.6 | 0.4 | 0.8 | 0.0 | 0.1 | 0.1 | 0.1 | 0.0 | 4.6 | 5.5 | 75.4 | 1.5 |
| **SI** | 0.0 | 0.0 | 0.0 | 0.0 | 0.0 | 0.0 | 0.1 | 0.1 | 0.0 | 0.1 | 0.0 | 3.7 | 0.3 |
| **SK** | 0.0 | 0.0 | 0.1 | 0.0 | 0.0 | 0.1 | 0.4 | 0.3 | 0.0 | 0.3 | 0.0 | 81.2 | 0.3 |
| **TJ** | 0.0 | 0.0 | 0.0 | 0.0 | 0.0 | 0.0 | 0.0 | 0.0 | 0.0 | 0.0 | 0.0 | 0.3 | 0.0 |
| **TM** | 0.0 | 0.0 | 0.0 | 0.0 | 0.0 | 0.0 | 0.0 | 0.1 | 0.0 | 0.0 | 0.0 | 1.5 | 0.1 |
| **TR** | 0.0 | 0.1 | 0.1 | 0.1 | 0.0 | 1.2 | 0.5 | 2.4 | 0.0 | 0.4 | 0.1 | 21.2 | 1.2 |
| **UA** | 0.0 | 0.5 | 0.4 | 0.4 | 0.0 | 11.6 | 1.1 | 2.3 | 0.0 | 1.7 | 0.3 | 287.9 | 1.5 |
| **UZ** | 0.0 | 0.0 | 0.0 | 0.0 | 0.0 | 0.0 | 0.0 | 0.1 | 0.0 | 0.0 | 0.0 | 1.7 | 0.1 |
| **SUM** | 0.1 | 23.7 | 28.5 | 24.6 | 0.2 | 35.8 | 25.5 | 62.7 | 0.1 | 121.5 | 36.3 | 3653.5 | 197.0 |
| **Emiss 2016** | 0.00 | 0.11 | 0.12 | 0.10 | 0.00 | 0.16 | 0.09 | 0.22 | 0.00 | 0.60 | 0.25 | 10.35 | 1.90 |
| **code** | **LI** | **LT** | **LU** | **LV** | **MC** | **MD** | **ME** | **MK** | **MT** | **NL** | **NO** | **PL** | **PT** |

***Table 3.4**. Matrix of Hg country-to-country deposition from anthropogenic sources in 2017, kg (continued)*

Receptors ↓ Emitters →

| code | RO | RS | RU | SE | SI | SK | TJ | TM | TR | UA | UZ | SUM |
|---|---|---|---|---|---|---|---|---|---|---|---|---|
| **AL** | 0.6 | 5.3 | 0.3 | 0.0 | 0.1 | 0.7 | 0.0 | 0.0 | 1.8 | 1.8 | 0.0 | 52.6 |
| **AM** | 0.1 | 0.1 | 0.6 | 0.0 | 0.0 | 0.1 | 0.0 | 0.1 | 6.8 | 1.7 | 0.0 | 30.3 |
| **AT** | 1.0 | 3.2 | 0.4 | 0.1 | 7.9 | 14.7 | 0.0 | 0.0 | 0.3 | 1.3 | 0.0 | 335.8 |
| **AZ** | 0.2 | 0.2 | 2.5 | 0.0 | 0.0 | 0.1 | 0.0 | 0.6 | 7.0 | 5.4 | 0.3 | 43.6 |
| **BA** | 3.8 | 31.4 | 0.7 | 0.0 | 1.0 | 10.4 | 0.0 | 0.0 | 1.7 | 3.6 | 0.0 | 395.3 |
| **BE** | 0.0 | 0.1 | 0.1 | 0.0 | 0.0 | 0.1 | 0.0 | 0.0 | 0.0 | 0.2 | 0.0 | 162.6 |
| **BG** | 31.9 | 41.8 | 8.7 | 0.1 | 0.5 | 6.0 | 0.0 | 0.0 | 81.6 | 63.2 | 0.1 | 417.4 |
| **BY** | 9.2 | 9.8 | 45.5 | 0.8 | 0.6 | 12.2 | 0.0 | 0.1 | 20.5 | 194.6 | 0.1 | 633.1 |
| **CH** | 0.0 | 0.1 | 0.1 | 0.0 | 0.1 | 0.2 | 0.0 | 0.0 | 0.1 | 0.1 | 0.0 | 156.6 |
| **CY** | 0.0 | 0.1 | 0.1 | 0.0 | 0.0 | 0.0 | 0.0 | 0.0 | 5.6 | 0.4 | 0.0 | 7.8 |
| **CZ** | 1.4 | 4.5 | 0.7 | 0.1 | 1.4 | 32.1 | 0.0 | 0.0 | 0.4 | 2.6 | 0.0 | 683.8 |
| **DE** | 1.0 | 2.0 | 2.7 | 0.6 | 0.8 | 6.5 | 0.0 | 0.0 | 0.8 | 6.6 | 0.0 | 2137 |
| **DK** | 0.1 | 0.2 | 0.6 | 0.6 | 0.0 | 0.4 | 0.0 | 0.0 | 0.1 | 1.1 | 0.0 | 91.3 |
| **EE** | 0.5 | 0.7 | 4.9 | 0.8 | 0.1 | 1.0 | 0.0 | 0.0 | 1.1 | 5.2 | 0.0 | 85.9 |
| **ES** | 0.2 | 0.4 | 0.3 | 0.0 | 0.2 | 0.5 | 0.0 | 0.0 | 0.4 | 0.9 | 0.0 | 393.9 |
| **FI** | 1.7 | 2.5 | 33.0 | 7.5 | 0.3 | 3.9 | 0.0 | 0.0 | 3.1 | 18.3 | 0.1 | 313.9 |
| **FR** | 0.4 | 1.5 | 0.9 | 0.2 | 0.6 | 1.3 | 0.0 | 0.0 | 1.2 | 1.6 | 0.0 | 660.3 |
| **GB** | 0.2 | 0.2 | 1.2 | 0.3 | 0.0 | 0.5 | 0.0 | 0.0 | 0.3 | 1.9 | 0.0 | 538.5 |
| **GE** | 0.9 | 0.8 | 3.2 | 0.0 | 0.0 | 0.4 | 0.0 | 0.1 | 30.0 | 14.3 | 0.1 | 79.1 |
| **GR** | 4.6 | 11.1 | 3.6 | 0.0 | 0.3 | 2.1 | 0.0 | 0.0 | 90.1 | 22.1 | 0.0 | 401.4 |
| **HR** | 3.0 | 17.3 | 0.5 | 0.0 | 5.6 | 10.8 | 0.0 | 0.0 | 0.9 | 2.8 | 0.0 | 205.6 |
| **HU** | 13.6 | 39.1 | 1.8 | 0.1 | 3.2 | 81.7 | 0.0 | 0.0 | 2.4 | 10.6 | 0.0 | 448.6 |
| **IE** | 0.0 | 0.1 | 0.2 | 0.0 | 0.0 | 0.1 | 0.0 | 0.0 | 0.1 | 0.2 | 0.0 | 48.7 |
| **IS** | 0.0 | 0.1 | 0.6 | 0.1 | 0.0 | 0.1 | 0.0 | 0.0 | 0.1 | 0.5 | 0.0 | 15.6 |
| **IT** | 2.5 | 7.8 | 1.1 | 0.1 | 5.7 | 5.6 | 0.0 | 0.0 | 4.4 | 4.3 | 0.0 | 1086.5 |
| **KY** | 0.2 | 0.3 | 2.4 | 0.0 | 0.0 | 0.2 | 4.0 | 0.8 | 4.6 | 4.3 | 122.2 | 220.6 |
| **KZ** | 7.8 | 6.3 | 284.5 | 0.7 | 0.5 | 6.0 | 5.1 | 9.5 | 73.7 | 350.6 | 182.1 | 3140.2 |
| **LI** | 0.0 | 0.0 | 0.0 | 0.0 | 0.0 | 0.0 | 0.0 | 0.0 | 0.0 | 0.0 | 0.0 | 0.7 |
| **LT** | 1.8 | 2.3 | 7.8 | 0.6 | 0.2 | 3.6 | 0.0 | 0.0 | 1.5 | 16.4 | 0.0 | 176.5 |
| **LU** | 0.0 | 0.0 | 0.0 | 0.0 | 0.0 | 0.0 | 0.0 | 0.0 | 0.0 | 0.0 | 0.0 | 11.5 |
| **LV** | 1.5 | 2.1 | 7.8 | 0.9 | 0.2 | 2.7 | 0.0 | 0.0 | 2.1 | 13.3 | 0.0 | 140.3 |
| **MC** | 0.0 | 0.0 | 0.0 | 0.0 | 0.0 | 0.0 | 0.0 | 0.0 | 0.0 | 0.0 | 0.0 | 0 |
| **MD** | 5.3 | 1.2 | 4.8 | 0.0 | 0.1 | 1.2 | 0.0 | 0.0 | 12.5 | 66.7 | 0.0 | 119.2 |
| **ME** | 0.5 | 6.1 | 0.1 | 0.0 | 0.1 | 1.0 | 0.0 | 0.0 | 0.7 | 0.8 | 0.0 | 42.9 |
| **MK** | 1.2 | 9.3 | 0.4 | 0.0 | 0.1 | 1.0 | 0.0 | 0.0 | 6.2 | 3.0 | 0.0 | 75.1 |
| **MT** | 0.0 | 0.0 | 0.0 | 0.0 | 0.0 | 0.0 | 0.0 | 0.0 | 0.0 | 0.0 | 0.0 | 0.1 |
| **NL** | 0.0 | 0.1 | 0.3 | 0.1 | 0.0 | 0.2 | 0.0 | 0.0 | 0.0 | 0.3 | 0.0 | 156.5 |
| **NO** | 0.6 | 0.9 | 9.9 | 6.2 | 0.1 | 1.9 | 0.0 | 0.0 | 1.2 | 9.1 | 0.1 | 196.5 |
| **PL** | 9.6 | 17.7 | 14.6 | 1.4 | 2.2 | 69.2 | 0.0 | 0.0 | 4.5 | 78.0 | 0.1 | 2751.4 |
| **PT** | 0.0 | 0.0 | 0.0 | 0.0 | 0.0 | 0.0 | 0.0 | 0.0 | 0.0 | 0.1 | 0.0 | 125.4 |
| **RO** | **212.7** | 63.5 | 16.8 | 0.2 | 1.8 | 26.7 | 0.0 | 0.1 | 65.7 | 139.5 | 0.1 | 764.7 |
| **RS** | 16.1 | **261.3** | 2.0 | 0.1 | 0.8 | 16.4 | 0.0 | 0.0 | 10.2 | 11.6 | 0.0 | 478.3 |
| **RU** | 55.6 | 54.4 | **4539.3** | 12.2 | 4.2 | 48.1 | 3.0 | 11.0 | 536.6 | 2897.4 | 78.8 | 11344.4 |
| **SE** | 1.0 | 1.9 | 17.7 | **41.5** | 0.3 | 4.1 | 0.0 | 0.0 | 1.6 | 12.4 | 0.1 | 381 |
| **SI** | 0.8 | 2.6 | 0.1 | 0.0 | **17.5** | 2.4 | 0.0 | 0.0 | 0.2 | 0.7 | 0.0 | 85.9 |
| **SK** | 5.3 | 14.1 | 1.5 | 0.1 | 1.4 | **162.7** | 0.0 | 0.0 | 1.1 | 8.2 | 0.0 | 418.3 |
| **TJ** | 0.1 | 0.1 | 0.9 | 0.0 | 0.0 | 0.1 | **13.2** | 0.7 | 2.2 | 1.7 | 29.5 | 56.3 |
| **TM** | 0.4 | 0.3 | 7.0 | 0.0 | 0.0 | 0.3 | 1.2 | **21.3** | 6.4 | 13.3 | 41.6 | 120 |
| **TR** | 15.1 | 14.3 | 31.8 | 0.2 | 0.6 | 5.3 | 0.0 | 0.3 | **2272.7** | 157.9 | 0.4 | 2663.7 |
| **UA** | 45.9 | 32.0 | 167.7 | 0.8 | 2.1 | 45.6 | 0.0 | 0.4 | 153.8 | **3221.0** | 0.7 | 4248.2 |
| **UZ** | 0.4 | 0.4 | 9.3 | 0.0 | 0.0 | 0.3 | 5.5 | 4.0 | 7.0 | 18.2 | **213.0** | 320.4 |
| **SUM** | 459.0 | 671.4 | 5241.1 | 76.6 | 60.7 | 590.4 | 32.1 | 49.3 | 3425.2 | 7389.9 | 669.7 | |
| **Emiss 2016** | 1.45 | 1.94 | 26.48 | 0.41 | 0.17 | 1.73 | 0.57 | 0.41 | 15.82 | 24.16 | 5.85 | |
| **code** | RO | RS | RU | SE | SI | SK | TJ | TM | TR | UA | UZ | |

# 4. EVALUATION OF MODELLING RESULTS VS. OBSERVATIONS

## 4.1. Lead

### *4.1.1. Air concentrations*

***Table 4.1.*** *Annual mean modelled and observed Pb air concentrations, ng/m$^3$, temporal correlation coefficient (Rc and relative bias (Bias) at EMEP stations in 2017*

| Station name | Code | Longitude | Latitude | Observed | Modelled | Rc | Bias |
|---|---|---|---|---|---|---|---|
| Koksijde | BE0014R | 2.66 | 51.12 | 5.31 | 6.22 | 0.91 | 16.7 |
| Ayia Maria | CY0002R | 33.06 | 35.04 | 0.28 | 7.29 | -0.04 | 2493.4 |
| Kosetice (NOAK) | CZ0003R | 15.08 | 49.57 | 2.79 | 2.77 | 0.69 | -0.8 |
| Churanov | CZ0005R | 13.6 | 49.07 | 1.44 | 1.68 | 0.77 | 16.2 |
| Westerland | DE0001R | 8.31 | 54.93 | 1.78 | 2.05 | 0.69 | 14.4 |
| Waldhof | DE0002R | 10.76 | 52.8 | 3.47 | 3.39 | 0.82 | -2.9 |
| Schauinsland | DE0003R | 7.91 | 47.91 | 1.10 | 2.80 | 0.31 | 155.1 |
| Neuglobsow | DE0007R | 13.03 | 53.17 | 3.25 | 2.88 | 0.86 | -12.4 |
| Schmucke | DE0008R | 10.77 | 50.65 | 1.66 | 2.75 | 0.84 | 65.0 |
| Zingst | DE0009R | 12.72 | 54.44 | 2.69 | 2.62 | 0.83 | -3.6 |
| Anholt | DK0008R | 11.52 | 56.72 | 1.16 | 1.48 | 0.72 | 26.2 |
| Riscoe | DK0012R | 12.09 | 55.69 | 1.72 | 3.25 | 0.9 | 87.2 |
| Lahemaa | EE0009R | 25.9 | 59.5 | 0.92 | 0.68 | 0.62 | -26.5 |
| San Pablo de los Montes | ES0001R | -4.35 | 39.55 | 1.44 | 1.62 | 0.44 | 12.7 |
| Viznar | ES0007R | -3.53 | 37.23 | 1.46 | 1.74 | 0.16 | 18.6 |
| Niembro | ES0008R | -4.85 | 43.44 | 3.85 | 1.79 | -0.37 | -53.6 |
| Campisabalos | ES0009R | -3.14 | 41.28 | 0.91 | 1.32 | 0.79 | 45.1 |
| ElTorms | ES0014R | 0.72 | 41.4 | 1.19 | 3.03 | 0.37 | 155 |
| Virolahti III | FI0018R | 27.67 | 60.53 | 1.05 | 0.73 | 0.59 | -30.4 |
| Pallas (Matorova) | FI0036R | 24.24 | 68 | 0.45 | 0.14 | 0.01 | -69.4 |
| Hyytiälä | FI0050R | 24.28 | 61.85 | 0.74 | 0.25 | 0.67 | -65.6 |
| Revin | FR0009R | 4.63 | 49.9 | 3.64 | 2.38 | 0.71 | -32.8 |
| Peyrusse Vieille | FR0013R | 0.18 | 43.62 | 1.49 | 1.01 | 0.69 | -32.9 |
| Saint-Nazaire-le-Desert | FR0023R | 5.28 | 44.57 | 1.37 | 1.17 | 0.09 | -14.8 |
| Guipry | FR0024R | -1.84 | 47.83 | 1.75 | 1.58 | 0.87 | -10.1 |
| Verneuil | FR0025R | 2.61 | 46.81 | 1.80 | 1.28 | 0.86 | -27.8 |
| Yarner Wood | GB0013R | -3.71 | 50.6 | 1.63 | 1.23 | 0.72 | -24.2 |
| Heigham Holmes | GB0017R | 1.62 | 52.72 | 4.00 | 3.29 | 0.72 | -17.3 |
| Auchencorth Moss | GB0048R | -3.24 | 55.79 | 1.04 | 0.94 | 0.87 | -9.8 |
| Chilbolton Observatory | GB1055 | -1.44 | 51.15 | 3.83 | 1.85 | 0.63 | -51.6 |
| K-puszta | HU0002R | 19.58 | 46.97 | 6.95 | 3.85 | 0.5 | -45.1 |
| Vestmannaeyjar | IS0091R | -20.28 | 63.4 | 0.11 | 0.65 | 0.86 | 442.7 |
| Rucava | LV0010R | 21.17 | 56.16 | 0.98 | 1.46 | -0.37 | 46.4 |
| Bilthoven | NL0008R | 5.2 | 52.12 | 4.16 | 4.01 | 0.75 | -2.5 |
| Birkenes II | NO0002R | 8.25 | 58.39 | 0.53 | 0.45 | 0.64 | -14.6 |
| Zeppelin mountain (Ny-Alesund) | NO0042G | 11.89 | 78.91 | 0.28 | 0.22 | -0.23 | -24.8 |
| Alomar | NO0090R | 16.01 | 69.28 | 0.22 | 0.34 | -0.61 | 27.1 |
| Diabla Gora | PL0005R | 22.07 | 54.15 | 2.64 | 3.36 | 0.82 | 27 |
| Zielonka | PL0009R | 17.93 | 53.66 | 4.15 | 4.38 | 0.81 | 6.9 |
| Bredkälen | SE0005R | 15.33 | 63.85 | 0.23 | 0.15 | 0.49 | -37 |
| Aspvreten | SE0012R | 17.38 | 58.8 | 0.89 | 0.52 | 0.82 | -39 |
| Råö | SE0014R | 11.91 | 57.39 | 1.04 | 1.00 | 0.68 | -4.6 |
| Hallahus | SE0020R | 13.15 | 56.04 | 1.19 | 1.84 | 0.52 | 61.4 |
| Iskrba | SI0008R | 14.87 | 45.57 | 1.81 | 2.15 | 0.61 | 16.6 |

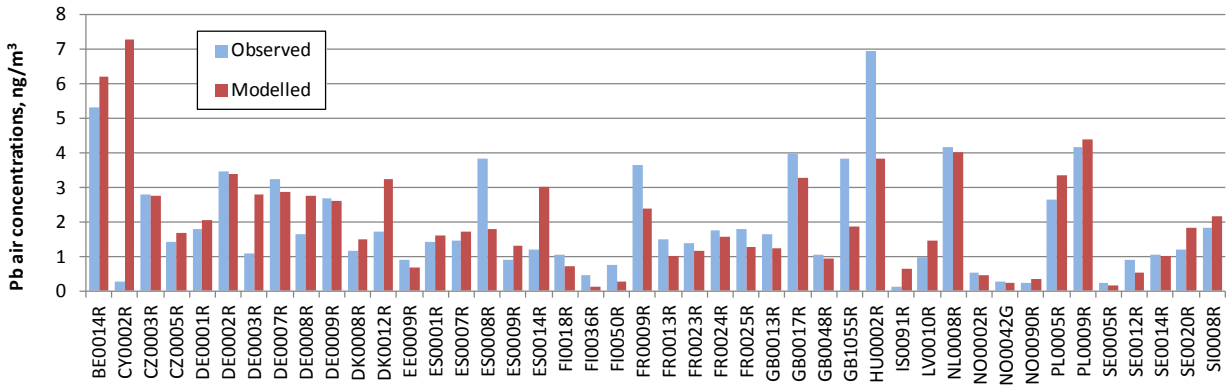


***Fig. 4.1.*** *Modelled and observed annual mean concentrations of Pb in air at the EMEP stations in 2017*

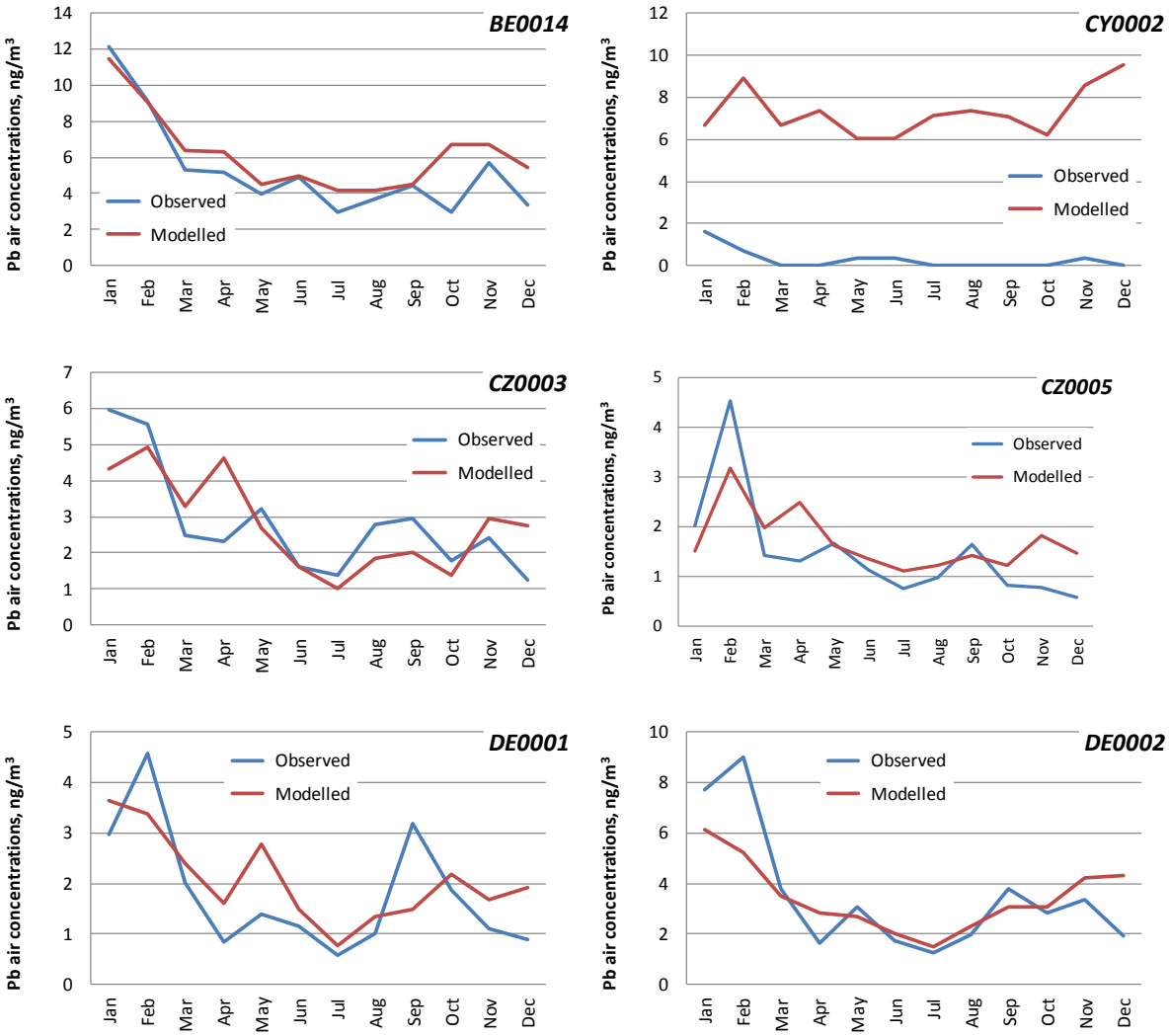

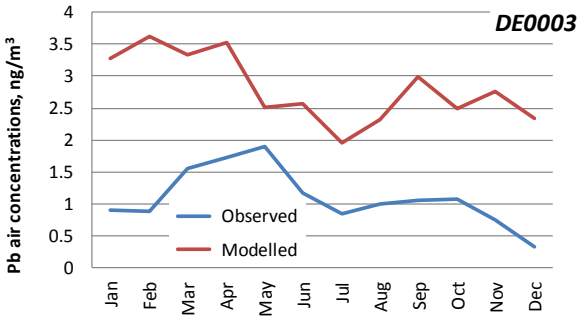
DE0003
Pb air concentrations, ng/m³
Observed
Modelled
Jan Feb Mar Apr May Jun Jul Aug Sep Oct Nov Dec

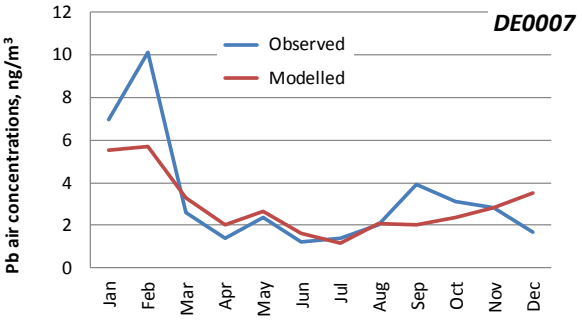
DE0007
Pb air concentrations, ng/m³
Observed
Modelled
Jan Feb Mar Apr May Jun Jul Aug Sep Oct Nov Dec

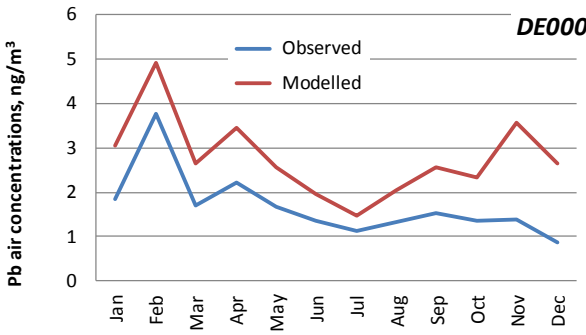
DE0008
Pb air concentrations, ng/m³
Observed
Modelled
Jan Feb Mar Apr May Jun Jul Aug Sep Oct Nov Dec

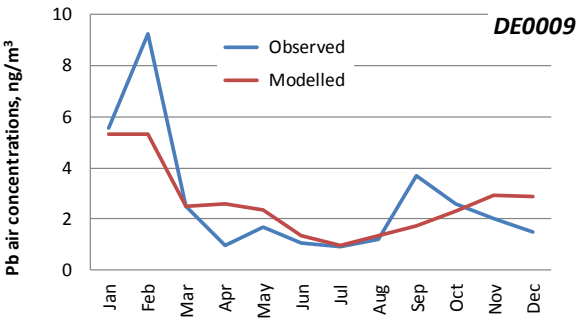
DE0009
Pb air concentrations, ng/m³
Observed
Modelled
Jan Feb Mar Apr May Jun Jul Aug Sep Oct Nov Dec

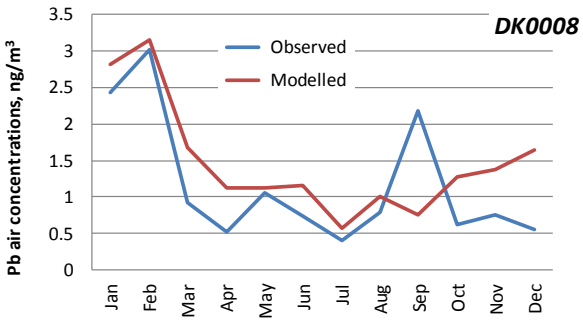
DK0008
Pb air concentrations, ng/m³
Observed
Modelled
Jan Feb Mar Apr May Jun Jul Aug Sep Oct Nov Dec

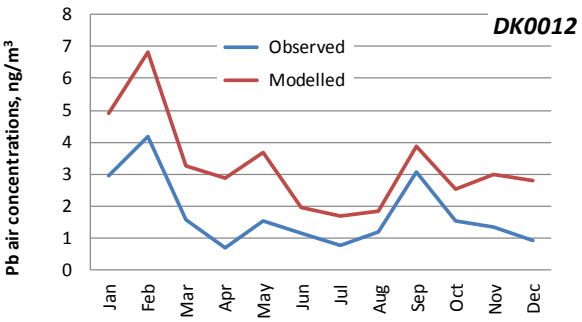
DK0012
Pb air concentrations, ng/m³
Observed
Modelled
Jan Feb Mar Apr May Jun Jul Aug Sep Oct Nov Dec

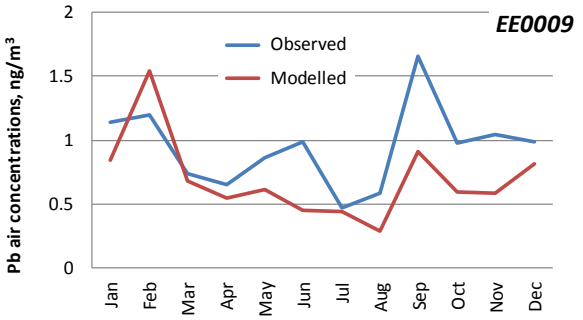
EE0009
Pb air concentrations, ng/m³
Observed
Modelled
Jan Feb Mar Apr May Jun Jul Aug Sep Oct Nov Dec

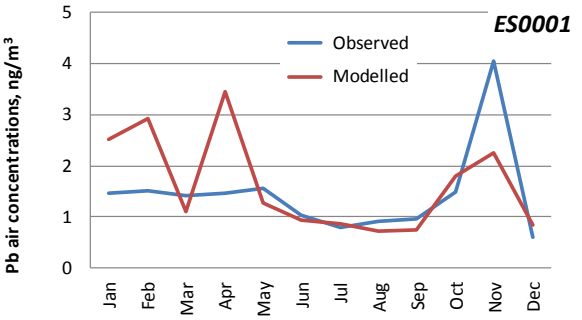
ES0001
Pb air concentrations, ng/m³
Observed
Modelled
Jan Feb Mar Apr May Jun Jul Aug Sep Oct Nov Dec

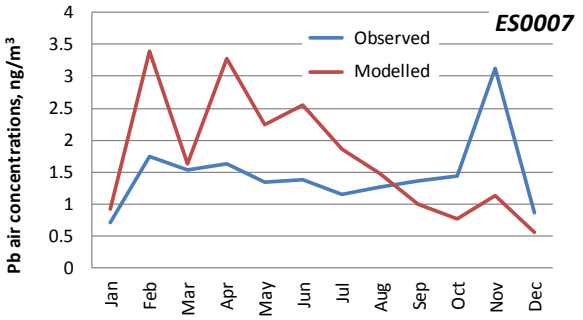
ES0007
Pb air concentrations, ng/m³
Observed
Modelled
Jan Feb Mar Apr May Jun Jul Aug Sep Oct Nov Dec

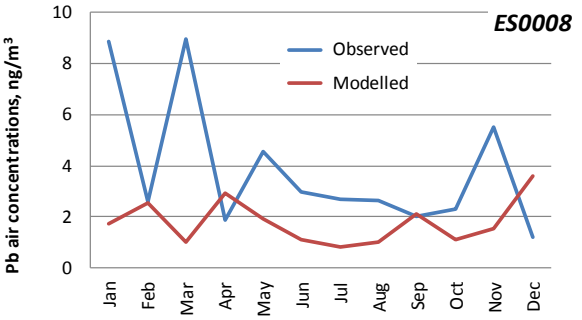
ES0008
Pb air concentrations, ng/m³
Observed
Modelled
Jan Feb Mar Apr May Jun Jul Aug Sep Oct Nov Dec

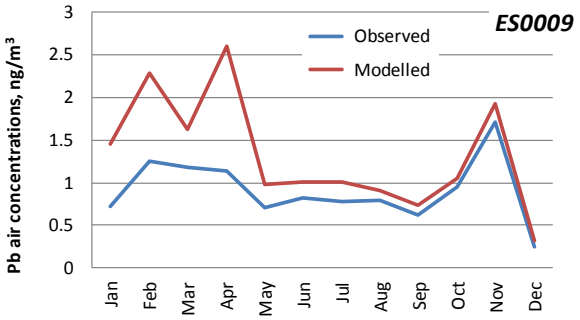
ES0009
Observed
Modelled
Pb air concentrations, ng/m³
0
0.5
1
1.5
2
2.5
3
Jan
Feb
Mar
Apr
May
Jun
Jul
Aug
Sep
Oct
Nov
Dec

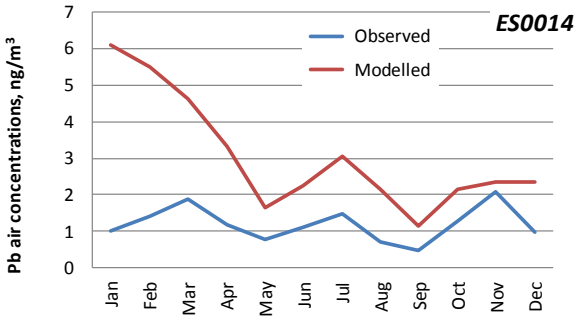
ES0014
Observed
Modelled
Pb air concentrations, ng/m³
0
1
2
3
4
5
6
7
Jan
Feb
Mar
Apr
May
Jun
Jul
Aug
Sep
Oct
Nov
Dec

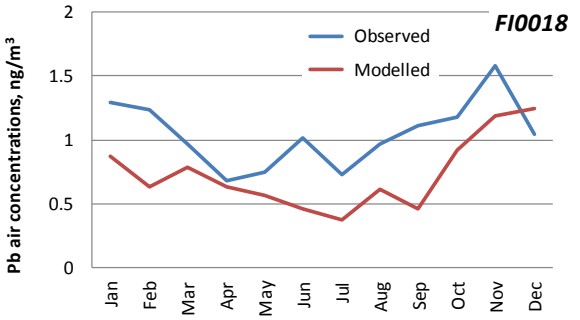
FI0018
Observed
Modelled
Pb air concentrations, ng/m³
0
0.5
1
1.5
2
Jan
Feb
Mar
Apr
May
Jun
Jul
Aug
Sep
Oct
Nov
Dec

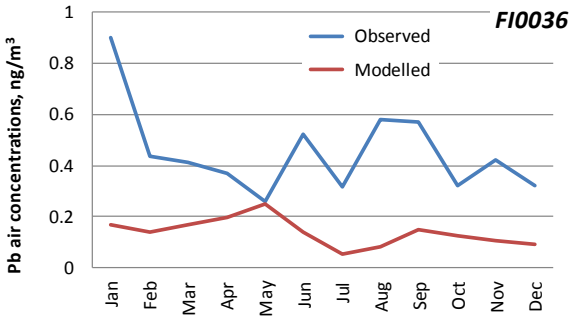
FI0036
Observed
Modelled
Pb air concentrations, ng/m³
0
0.2
0.4
0.6
0.8
1
Jan
Feb
Mar
Apr
May
Jun
Jul
Aug
Sep
Oct
Nov
Dec

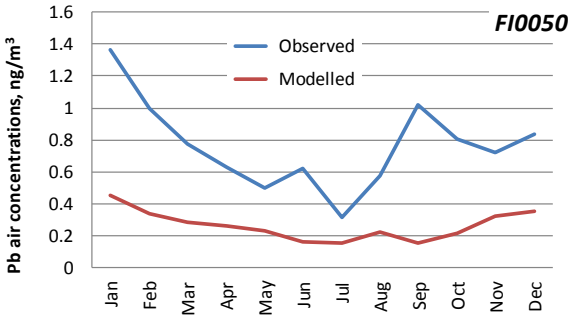
FI0050
Observed
Modelled
Pb air concentrations, ng/m³
0
0.2
0.4
0.6
0.8
1
1.2
1.4
1.6
Jan
Feb
Mar
Apr
May
Jun
Jul
Aug
Sep
Oct
Nov
Dec

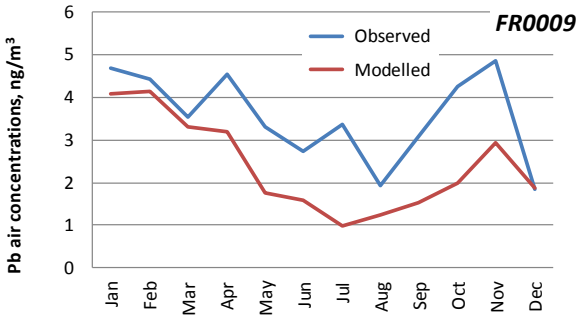
FR0009
Observed
Modelled
Pb air concentrations, ng/m³
0
1
2
3
4
5
6
Jan
Feb
Mar
Apr
May
Jun
Jul
Aug
Sep
Oct
Nov
Dec

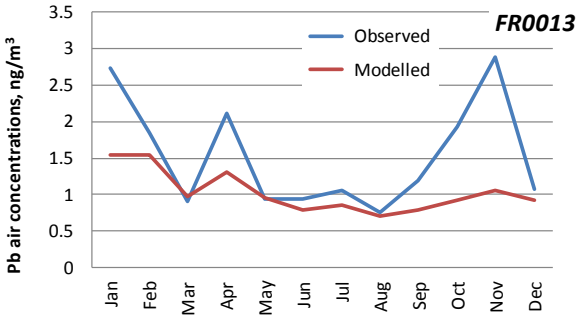
FR0013
Observed
Modelled
Pb air concentrations, ng/m³
0
0.5
1
1.5
2
2.5
3
3.5
Jan
Feb
Mar
Apr
May
Jun
Jul
Aug
Sep
Oct
Nov
Dec

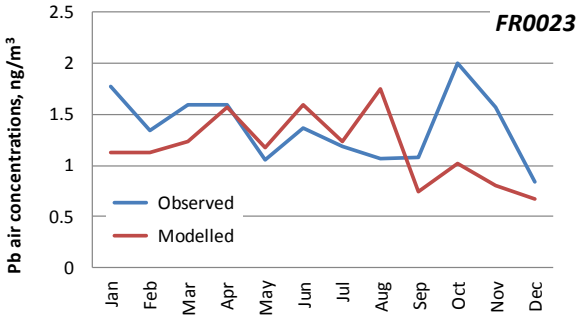
FR0023
Observed
Modelled
Pb air concentrations, ng/m³
0
0.5
1
1.5
2
2.5
Jan
Feb
Mar
Apr
May
Jun
Jul
Aug
Sep
Oct
Nov
Dec

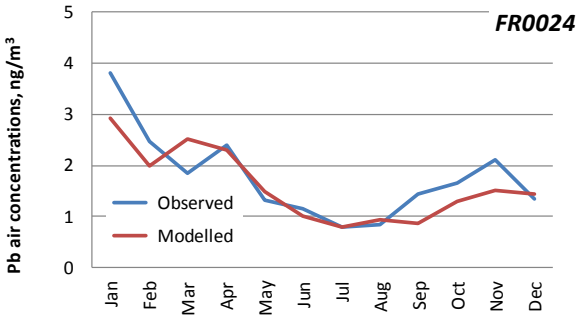
FR0024
Observed
Modelled
Pb air concentrations, ng/m³
0
1
2
3
4
5
Jan
Feb
Mar
Apr
May
Jun
Jul
Aug
Sep
Oct
Nov
Dec

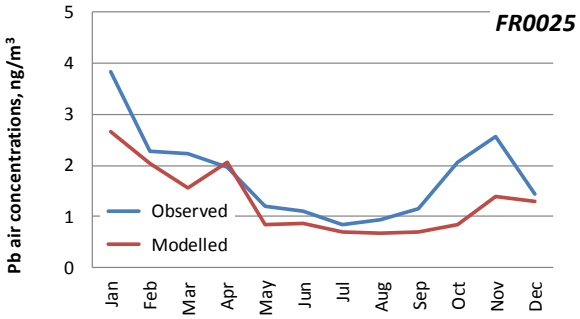
FR0025
Observed
Modelled
Pb air concentrations, ng/m³
0
1
2
3
4
5
Jan
Feb
Mar
Apr
May
Jun
Jul
Aug
Sep
Oct
Nov
Dec

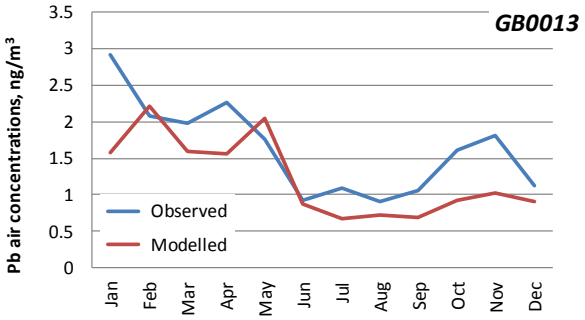
GB0013
Pb air concentrations, ng/m³
Observed
Modelled
Jan Feb Mar Apr May Jun Jul Aug Sep Oct Nov Dec

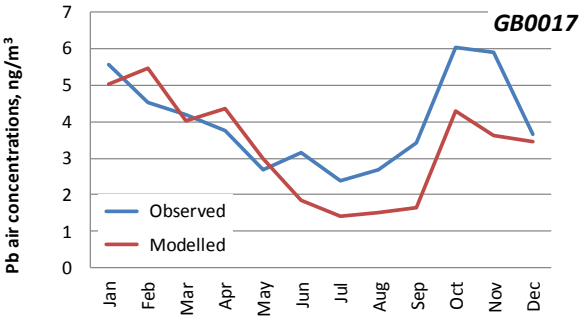
GB0017
Pb air concentrations, ng/m³
Observed
Modelled
Jan Feb Mar Apr May Jun Jul Aug Sep Oct Nov Dec

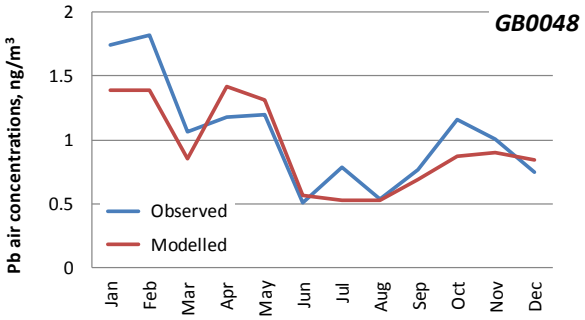
GB0048
Pb air concentrations, ng/m³
Observed
Modelled
Jan Feb Mar Apr May Jun Jul Aug Sep Oct Nov Dec

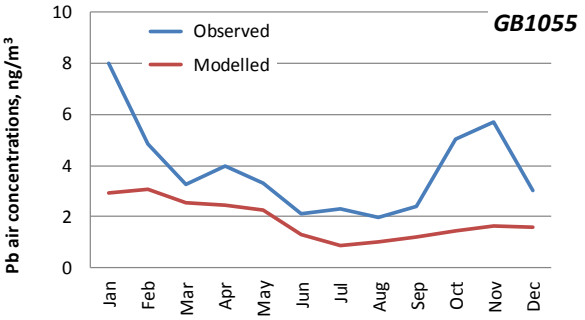
GB1055
Pb air concentrations, ng/m³
Observed
Modelled
Jan Feb Mar Apr May Jun Jul Aug Sep Oct Nov Dec

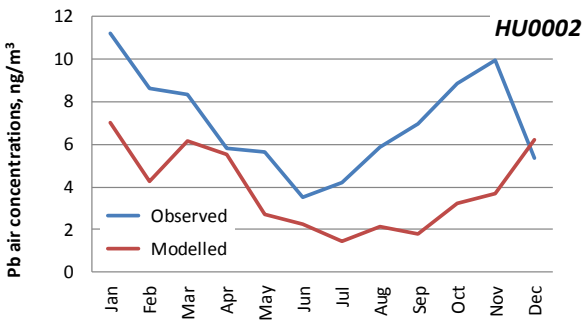
HU0002
Pb air concentrations, ng/m³
Observed
Modelled
Jan Feb Mar Apr May Jun Jul Aug Sep Oct Nov Dec

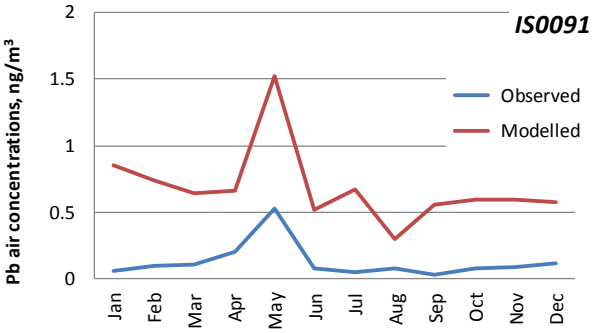
IS0091
Pb air concentrations, ng/m³
Observed
Modelled
Jan Feb Mar Apr May Jun Jul Aug Sep Oct Nov Dec

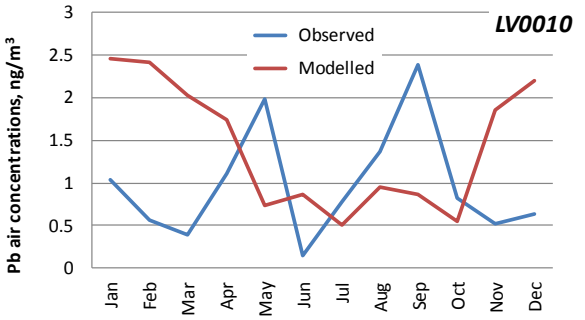
LV0010
Pb air concentrations, ng/m³
Observed
Modelled
Jan Feb Mar Apr May Jun Jul Aug Sep Oct Nov Dec

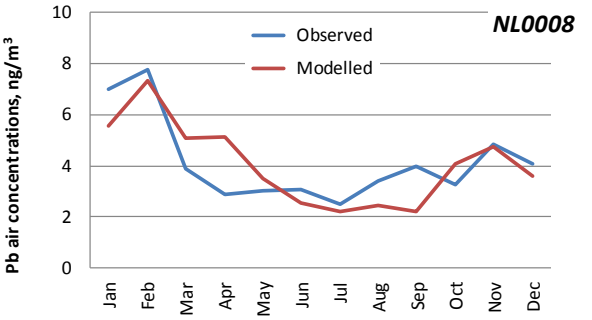
NL0008
Pb air concentrations, ng/m³
Observed
Modelled
Jan Feb Mar Apr May Jun Jul Aug Sep Oct Nov Dec

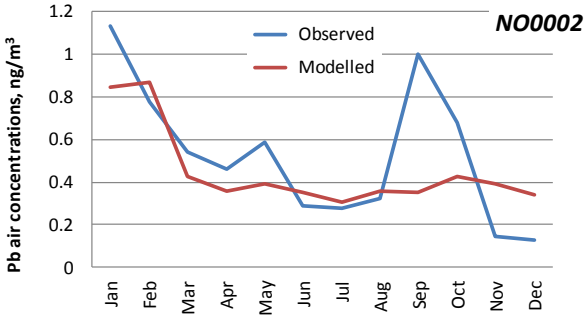
NO0002
Pb air concentrations, ng/m³
Observed
Modelled
Jan Feb Mar Apr May Jun Jul Aug Sep Oct Nov Dec

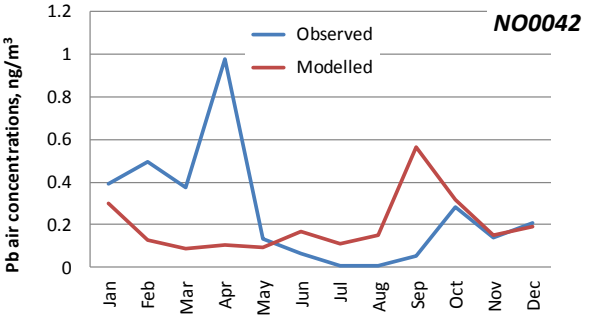
NO0042
Pb air concentrations, ng/m³
Observed
Modelled
Jan Feb Mar Apr May Jun Jul Aug Sep Oct Nov Dec

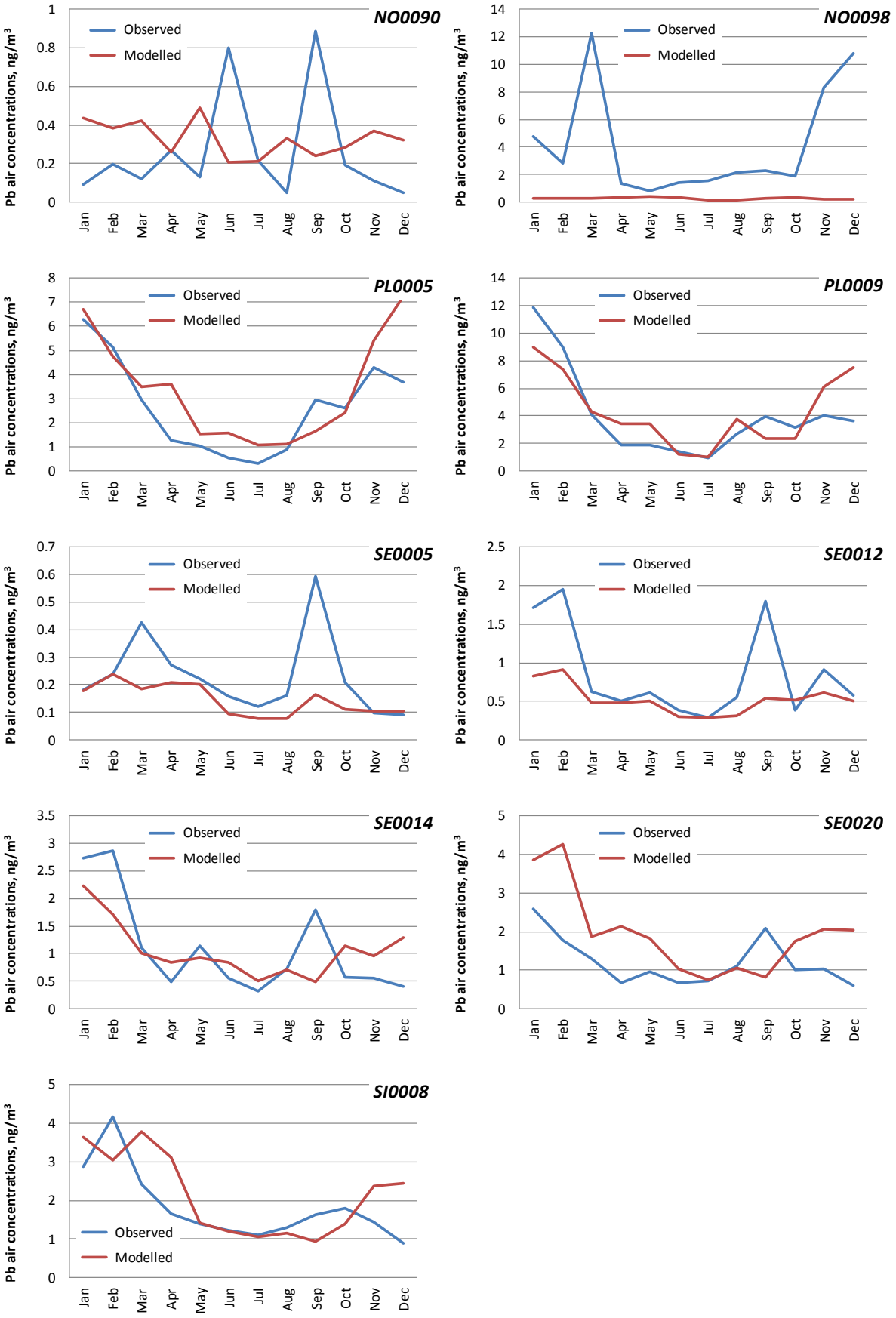


***Fig. 4.2.*** *Modelled and observed monthly mean concentrations of Pb in air at the EMEP stations in 2017*

### *4.1.2. Wet deposition*

***Table 4.2.*** *Annual sums of modelled and observed Pb wet deposition fluxes, g/km$^2$/y, temporal correlation coefficient (Rc) and relative bias (Bias) at EMEP stations in 2017*

| Station name | Code | Longit | Latit | Observed flux | Modelled flux | Observed precip | Modelled precip | R | Bias |
|---|---|---|---|---|---|---|---|---|---|
| Koksijde | BE0014R | 2.66 | 51.12 | 317.6 | 307.9 | 555.9 | 567.5 | 0.45 | -3.1 |
| Kosetice (NOAK) | CZ0003R | 15.08 | 49.57 | 382.1 | 268.9 | 586.1 | 613.7 | 0.79 | -29.6 |
| Churanov | CZ0005R | 13.6 | 49.07 | 270.7 | 207.4 | 768.6 | 765.8 | 0.64 | -23.4 |
| Westerland | DE0001R | 8.31 | 54.93 | 180.6 | 270.5 | 708.9 | 1002.4 | 0.48 | 49.8 |
| Waldhof | DE0002R | 10.76 | 52.8 | 369.1 | 302.4 | 797.2 | 541.1 | 0.31 | -18.1 |
| Schauinsland | DE0003R | 7.91 | 47.91 | 378.4 | 368.2 | 1587.1 | 1354.0 | 0.28 | -2.7 |
| Neuglobsow | DE0007R | 13.03 | 53.17 | 342.7 | 264.9 | 771.4 | 603.6 | 0.57 | -22.7 |
| Schmucke | DE0008R | 10.77 | 50.65 | 558.2 | 378.0 | 1382.5 | 971.4 | 0.35 | -32.3 |
| Zingst | DE0009R | 12.72 | 54.44 | 231.8 | 145.3 | 572.1 | 368.3 | -0.15 | -37.3 |
| Keldsnor | DK0005R | 10.74 | 54.75 | 603.7 | 132.3 | 536.6 | 326.4 | 0.53 | -78.1 |
| Anholt | DK0008R | 11.52 | 56.72 | 279.5 | 192.9 | 729.8 | 627.4 | 0.23 | -31 |
| Riscoe | DK0012R | 12.09 | 55.69 | 309.5 | 270.6 | 706.1 | 672.1 | 0.16 | -12.6 |
| Sepstrup Sande | DK0022R | 9.42 | 56.08 | 689.4 | 232.3 | 1043.2 | 478.5 | -0.01 | -66.3 |
| Lahemaa | EE0009R | 25.9 | 59.5 | 377.6 | 109.0 | 776.2 | 510.2 | 0.48 | -71.1 |
| Vilsandi | EE0011R | 21.82 | 58.38 | 419.1 | 195.1 | 683.0 | 817.2 | 0.22 | -53.4 |
| Niembro | ES0008R | -4.85 | 43.44 | 844.6 | 152.6 | 1068.9 | 334.6 | 0.02 | -81.9 |
| Campisabalos | ES0009R | -3.14 | 41.28 | 214.3 | 88.5 | 274.2 | 242.8 | 0.54 | -58.7 |
| Virolahti III | FI0018R | 27.67 | 60.53 | 456.1 | 218.7 | 816.4 | 719.2 | 0.89 | -52.1 |
| Pallas (Matorova) | FI0036R | 24.24 | 68 | 87.8 | 34.0 | 557.6 | 587.0 | 0.55 | -61.3 |
| Hyytiälä | FI0050R | 24.28 | 61.85 | 166.3 | 96.6 | 594.2 | 602.4 | 0.60 | -41.9 |
| Hailuoto II | FI0053R | 24.69 | 65 | 89.8 | 65.9 | 376.9 | 470.5 | 0.87 | -26.6 |
| Hietajärvi | FI0092R | 30.72 | 63.17 | 191.2 | 107.2 | 701.0 | 729.5 | 0.75 | -44 |
| Kotinen | FI0093R | 25.07 | 61.23 | 160.0 | 89.8 | 598.9 | 556.4 | 0.61 | -43.9 |
| Revin | FR0009R | 4.63 | 49.9 | 724.6 | 308.0 | 1047.8 | 736.8 | 0.55 | -57.5 |
| Peyrusse Vieille | FR0013R | 0.18 | 43.62 | 357.4 | 134.1 | 665.5 | 429.0 | -0.11 | -62.5 |
| Saint-Nazaire-le-Desert | FR0023R | 5.28 | 44.57 | 738.6 | 215.3 | 679.2 | 640.3 | 0.72 | -70.8 |
| Guipry | FR0024R | -1.84 | 47.83 | 433.5 | 96.2 | 456.5 | 391.0 | 0.52 | -77.8 |
| Verneuil | FR0025R | 2.61 | 46.81 | 504.2 | 162.0 | 655.7 | 648.9 | 0.36 | -67.9 |
| Lough Navar | GB0006R | -7.87 | 54.44 | 99.4 | 70.1 | 739.3 | 418.0 | 0.90 | -29.4 |
| Yarner Wood | GB0013R | -3.71 | 50.6 | 150.3 | 102.7 | 712.7 | 414.7 | 0.85 | -31.7 |
| Heigham Holmes | GB0017R | 1.62 | 52.72 | 223.5 | 126.8 | 444.5 | 334.6 | 0.82 | -43.3 |
| Auchencorth Moss | GB0048R | -3.24 | 55.79 | 54.7 | 62.0 | 363.0 | 283.0 | 0.70 | 13.3 |
| Chilbolton Observatory | GB1055 | -1.44 | 51.15 | 134.5 | 108.6 | 527.4 | 459.9 | 0.51 | -19.2 |
| K-puszta | HU0002R | 19.58 | 46.97 | 641.3 | 337.6 | 688.6 | 627.6 | 0.21 | -47.4 |
| Vestmannaeyjar | IS0091R | -20.28 | 63.4 | 578.3 | 266.6 | 1365.0 | 1395.0 | -0.06 | -53.9 |
| Rucava | LV0010R | 21.17 | 56.16 | 216.1 | 162.4 | 472.9 | 649.6 | 0.77 | -24.9 |
| Aluksne | LV1000R | 27.04 | 57.44 | 185.5 | 82.9 | 428.4 | 361.6 | 0.50 | -55.3 |
| Dobele | LV2000R | 23.32 | 56.62 | 127.9 | 72.5 | 319.6 | 228.4 | 0.43 | -43.3 |
| Skriveri | LV5000R | 25.13 | 56.64 | 166.3 | 163.5 | 415.7 | 486.1 | 0.81 | -1.7 |
| Riga | LV6000R | 24.1 | 56.95 | 724.4 | 140.2 | 220.8 | 273.9 | 0.30 | -80.6 |
| Vredepeel | NL0010R | 5.85 | 51.54 | 424.8 | 323.9 | 392.8 | 469.0 | 0.41 | -23.8 |
| De Zilk | NL0091R | 4.5 | 52.3 | 178.6 | 132.6 | 266.6 | 208.1 | 0.06 | -25.7 |
| Birkenes | NO0001R | 8.25 | 58.38 | 685.4 | 243.5 | 1496.2 | 1024.0 | 0.71 | -64.5 |
| Kårvatn | NO0039R | 8.88 | 62.78 | 106.0 | 109.7 | 1575.8 | 1826.7 | 0.40 | 3.5 |
| Hurdal | NO00056R | 11.08 | 60.37 | 301.9 | 104.9 | 879.4 | 703.6 | 0.46 | -65.3 |
| Leba | PL0004R | 17.53 | 54.75 | 211.0 | 315.2 | 829.8 | 837.6 | 0.62 | 49.4 |
| Diabla Gora | PL0005R | 22.07 | 54.15 | 474.2 | 480.1 | 838.5 | 876.3 | 0.41 | 1.2 |
| Bredkälen | SE0005R | 15.33 | 63.85 | 32.1 | 49.5 | 440.4 | 583.5 | -0.06 | 54.3 |
| Aspvreten | SE0012R | 17.38 | 58.8 | 130.9 | 129.0 | 451.6 | 543.8 | 0.50 | -1.4 |
| Råö | SE0014R | 11.91 | 57.39 | 220.0 | 269.8 | 695.8 | 914.0 | 0.12 | 22.6 |
| Hallahus | SE0020R | 13.15 | 56.04 | 286.1 | 300.7 | 843.9 | 926.4 | 0.55 | 5.1 |
| Iskrba | SI0008R | 14.87 | 45.57 | 322.9 | 377.0 | 867.8 | 795.6 | 0.34 | 16.8 |

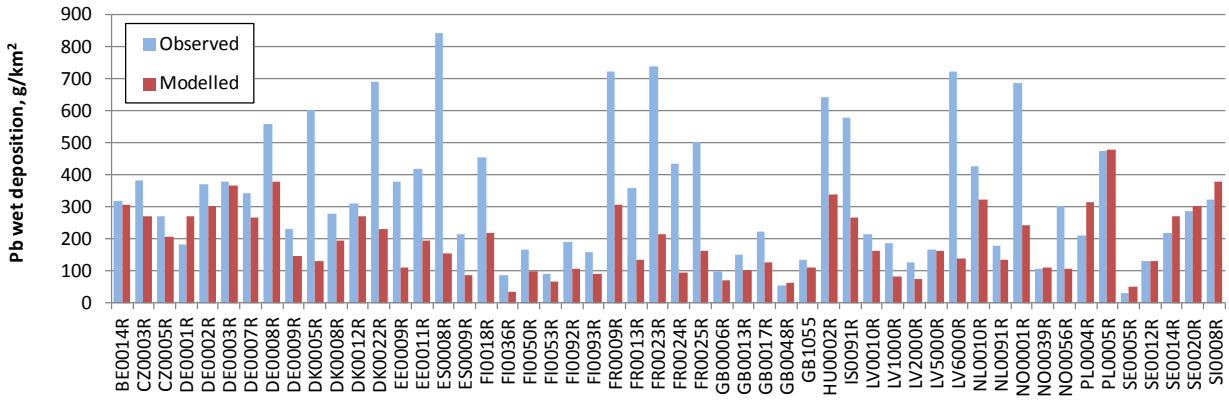


***Fig. 4.3.*** *Modelled and observed annual wet deposition fluxes of Pb at the EMEP stations in 2017*

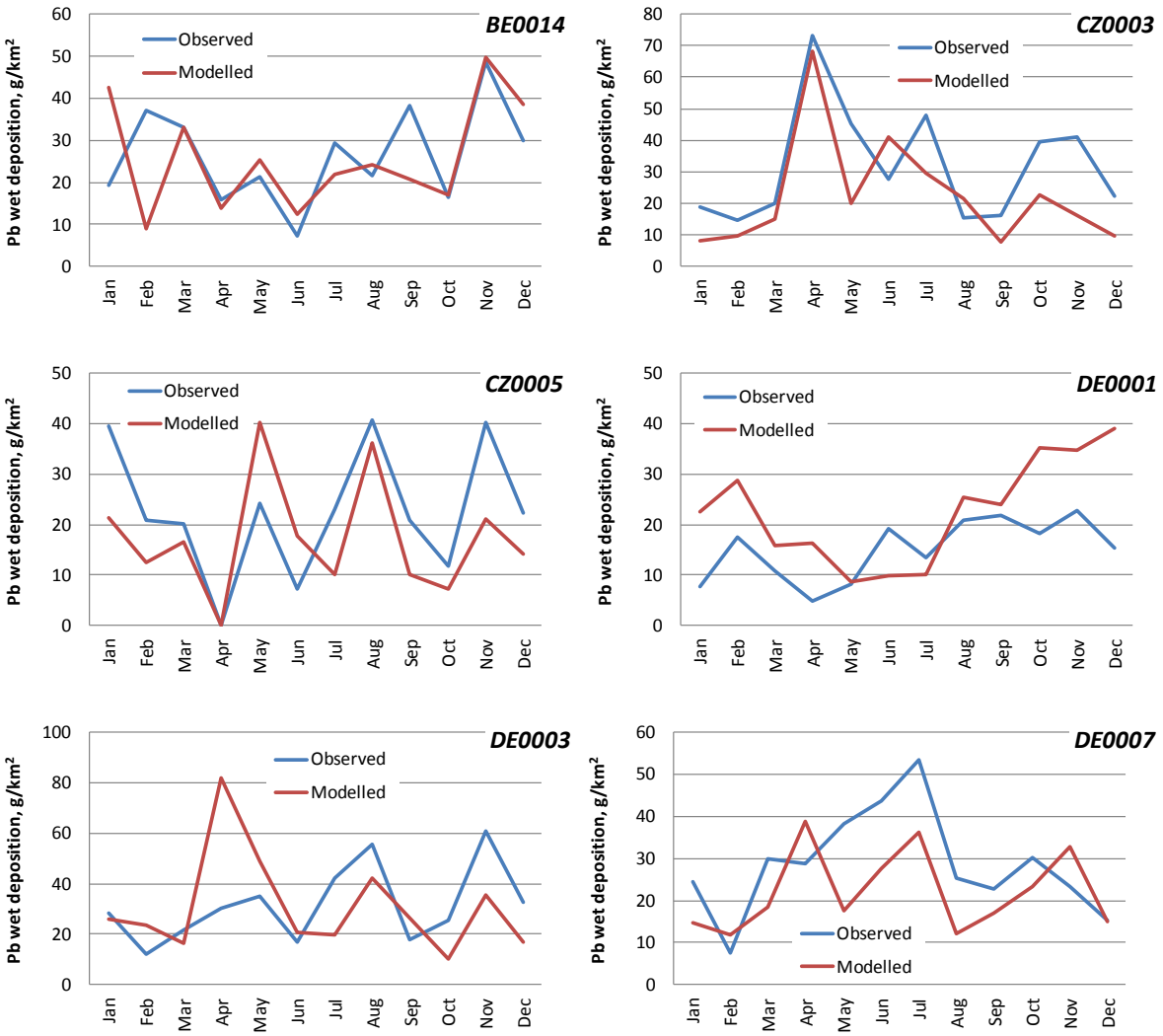

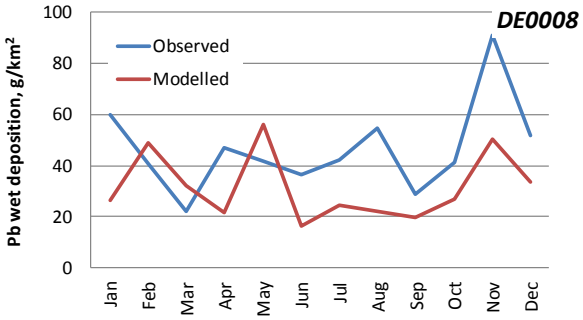
DE0008
Observed
Modelled
Pb wet deposition, g/km²
0
20
40
60
80
100
Jan Feb Mar Apr May Jun Jul Aug Sep Oct Nov Dec

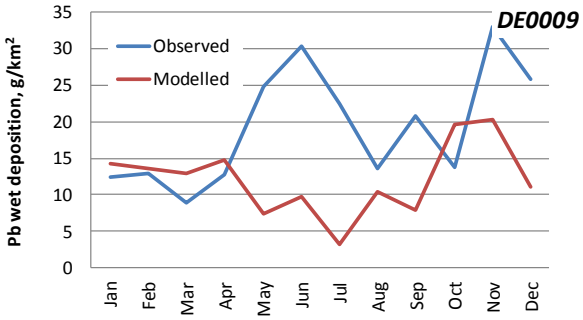
DE0009
Observed
Modelled
Pb wet deposition, g/km²
0
5
10
15
20
25
30
35
Jan Feb Mar Apr May Jun Jul Aug Sep Oct Nov Dec

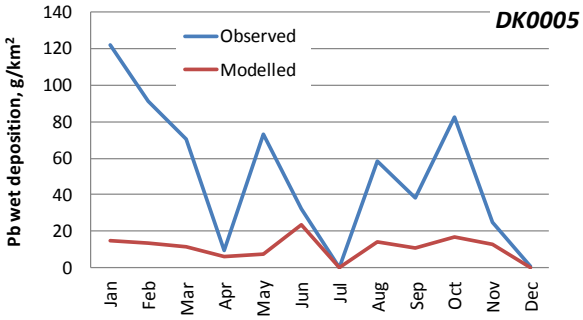
DK0005
Observed
Modelled
Pb wet deposition, g/km²
0
20
40
60
80
100
120
140
Jan Feb Mar Apr May Jun Jul Aug Sep Oct Nov Dec

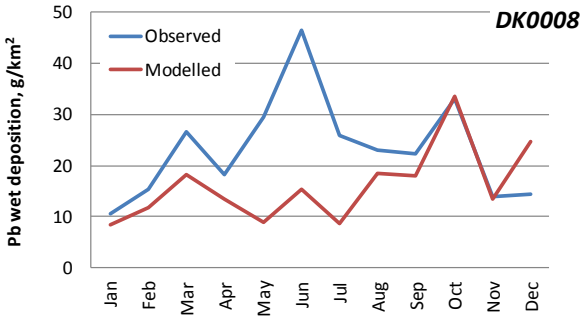
DK0008
Observed
Modelled
Pb wet deposition, g/km²
0
10
20
30
40
50
Jan Feb Mar Apr May Jun Jul Aug Sep Oct Nov Dec

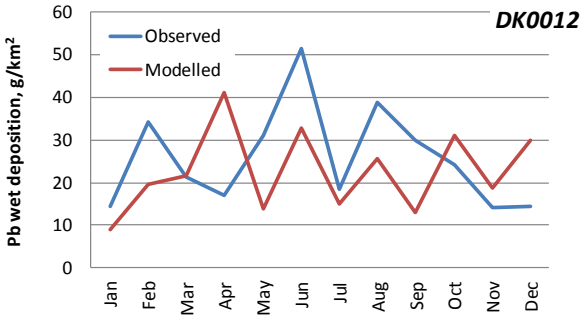
DK0012
Observed
Modelled
Pb wet deposition, g/km²
0
10
20
30
40
50
60
Jan Feb Mar Apr May Jun Jul Aug Sep Oct Nov Dec

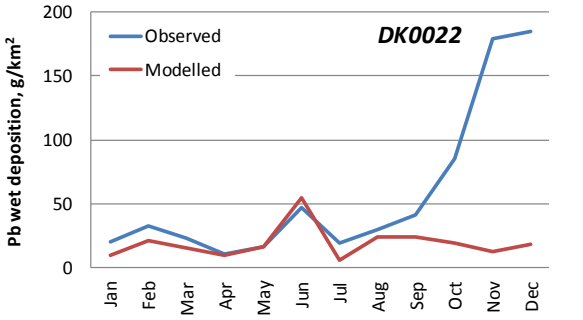
DK0022
Observed
Modelled
Pb wet deposition, g/km²
0
50
100
150
200
Jan Feb Mar Apr May Jun Jul Aug Sep Oct Nov Dec

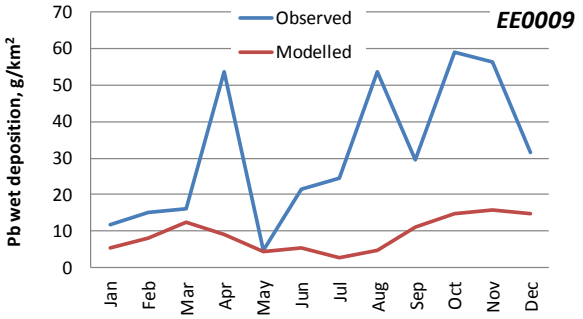
EE0009
Observed
Modelled
Pb wet deposition, g/km²
0
10
20
30
40
50
60
70
Jan Feb Mar Apr May Jun Jul Aug Sep Oct Nov Dec

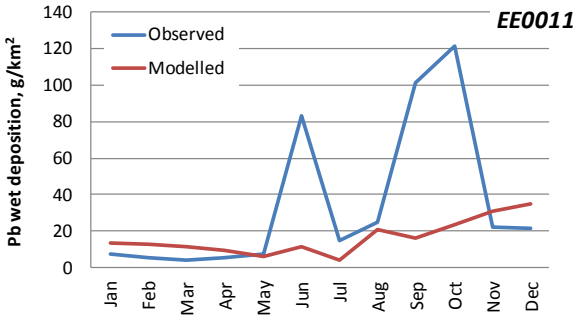
EE0011
Observed
Modelled
Pb wet deposition, g/km²
0
20
40
60
80
100
120
140
Jan Feb Mar Apr May Jun Jul Aug Sep Oct Nov Dec

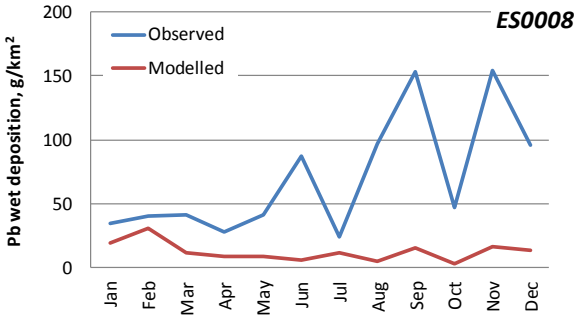
ES0008
Observed
Modelled
Pb wet deposition, g/km²
0
50
100
150
200
Jan Feb Mar Apr May Jun Jul Aug Sep Oct Nov Dec

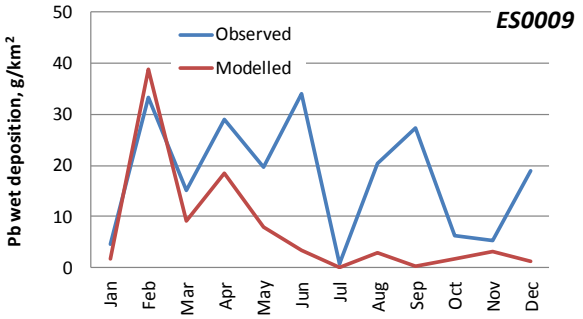
ES0009
Observed
Modelled
Pb wet deposition, g/km²
0
10
20
30
40
50
Jan Feb Mar Apr May Jun Jul Aug Sep Oct Nov Dec

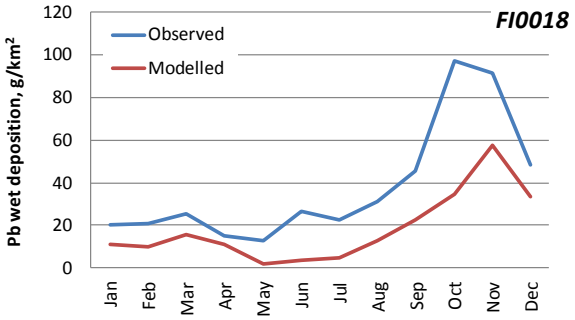
FI0018
Observed
Modelled
Pb wet deposition, g/km²
0
20
40
60
80
100
120
Jan
Feb
Mar
Apr
May
Jun
Jul
Aug
Sep
Oct
Nov
Dec

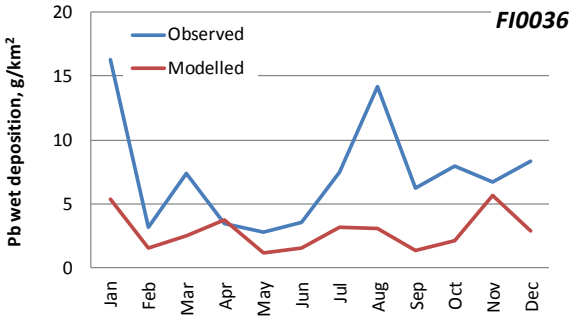
FI0036
Observed
Modelled
Pb wet deposition, g/km²
0
5
10
15
20
Jan
Feb
Mar
Apr
May
Jun
Jul
Aug
Sep
Oct
Nov
Dec

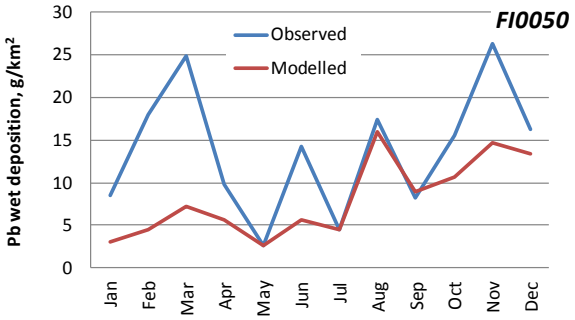
FI0050
Observed
Modelled
Pb wet deposition, g/km²
0
5
10
15
20
25
30
Jan
Feb
Mar
Apr
May
Jun
Jul
Aug
Sep
Oct
Nov
Dec

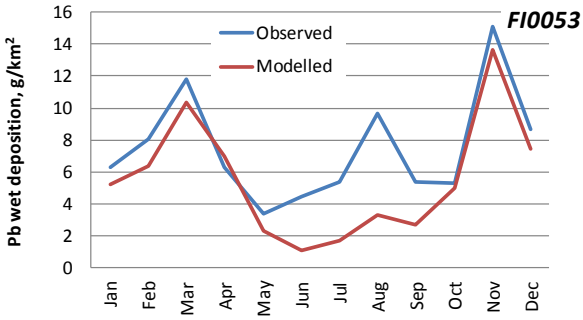
FI0053
Observed
Modelled
Pb wet deposition, g/km²
0
2
4
6
8
10
12
14
16
Jan
Feb
Mar
Apr
May
Jun
Jul
Aug
Sep
Oct
Nov
Dec

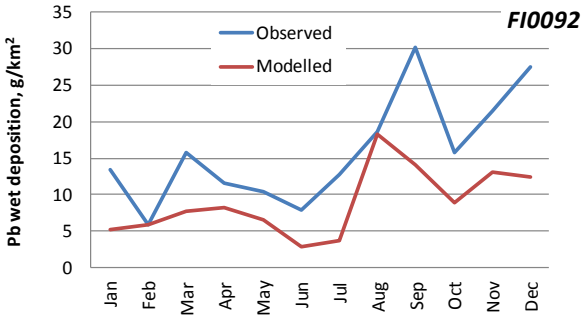
FI0092
Observed
Modelled
Pb wet deposition, g/km²
0
5
10
15
20
25
30
35
Jan
Feb
Mar
Apr
May
Jun
Jul
Aug
Sep
Oct
Nov
Dec

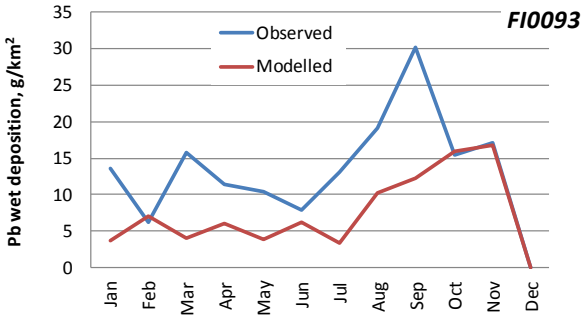
FI0093
Observed
Modelled
Pb wet deposition, g/km²
0
5
10
15
20
25
30
35
Jan
Feb
Mar
Apr
May
Jun
Jul
Aug
Sep
Oct
Nov
Dec

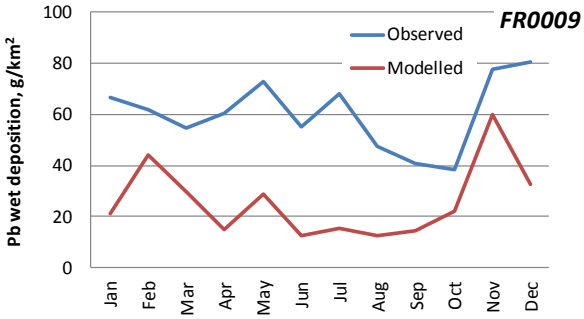
FR0009
Observed
Modelled
Pb wet deposition, g/km²
0
20
40
60
80
100
Jan
Feb
Mar
Apr
May
Jun
Jul
Aug
Sep
Oct
Nov
Dec

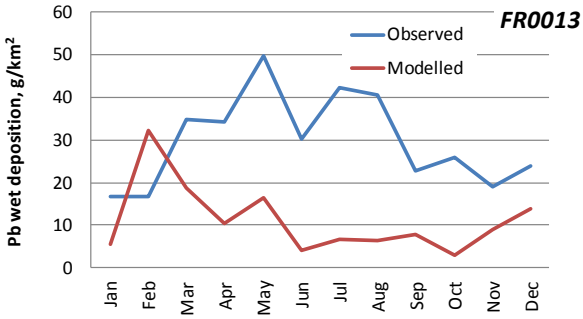
FR0013
Observed
Modelled
Pb wet deposition, g/km²
0
10
20
30
40
50
60
Jan
Feb
Mar
Apr
May
Jun
Jul
Aug
Sep
Oct
Nov
Dec

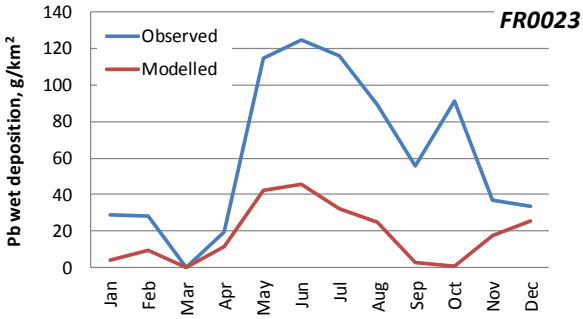
FR0023
Observed
Modelled
Pb wet deposition, g/km²
0
20
40
60
80
100
120
140
Jan
Feb
Mar
Apr
May
Jun
Jul
Aug
Sep
Oct
Nov
Dec

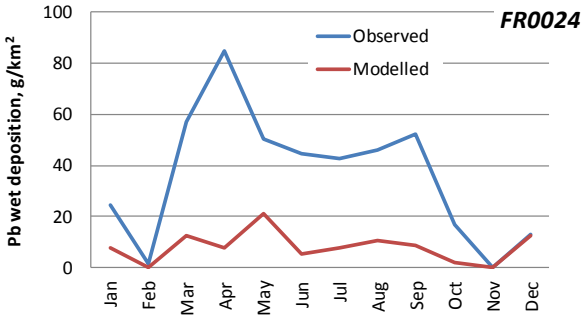
FR0024
Observed
Modelled
Pb wet deposition, g/km²
0
20
40
60
80
100
Jan
Feb
Mar
Apr
May
Jun
Jul
Aug
Sep
Oct
Nov
Dec

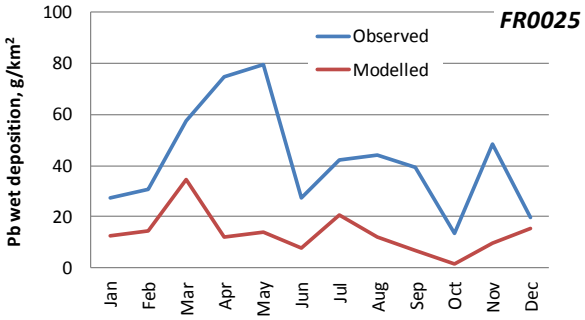
FR0025
Observed
Modelled
Pb wet deposition, g/km²
0
20
40
60
80
100
Jan
Feb
Mar
Apr
May
Jun
Jul
Aug
Sep
Oct
Nov
Dec

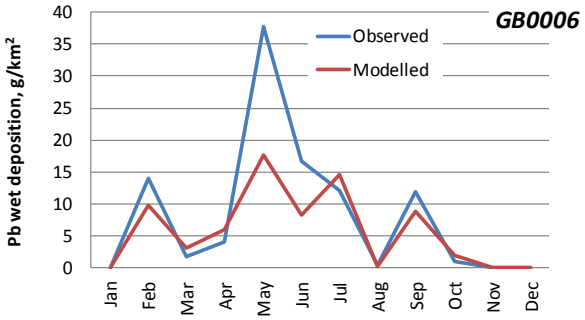
GB0006
Observed
Modelled
Pb wet deposition, g/km²
0
5
10
15
20
25
30
35
40
Jan
Feb
Mar
Apr
May
Jun
Jul
Aug
Sep
Oct
Nov
Dec

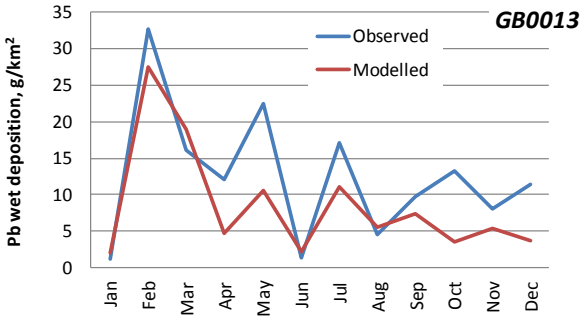
GB0013
Observed
Modelled
Pb wet deposition, g/km²
0
5
10
15
20
25
30
35
Jan
Feb
Mar
Apr
May
Jun
Jul
Aug
Sep
Oct
Nov
Dec

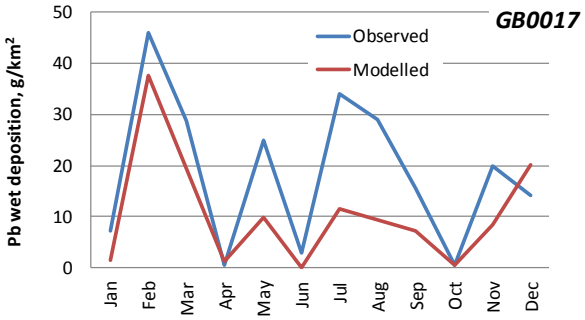
GB0017
Observed
Modelled
Pb wet deposition, g/km²
0
10
20
30
40
50
Jan
Feb
Mar
Apr
May
Jun
Jul
Aug
Sep
Oct
Nov
Dec

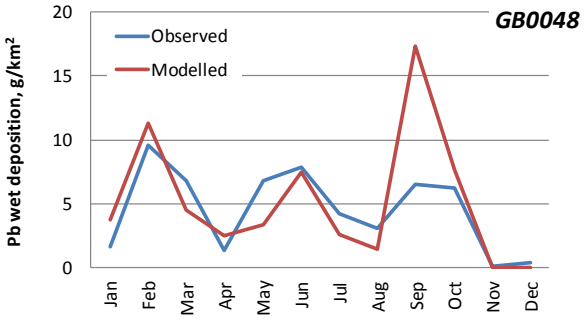
GB0048
Observed
Modelled
Pb wet deposition, g/km²
0
5
10
15
20
Jan
Feb
Mar
Apr
May
Jun
Jul
Aug
Sep
Oct
Nov
Dec

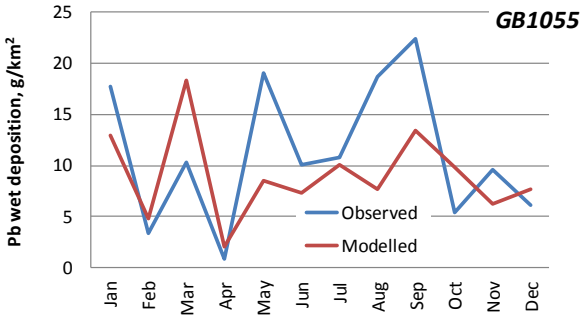
GB1055
Observed
Modelled
Pb wet deposition, g/km²
0
5
10
15
20
25
Jan
Feb
Mar
Apr
May
Jun
Jul
Aug
Sep
Oct
Nov
Dec

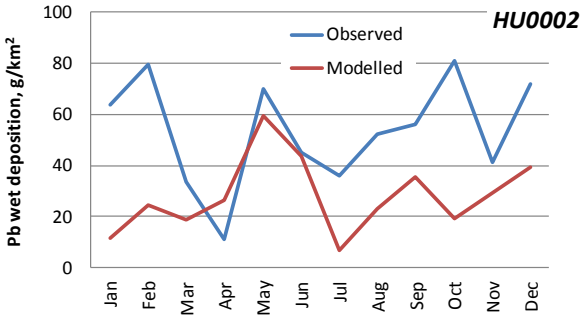
HU0002
Observed
Modelled
Pb wet deposition, g/km²
0
20
40
60
80
100
Jan
Feb
Mar
Apr
May
Jun
Jul
Aug
Sep
Oct
Nov
Dec

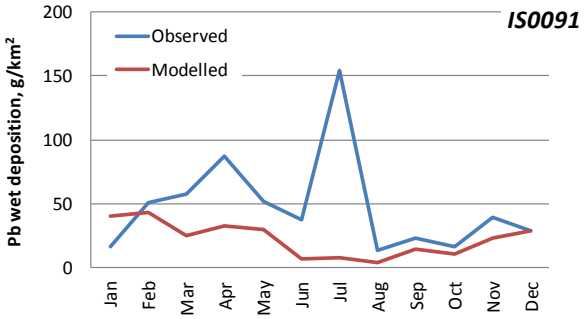
IS0091
Observed
Modelled
Pb wet deposition, g/km²
0
50
100
150
200
Jan
Feb
Mar
Apr
May
Jun
Jul
Aug
Sep
Oct
Nov
Dec

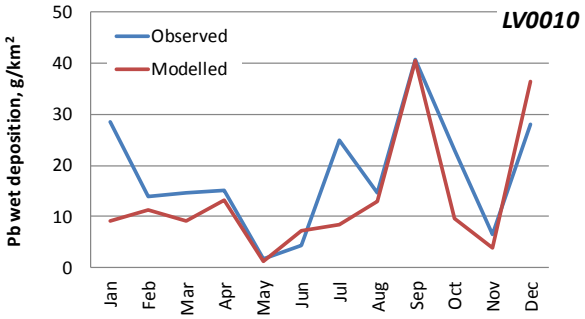
LV0010
Observed
Modelled
Pb wet deposition, g/km²
0
10
20
30
40
50
Jan
Feb
Mar
Apr
May
Jun
Jul
Aug
Sep
Oct
Nov
Dec

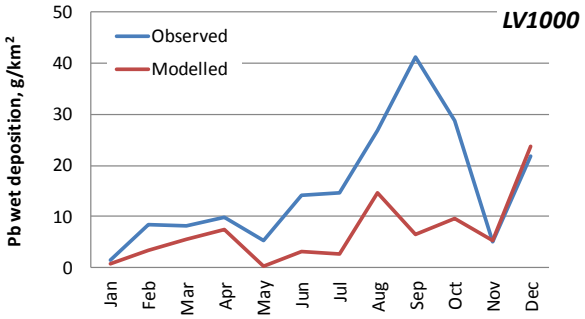
LV1000
Observed
Modelled
Pb wet deposition, g/km²
0
10
20
30
40
50
Jan
Feb
Mar
Apr
May
Jun
Jul
Aug
Sep
Oct
Nov
Dec

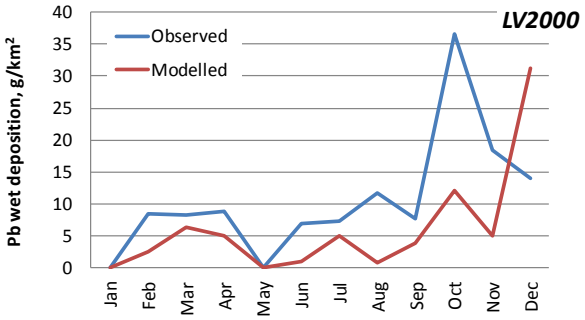
LV2000
Observed
Modelled
Pb wet deposition, g/km²
0
5
10
15
20
25
30
35
40
Jan
Feb
Mar
Apr
May
Jun
Jul
Aug
Sep
Oct
Nov
Dec

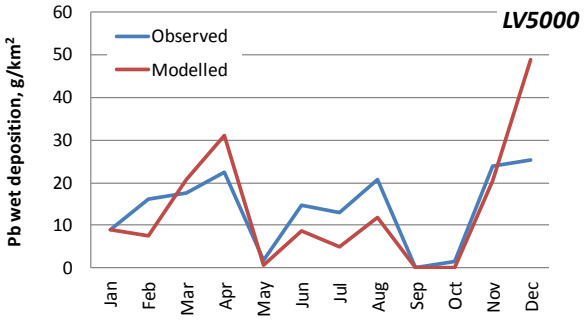
LV5000
Observed
Modelled
Pb wet deposition, g/km²
0
10
20
30
40
50
60
Jan
Feb
Mar
Apr
May
Jun
Jul
Aug
Sep
Oct
Nov
Dec

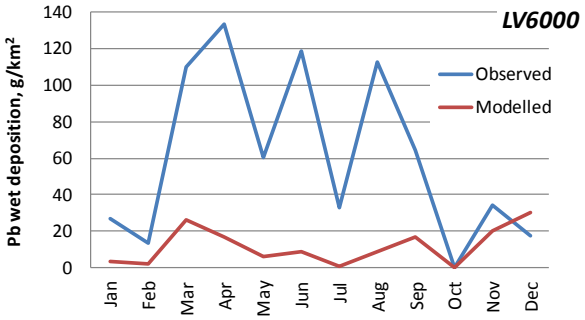
LV6000
Observed
Modelled
Pb wet deposition, g/km²
0
20
40
60
80
100
120
140
Jan
Feb
Mar
Apr
May
Jun
Jul
Aug
Sep
Oct
Nov
Dec

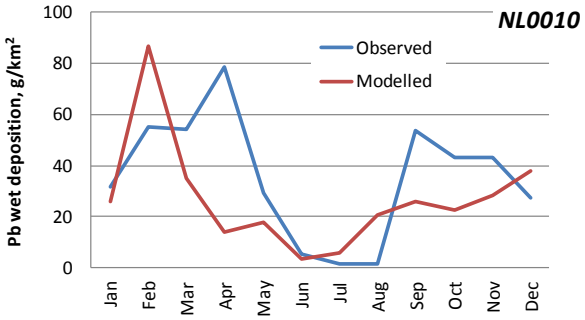
NL0010
Observed
Modelled
Pb wet deposition, g/km²
0
20
40
60
80
100
Jan
Feb
Mar
Apr
May
Jun
Jul
Aug
Sep
Oct
Nov
Dec

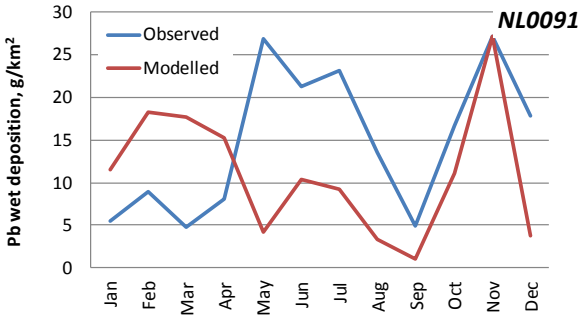
NL0091
Observed
Modelled
Pb wet deposition, g/km²
0
5
10
15
20
25
30
Jan
Feb
Mar
Apr
May
Jun
Jul
Aug
Sep
Oct
Nov
Dec

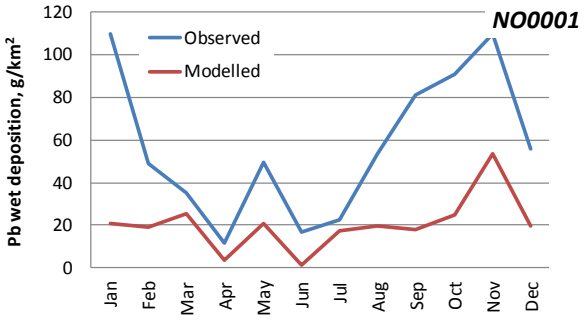
NO0001
Observed
Modelled
Pb wet deposition, g/km²
0
20
40
60
80
100
120
Jan
Feb
Mar
Apr
May
Jun
Jul
Aug
Sep
Oct
Nov
Dec

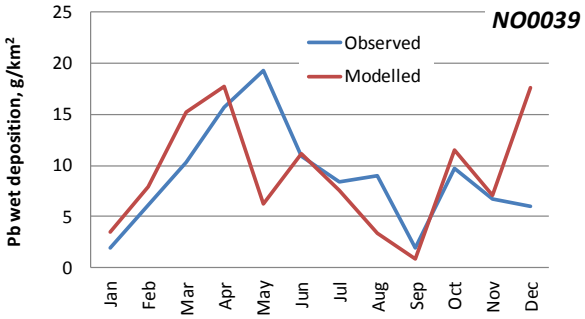
NO0039
Observed
Modelled
Pb wet deposition, g/km²
0
5
10
15
20
25
Jan
Feb
Mar
Apr
May
Jun
Jul
Aug
Sep
Oct
Nov
Dec

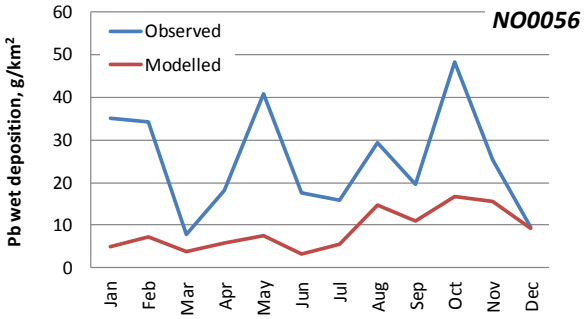
NO0056
Observed
Modelled
Pb wet deposition, g/km²
0
10
20
30
40
50
60
Jan
Feb
Mar
Apr
May
Jun
Jul
Aug
Sep
Oct
Nov
Dec

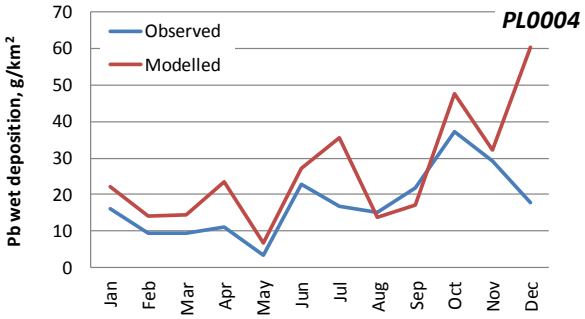
PL0004
Observed
Modelled
Pb wet deposition, g/km²
0
10
20
30
40
50
60
70
Jan
Feb
Mar
Apr
May
Jun
Jul
Aug
Sep
Oct
Nov
Dec

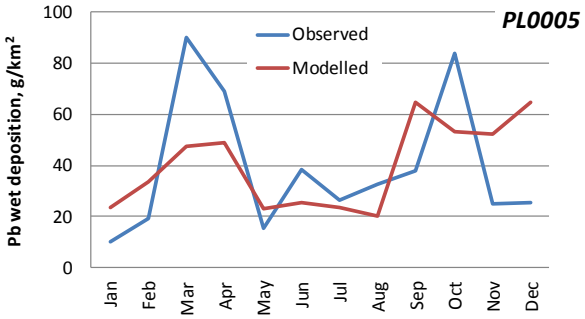
PL0005
Observed
Modelled
Pb wet deposition, g/km²
0
20
40
60
80
100
Jan
Feb
Mar
Apr
May
Jun
Jul
Aug
Sep
Oct
Nov
Dec

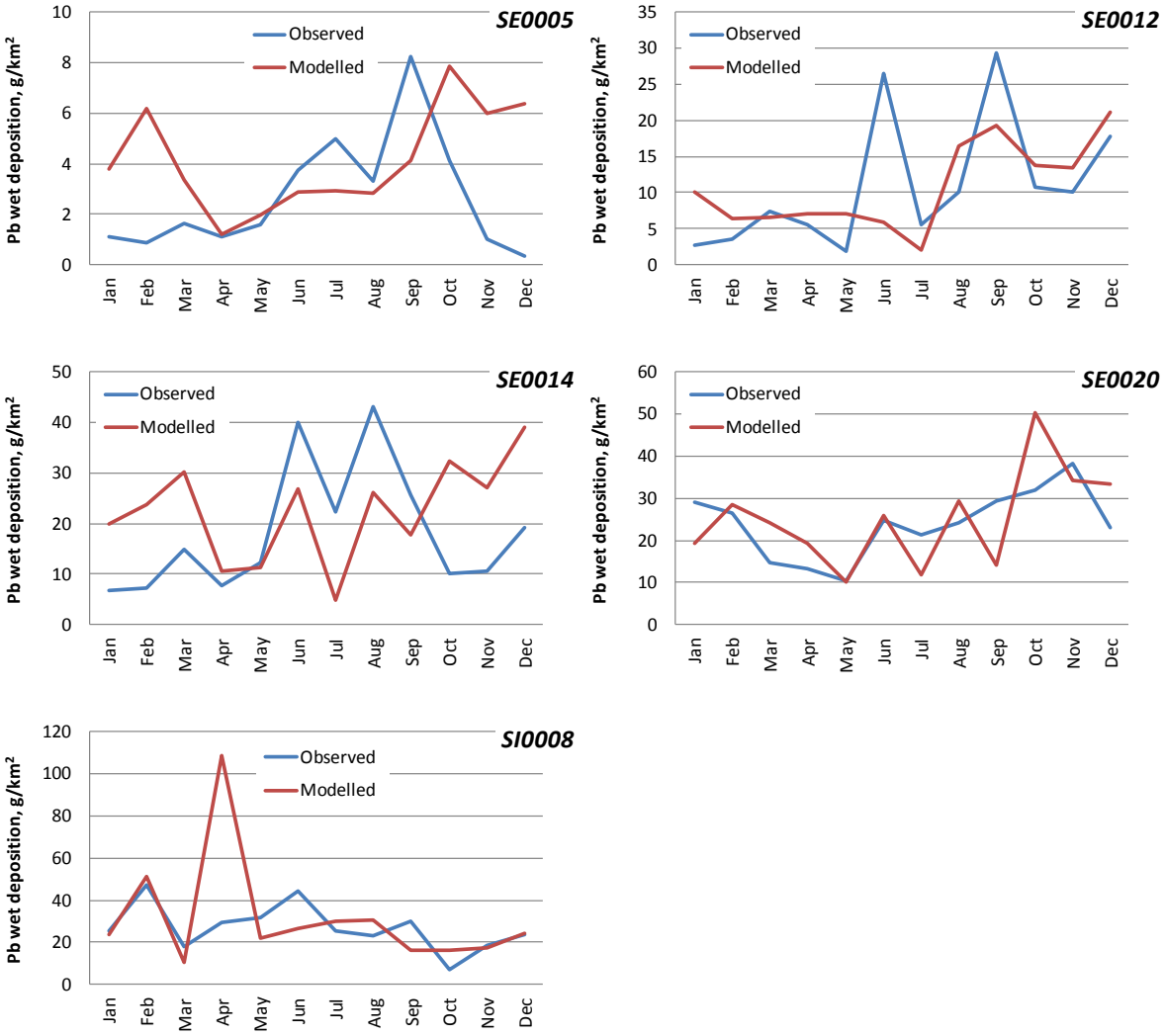


***Fig. 4.4.*** *Modelled and observed monthly wet deposition fluxes of Pb at the EMEP stations in 2017*

## 4.2. Cadmium

### *4.2.1. Air concentrations*

***Table 4.3.*** *Annual mean modelled and observed Cd air concentrations, ng/m$^3$, temporal correlation coefficient (Rc) and relative bias (Bias) at EMEP stations in 2017*

| Station name | Code | Longit | Latid | Observed | Modelled | R | Bias |
|---|---|---|---|---|---|---|---|
| Koksijde | BE0014R | 2.66 | 51.12 | 0.15 | 0.25 | 0.93 | 70.6 |
| Ayia Maria | CY0002R | 33.06 | 35.04 | 0.10 | 0.05 | -0.36 | -49.6 |
| Kosetice (NOAK) | CZ0003R | 15.08 | 49.57 | 0.08 | 0.10 | 0.91 | 19.3 |
| Churanov | CZ0005R | 13.6 | 49.07 | 0.03 | 0.08 | 0.48 | 156.4 |
| Westerland | DE0001R | 8.31 | 54.93 | 0.05 | 0.07 | 0.86 | 37.7 |
| Waldhof | DE0002R | 10.76 | 52.8 | 0.09 | 0.12 | 0.84 | 32.7 |
| Schauinsland | DE0003R | 7.91 | 47.91 | 0.02 | 0.10 | 0.46 | 353.1 |
| Neuglobsow | DE0007R | 13.03 | 53.17 | 0.09 | 0.08 | 0.92 | -15.7 |
| Schmucke | DE0008R | 10.77 | 50.65 | 0.04 | 0.09 | 0.8 | 123.7 |
| Zingst | DE0009R | 12.72 | 54.44 | 0.07 | 0.08 | 0.86 | 4.4 |
| Anholt | DK0008R | 11.52 | 56.72 | 0.03 | 0.05 | 0.66 | 49.3 |
| Riscoe | DK0012R | 12.09 | 55.69 | 0.05 | 0.11 | 0.81 | 126.2 |
| Lahemaa | EE0009R | 25.9 | 59.5 | 0.04 | 0.03 | 0.57 | -30.5 |
| San Pablo de los Montes | ES0001R | -4.35 | 39.55 | 0.02 | 0.04 | 0.56 | 60.6 |
| Viznar | ES0007R | -3.53 | 37.23 | 0.03 | 0.04 | 0.37 | 53.7 |
| Niembro | ES0008R | -4.85 | 43.44 | 0.13 | 0.05 | -0.16 | -58.6 |
| Campisabalos | ES0009R | -3.14 | 41.28 | 0.02 | 0.03 | 0.74 | 65.8 |
| ElTorms | ES0014R | 0.72 | 41.4 | 0.03 | 0.06 | 0.65 | 116.1 |
| Virolahti III | FI0018R | 27.67 | 60.53 | 0.03 | 0.03 | 0.57 | -24.0 |
| Pallas (Matorova) | FI0036R | 24.24 | 68 | 0.01 | 0.00 | 0.09 | -70.4 |
| Hyytiälä | FI0050R | 24.28 | 61.85 | 0.03 | 0.01 | 0.83 | -68.5 |
| Revin | FR0009R | 4.63 | 49.9 | 0.09 | 0.08 | 0.54 | -6.7 |
| Peyrusse Vieille | FR0013R | 0.18 | 43.62 | 0.04 | 0.02 | 0.6 | -42.4 |
| Saint-Nazaire-le-Desert | FR0023R | 5.28 | 44.57 | 0.04 | 0.03 | 0.67 | -16.8 |
| Guipry | FR0024R | -1.84 | 47.83 | 0.06 | 0.03 | 0.8 | -51.7 |
| Verneuil | FR0025R | 2.61 | 46.81 | 0.06 | 0.03 | 0.81 | -49.7 |
| Yarner Wood | GB0013R | -3.71 | 50.6 | 0.05 | 0.05 | 0.67 | -7.6 |
| Heigham Holmes | GB0017R | 1.62 | 52.72 | 0.09 | 0.12 | 0.85 | 32.1 |
| Auchencorth Moss | GB0048R | -3.24 | 55.79 | 0.03 | 0.03 | 0.95 | 13.4 |
| Chilbolton Observatory | GB1055R | -1.44 | 51.15 | 0.11 | 0.08 | 0.73 | -31.4 |
| K-puszta | HU0002R | 19.58 | 46.97 | 0.17 | 0.16 | 0.74 | 0.1 |
| Vestmannaeyjar | IS0091R | -20.28 | 63.4 | 0.00 | 0.02 | 0.78 | 261.7 |
| Monte Martano | IT0019R | 12.57 | 42.81 | 0.03 | 0.04 | 0.62 | 47.2 |
| Rucava | LV0010R | 21.17 | 56.16 | 0.05 | 0.05 | 0.62 | 47.2 |
| Bilthoven | NL0008R | 5.2 | 52.12 | 0.11 | 0.18 | 0.88 | 73.3 |
| Birkenes II | NO0002R | 8.25 | 58.39 | 0.02 | 0.01 | 0.63 | -41.4 |
| Zeppelin mountain (Ny-Alesund) | NO0042G | 11.89 | 78.91 | 0.01 | 0.01 | -0.29 | -45.9 |
| Alomar | NO0090R | 16.01 | 69.28 | 0.01 | 0.01 | 0.34 | -3.0 |
| Diabla Gora | PL0005R | 22.07 | 54.15 | 0.10 | 0.09 | 0.49 | -2.5 |
| Zielonka | PL0009R | 17.93 | 53.66 | 0.12 | 0.10 | 0.87 | -13.0 |
| Bredkälen | SE0005R | 15.33 | 63.85 | 0.01 | 0.00 | 0.73 | -54.9 |
| Aspvreten | SE0012R | 17.38 | 58.8 | 0.03 | 0.02 | 0.87 | -42.1 |
| Råö | SE0014R | 11.91 | 57.39 | 0.03 | 0.03 | 0.62 | 5.0 |
| Hallahus | SE0020R | 13.15 | 56.04 | 0.03 | 0.06 | 0.55 | 99.6 |
| Iskrba | SI0008R | 14.87 | 45.57 | 0.07 | 0.08 | 0.79 | 19.2 |

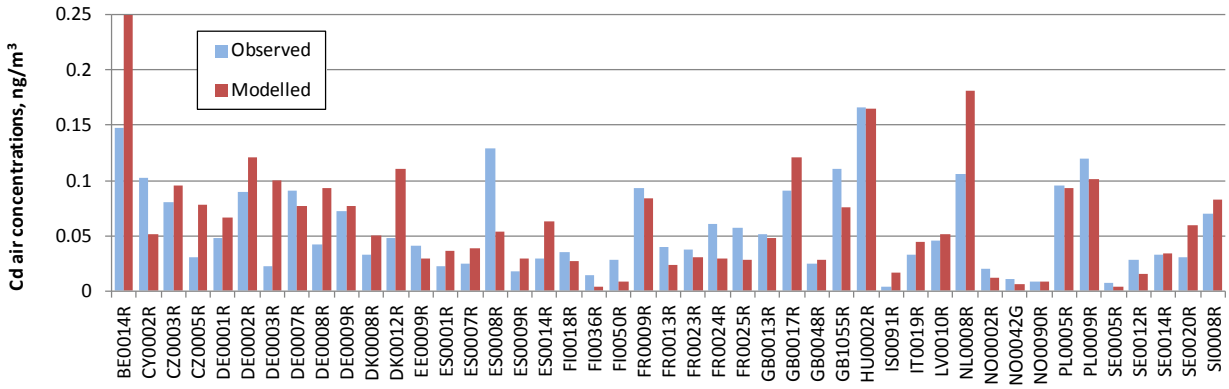


***Fig. 4.5.*** *Modelled and observed annual mean concentrations of Cd in air at the EMEP stations in 2017*

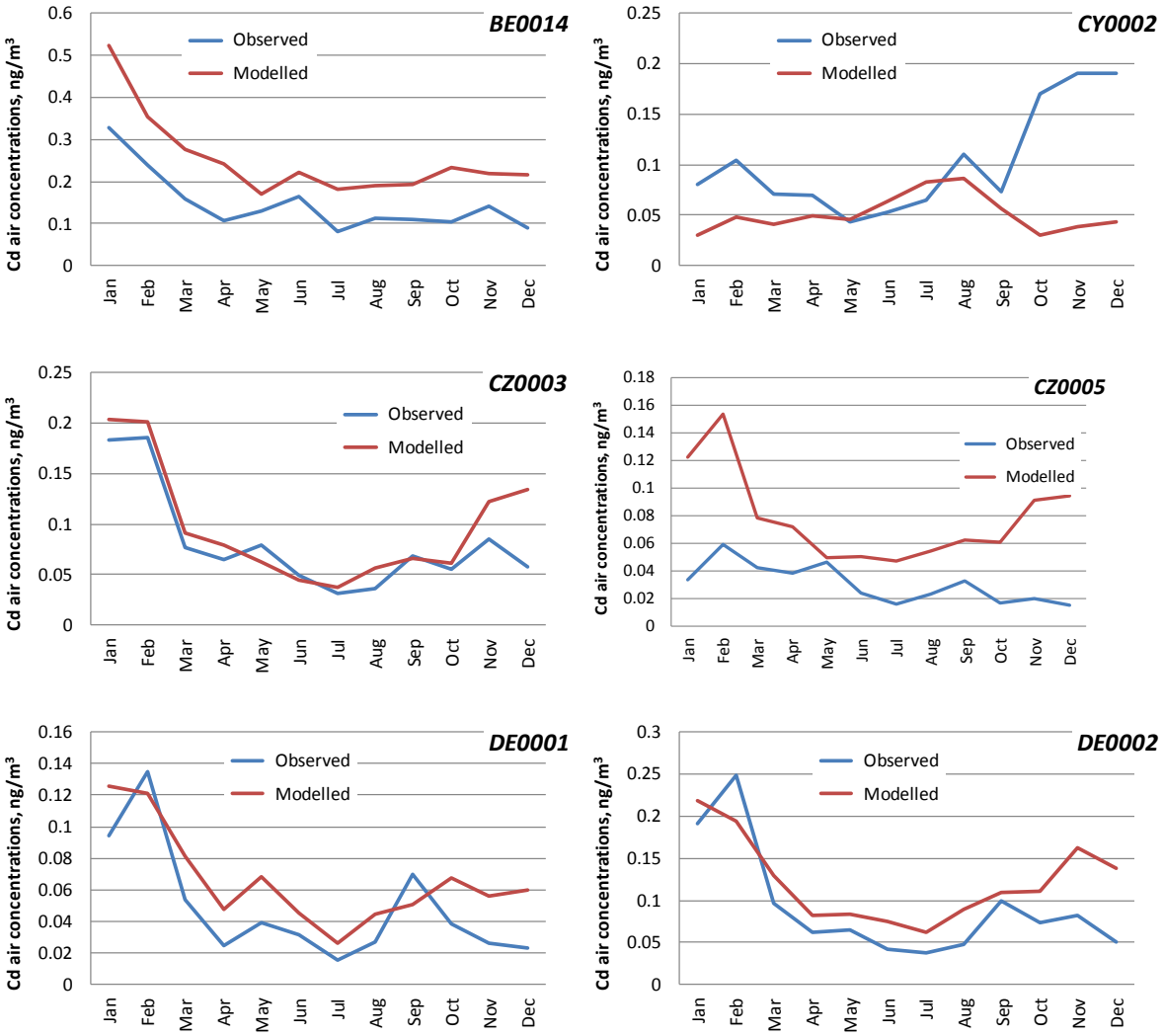

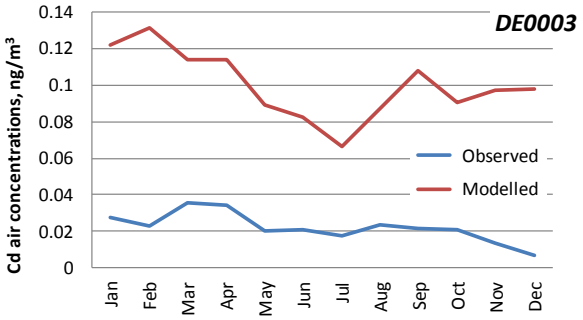
DE0003
Cd air concentrations, ng/m³
0.14
0.12
0.1
0.08
0.06
0.04
0.02
0
Observed
Modelled
Jan Feb Mar Apr May Jun Jul Aug Sep Oct Nov Dec

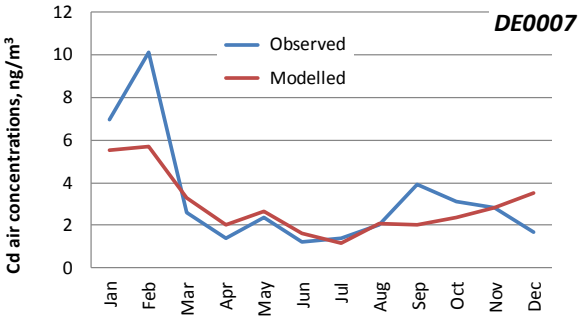
DE0007
Cd air concentrations, ng/m³
12
10
8
6
4
2
0
Observed
Modelled
Jan Feb Mar Apr May Jun Jul Aug Sep Oct Nov Dec

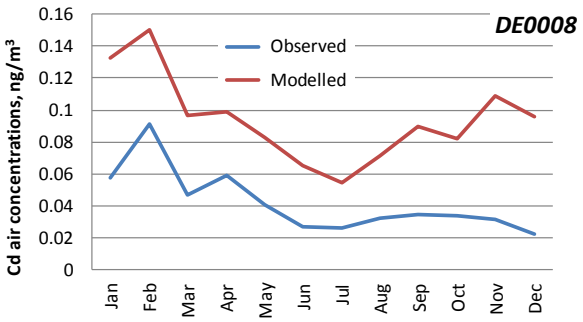
DE0008
Cd air concentrations, ng/m³
0.16
0.14
0.12
0.1
0.08
0.06
0.04
0.02
0
Observed
Modelled
Jan Feb Mar Apr May Jun Jul Aug Sep Oct Nov Dec

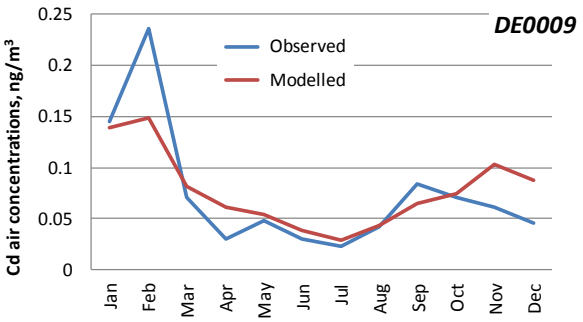
DE0009
Cd air concentrations, ng/m³
0.25
0.2
0.15
0.1
0.05
0
Observed
Modelled
Jan Feb Mar Apr May Jun Jul Aug Sep Oct Nov Dec

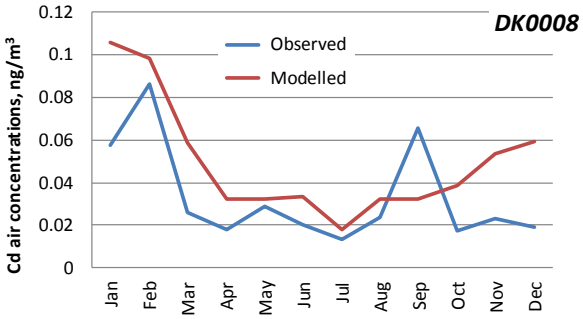
DK0008
Cd air concentrations, ng/m³
0.12
0.1
0.08
0.06
0.04
0.02
0
Observed
Modelled
Jan Feb Mar Apr May Jun Jul Aug Sep Oct Nov Dec

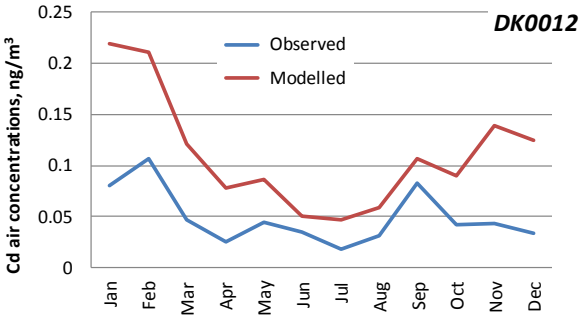
DK0012
Cd air concentrations, ng/m³
0.25
0.2
0.15
0.1
0.05
0
Observed
Modelled
Jan Feb Mar Apr May Jun Jul Aug Sep Oct Nov Dec

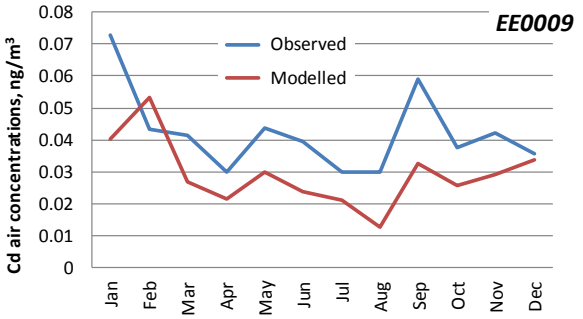
EE0009
Cd air concentrations, ng/m³
0.08
0.07
0.06
0.05
0.04
0.03
0.02
0.01
0
Observed
Modelled
Jan Feb Mar Apr May Jun Jul Aug Sep Oct Nov Dec

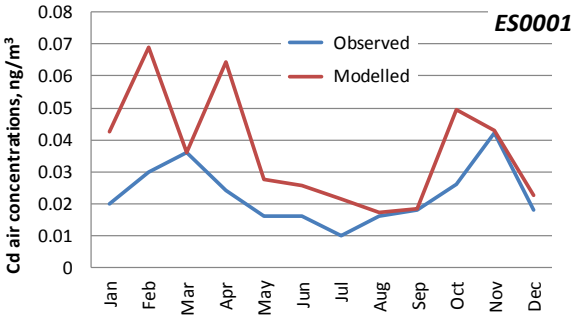
ES0001
Cd air concentrations, ng/m³
0.08
0.07
0.06
0.05
0.04
0.03
0.02
0.01
0
Observed
Modelled
Jan Feb Mar Apr May Jun Jul Aug Sep Oct Nov Dec

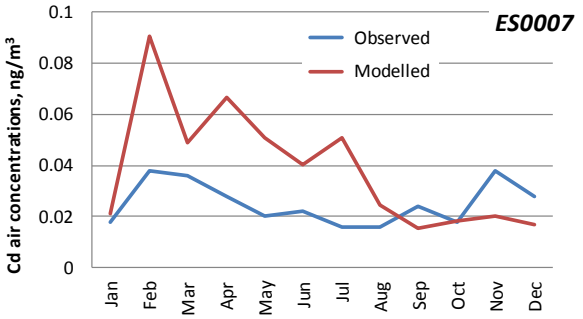
ES0007
Cd air concentrations, ng/m³
0.1
0.08
0.06
0.04
0.02
0
Observed
Modelled
Jan Feb Mar Apr May Jun Jul Aug Sep Oct Nov Dec

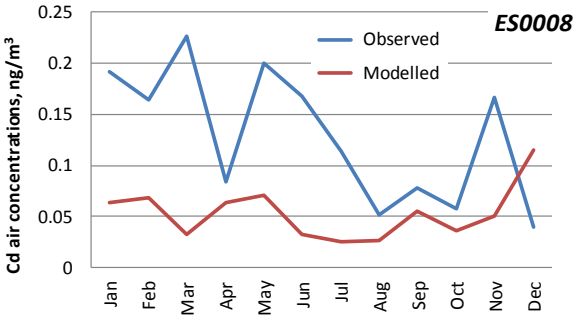
ES0008
Cd air concentrations, ng/m³
0.25
0.2
0.15
0.1
0.05
0
Observed
Modelled
Jan Feb Mar Apr May Jun Jul Aug Sep Oct Nov Dec

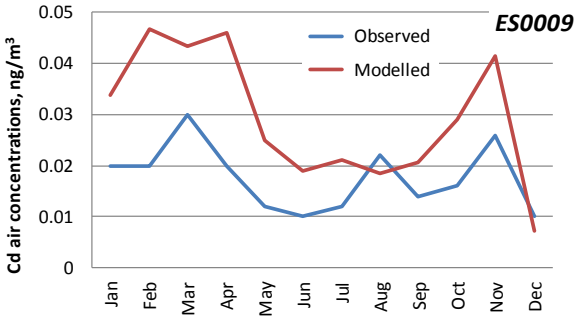
ES0009
Observed
Modelled
Cd air concentrations, ng/m³
0.05
0.04
0.03
0.02
0.01
0
Jan Feb Mar Apr May Jun Jul Aug Sep Oct Nov Dec

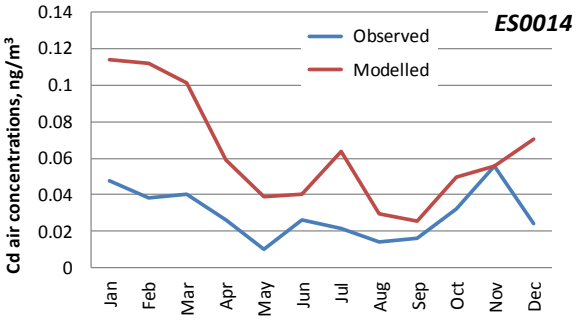
ES0014
Observed
Modelled
Cd air concentrations, ng/m³
0.14
0.12
0.1
0.08
0.06
0.04
0.02
0
Jan Feb Mar Apr May Jun Jul Aug Sep Oct Nov Dec

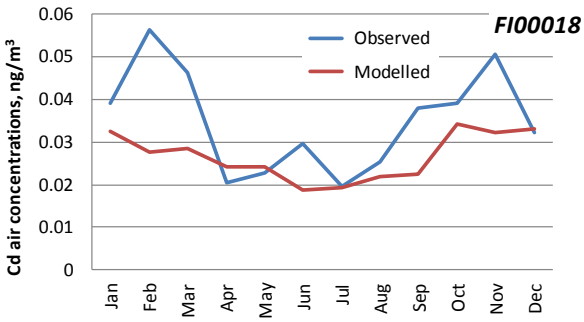
FI00018
Observed
Modelled
Cd air concentrations, ng/m³
0.06
0.05
0.04
0.03
0.02
0.01
0
Jan Feb Mar Apr May Jun Jul Aug Sep Oct Nov Dec

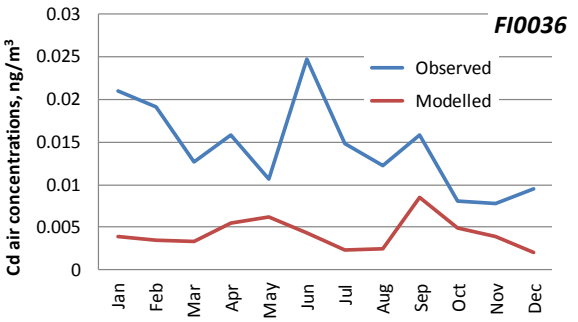
FI0036
Observed
Modelled
Cd air concentrations, ng/m³
0.03
0.025
0.02
0.015
0.01
0.005
0
Jan Feb Mar Apr May Jun Jul Aug Sep Oct Nov Dec

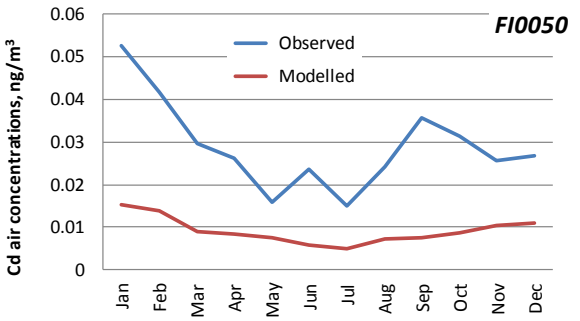
FI0050
Observed
Modelled
Cd air concentrations, ng/m³
0.06
0.05
0.04
0.03
0.02
0.01
0
Jan Feb Mar Apr May Jun Jul Aug Sep Oct Nov Dec

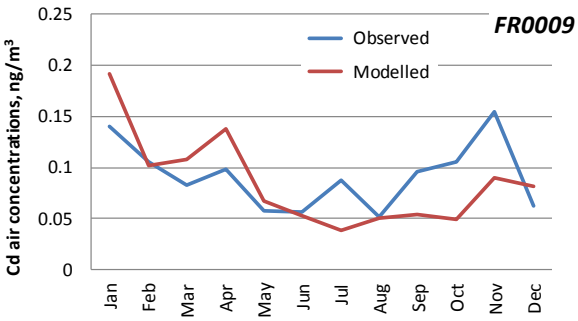
FR0009
Observed
Modelled
Cd air concentrations, ng/m³
0.25
0.2
0.15
0.1
0.05
0
Jan Feb Mar Apr May Jun Jul Aug Sep Oct Nov Dec

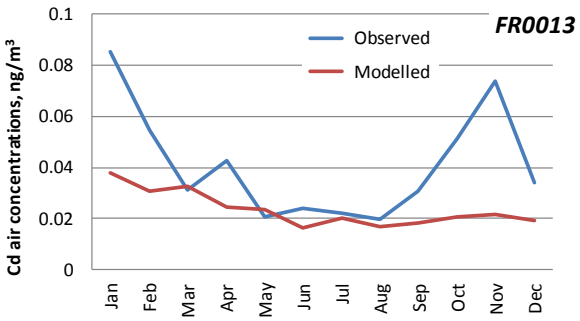
FR0013
Observed
Modelled
Cd air concentrations, ng/m³
0.1
0.08
0.06
0.04
0.02
0
Jan Feb Mar Apr May Jun Jul Aug Sep Oct Nov Dec

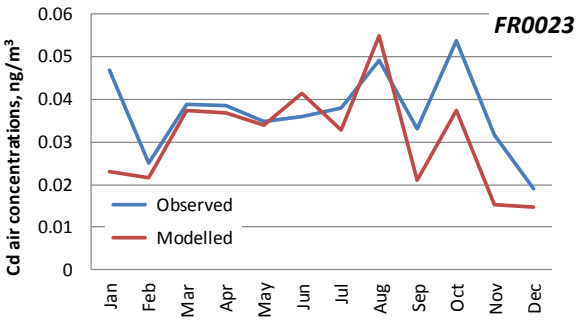
FR0023
Observed
Modelled
Cd air concentrations, ng/m³
0.06
0.05
0.04
0.03
0.02
0.01
0
Jan Feb Mar Apr May Jun Jul Aug Sep Oct Nov Dec

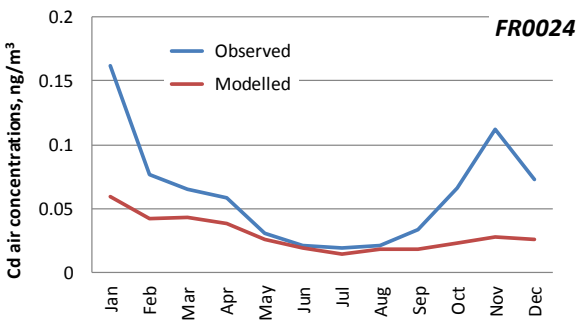
FR0024
Observed
Modelled
Cd air concentrations, ng/m³
0.2
0.15
0.1
0.05
0
Jan Feb Mar Apr May Jun Jul Aug Sep Oct Nov Dec

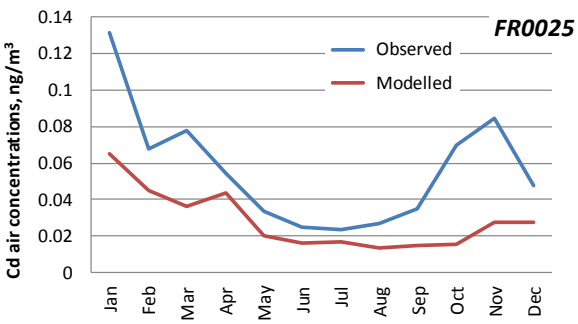
FR0025
Observed
Modelled
Cd air concentrations, ng/m³
0.14
0.12
0.1
0.08
0.06
0.04
0.02
0
Jan Feb Mar Apr May Jun Jul Aug Sep Oct Nov Dec

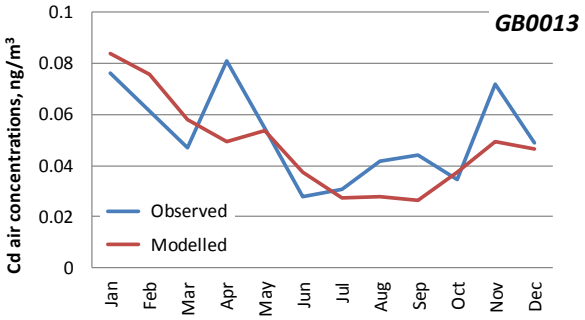
GB0013
Cd air concentrations, ng/m³
0.1
0.08
0.06
0.04
0.02
0
Observed
Modelled
Jan Feb Mar Apr May Jun Jul Aug Sep Oct Nov Dec

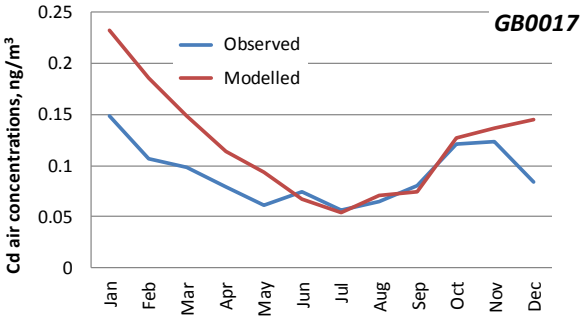
GB0017
Cd air concentrations, ng/m³
0.25
0.2
0.15
0.1
0.05
0
Observed
Modelled
Jan Feb Mar Apr May Jun Jul Aug Sep Oct Nov Dec

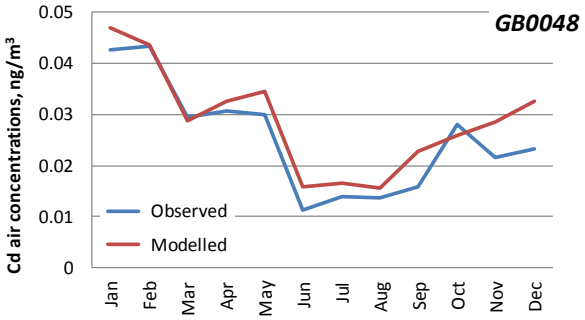
GB0048
Cd air concentrations, ng/m³
0.05
0.04
0.03
0.02
0.01
0
Observed
Modelled
Jan Feb Mar Apr May Jun Jul Aug Sep Oct Nov Dec

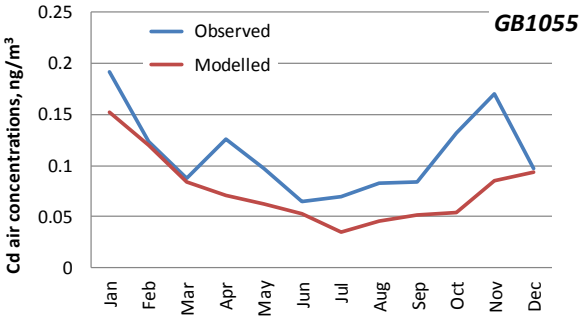
GB1055
Cd air concentrations, ng/m³
0.25
0.2
0.15
0.1
0.05
0
Observed
Modelled
Jan Feb Mar Apr May Jun Jul Aug Sep Oct Nov Dec

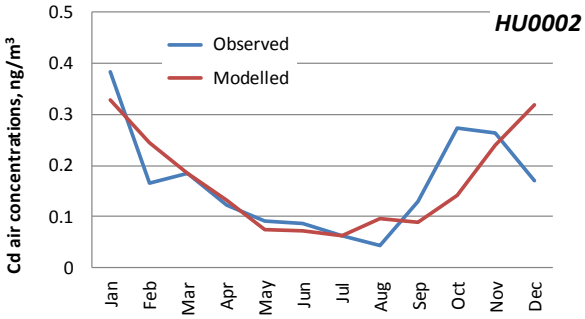
HU0002
Cd air concentrations, ng/m³
0.5
0.4
0.3
0.2
0.1
0
Observed
Modelled
Jan Feb Mar Apr May Jun Jul Aug Sep Oct Nov Dec

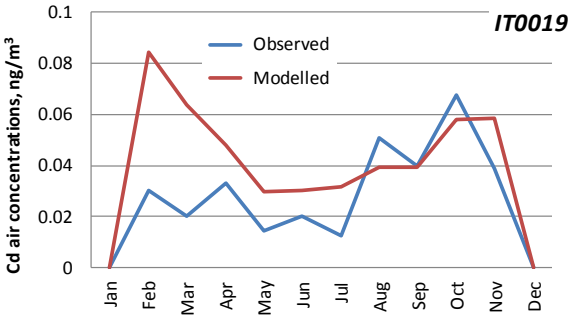
IT0019
Cd air concentrations, ng/m³
0.1
0.08
0.06
0.04
0.02
0
Observed
Modelled
Jan Feb Mar Apr May Jun Jul Aug Sep Oct Nov Dec

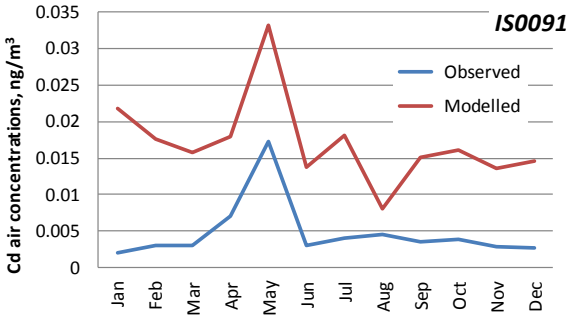
IS0091
Cd air concentrations, ng/m³
0.035
0.03
0.025
0.02
0.015
0.01
0.005
0
Observed
Modelled
Jan Feb Mar Apr May Jun Jul Aug Sep Oct Nov Dec

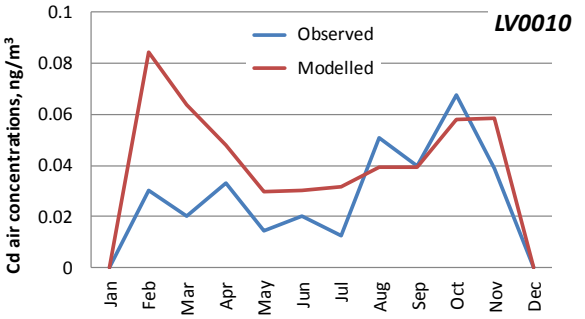
LV0010
Cd air concentrations, ng/m³
0.1
0.08
0.06
0.04
0.02
0
Observed
Modelled
Jan Feb Mar Apr May Jun Jul Aug Sep Oct Nov Dec

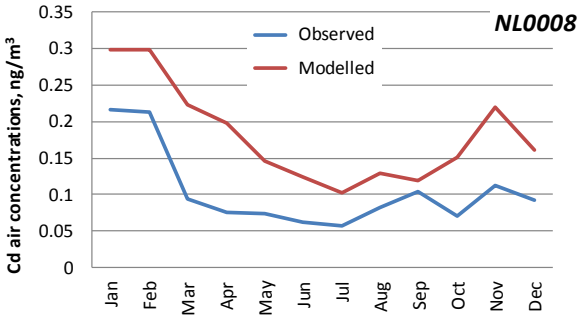
NL0008
Cd air concentrations, ng/m³
0.35
0.3
0.25
0.2
0.15
0.1
0.05
0
Observed
Modelled
Jan Feb Mar Apr May Jun Jul Aug Sep Oct Nov Dec

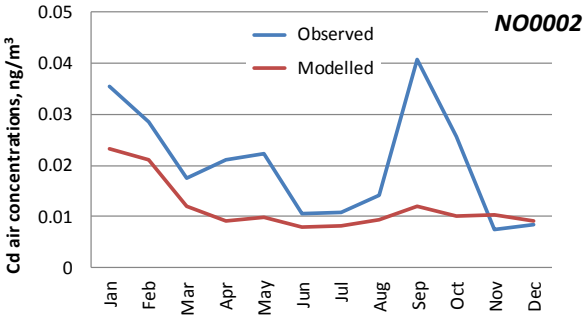
NO0002
Cd air concentrations, ng/m³
0.05
0.04
0.03
0.02
0.01
0
Observed
Modelled
Jan Feb Mar Apr May Jun Jul Aug Sep Oct Nov Dec

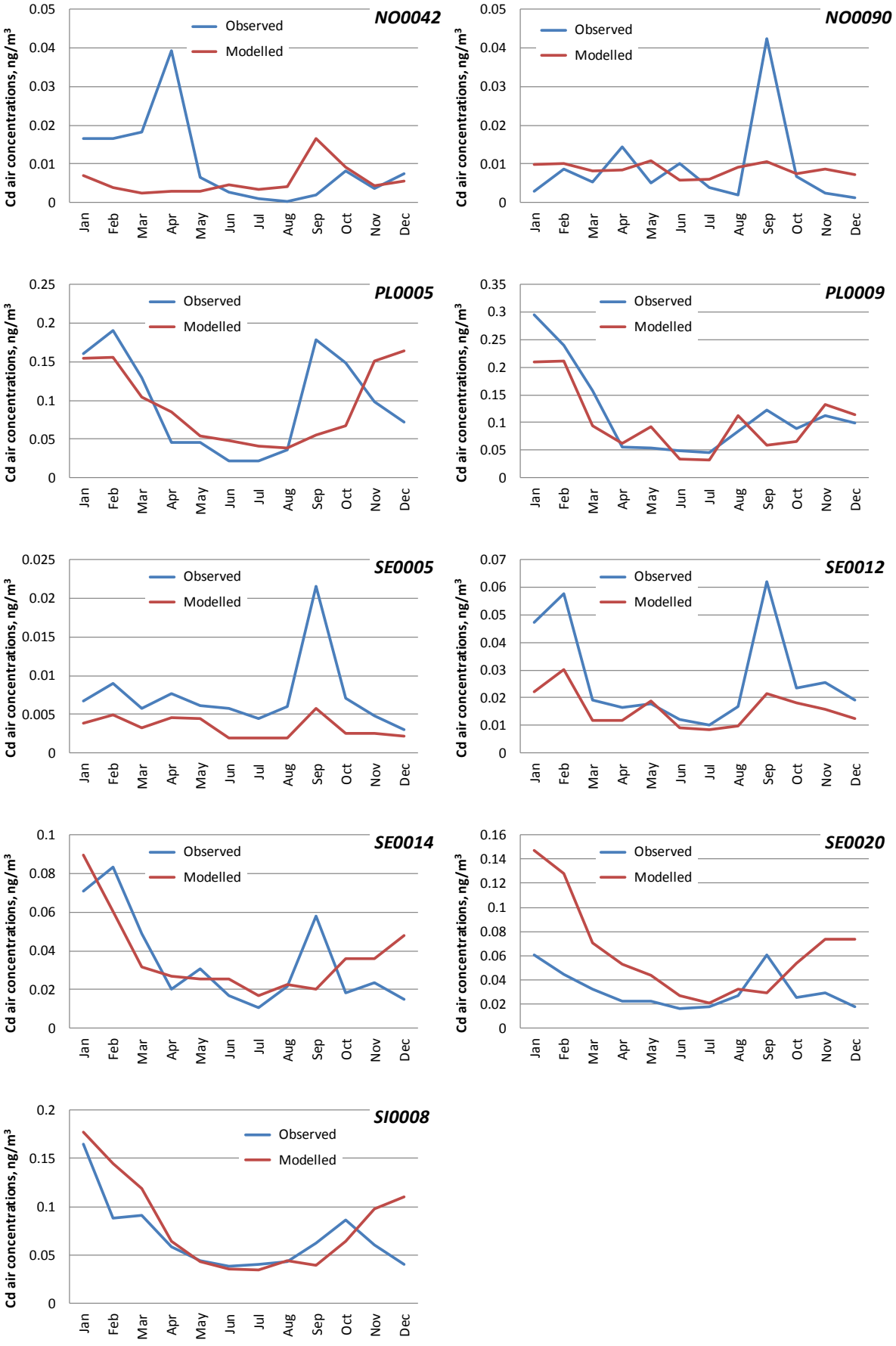


***Fig. 4.6.*** *Modelled and observed annual mean concentrations of Cd in air at the EMEP stations in 2017*

### *4.2.2. Wet deposition*

***Table 4.4.*** *Annual sums of modelled and observed Cd wet deposition fluxes, g/km$^2$/y, temporal correlation coefficient (Rc) and relative bias (Bias) at EMEP stations in 2017*

| Station name | Code | Longit | Latit | Observed flux | Modelled flux | Observed precip | Modelled precip | R | Bias |
|---|---|---|---|---|---|---|---|---|---|
| Koksijde | BE0014R | 2.66 | 51.12 | 12.0 | 12.7 | 578.0 | 573.6 | 0.50 | 5.7 |
| Kosetice (NOAK) | CZ0003R | 15.08 | 49.57 | 14.1 | 8.1 | 634.1 | 557.6 | 0.77 | -42.2 |
| Churanov | CZ0005R | 13.6 | 49.07 | 8.2 | 6.2 | 689.1 | 637.7 | 0.69 | -24.2 |
| Westerland | DE0001R | 8.31 | 54.93 | 7.4 | 10.5 | 755.4 | 1020.4 | 0.69 | 41.7 |
| Waldhof | DE0002R | 10.76 | 52.8 | 12.2 | 11.1 | 797.2 | 528.5 | 0.21 | -9.7 |
| Schauinsland | DE0003R | 7.91 | 47.91 | 10.4 | 11.8 | 1501.6 | 1263.8 | 0.02 | 13.4 |
| Neuglobsow | DE0007R | 13.03 | 53.17 | 10.9 | 8.9 | 692.8 | 535.3 | 0.59 | -18.2 |
| Schmucke | DE0008R | 10.77 | 50.65 | 20.2 | 12.3 | 1449.1 | 949.3 | 0.58 | -39.1 |
| Zingst | DE0009R | 12.72 | 54.44 | 9.2 | 7.0 | 657.8 | 430.4 | 0.50 | -24.2 |
| Keldsnor | DK0005R | 10.74 | 54.75 | 13.8 | 5.7 | 536.6 | 321.9 | 0.18 | -58.6 |
| Anholt | DK0008R | 11.52 | 56.72 | 10.9 | 6.8 | 604.6 | 515.2 | 0.61 | -40.2 |
| Riscoe | DK0012R | 12.09 | 55.69 | 14.8 | 8.9 | 604.8 | 558.8 | 0.61 | -40.2 |
| Sepstrup Sande | DK0022R | 9.42 | 56.08 | 18.0 | 8.8 | 1043.2 | 466.6 | 0.40 | -53.3 |
| Lahemaa | EE0009R | 25.9 | 59.5 | 25.6 | 5.2 | 776.2 | 509.1 | -0.20 | -79.7 |
| Vilsandi | EE0011R | 21.82 | 58.38 | 39.8 | 7.1 | 683.0 | 810.2 | 0.02 | -82.2 |
| Niembro | ES0008R | -4.85 | 43.44 | 64.2 | 5.4 | 1055.1 | 389.2 | 0.73 | -91.6 |
| Campisabalos | ES0009R | -3.14 | 41.28 | 7.3 | 1.0 | 116.9 | 118.8 | 0.74 | -86.8 |
| Virolahti III | FI0018R | 27.67 | 60.53 | 22.6 | 8.0 | 816.4 | 709.9 | 0.60 | -64.5 |
| Pallas (Matorova) | FI0036R | 24.24 | 68 | 3.1 | 1.5 | 557.6 | 585.1 | -0.02 | -53.6 |
| Hyytiälä | FI0050R | 24.28 | 61.85 | 6.8 | 3.7 | 594.2 | 599.1 | 0.70 | -44.5 |
| Hailuoto II | FI0053R | 24.69 | 65 | 3.8 | 2.8 | 377.8 | 466.8 | 0.38 | -24.8 |
| Hietajärvi | FI0092R | 30.72 | 63.17 | 8.6 | 4.7 | 701.0 | 715.7 | 0.61 | -45.3 |
| Kotinen | FI0093R | 25.07 | 61.23 | 7.3 | 3.6 | 598.9 | 549.6 | 0.39 | -51.0 |
| Revin | FR0009R | 4.63 | 49.9 | 29.9 | 8.9 | 1047.8 | 730.3 | -0.09 | -70.2 |
| Peyrusse Vieille | FR0013R | 0.18 | 43.62 | 16.2 | 4.4 | 620.0 | 377.1 | 0.23 | -72.8 |
| Saint-Nazaire-le-Desert | FR0023R | 5.28 | 44.57 | 43.7 | 6.3 | 695.7 | 612.1 | -0.11 | -85.7 |
| Guipry | FR0024R | -1.84 | 47.83 | 11.5 | 3.0 | 495.3 | 414.6 | 0.46 | -73.8 |
| Verneuil | FR0025R | 2.61 | 46.81 | 36.5 | 4.1 | 491.3 | 533.2 | 0.32 | -88.7 |
| Porspoder | FR0090R | -4.75 | 48.52 | 19.6 | 7.6 | 633.4 | 1015.5 | 0.29 | -61.3 |
| Lough Navar | GB0006R | -7.87 | 54.44 | 5.7 | 4.0 | 1338.8 | 700.1 | 0.75 | -30.1 |
| Yarner Wood | GB0013R | -3.71 | 50.6 | 6.0 | 3.3 | 722.0 | 408.2 | 0.67 | -30.7 |
| Heigham Holmes | GB0017R | 1.62 | 52.72 | 6.7 | 4.7 | 444.5 | 311.1 | 0.93 | -30.7 |
| Auchencorth Moss | GB0048R | -3.24 | 55.79 | 0.0 | 3.1 | 0.3 | 460.8 | 0.23 | 5.4 |
| Chilbolton Observatory | GB1055 | -1.44 | 51.15 | 6.1 | 4.0 | 498.8 | 433.0 | 0.58 | -33.8 |
| K-puszta | HU0002R | 19.58 | 46.97 | 15.7 | 10.7 | 681.1 | 593.1 | 0.31 | -31.6 |
| Vestmannaeyjar | IS0091R | -20.28 | 63.4 | 21.8 | 8.6 | 1365.0 | 1381.5 | -0.07 | -60.4 |
| Rucava | LV0010R | 21.17 | 56.16 | 16.0 | 7.3 | 666.1 | 787.5 | 0.82 | -54.5 |
| Aluksne | LV1000R | 27.04 | 57.44 | 11.1 | 3.3 | 368.0 | 388.3 | 0.85 | -70.5 |
| Dobele | LV2000R | 23.32 | 56.62 | 6.8 | 3.1 | 313.3 | 206.9 | 0.64 | -54.1 |
| Skriveri | LV5000R | 25.13 | 56.64 | 8.0 | 3.4 | 261.9 | 322.2 | 0.75 | -57.7 |
| Riga | LV6000R | 24.1 | 56.95 | 24.9 | 7.7 | 388.1 | 446.7 | 0.13 | -69.3 |
| Vredepeel | NL0010R | 5.85 | 51.54 | 18.1 | 11.2 | 228.2 | 308.7 | 0.13 | -38.0 |
| Birkenes | NO0001R | 8.25 | 58.38 | 16.7 | 7.8 | 1496.2 | 1015.2 | 0.84 | -53.5 |
| Kårvatn | NO0039R | 8.88 | 62.78 | 4.7 | 3.2 | 1642.3 | 1875.5 | 0.52 | -32.6 |
| Hurdal | NO0056R | 11.08 | 60.37 | 9.8 | 3.7 | 858.3 | 694.9 | 0.57 | -61.6 |
| Karpdalen | NO0098R | 30.43 | 69.65 | 20.7 | 2.6 | 347.1 | 572.1 | -0.57 | -87.7 |
| Leba | PL0004R | 17.53 | 54.75 | 11.2 | 10.5 | 829.8 | 800.6 | 0.46 | -6.0 |
| Diabla Gora | PL0005R | 22.07 | 54.15 | 19.5 | 13.3 | 691.2 | 755.0 | 0.55 | -31.9 |
| Bredkälen | SE0005R | 15.33 | 63.85 | 8.7 | 1.7 | 440.4 | 581.3 | -0.27 | -80.7 |
| Aspvreten | SE0012R | 17.38 | 58.8 | 7.1 | 4.5 | 451.6 | 522.4 | 0.26 | -36.0 |
| Råö | SE0014R | 11.91 | 57.39 | 10.3 | 9.4 | 606.5 | 756.1 | 0.32 | -8.6 |
| Hallahus | SE0020R | 13.15 | 56.04 | 11.8 | 10.8 | 843.9 | 912.8 | 0.54 | -8.8 |
| Iskrba | SI0008R | 14.87 | 45.57 | 12.3 | 11.3 | 1098.0 | 967.0 | 0.37 | -8.2 |

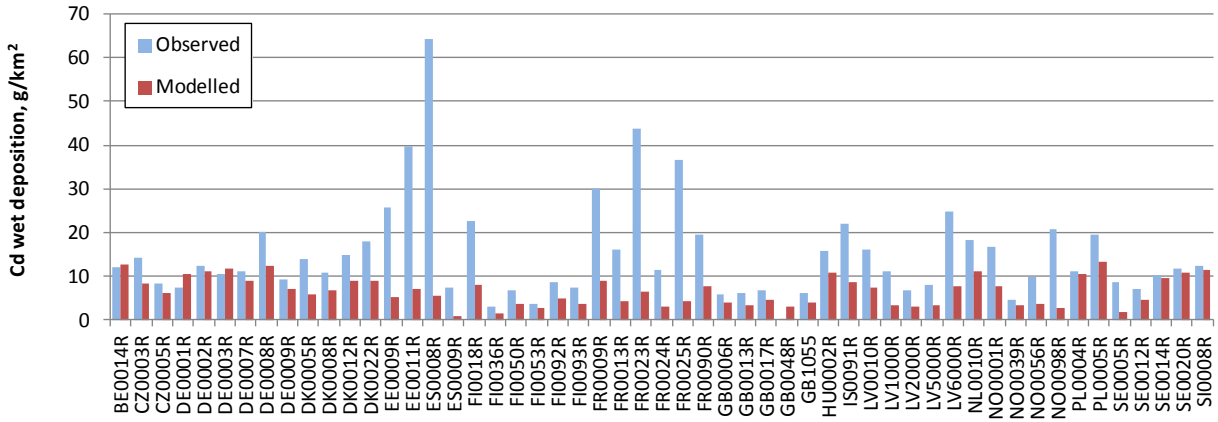


***Fig. 4.7.*** *Modelled and observed annual wet deposition fluxes of Cd at the EMEP stations in 2017*

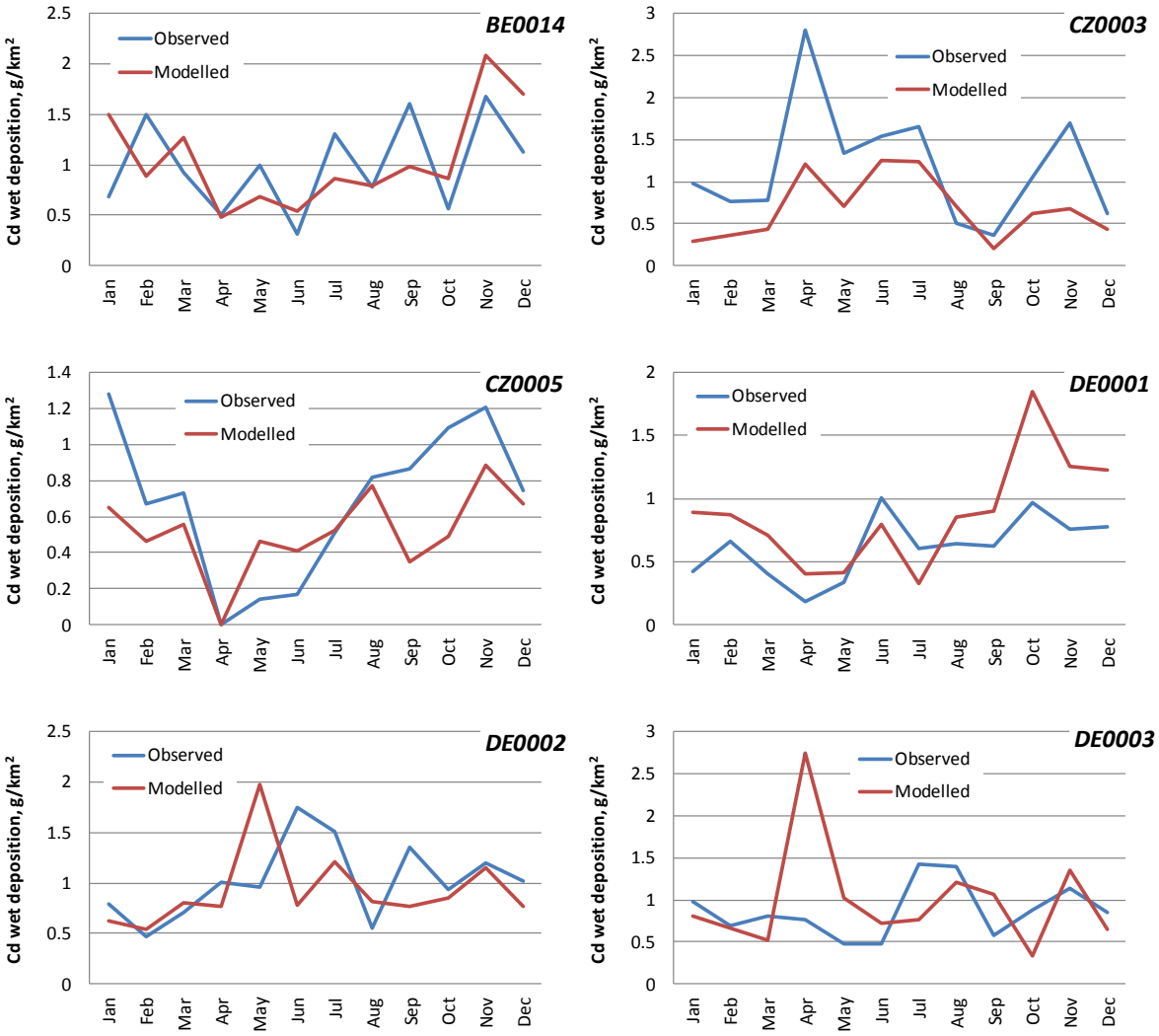

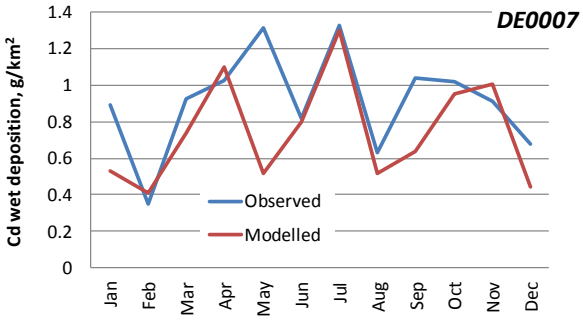
DE0007
Cd wet deposition, g/km²
Observed
Modelled
Jan Feb Mar Apr May Jun Jul Aug Sep Oct Nov Dec

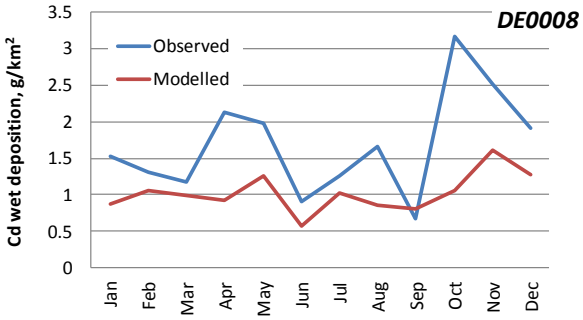
DE0008
Cd wet deposition, g/km²
Observed
Modelled
Jan Feb Mar Apr May Jun Jul Aug Sep Oct Nov Dec

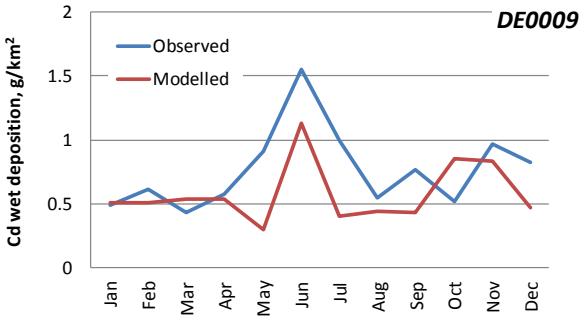
DE0009
Cd wet deposition, g/km²
Observed
Modelled
Jan Feb Mar Apr May Jun Jul Aug Sep Oct Nov Dec

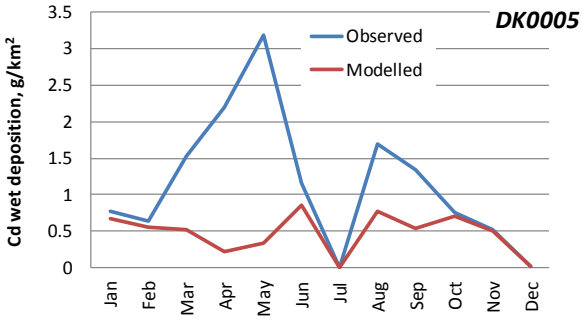
DK0005
Cd wet deposition, g/km²
Observed
Modelled
Jan Feb Mar Apr May Jun Jul Aug Sep Oct Nov Dec

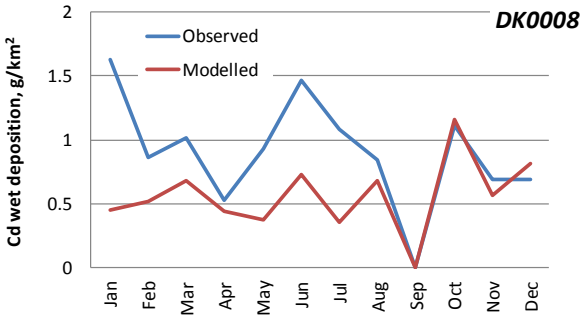
DK0008
Cd wet deposition, g/km²
Observed
Modelled
Jan Feb Mar Apr May Jun Jul Aug Sep Oct Nov Dec

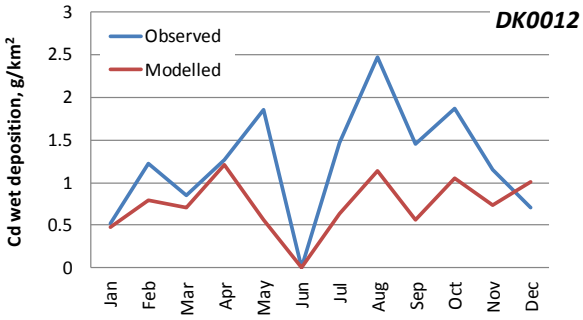
DK0012
Cd wet deposition, g/km²
Observed
Modelled
Jan Feb Mar Apr May Jun Jul Aug Sep Oct Nov Dec

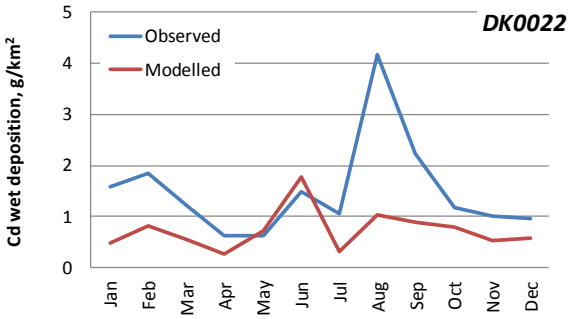
DK0022
Cd wet deposition, g/km²
Observed
Modelled
Jan Feb Mar Apr May Jun Jul Aug Sep Oct Nov Dec

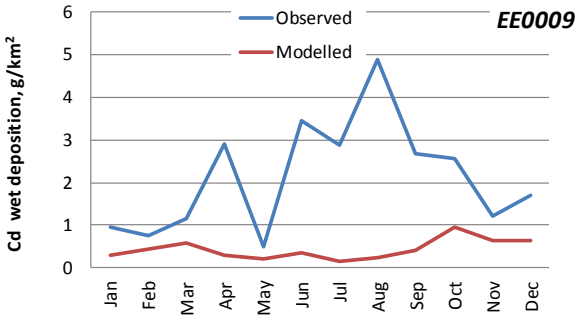
EE0009
Cd wet deposition, g/km²
Observed
Modelled
Jan Feb Mar Apr May Jun Jul Aug Sep Oct Nov Dec

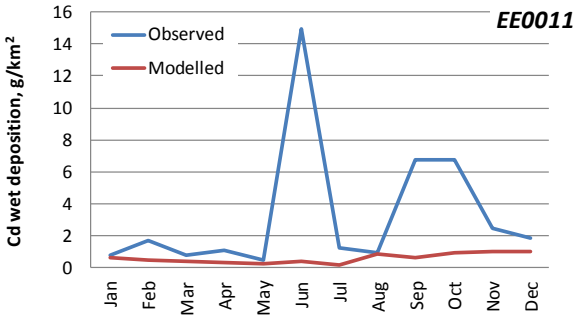
EE0011
Cd wet deposition, g/km²
Observed
Modelled
Jan Feb Mar Apr May Jun Jul Aug Sep Oct Nov Dec

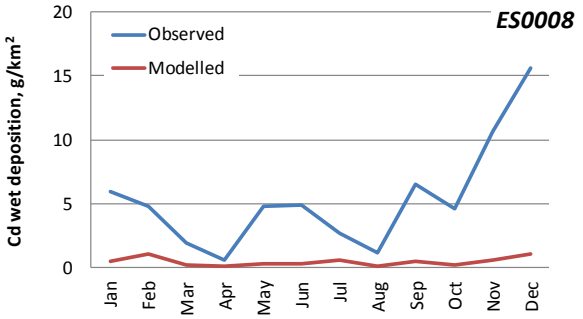
ES0008
Cd wet deposition, g/km²
Observed
Modelled
Jan Feb Mar Apr May Jun Jul Aug Sep Oct Nov Dec

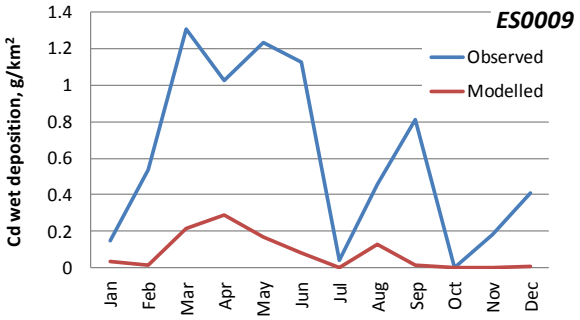
ES0009
Observed
Modelled
Cd wet deposition, g/km²
1.4
1.2
1
0.8
0.6
0.4
0.2
0
Jan Feb Mar Apr May Jun Jul Aug Sep Oct Nov Dec

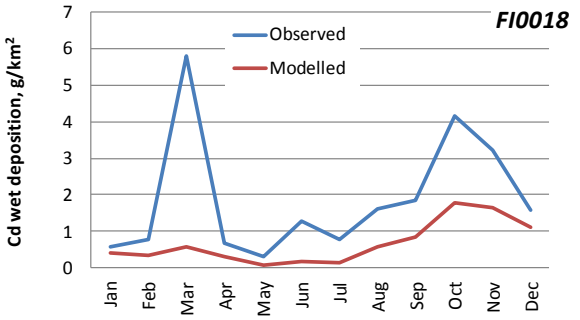
FI0018
Observed
Modelled
Cd wet deposition, g/km²
7
6
5
4
3
2
1
0
Jan Feb Mar Apr May Jun Jul Aug Sep Oct Nov Dec

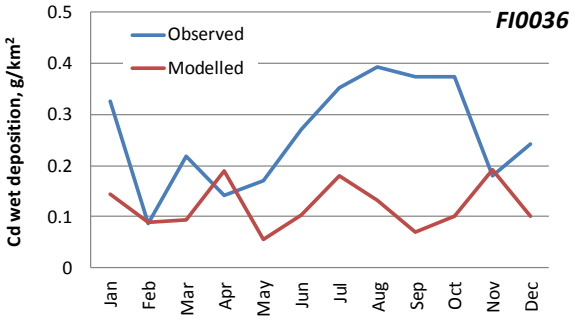
FI0036
Observed
Modelled
Cd wet deposition, g/km²
0.5
0.4
0.3
0.2
0.1
0
Jan Feb Mar Apr May Jun Jul Aug Sep Oct Nov Dec

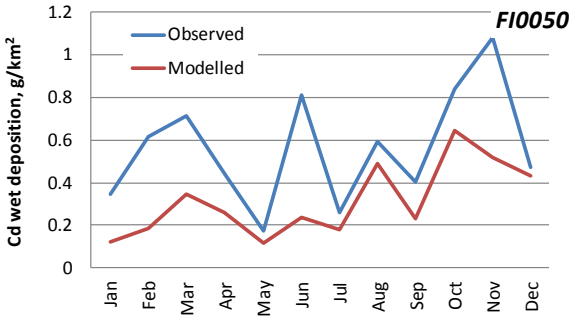
FI0050
Observed
Modelled
Cd wet deposition, g/km²
1.2
1
0.8
0.6
0.4
0.2
0
Jan Feb Mar Apr May Jun Jul Aug Sep Oct Nov Dec

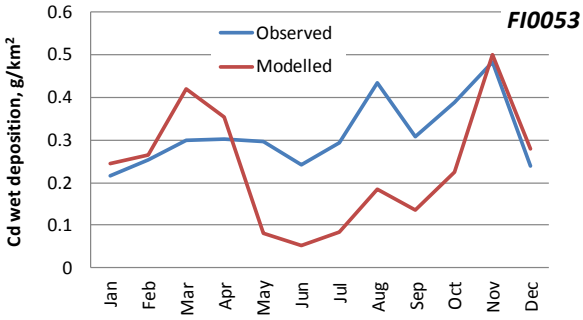
FI0053
Observed
Modelled
Cd wet deposition, g/km²
0.6
0.5
0.4
0.3
0.2
0.1
0
Jan Feb Mar Apr May Jun Jul Aug Sep Oct Nov Dec

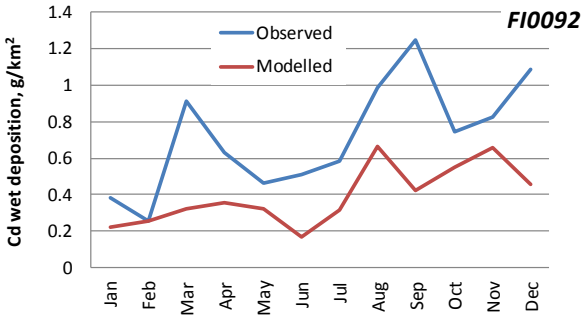
FI0092
Observed
Modelled
Cd wet deposition, g/km²
1.4
1.2
1
0.8
0.6
0.4
0.2
0
Jan Feb Mar Apr May Jun Jul Aug Sep Oct Nov Dec

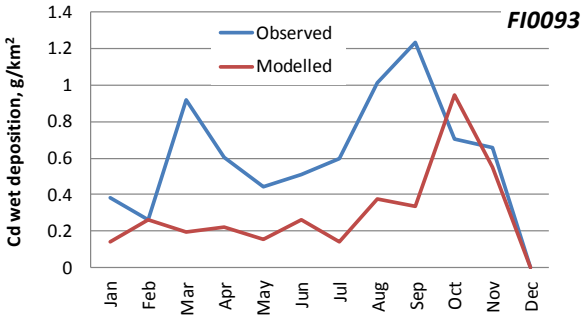
FI0093
Observed
Modelled
Cd wet deposition, g/km²
1.4
1.2
1
0.8
0.6
0.4
0.2
0
Jan Feb Mar Apr May Jun Jul Aug Sep Oct Nov Dec

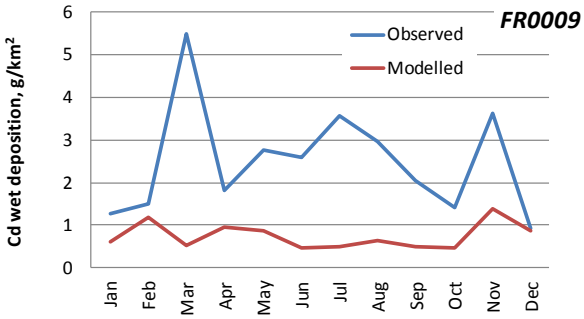
FR0009
Observed
Modelled
Cd wet deposition, g/km²
6
5
4
3
2
1
0
Jan Feb Mar Apr May Jun Jul Aug Sep Oct Nov Dec

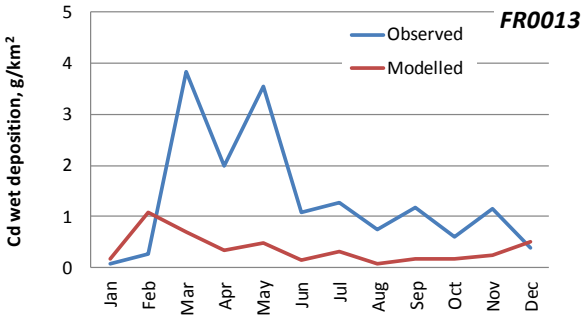
FR0013
Observed
Modelled
Cd wet deposition, g/km²
5
4
3
2
1
0
Jan Feb Mar Apr May Jun Jul Aug Sep Oct Nov Dec

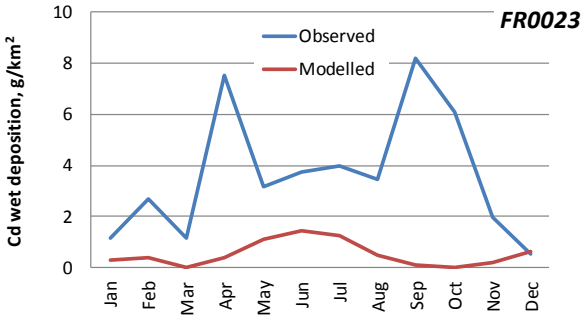
FR0023
Observed
Modelled
Cd wet deposition, g/km²
10
8
6
4
2
0
Jan Feb Mar Apr May Jun Jul Aug Sep Oct Nov Dec

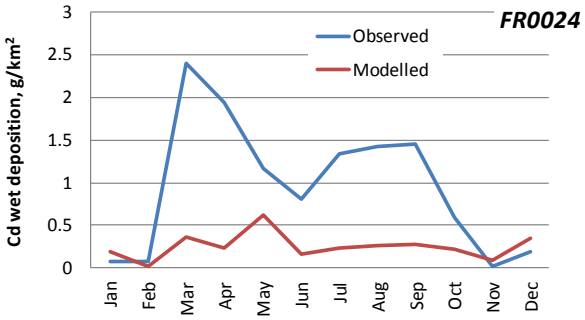
FR0024
Observed
Modelled
Cd wet deposition, g/km²
0
0.5
1
1.5
2
2.5
3
Jan Feb Mar Apr May Jun Jul Aug Sep Oct Nov Dec

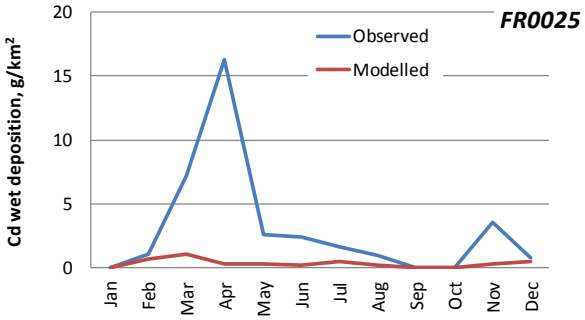
FR0025
Observed
Modelled
Cd wet deposition, g/km²
0
5
10
15
20
Jan Feb Mar Apr May Jun Jul Aug Sep Oct Nov Dec

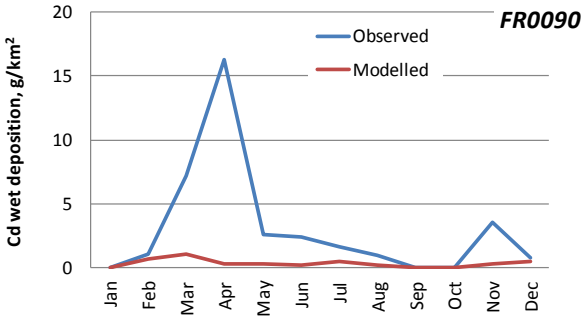
FR0090
Observed
Modelled
Cd wet deposition, g/km²
0
5
10
15
20
Jan Feb Mar Apr May Jun Jul Aug Sep Oct Nov Dec

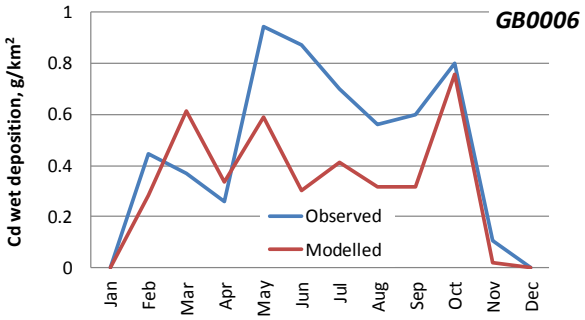
GB0006
Observed
Modelled
Cd wet deposition, g/km²
0
0.2
0.4
0.6
0.8
1
Jan Feb Mar Apr May Jun Jul Aug Sep Oct Nov Dec

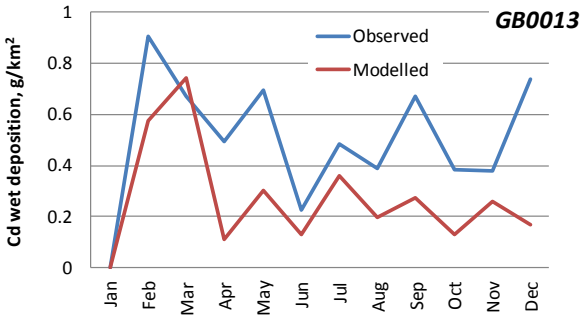
GB0013
Observed
Modelled
Cd wet deposition, g/km²
0
0.2
0.4
0.6
0.8
1
Jan Feb Mar Apr May Jun Jul Aug Sep Oct Nov Dec

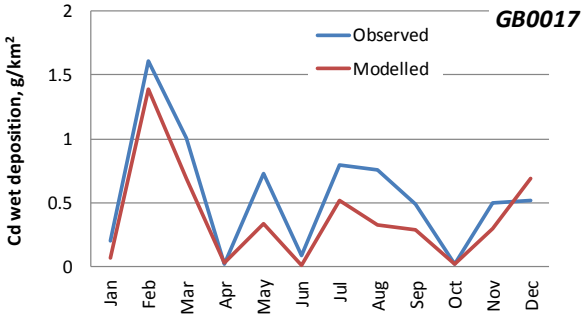
GB0017
Observed
Modelled
Cd wet deposition, g/km²
0
0.5
1
1.5
2
Jan Feb Mar Apr May Jun Jul Aug Sep Oct Nov Dec

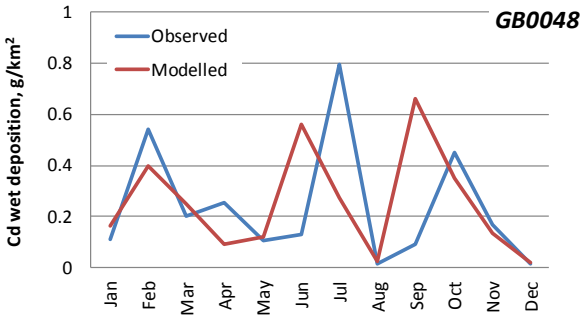
GB0048
Observed
Modelled
Cd wet deposition, g/km²
0
0.2
0.4
0.6
0.8
1
Jan Feb Mar Apr May Jun Jul Aug Sep Oct Nov Dec

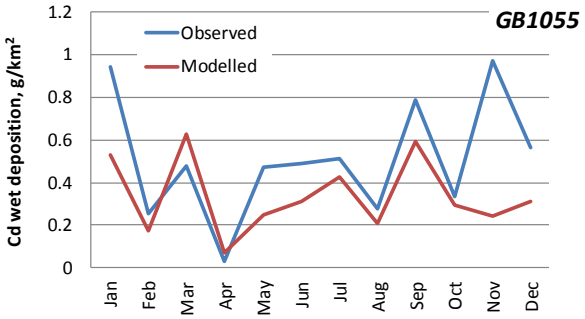
GB1055
Observed
Modelled
Cd wet deposition, g/km²
0
0.2
0.4
0.6
0.8
1
1.2
Jan Feb Mar Apr May Jun Jul Aug Sep Oct Nov Dec

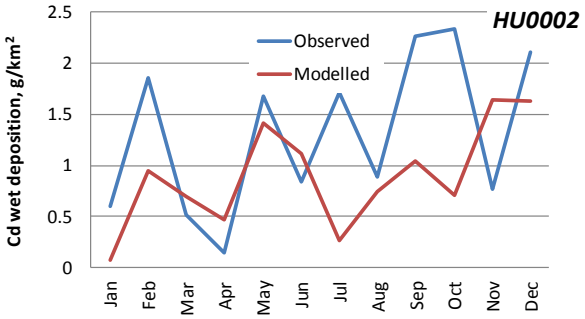
HU0002
Observed
Modelled
Cd wet deposition, g/km²
0
0.5
1
1.5
2
2.5
Jan Feb Mar Apr May Jun Jul Aug Sep Oct Nov Dec

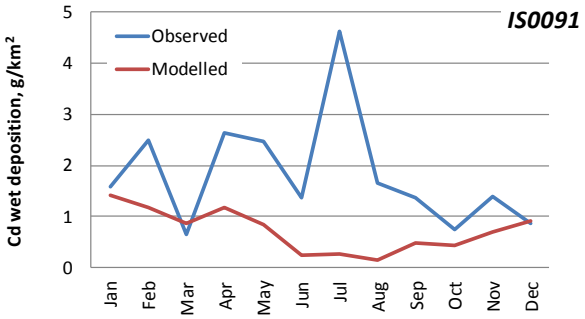
IS0091
Observed
Modelled
Cd wet deposition, g/km²
0
1
2
3
4
5
Jan Feb Mar Apr May Jun Jul Aug Sep Oct Nov Dec

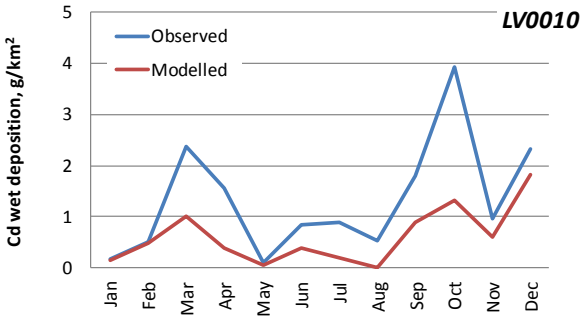
LV0010
Observed
Modelled
Cd wet deposition, g/km²
0
1
2
3
4
5
Jan
Feb
Mar
Apr
May
Jun
Jul
Aug
Sep
Oct
Nov
Dec

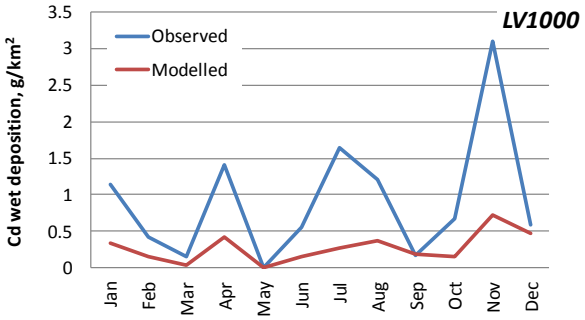
LV1000
Observed
Modelled
Cd wet deposition, g/km²
0
0.5
1
1.5
2
2.5
3
3.5
Jan
Feb
Mar
Apr
May
Jun
Jul
Aug
Sep
Oct
Nov
Dec

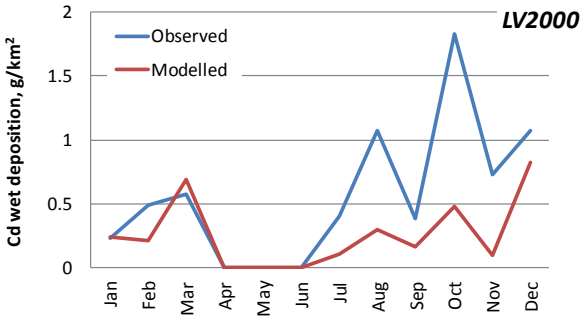
LV2000
Observed
Modelled
Cd wet deposition, g/km²
0
0.5
1
1.5
2
Jan
Feb
Mar
Apr
May
Jun
Jul
Aug
Sep
Oct
Nov
Dec

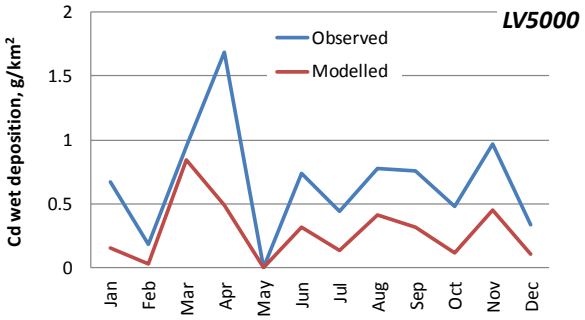
LV5000
Observed
Modelled
Cd wet deposition, g/km²
0
0.5
1
1.5
2
Jan
Feb
Mar
Apr
May
Jun
Jul
Aug
Sep
Oct
Nov
Dec

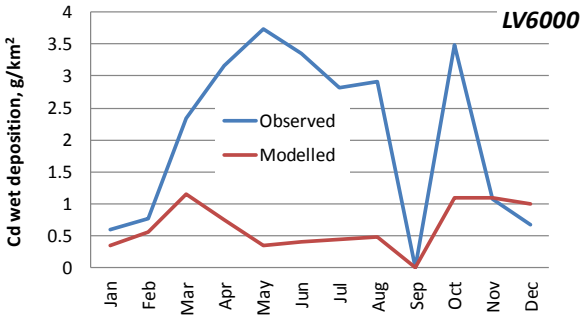
LV6000
Observed
Modelled
Cd wet deposition, g/km²
0
0.5
1
1.5
2
2.5
3
3.5
4
Jan
Feb
Mar
Apr
May
Jun
Jul
Aug
Sep
Oct
Nov
Dec

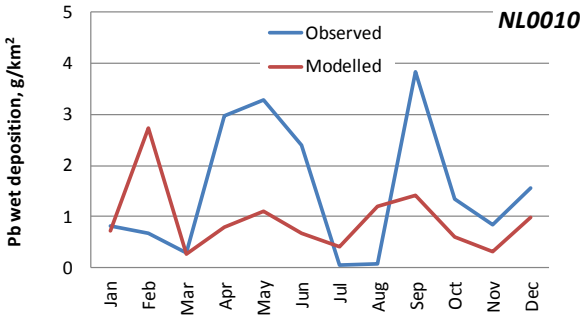
NL0010
Observed
Modelled
Pb wet deposition, g/km²
0
1
2
3
4
5
Jan
Feb
Mar
Apr
May
Jun
Jul
Aug
Sep
Oct
Nov
Dec

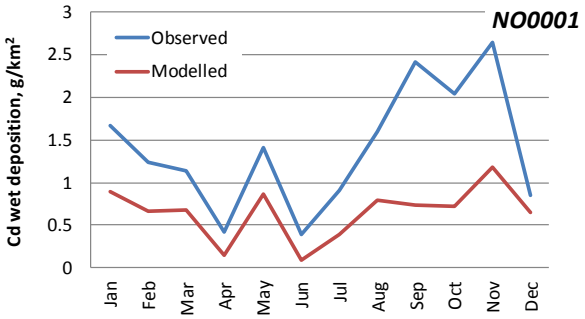
NO0001
Observed
Modelled
Cd wet deposition, g/km²
0
0.5
1
1.5
2
2.5
3
Jan
Feb
Mar
Apr
May
Jun
Jul
Aug
Sep
Oct
Nov
Dec

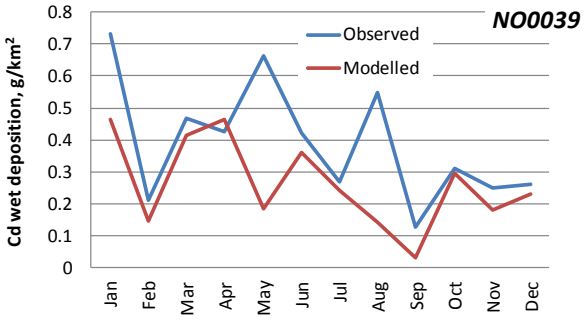
NO0039
Observed
Modelled
Cd wet deposition, g/km²
0
0.1
0.2
0.3
0.4
0.5
0.6
0.7
0.8
Jan
Feb
Mar
Apr
May
Jun
Jul
Aug
Sep
Oct
Nov
Dec

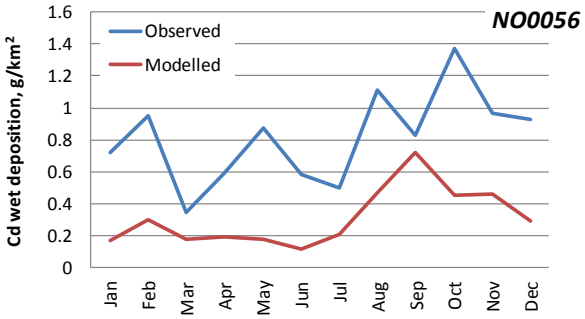
NO0056
Observed
Modelled
Cd wet deposition, g/km²
0
0.2
0.4
0.6
0.8
1
1.2
1.4
1.6
Jan
Feb
Mar
Apr
May
Jun
Jul
Aug
Sep
Oct
Nov
Dec

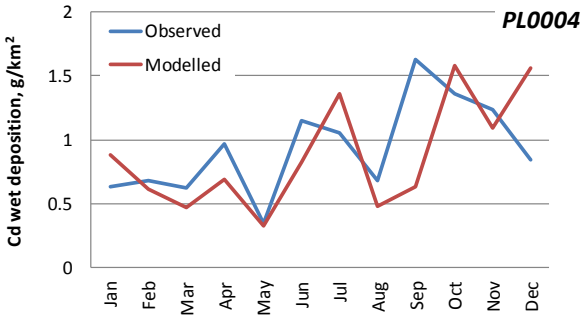
PL0004
Observed
Modelled
Cd wet deposition, g/km²
0
0.5
1
1.5
2
Jan
Feb
Mar
Apr
May
Jun
Jul
Aug
Sep
Oct
Nov
Dec

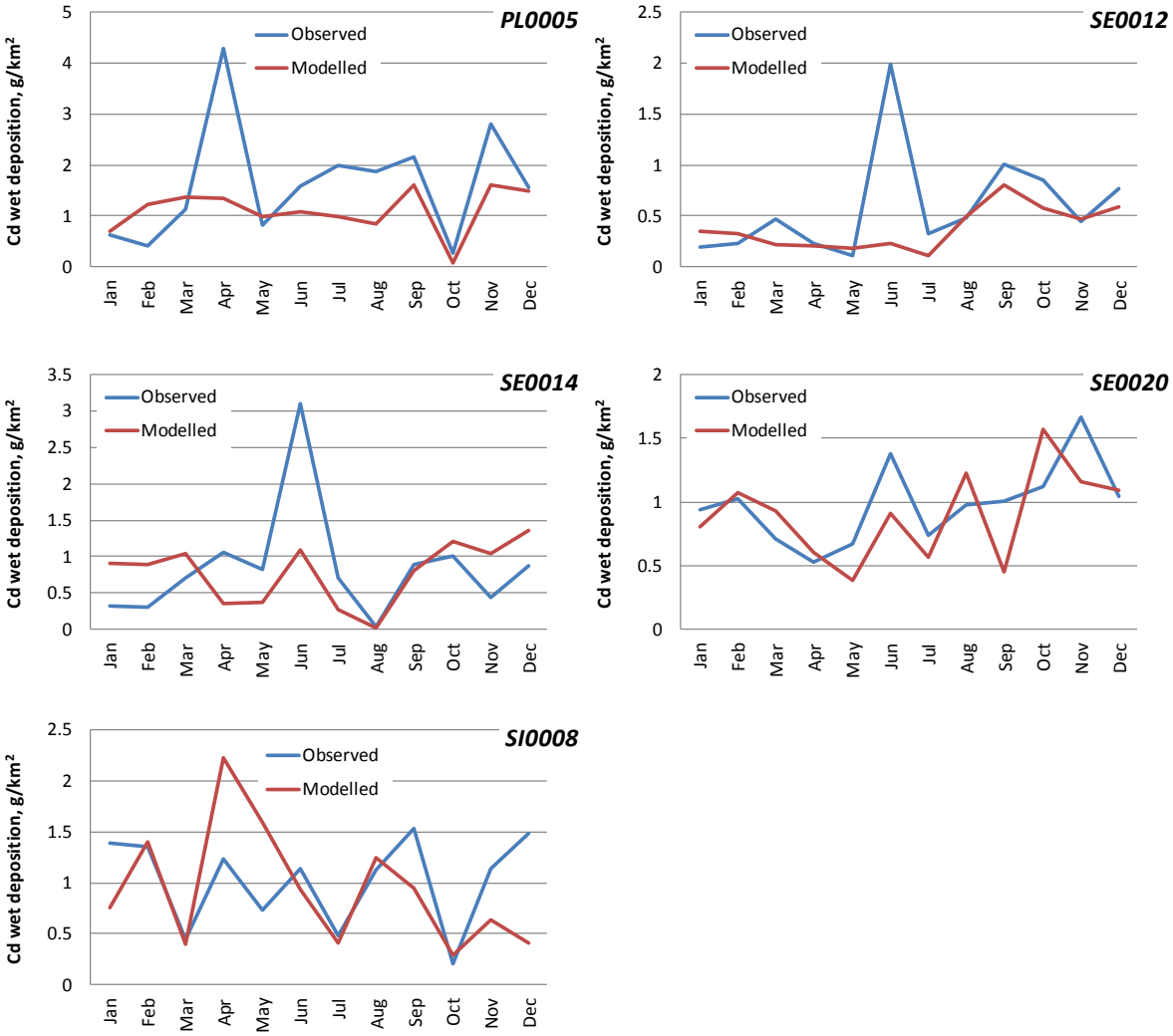


***Fig. 4.8.*** *Modelled and observed monthly wet deposition fluxes of Cd at the EMEP stations in 2017*

## 4.3. Mercury

### *4.3.1. Air concentrations*

***Table 4.5.*** *Annual mean modelled and observed Hg air concentrations, ng/m$^3$, temporal correlation coefficient (Rc) and relative bias (Bias) at EMEP stations in 2017*

| Station Name | Code | Longitude | Latitude | Observed | Modelled | R | Bias |
|---|---|---|---|---|---|---|---|
| Waldhof | DE0002R | 10.76 | 52.8 | 1.33 | 1.48 | 0.29 | -1.4 |
| Schauinsland | DE0003R | 7.91 | 47.91 | 1.33 | 1.48 | -0.44 | 11.5 |
| Schmucke | DE0008R | 10.77 | 50.65 | 1.5 | 1.56 | -0.34 | 4.3 |
| Zingst | DE0009R | 12.72 | 54.44 | 1.48 | 1.59 | -0.24 | 7.2 |
| Lahemaa | EE0009R | 25.9 | 59.5 | 1.17 | 1.51 | -0.45 | 29.3 |
| Pallas (Matorova) | FI0036R | 24.24 | 68 | 1.35 | 1.41 | 0.32 | 3.8 |
| Auchencorth Moss | GB0048R | -3.24 | 55.79 | 1.38 | 1.5 | -0.32 | 5.7 |
| Diabla Gora | PL0005R | 22.07 | 54.15 | 1.12 | 1.47 | 0.11 | 28.8 |
| Bredkälen | SE0005R | 15.33 | 63.85 | 1.37 | 1.39 | -0.32 | 1.5 |
| Råö | SE0014R | 11.91 | 57.39 | 1.35 | 1.52 | -0.46 | 12 |
| Chilbolton Observatory | GB1055R | -1.44 | 51.15 | 1.41 | 1.55 | | 9.6 |
| Halla | SE0020R | 13.15 | 56.04 | 1.34 | 1.51 | | 12.6 |

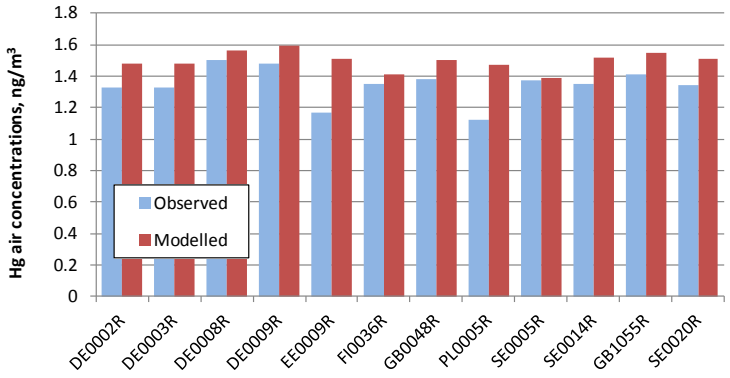


***Fig. 4.9.*** *Modelled and observed annual mean concentrations of Hg in air at the EMEP stations in 2017*

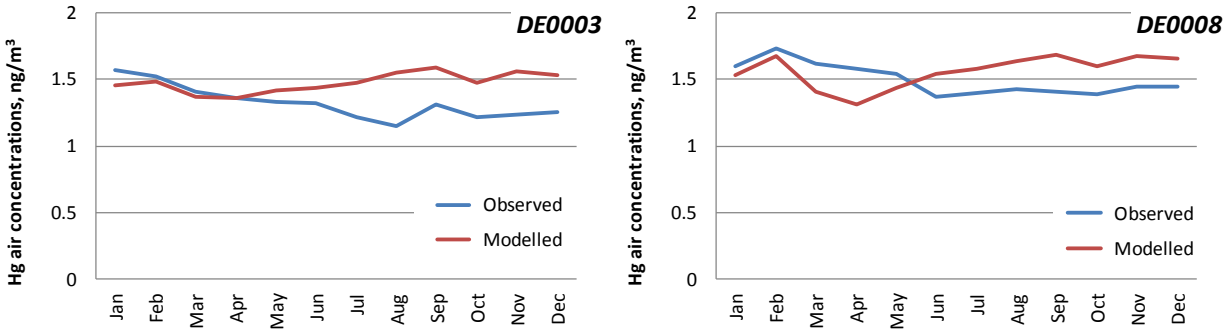

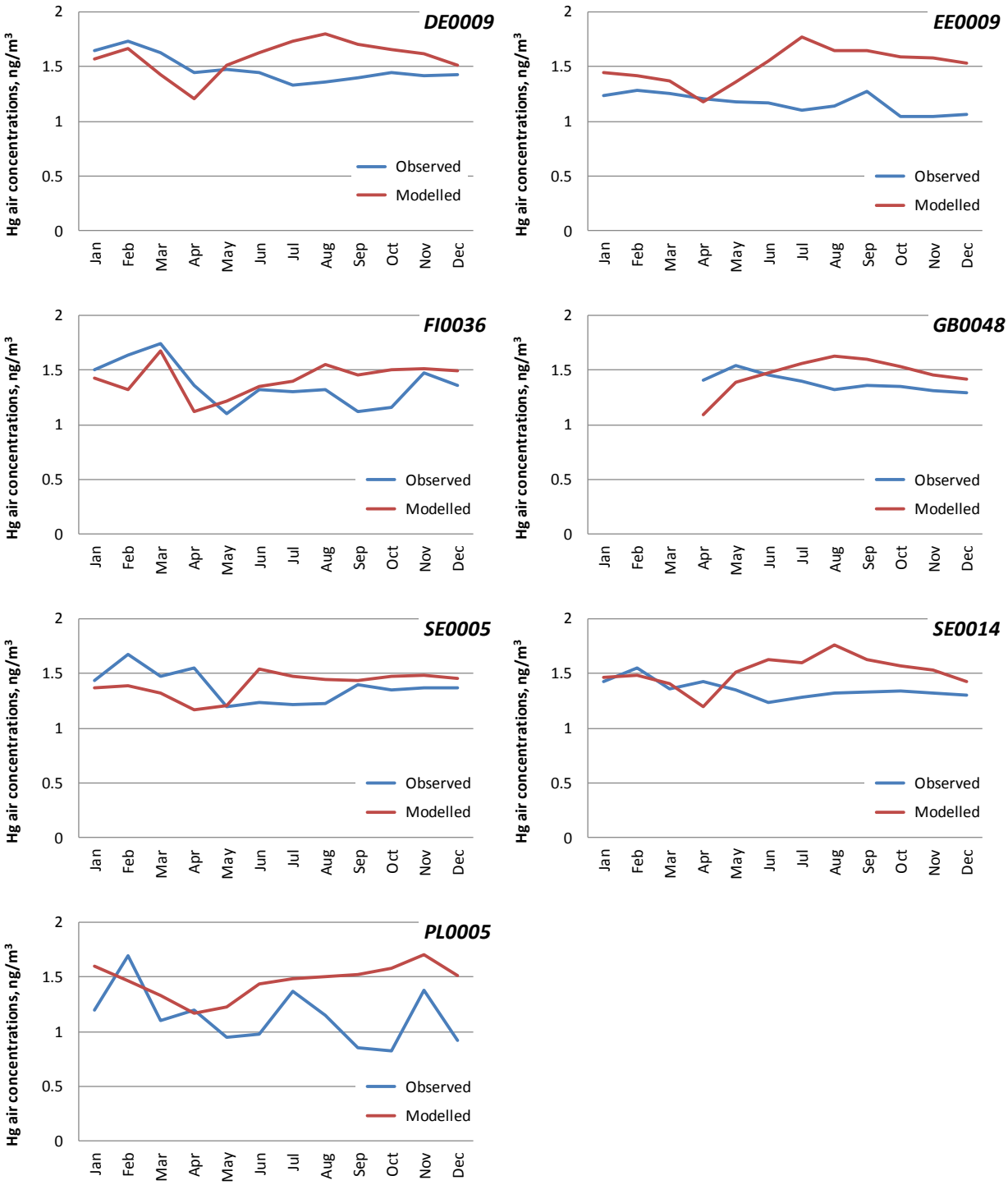


***Fig. 4.10.*** *Modelled and observed monthly mean concentrations of Hg in air at the EMEP stations in 2017*

### 4.3.2. Wet deposition

***Table 4.6.*** *Annual sums of modelled and observed Hg wet deposition fluxes, g/km$^2$/y, temporal correlation coefficient (Rc) and relative bias (Bias) at EMEP stations in 2017*

| Station name | Code | Longit | Latit | Observed flux | Modelled flux | Observed precip | Modelled precip | R | Bias |
|---|---|---|---|---|---|---|---|---|---|
| Koksijde | BE0014R | 2.66 | 51.12 | 4.06 | 7.47 | 681.5 | 260.2 | 0.88 | 115.9 |
| Kosetice (NOAK) | CZ0003R | 15.08 | 49.57 | 8.33 | 11.48 | 603.6 | 343.7 | 0.78 | 97.8 |
| Westerland | DE0001R | 8.31 | 54.93 | 5.07 | 9.39 | 891.4 | 496.1 | 0.87 | 140.7 |
| Waldhof | DE0002R | 10.76 | 52.8 | 6.39 | 8.81 | 864.9 | 323.2 | 0.68 | 50.1 |
| Schauinsland | DE0003R | 7.91 | 47.91 | 9.88 | 13.59 | 1605.4 | 849.1 | 0.53 | 44.1 |
| Schmucke | DE0008R | 10.77 | 50.65 | 8.13 | 10.37 | 1414.4 | 798.1 | 0.69 | 55.7 |
| Zingst | DE0009R | 12.72 | 54.44 | 3.79 | 5.40 | 548.2 | 196.8 | 0.97 | 27.4 |
| Lahemaa | EE0009R | 25.9 | 59.5 | 4.80 | 4.51 | 690.1 | 351.0 | 0.44 | -3.3 |
| Pallas (Matorova) | FI0036R | 24.24 | 68 | 2.86 | 6.65 | 569.0 | 600.6 | -0.09 | 158.1 |
| Yarner Wood | GB0013R | -3.71 | 50.6 | 3.61 | 5.44 | 829.4 | 267.0 | 0.40 | 64.5 |
| Heigham Holmes | GB0017R | 1.62 | 52.72 | 2.48 | 4.16 | 460.7 | 162.5 | 0.90 | 58.9 |
| Auchencorth Moss | GB0048R | -3.24 | 55.79 | 3.61 | 5.03 | 707.9 | 374.0 | 0.64 | 33.0 |
| De Zilk | NL0091R | 4.5 | 52.3 | 5.38 | 6.90 | 613.8 | 373.4 | 0.70 | 62.9 |
| Birkenes | NO0001R | 8.25 | 58.38 | 10.98 | 13.71 | 1884.0 | 1413.3 | 0.56 | 34.3 |
| Diabla Gora | PL0005R | 22.07 | 54.15 | 4.32 | 8.98 | 710.0 | 516.6 | 0.56 | 104.8 |
| Rao | SE0014R | 11.91 | 57.39 | 5.58 | 8.23 | 749.5 | 402.3 | 0.78 | 42.6 |
| Iskrba | SI0008R | 14.87 | 45.57 | 6.34 | 15.90 | 1528.0 | 902.0 | 0.13 | 151.8 |

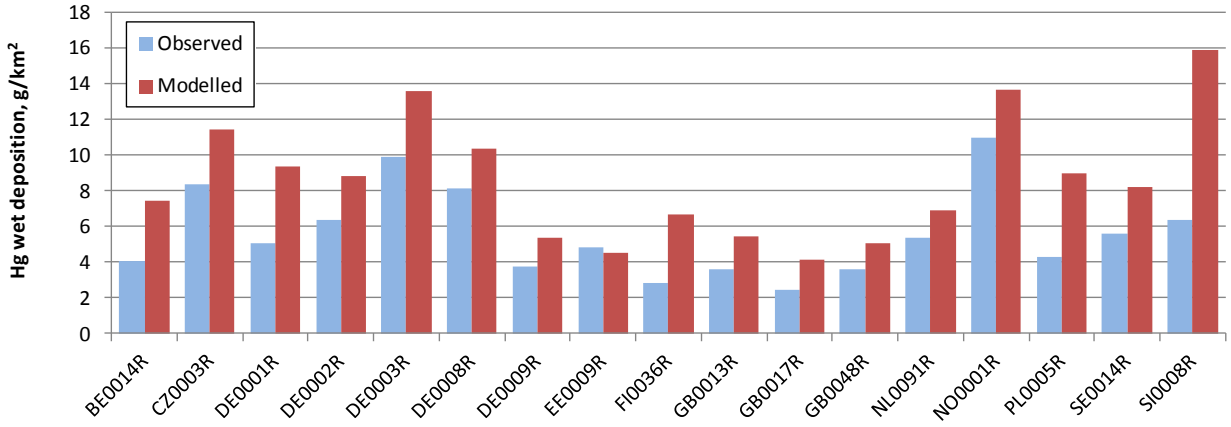


***Fig. 4.11.*** *Modelled and observed annual wet deposition fluxes of Hg at the EMEP stations in 2017*

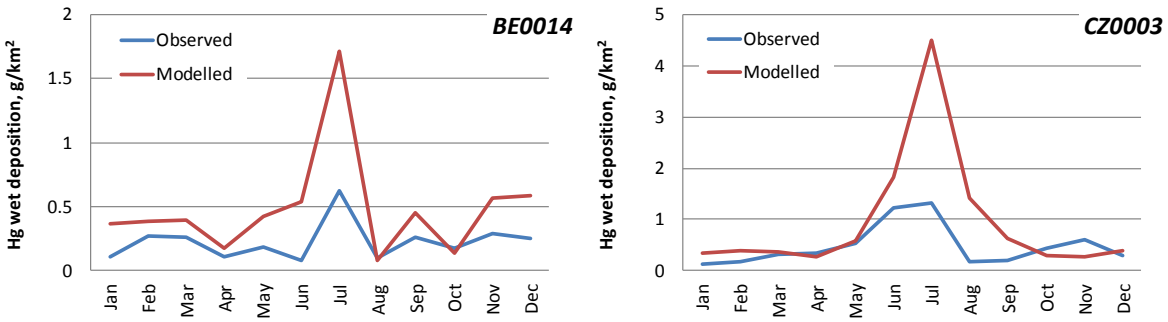

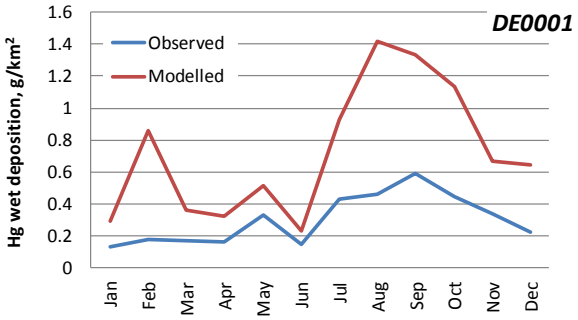
DE0001
Observed
Modelled
Hg wet deposition, g/km²
0
0.2
0.4
0.6
0.8
1
1.2
1.4
1.6
Jan
Feb
Mar
Apr
May
Jun
Jul
Aug
Sep
Oct
Nov
Dec

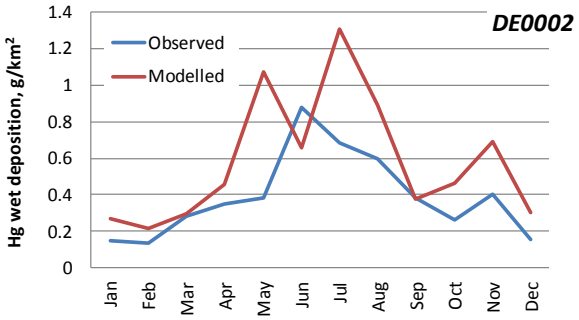
DE0002
Observed
Modelled
Hg wet deposition, g/km²
0
0.2
0.4
0.6
0.8
1
1.2
1.4
Jan
Feb
Mar
Apr
May
Jun
Jul
Aug
Sep
Oct
Nov
Dec

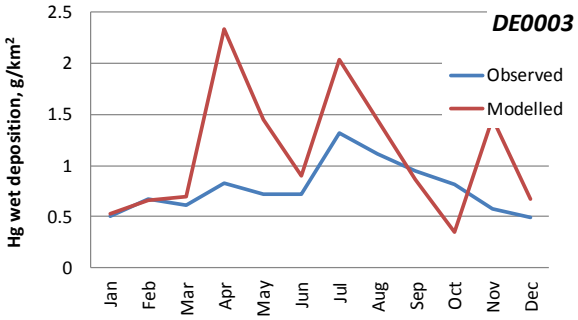
DE0003
Observed
Modelled
Hg wet deposition, g/km²
0
0.5
1
1.5
2
2.5
Jan
Feb
Mar
Apr
May
Jun
Jul
Aug
Sep
Oct
Nov
Dec

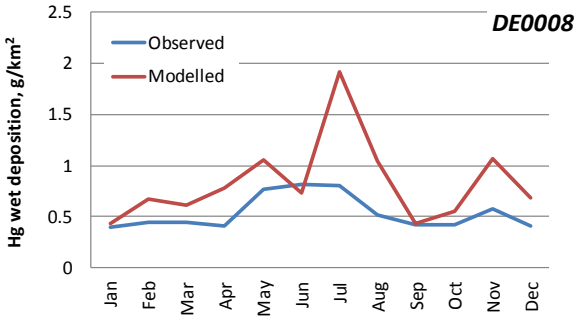
DE0008
Observed
Modelled
Hg wet deposition, g/km²
0
0.5
1
1.5
2
2.5
Jan
Feb
Mar
Apr
May
Jun
Jul
Aug
Sep
Oct
Nov
Dec

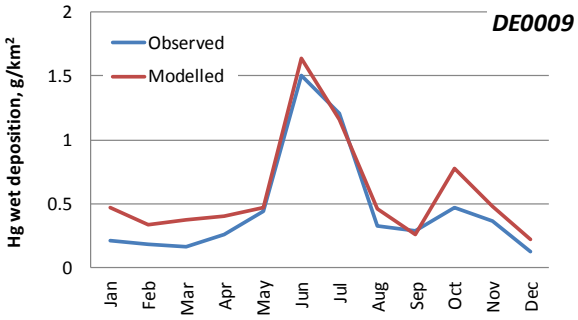
DE0009
Observed
Modelled
Hg wet deposition, g/km²
0
0.5
1
1.5
2
Jan
Feb
Mar
Apr
May
Jun
Jul
Aug
Sep
Oct
Nov
Dec

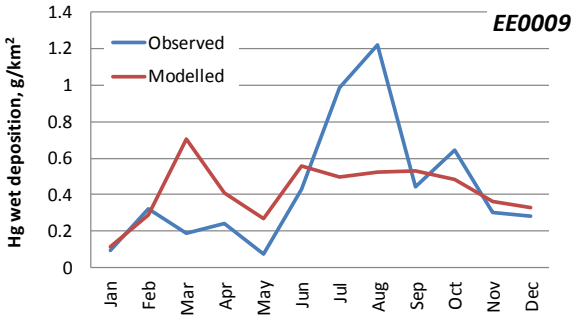
EE0009
Observed
Modelled
Hg wet deposition, g/km²
0
0.2
0.4
0.6
0.8
1
1.2
1.4
Jan
Feb
Mar
Apr
May
Jun
Jul
Aug
Sep
Oct
Nov
Dec

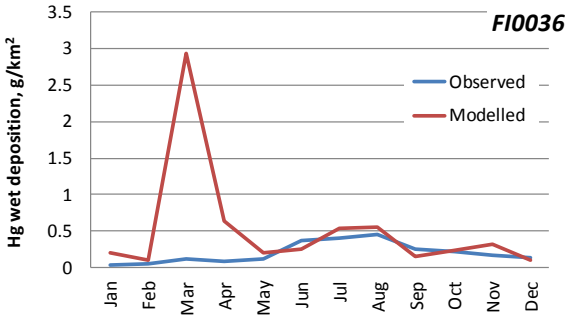
FI0036
Observed
Modelled
Hg wet deposition, g/km²
0
0.5
1
1.5
2
2.5
3
3.5
Jan
Feb
Mar
Apr
May
Jun
Jul
Aug
Sep
Oct
Nov
Dec

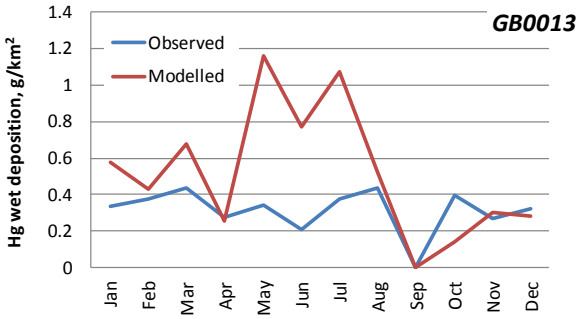
GB0013
Observed
Modelled
Hg wet deposition, g/km²
0
0.2
0.4
0.6
0.8
1
1.2
1.4
Jan
Feb
Mar
Apr
May
Jun
Jul
Aug
Sep
Oct
Nov
Dec

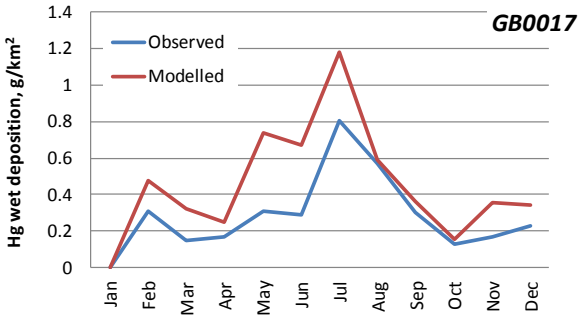
GB0017
Observed
Modelled
Hg wet deposition, g/km²
0
0.2
0.4
0.6
0.8
1
1.2
1.4
Jan
Feb
Mar
Apr
May
Jun
Jul
Aug
Sep
Oct
Nov
Dec

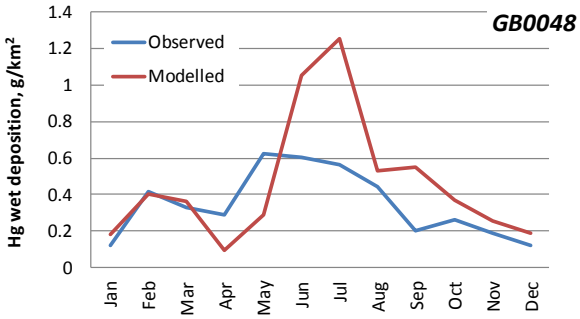
GB0048
Observed
Modelled
Hg wet deposition, g/km²
0
0.2
0.4
0.6
0.8
1
1.2
1.4
Jan
Feb
Mar
Apr
May
Jun
Jul
Aug
Sep
Oct
Nov
Dec

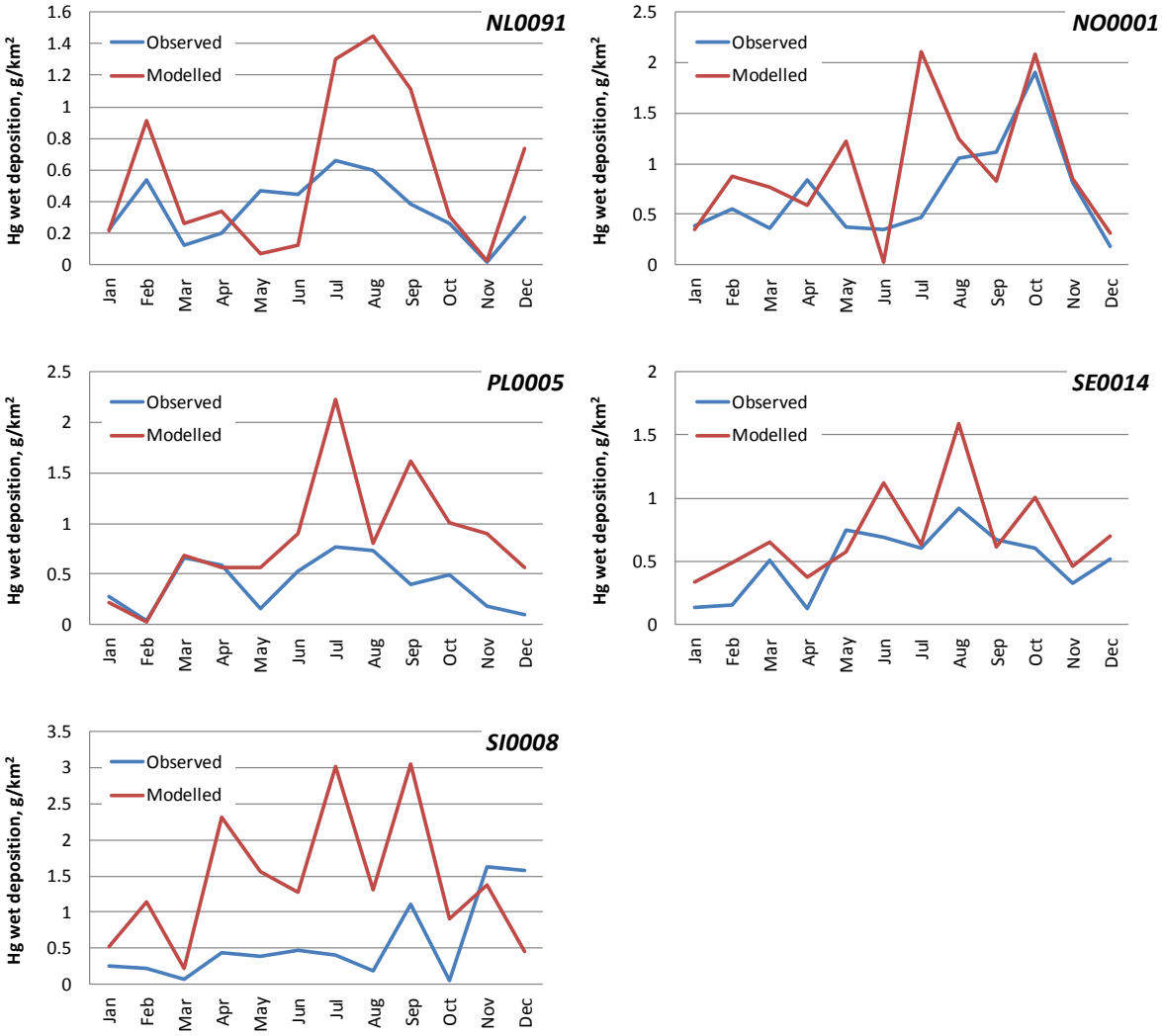


***Fig. 4.13.*** *Modelled and observed monthly wet deposition fluxes of Hg at the EMEP stations in 2017*

## 4.4. Discussion

Mean annual concentrations in air and wet deposition fluxes of Pb, Cd and Hg simulated by GLEMOS model were compared with the available EMEP monitoring data. This section presents the results of the comparison for 2017.

Results of the comparison between modelled and observed levels depend on uncertainties of the model parameterization, uncertainties of input data, especially emissions and on quality of measurement data. Analysis of the model uncertainties [*Travnikov and Ilyin*, 2005] demonstrated that intrinsic model uncertainty (i.e. uncertainty of the model as such, without effect of emission data) of modelled deposition of heavy metals was amounted to ±30-40% for Europe as a whole. Intrinsic uncertainty for air concentrations of particulate metals (Pb, Cd) is around ±40%, and Hg - around ±20%.

Information on uncertainties of the emission data is provided by some EMEP countries. Table ## summarizes estimates of uncertainties of Pb, Cd and Hg emission totals prepared by national experts. Uncertainty of total emissions in some counties may reach 500% for Pb, 430% for Cd and 180% for Hg. Median values of these emission uncertainties are about 50% for the considered metals. Therefore, uncertainties of emissions may affect quality of the model assessment results and interpretation of the results of comparison between modelled and observed concentrations and deposition.

***Table 4.7.*** *Uncertainties (%) of the national total values of heavy emission data used in calculations for 2017*

| Country | Pb | Cd | Hg | Reference |
|---|---|---|---|---|
| Belarus | 192 | 266 | 111 | *IIR Belarus* [2016] |
| Belgium | 104 | 85 | 33 | *IIR Belgium* [2018] |
| Croatia | 141 | 295 | 77 | *Poljanac et al.* [2018] |
| Cyprus | 30 | 25 | 8 | *Papadopoulos and Charalambous* [2018] |
| Denmark | 511 | 431 | 101 | *Nielsen et al.* [2018] |
| Estonia | 184 | 134 | 182 | *Kohv et al*. [2018] |
| Finland | 27 | 28 | 19 | *IIR Finland* [2018] |
| France | 160 | 37 | 32 | *Durand and Robert* [2018] |
| Latvia | 11 | 29 | 17 | *Skrebele at al*. [2018] |
| Poland | 55 | 53 | 59 | *Dębski et al*. [2018] |
| Sweden | 21 | 37 | 68 | *IIR Sweden* [2018] |
| Switzerland | 20-50 | 20-50 | 20-50 | *IIR Switzerland* [2018] |
| United Kingdom | 47 | -30 to >50 | -30 to 50 | *Wakeling et al*. [2018] |

Quality of Pb and Cd monitoring data is regularly evaluated via laboratory intercomparison tests. According to the most recent results, related to measurements in 2017, almost all laboratories managed to predict theoretical values of Cd and Pb concentrations in precipitation with satisfactory accuracy (within ±25%) [*CCC,* 2019]. However, these tests characterize only uncertainty of analytical methods applied in country's laboratories. Uncertainties arisen at other steps of monitoring (e.g., sampling, transportation, storing etc.) are not taken into account. Therefore, full uncertainty is most likely higher than the uncertainty estimated via considered tests.

Statistical indicators for lead, cadmium and mercury concentrations in air and wet deposition are summarized in Table 4.8. Statistical parameters used in the comparison include mean relative bias,

Pearson's correlation coefficient, normalized root mean square error (NRMSE) and fraction of fitting modelled and observed values within two-fold or three-fold difference (F2, F3).

***Table 4.8.*** *Main statistical indicators of agreement between annual modelled and measured levels of air concentrations and wet deposition fluxes in 2016*

| | Pb | | Cd | | Hg | |
|---|---|---|---|---|---|---|
| | $C_{air}$ | Wet Dep | $C_{air}$ | Wet Dep | $C_{air}$ | Wet Dep |
| Mean relative bias, % | 0.7 | -40 | 12.6 | -43 | 11 | 52 |
| Correlation coefficient | 0.82 | 0.51 | 0.76 | 0.45 | 0.39 | 0.81 |
| NRMSE | 0.45 | 0.65 | 0.61 | 0.67 | 0.13 | 0.63 |
| F2, % | 84 | 68 | 73 | 65 | 100 | 84 |
| F3, % | 96 | 88 | 91 | 91 | 100 | 100 |
| N | 45 | 50 | 45 | 43 | 12 | 19 |

$C_{air}$ – concentration in air F2 – fraction of values fitting to factor of 2 difference

Wet Dep – wet deposition flux F3 – fraction of values fitting to factor of 3 difference

NRMSE – Normalized Root Mean Square Error N – number of model-observation pairs

Mean relative bias for concentrations in air, calculated for all stations is -5.5%, and spatial correlation coefficient is 0.74. Corresponding values for Cd concentrations in air are 13% and 0.76. The agreement between modelled and observed concentrations at particulate stations differs markedly from the mean value. Fig. 4.14 and 4.15 depicts modelled and observed concentrations of Pb and Cd in air for each EMEP station. Bars showing modelled concentrations are split in contributions of several components: EMEP anthropogenic sources, re-suspension from various land-cover surfaces (bare lands, arable lands, urban territories, sea surface) and non-EMEP sources.

Satisfactory agreement (within ±50%) between modelled and observed annual mean concentrations of Pb and Cd is noted for stations in Czech Republic, Poland, Slovenia, most of stations in Germany and the United Kingdom. Significant overestimation of both metals occurs at stations DE3 and DE8 (Germany), DK12 (Denmark), ES14 (Spain), IS91 (Iceland), and SE20 (Sweden). At DE3, DE8 and ES14 (both metals), DK12 and SE20 (Cd) the overestimation takes place even if anthropogenic component is taken into account. In this case overestimation may be caused by uncertainties of anthropogenic emissions. Another possible reason can be associated with modelling, for example, treatment of near-surface temperature inversions in cold season, but this idea requires special research. Probably, similar reasons are related to stations in Belgium and the Netherlands where Cd concentrations were overestimated. Overestimation at costal stations IS91 and NO90 is caused mainly by too high contribution of re-suspension from sea surface. Although at other stations the contribution of this component is relatively low, more attention should be paid to verification of suspension of marine aerosols due to wind action. For stations located in Scandinavia the model tends to underestimate the observed levels. For most of Swedish and Norwegian sites the underestimation is better than -50%, but for stations in Finland it ranges from -20% to -70%. This underestimation can be explained by uncertainties of emission data. Similar possible reason can be proposed to explain underestimation of Cd and Pb levels at stations in France from -10% to -50%.

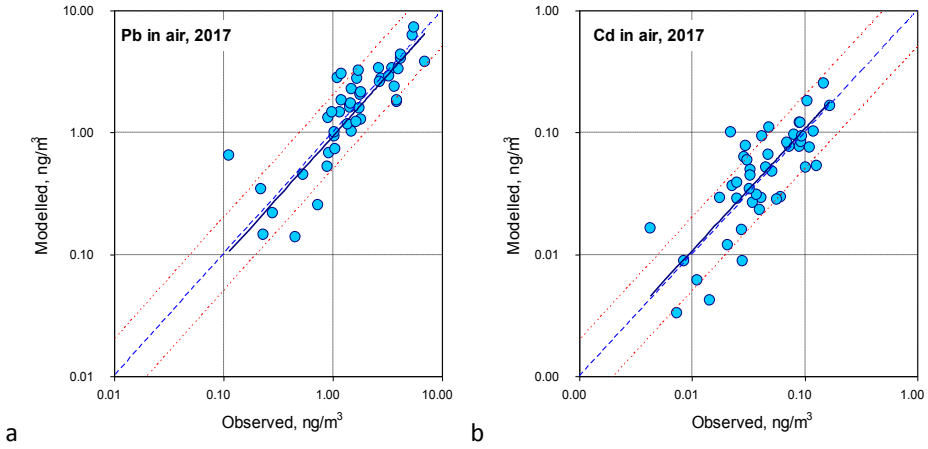


a b

***Fig. 4.14.*** *Modelled and observed concentrations of lead (a) and cadmium (b) in air in 2017*

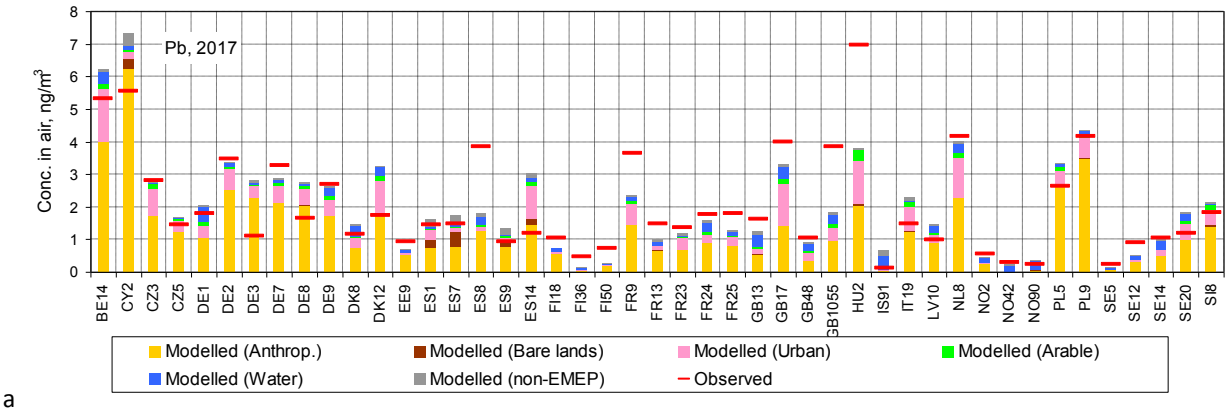


a

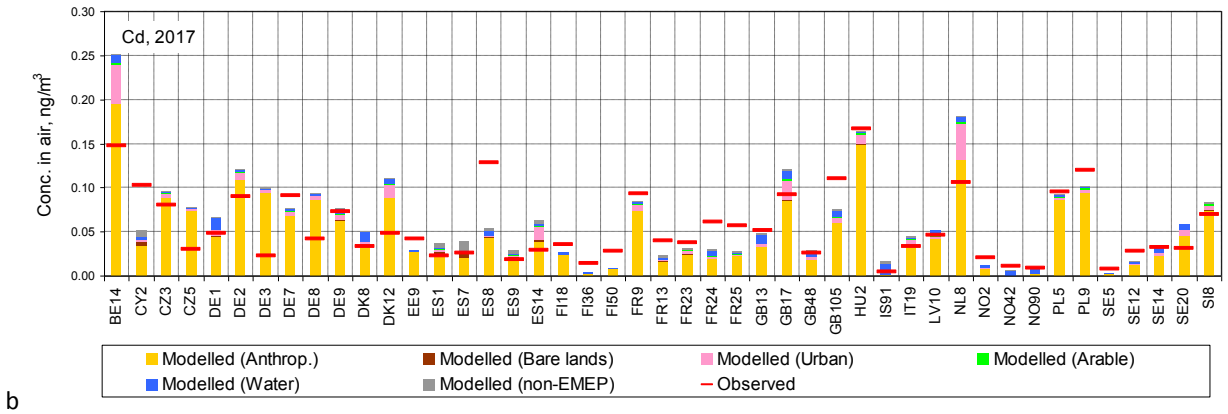


b

***Fig. 4.15.*** *Modelled and observed concentrations of lead (a) and cadmium (b) in air at the EMEP stations in 2017.*

Unlike concentrations in air, wet deposition fluxes of Pb and Cd were generally underestimated by the model. Mean relative bias for the totality of stations is -40% for lead and -43 for Cd. Correlation coefficients are about 0.51 for Pb and 0.45 for Cd(Fig. 4.16, 4.17). These statistical indicators do not include information on wet deposition from Spanish stations. No information is available for quality of measurements in Spain. Hence, although the model strongly (2.4 – 12 fold) underestimates observed Pb and Cd levels at these stations, it is not clear whether it is caused by uncertainties of measurements or

model parameterizations. Besides, measurements of Cd wet deposition from French stations were also excluded from the comparison. Before this year measured Cd concentrations in precipitation reported for the French stations were mostly below detection limit. This year the data are reported with lower detection limit. Observed wet deposition fluxes are much higher compared to those measured in neighbouring Germany and the United Kingdom. But the model underestimates the observed levels by 3- 9 times. These high observed levels may be explained by measurement uncertainties. Although this assumption needs to be checked, it was decided not to include Cd concentrations from French stations in 2017 in the statistical analysis.

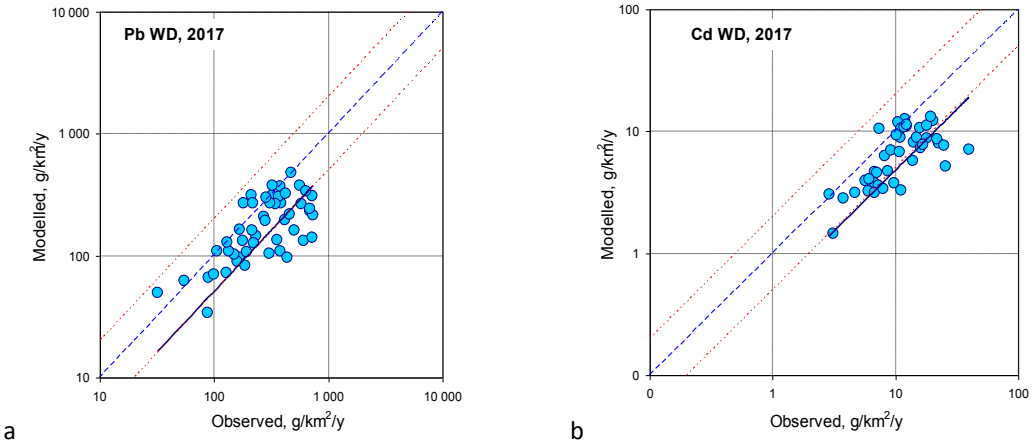


***Fig. 4.16.*** *Modelled and observed wet deposition fluxes of lead (a) and cadmium (b) in 2017*

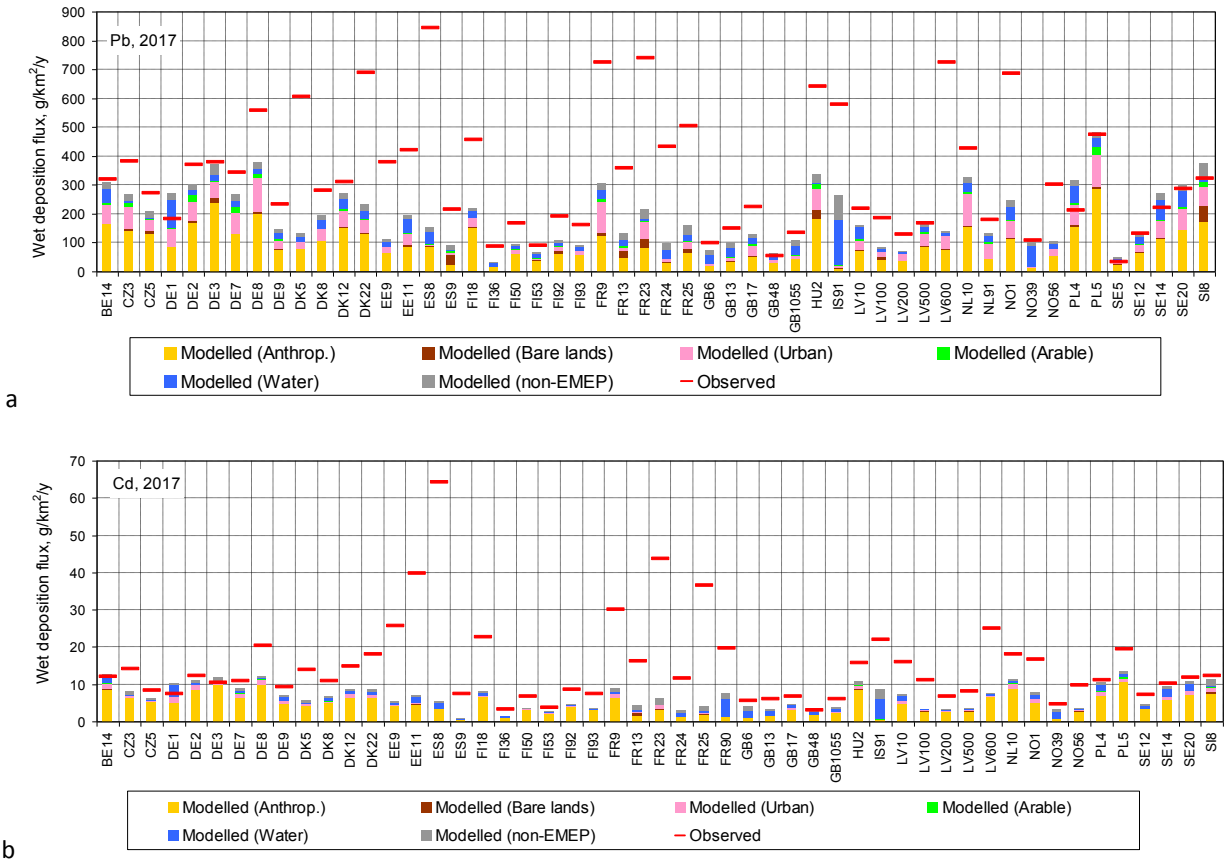


***Fig. 4.17.*** *Modelled and observed wet deposition fluxes of lead (a) and cadmium (b) at the EMEP stations in 2017.*

At stations located in Germany, the Czech Republic, Belgium, the United Kingdom, the Netherlands, Poland, Slovenia, most of stations in Sweden the bias between modelled and observed wet deposition fluxes lies within ±50% (Fig. 4.17). However, there is a large group of stations where observed wet deposition 2-5 fold higher than that predicted by the model. These are, for example, stations in Finland, France, Estonia, Spain, Latvia, DK5 and DK22 in Denmark. At some stations, such as DE1 (Pb, Cd), PL4, SE5 (Pb) overestimation of the observed concentrations (about 50%) takes place. Anthropogenic component of wet deposition is below than the observed value at these stations. Therefore, this overestimation can be caused by wind re-suspension components.

Most stations measurement lead levels in the atmosphere are co-located, i.e. both concentrations in air and wet deposition are measured. At these stations the results of modelled and measured concentrations in air and wet deposition can be analyzed jointly. In Fig. 4.18 ratios of modelled to observed parameters are shown. In the ideal case, the ratios both for concentrations in air and wet deposition should be equal to unity. In fact, the ratios close to unity are noted for Belgium (Pb), the Czech Republic (Pb), Poland, Slovenia, most stations of Germany and Sweden. At stations in Spain, Hungary and Finland the model tends to underestimate both parameters. Most likely it is explained by insufficient Pb and Cd emissions in these or neighbouring countries.

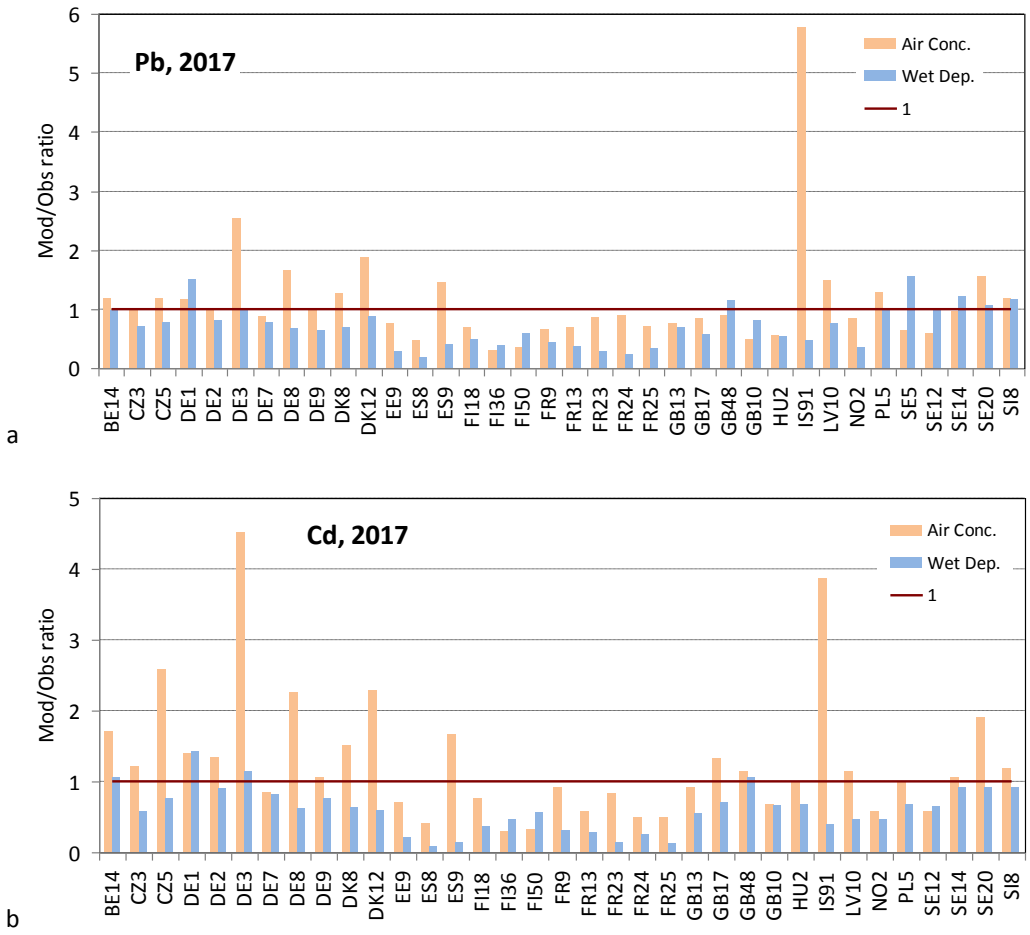


***Fig. 4.18****. Ratios of modelled to observed annual mean concentrations in air and wet deposition fluxes of lead (a) and cadmium (b)*

At stations in Denmark, Spain, France, Norway, Iceland and some stations in Germany the imbalance between modelled air concentrations and wet deposition is noted: ratio for concentrations in air is close or even exceeds unity, while wet deposition is underestimated. For cadmium we can see that air concentrations are overestimated at some stations, while wet deposition is underestimated. On one hand, in order to explain this imbalance peculiarities of modelling have to be studied. Air concentrations characterize pollution in the near-surface layer of the atmosphere, whereas wet deposition is formed when pollutants are scavenged through the atmosphere vertical column (hundreds – thousands meters). Underpredicted wet deposition could be caused by underestimated mass of lead in the atmospheric boundary layer or even above it. Therefore, analysis of vertical distribution of pollution produced by the model is needed. Besides, the effect of frequency of atmospheric precipitation on modelled concentrations in precipitation deserves special investigation. On the other hand, quality of wet deposition measurements remains unknown. Intercomparison tests regularly carried out by CCC characterize only analytical part of uncertainty of measured concentrations. Besides, some countries (e.g., Spain) do not participate in these tests. Hence, no information on quality of measurements at stations in these countries is available.

Mercury is a global-scale pollutant which atmospheric residence is about a year. Hence, mercury is well mixed in the troposphere of the North Hemisphere where its concentrations in air are relatively uniform except for locations close to strong emission sources. Therefore, both modelled and observed concentrations at the EMEP stations lie within 1.1-1.6 ng/$m^3$ limits (Fig. 4.19a).Mean relative bias for Hg concentrations in air is 11%. For most of stations relative bias between modelled and calculated values varies from 4% to 13%, except for the station EE9 and PL5, where the bias is around 30% (Fig. 4.9). Observed concentrations at these two stations are considerably lower than the concentrations observed at other EMEP stations probably because of measurement issues. Since both modelled and observed concentrations do not exhibit significant spatial variability, spatial correlation coefficient is relatively low (0.39).

The model tends to overestimate wet deposition of mercury at the EMEP stations. Mean relative bias is about 50%. However, spatial correlation is relatively reaching 0.82 (Fig. 4.19b) assuming that the model capable of reproducing spatial gradients of wet deposition fluxes. For particular stations relative bias varies from -6% (EE9) to 150% (SI8). For stations located Norway, the Netherlands, the Czech Republic and most of stations in Germany the bias is about 25-40%. For stations of Sweden and the United Kingdom it is somewhat higher (50-60%).

There are two main possible reasons leading to overestimation of the observed Hg deposition fluxes by the model. First of all, information about mercury speciation is uncertain. Countries are not obliged to report information on speciation of mercury emissions between relatively chemically inert are poorly soluble elemental form and easily washed out gaseous oxidized and particulate forms. Therefore, expert estimates are applied to establish the ratios between contributions of these forms to emission. The second reason is associated with uncertainties of atmospheric chemistry of mercury. Despite the progress in this field reached for recent decades, knowledge about rates, pathways and products of key reactions is still insufficient and requires further research. Details about progress in atmospheric chemistry of mercury are available in Section 4.2 of the EMEP status report [*Gusev et al*., 2019].

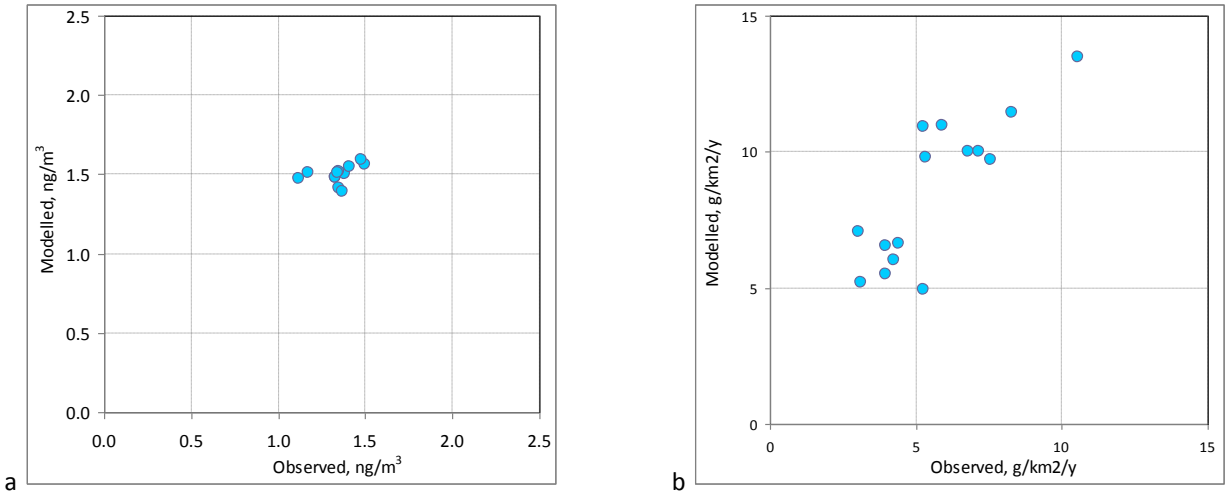


***Fig. 4.19.*** *Modelled and observed concentrations of mercury in air (a) and mercury wet deposition fluxes (b) in 2017*

# 5. POLLUTION OF MARGINAL SEAS

## 5.1. Lead

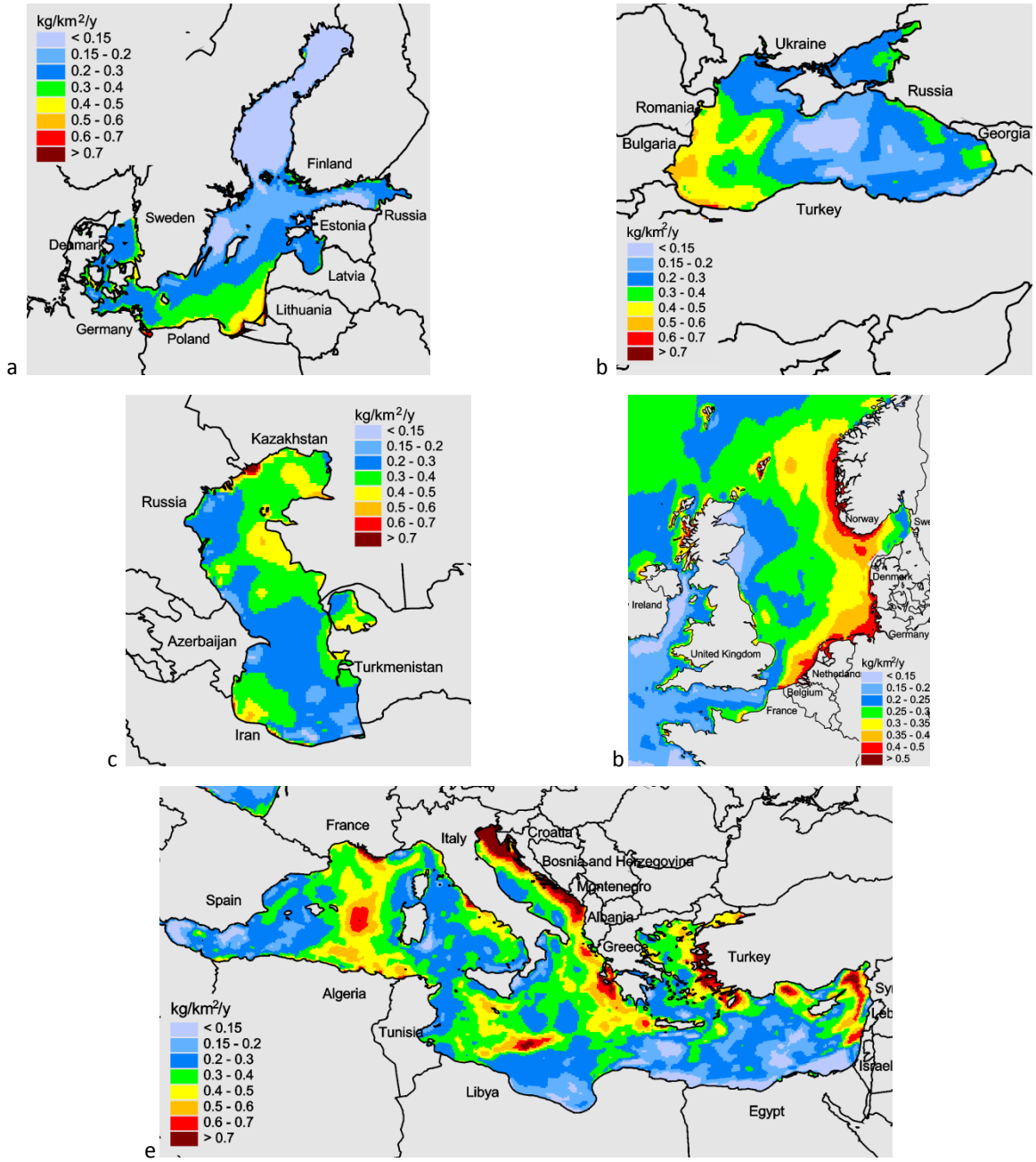


***Fig. 5.1.*** *Lead atmospheric input to the Baltic (a), Black (b), Caspian (c), North (d) and Mediterranean (d) Seas*

## 5.2. Cadmium

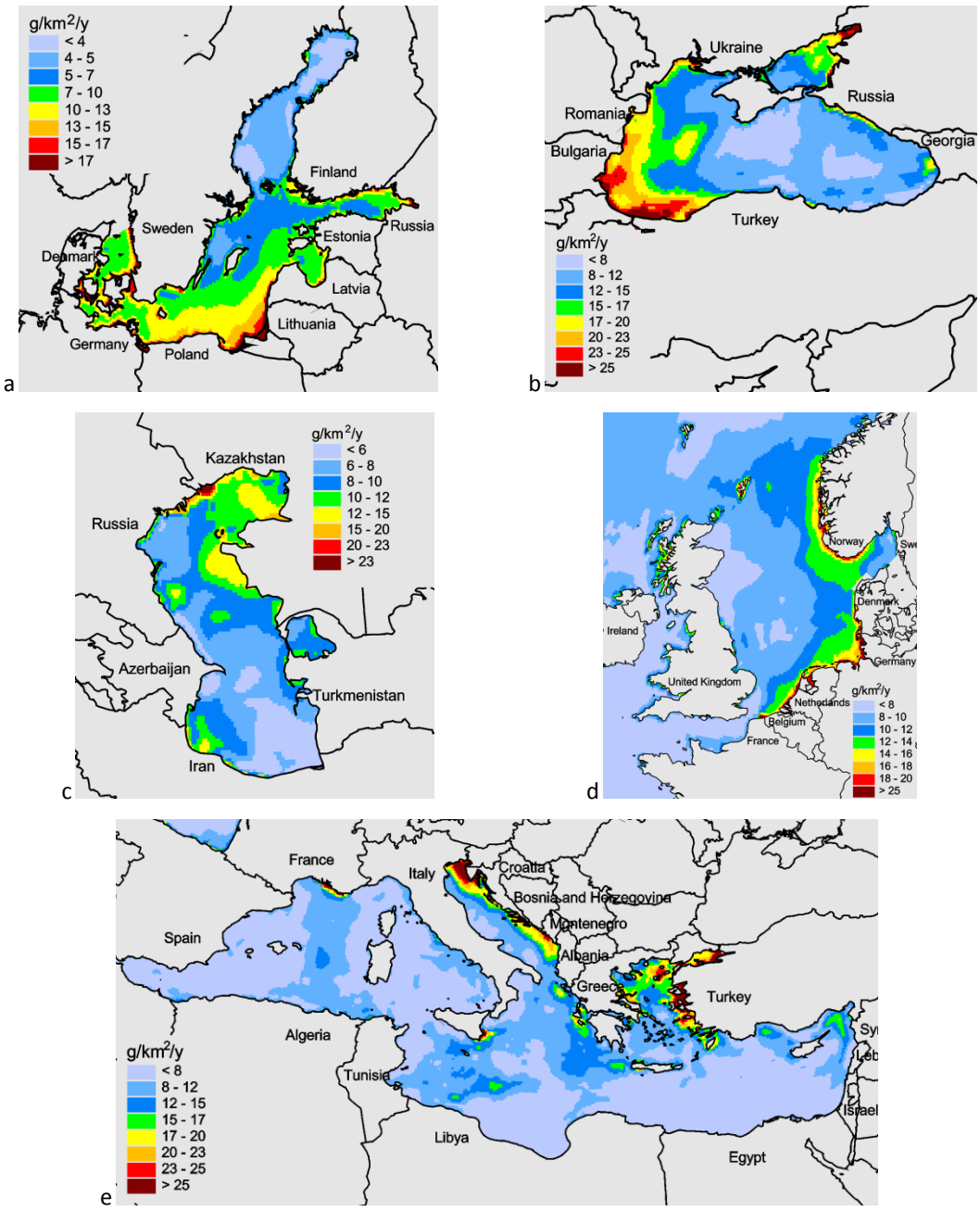


***Fig. 5.2.*** *Cadmium atmospheric input to the Baltic (a), Black (b), Caspian (c), North (d) and Mediterranean (d) Seas*

## 5.3. Mercury

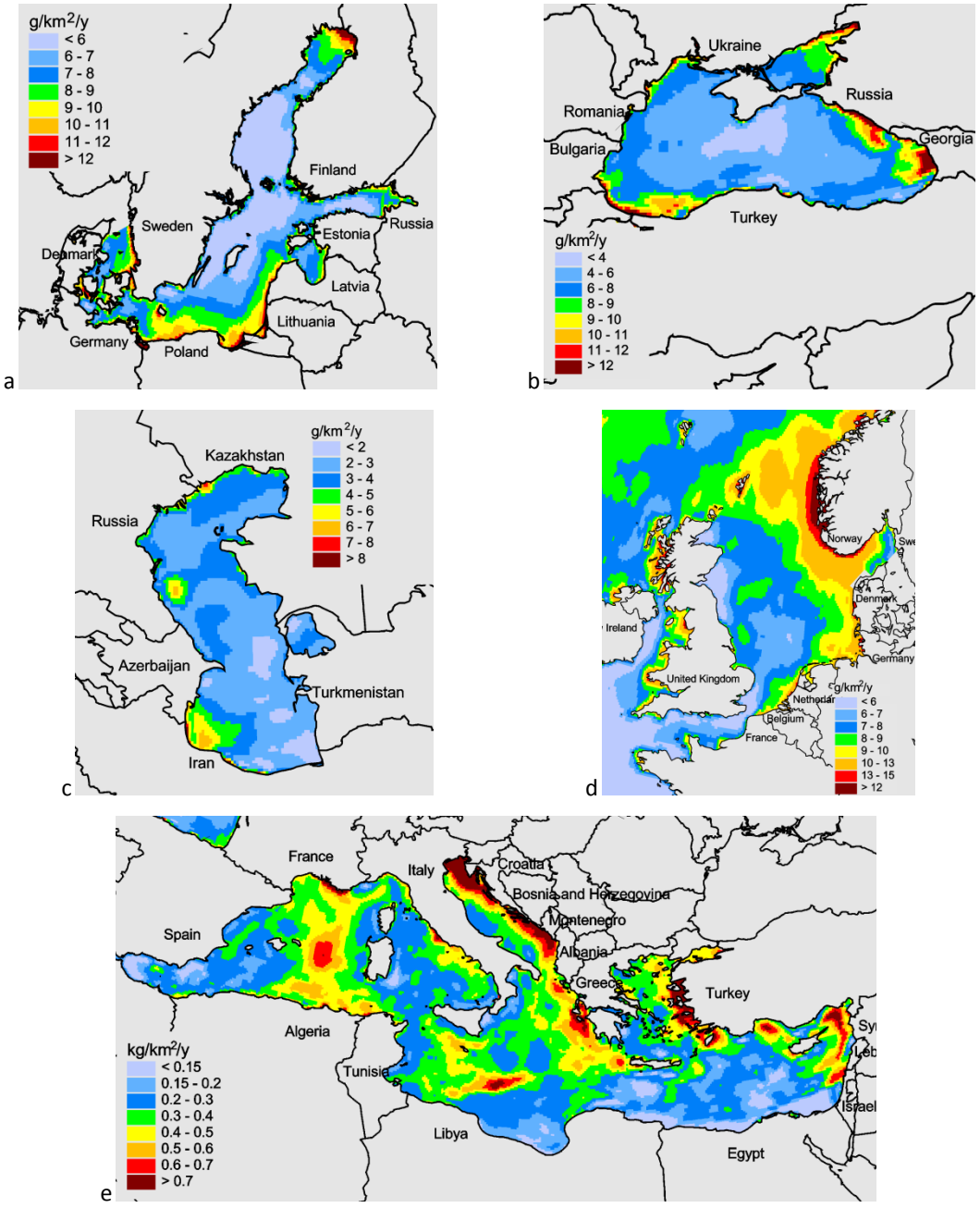


***Fig. 5.3.*** *Mercury atmospheric input to the Baltic (a), Black (b), Caspian (c), North (d) and Mediterranean (d) Seas*

# 6. ECOSYSTEM-SPECIFIC DEPOSITION

***Table 6.1.*** *Classification of land-cover types used for modelling of ecosystem-dependent deposition [Strahler et al, 1999]*

| Land-cover type | Description |
|---|---|
| Evergreen Needleleaf Forests | Lands dominated by woody vegetation with a percent cover >60% and height exceeding 2 meters. Almost all trees remain green all year. Canopy is never without green foliage. |
| Evergreen Broadleaf Forests | Lands dominated by woody vegetation with a percent cover >60% and height exceeding 2 meters. Almost all trees and shrubs remain green year round. Canopy is never without green foliage. |
| Deciduous Needleleaf Forests | Lands dominated by woody vegetation with a percent cover >60% and height exceeding 2 meters. Consists of seasonal needleleaf tree communities with an annual cycle of leaf-on and leaf-off periods. |
| Deciduous Broadleaf Forests | Lands dominated by woody vegetation with a percent cover >60% and height exceeding 2 meters. Consists of broadleaf tree communities with an annual cycle of leaf-on and leaf-off periods. |
| Mixed Forests | Lands dominated by trees with a percent cover >60% and height exceeding 2 meters. Consists of tree communities with interspersed mixtures or mosaics of the other four forest types. None of the forest types exceeds 60% of landscape. |
| Closed Shrublands | Lands with woody vegetation less than 2 meters tall and with shrub canopy cover >60%. The shrub foliage can be either evergreen or deciduous. |
| Open Shrublands | Lands with woody vegetation less than 2 meters tall and with shrub canopy cover between 10-60%. The shrub foliage can be either evergreen or deciduous. |
| Woody Savannas | Lands with herbaceous and other understory systems, and with forest canopy cover between 30-60%. The forest cover height exceeds 2 meters. |
| Savannas | Lands with herbaceous and other understory systems, and with forest canopy cover between 10-30%. The forest cover height exceeds 2 meters. |
| Grasslands | Lands with herbaceous types of cover. Tree and shrub cover is less than 10%. |
| Permanent Wetlands | Lands with a permanent mixture of water and herbaceous or woody vegetation. The vegetation can be present in either salt, brackish, or fresh water. |
| Croplands | Lands covered with temporary crops followed by harvest and a bare soil period (*e.g.*, single and multiple cropping systems). Note that perennial woody crops will be classified as the appropriate forest or shrub land cover type. |
| Urban and Built-Up Lands | Land covered by buildings and other man-made structures. |
| Cropland/Natural Vegetation Mosaics | Lands with a mosaic of croplands, forests, shrubland, and grasslands in which no one component comprises more than 60% of the landscape. |
| Snow and Ice | Lands under snow/ice cover throughout the year. |
| Barren | Lands with exposed soil, sand, rocks, or snow and never has more than 10% vegetated cover during any time of the year. |
| Water Bodies | Oceans, seas, lakes, reservoirs, and rivers. Can be either fresh or salt-water bodies. |

## 6.1. Lead

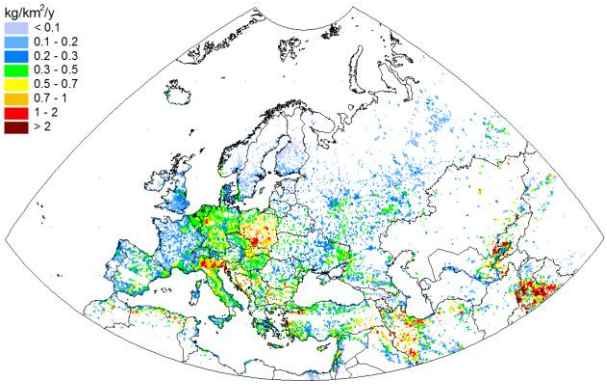


***Fig. 6.1.*** *Annual total deposition of Pb on urban and built-up lands in the EMEP region in 2017, kg/km²/y*

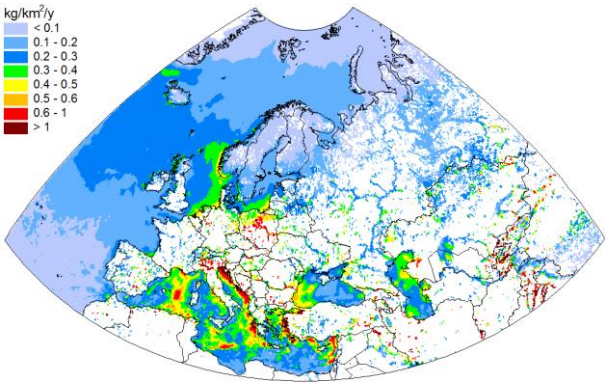


***Fig. 6.2.****Annual total deposition of Pb on water bodies in the EMEP region in 2017, kg/km²/y*

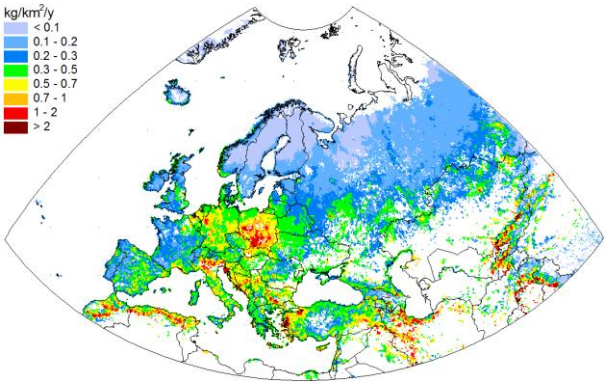


***Fig. 6.3.****Annual total deposition of Pb on woody savannas in the EMEP region in 2017, kg/km²/y*

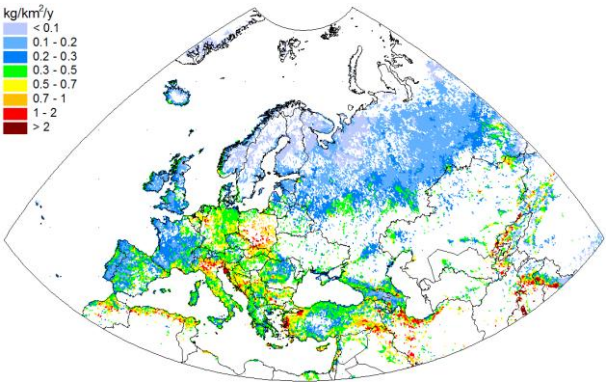


***Fig. 6.4.****Annual total deposition of Pb on savannas in the EMEP region in 2017, kg/km²/y*

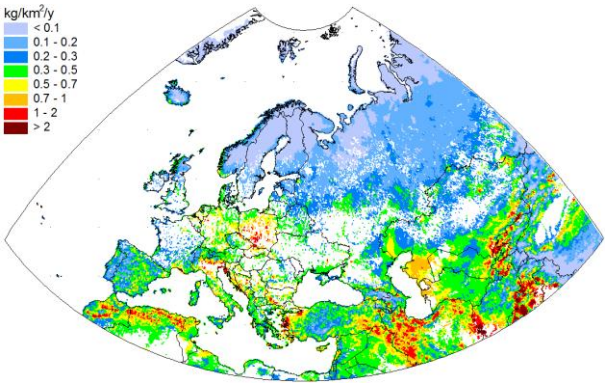


***Fig. 6.5.****Annual total deposition of Pb on open shrublands in the EMEP region in 2017, kg/km²/y*

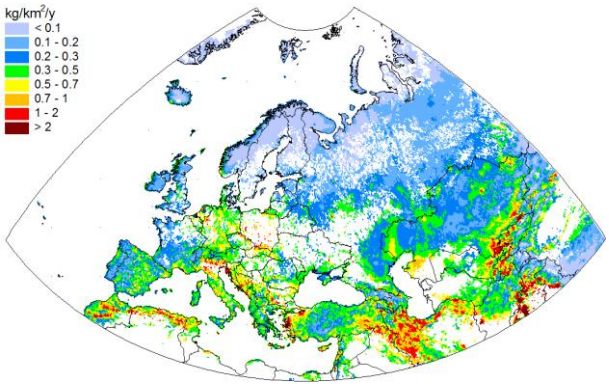


***Fig. 6.6.****Annual total deposition of Pb on grasslands in the EMEP region in 2017, kg/km²/y*

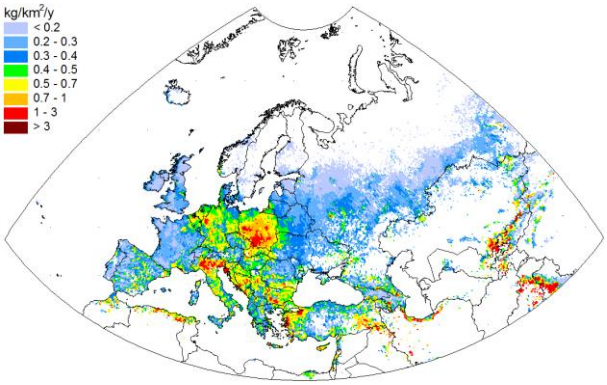


***Fig. 6.7.****Annual total deposition of Pb on cropland/natural vegetation mosaics in the EMEP region in 2017, kg/km²/y*

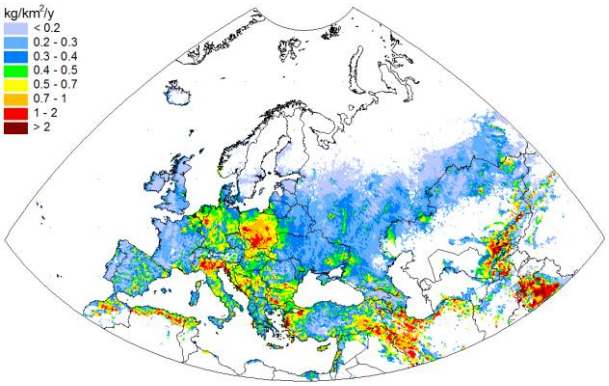


***Fig. 6.8.****Annual total deposition of Pb on croplands in the EMEP region in 2017, kg/km²/y*

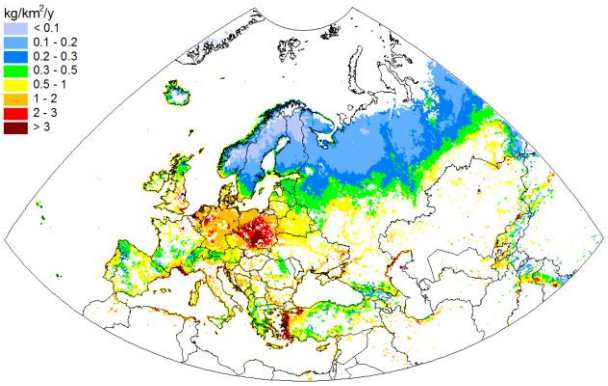


***Fig. 6.9.****Annual total deposition of Pb on evergreen needleleaf forests in the EMEP region in 2017, kg/km²/y*

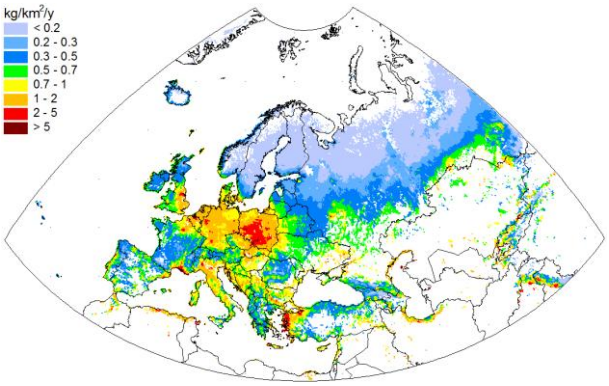


***Fig. 6.10.****Annual total deposition of Pb on mixed forests in the EMEP region in 2017, kg/km²/y*

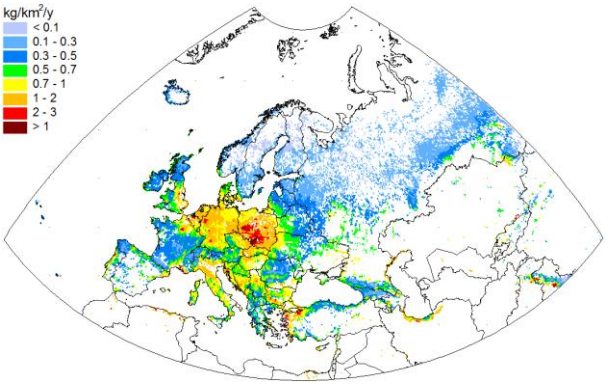


***Fig. 6.11.****Annual total deposition of Pb on deciduous broadleaf forests in the EMEP region in 2017, kg/km²/y*

## 6.2. Cadmium

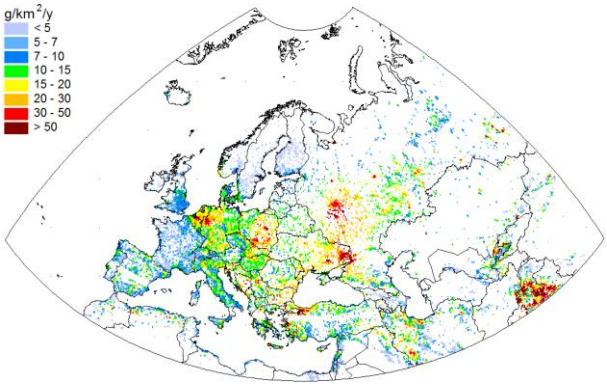


***Fig. 6.12.****Annual total deposition of Cd on urban and built-up lands in the EMEP region in 2017, g/km²/y*

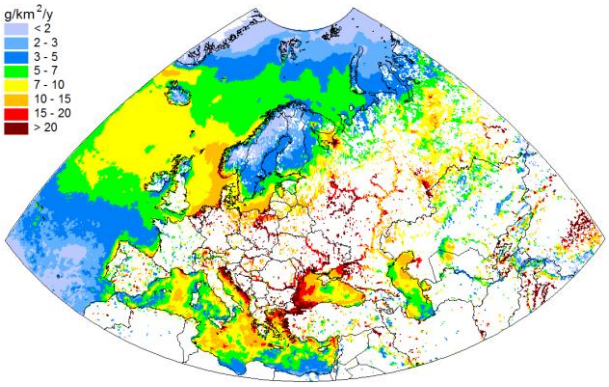


***Fig. 6.13.****Annual total deposition of Cd on water bodies in the EMEP region in 2017, g/km²/y*

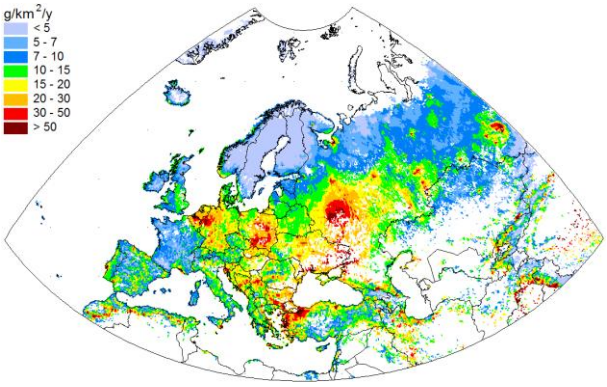


***Fig. 6.14.*** *Annual total deposition of Cd on woody savannas in the EMEP region in 2017, g/km²/y*

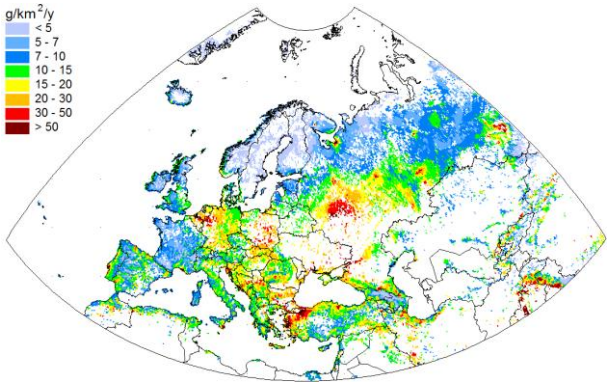


***Fig. 6.15.*** *Annual total deposition of Cd on savannas in the EMEP region in 2017, g/km²/y*

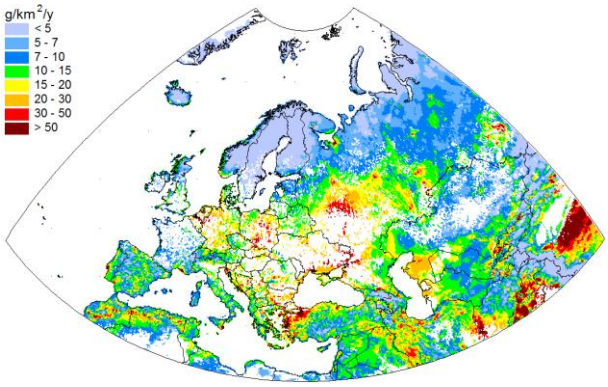


***Fig. 6.16.*** *Annual total deposition of Cd on open shrublands in the EMEP region in 2017, g/km²/y*

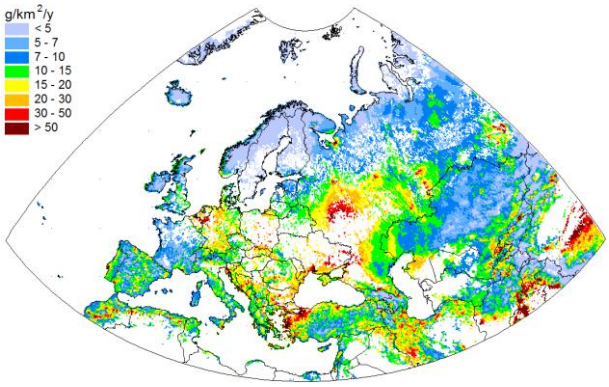


***Fig. 6.17.*** *Annual total deposition of Cd on grasslands in the EMEP region in 2017, g/km²/y*

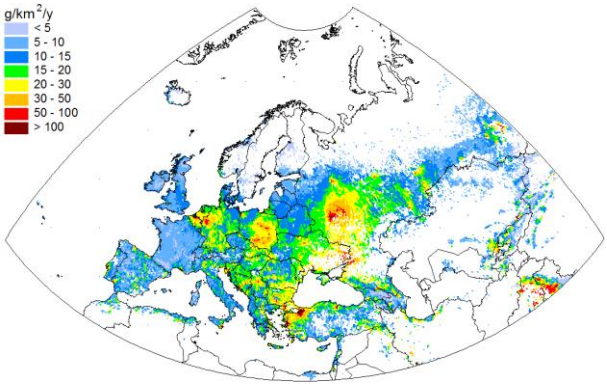


***Fig. 6.18.*** *Annual total deposition of Cd on cropland/natural vegetation mosaics in the EMEP region in 2017, g/km²/y*

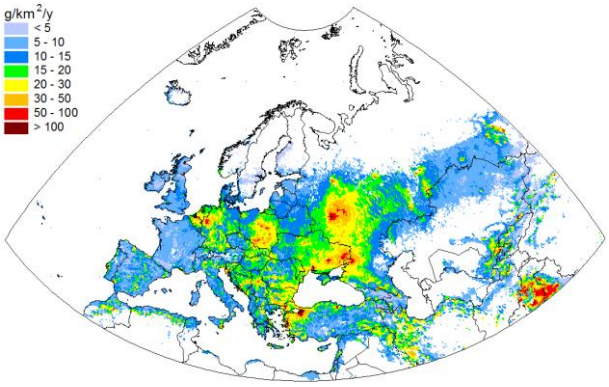


***Fig. 6.19.*** *Annual total deposition of Cd on croplands in the EMEP region in 2017, g/km²/y*

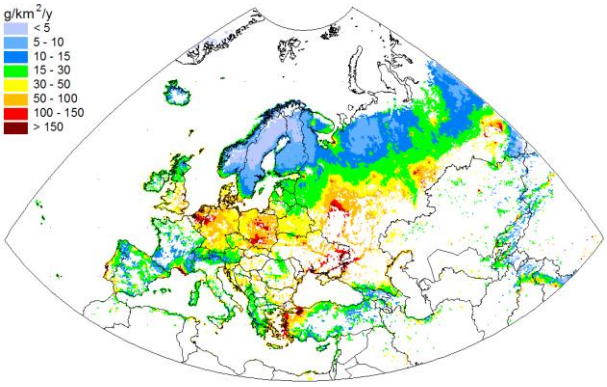


***Fig. 6.20.*** *Annual total deposition of Cd on evergreen needleleaf forests in the EMEP region in 2017, g/km²/y*

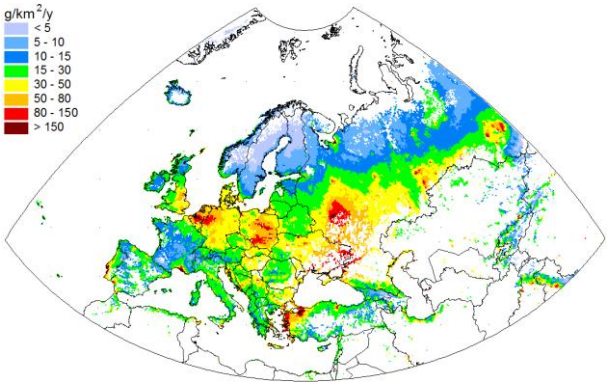


***Fig. 6.21.*** *Annual total deposition of Cd on mixed forests in the EMEP region in 2017, g/km²/y*

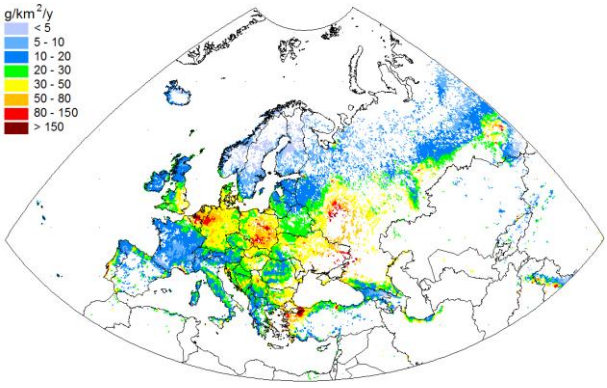


***Fig. 6.22.*** *Annual total deposition of Cd on deciduous broadleaf forests in the EMEP region in 2017, g/km²/y*

## 6.3. Mercury

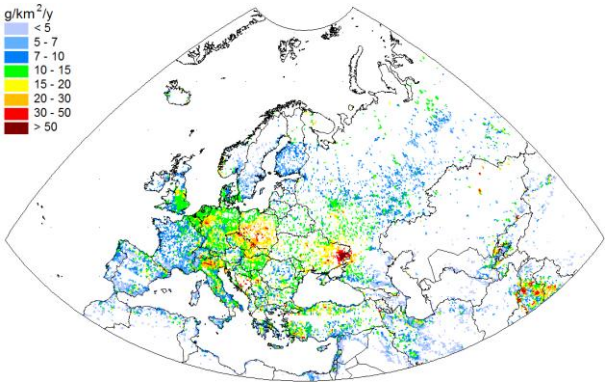


***Fig. 6.23.****Annual total deposition of Hg on urban and built-up lands in the EMEP region in 2017, g/km²/y*

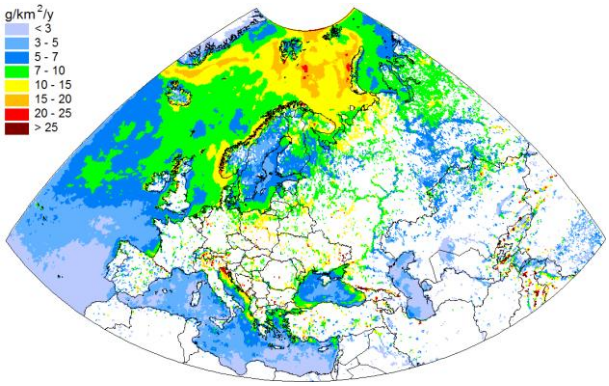


***Fig. 6.24.****Annual total deposition of Hg on water bodies in the EMEP region in 2017, g/km²/y*

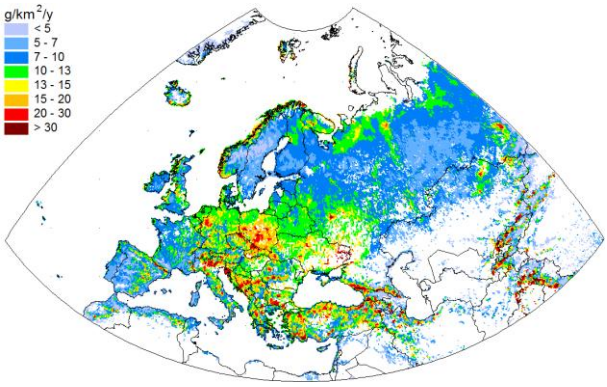


***Fig. 6.25.****Annual total deposition of Hg on woody savannas in the EMEP region in 2017, g/km²/y*

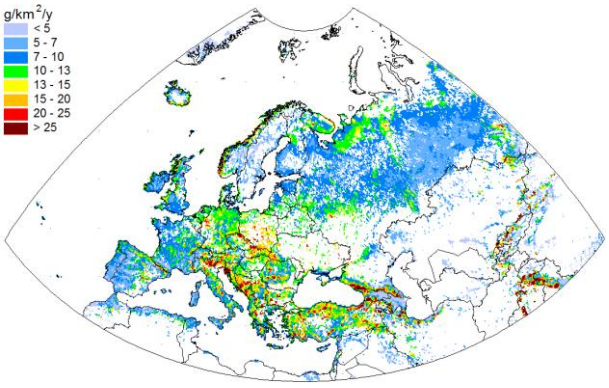


***Fig. 6.26.****Annual total deposition of Hg on savannas in the EMEP region in 2017, g/km²/y*

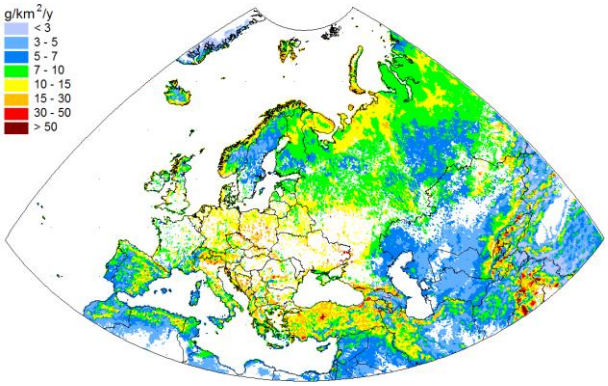


***Fig. 6.27.****Annual total deposition of Hg on open shrublands in the EMEP region in 2017, g/km²/y*

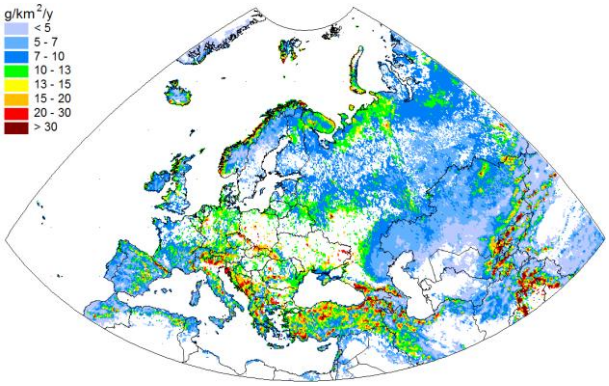


***Fig. 6.28.****Annual total deposition of Hg on grasslands in the EMEP region in 2017, g/km²/y*

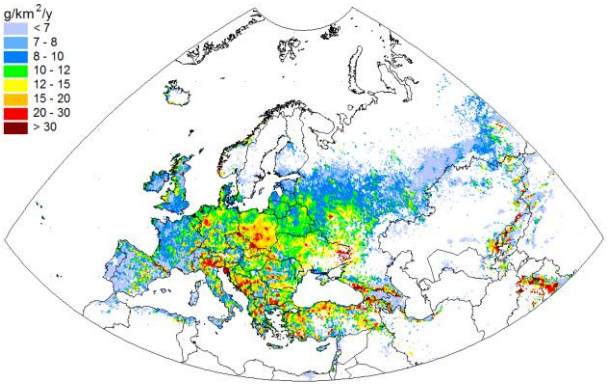


***Fig. 6.29.*** *Annual total deposition of Hg on cropland/natural vegetation mosaics in the EMEP region in 2017, g/km$^2$/y*

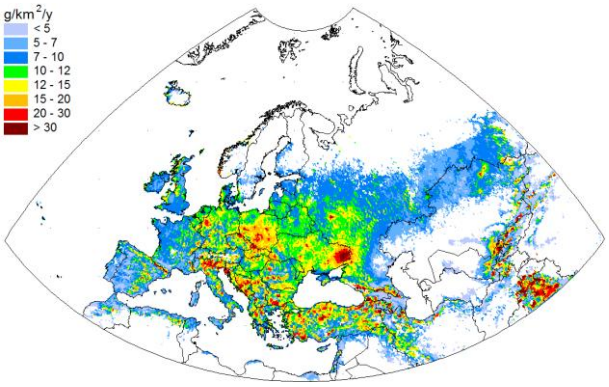


***Fig. 6.30.*** *Annual total deposition of Hg on croplands in the EMEP region in 2017, g/km$^2$/y*

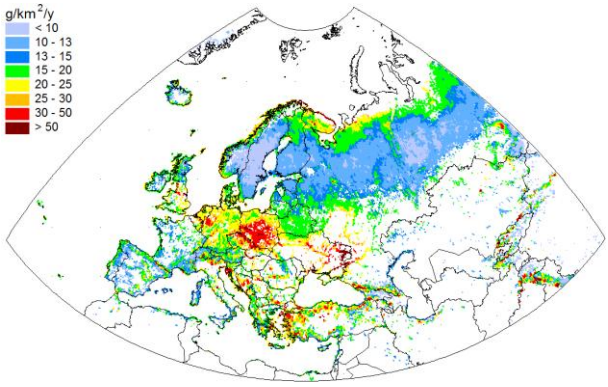


***Fig. 6.31.*** *Annual total deposition of Hg on evergreen needleleaf forests in the EMEP region in 2017, g/km$^2$/y*

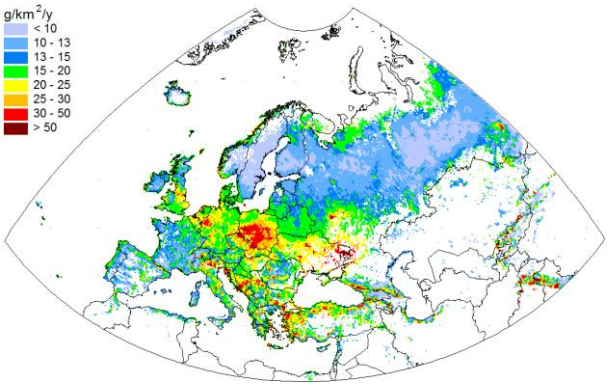


***Fig. 6.32.*** *Annual total deposition of Hg on mixed forests in the EMEP region in 2017, g/km$^2$/y*

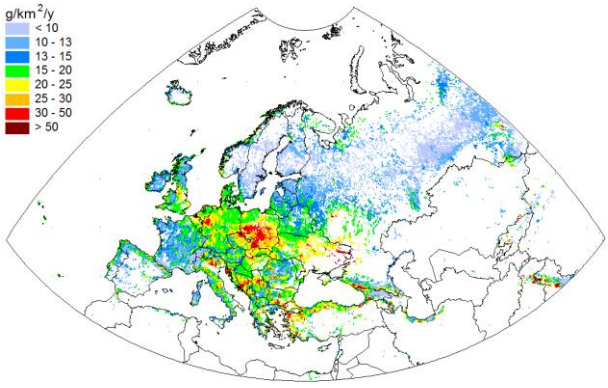


***Fig. 6.33.*** *Annual total deposition of Hg on deciduous broadleaf forests in the EMEP region in 2017, g/km$^2$/y*

# REFERENCES


CCC [2019]. EMEP laboratory intercomparison. https://projects.nilu.no//ccc/intercomparison/index.html.Accessed on June 18, 2019.

Dębski B., Olecka A., Bebkiewicz K., Chłopek Z., Kargulewicz I., Rutkowski J., Zasina D., Zimakowska–Laskowska M., Żaczek M. and S.Waśniewska [2018] Poland's Informative Inventory Report 2018. Submission under the UN ECE Convention on Long-range Transboundary Air Pollution and the DIRECTIVE (EU) 2016/2284. IOS-PIB/KOBiZE, Warsaw, February 2018.

Durand A. and C.Robert (ed.) [2018] Inventaire des émissions de polluants atmosphériques en France au titre de la convention sur la pollution atmosphérique transfrontalière à longue distance et de la directive européenne concernant la réduction des émissions nationales de certains polluants atmosphériques. CITEPA, Mars 2018. 598 p.

Gusev A., I. Ilyin, V. Shatalov, O. Travnikov, N. Batrakova, O. Rozovskaya, I. Strijkina, K.Brevik, Nizzetto P.B., W. Aas, K. Mareckova, S. Poupa, C. Sosa, M. Tista, R. Wankmueller, F. Couvidat [2019] Assessment of transboundary pollution by toxic substances: Heavy metals and POPs. EMEP Status Report 2/2019. July 2019.

IIR Belarus [2016] Belarusian emission inventory data. Informative Inventory Report to CLRTAP/EMEP 2016. 64 p.

IIR Belgium [2018] Informative Inventory Report about Belgium's air emissions submitted under the Convention on Long Range Transboundary Air Pollution CLRTAP and National Emission Ceiling Directive NECD. March 2018. VMM, AWAC, IBGE-BIM, IRCEL-CELINE, EKG. 193 p.

IIR Finland [2018] Air Pollutant Emissions in Finland 1990 – 2016. Informative Inventory Report to the secretariat of the UNECE Convention on long-range transboundary air pollution. Part 5 Annexes. Finish Environmental Institute.

IIR Sweden [2018] Informative Inventory Report Sweden 2018. Submitted under the Convention on Long-Range Transboundary Air Pollution. Swedish Environmental Protection Agency Report 2018. 261 p.

IIR Switzerland [2018] Switzerland's Informative Inventory Report 2018. Submission under the UNECE Convention on Long-range Transboundary Air Pollution. Federal Office for the Environment FOEN. Air Pollution Control and Chemicals Division. 345 p.

Kohv N., Heintalu H., Mandel E. and A.Link [2018] Estonian Informative Inventory Report 1990-2016 Submitted under the Convention on Long-Range Transboundary Air Pollution. Environment Agency, Tallinn 2018, 316 p.

Nielsen O-K., Plejdrup M.S., Winther M., Mikkelsen M.H., Nielsen M., Gyldenkærne S., Fauser P., Albrektsen R., Hjelgaard K.H., Bruun H.G. and M.Thomsen [2018] ANNUAL DANISH INFORMATIVE INVENTORY REPORT TO UNECE. Emission inventories from the base year of the protocols to year 2016. Aarhus University, Department of Environmental Science., 495 p.

Papadopoulos C. and Charalambous C. [2018] Cyprus Informative Inventory Report 2016. Ministry of Labour, Welfare and Social Insurance. Department of Labour Inspection. Nicosia, March 2018. 270 p.

Poljanac M., Marković B., Švedek I., Hublin A., Kos R., Herenčić L., Delija-Ružić V. and A.Abrashi [2018] Republic of Croatia 2018 Informative Inventory Report (1990 – 2016). Submission to the Convention on Long-range Transboundary Air Pollution and National Emission Ceilings Directive (NECD 2016/2284/EU). Croatian Agency for Environment and Nature. 445 p.

Skrebele A., Ratniece V., Rubene L., Ozoliņa Z., Cakars I., Siņics L., Klāvs G., Gračkova L., Bērziņa L., Frolova O., Lazdiņš A., Bārdule A., Šustere L., Maslova L., Gancone A., Braņicka I., Lavrinoviča I., Ozoliņa I., Raubena A. and L.Meļko [2018] Latvia's Informative Inventory Report 1990 - 2016. Submitted under the Convention on Long-Range Transboundary Air Pollution. Latvian Environment, Geology and Meteorology Centre.

Strahler A., Muchoney D.,Borak J., Friedl M., Gopal S., Lambin E. and Moody A. [1999]. MODIS Land Cover Product Algorithm Theoretical Basis Document (ATBD) Version 5.0. 66 p.

Wakeling D., Passant N.R., Murrells T.P., Misra A., Pang Y., Thistlethwaite G., Walker C., Brown P., Del Vento S., Hunter R., Wiltshire J., Broomfield M., Watterson J., Pearson B., Rushton K., Hobson M., Dore C. and T.Misselbrook [2018] UK Informative Inventory Report (1990 to 2016). 320 p.